UNIVERSITY OF SOUTHAMPTON

Faculty of Social Sciences

Department of Applied Mathematics

Analytic exploration of the non-perturbative domain of asymptotic observables.

by

Daniel Hasenbichler

ORCiD: 0000-0002-5390-5175

A thesis for the degree of

Doctor of Philosophy

January 2024

University of Southampton

Abstract

Faculty of Social Sciences
Department of Applied Mathematics

Doctor of Philosophy

Analytic exploration of the non-perturbative domain of asymptotic observables.

by Daniel Hasenbichler

Transseries expansions are natural extensions of ordinary power series and include non-perturbative monomials such as exponentials as additional basis elements. By using a range of highly accurate asymptotic methods an analytic understanding of the full non-perturbative domain of asymptotic observables can be obtained which can go far beyond the results of numerical computations. This is the focus of this thesis, where such asymptotic methods have proven crucial for the full non-perturbative understanding of observables in three separate research directions. The so-called transasymptotic summation is used to arrive at a novel analytic understanding of the bifurcation behaviour of discrete non-linear systems. It is shown that such transasymptotic summations can be used to naturally explain the emergence of so-called delayed bifurcations widely known as 'canards' in singularly perturbed systems. In the context of relativistic hydrodynamics, several distinct summation techniques are used and compared to match the late time temperature evolution of an expanding fluid to its early time behaviour. The power of the transasymptotic summation method is further exploited to derive global analytical properties such as analytic approximations to the locations of square-root branch points. In the context of mathematical relativity, the exponentially decaying and oscillatory corrections to the perturbative WKB approximation of the quasinormal mode frequencies of a charged scalar field in an expanding charged black hole spacetime background (RNdS) are captured in a transseries and analysed using Borel techniques and new analytic properties are found. These approaches to study non-perturbative phenomena are quite generic and can be applied to a large class of problems.

Contents

List of Figures

List of Tables

Declaration of Authorship

I declare that this thesis and the work presented in it is my own and has been generated by me as the result of my own original research.

I confirm that:

1. This work was done wholly or mainly while in candidature for a research degree at this University;
2. Where any part of this thesis has previously been submitted for a degree or any other qualification at this University or any other institution, this has been clearly stated;
3. Where I have consulted the published work of others, this is always clearly attributed;
4. Where I have quoted from the work of others, the source is always given. With the exception of such quotations, this thesis is entirely my own work;
5. I have acknowledged all main sources of help;
6. Where the thesis is based on work done by myself jointly with others, I have made clear exactly what was done by others and what I have contributed myself;
7. Parts of this work have been published as: [4, 2]

Signed:..... Date:.....

Acknowledgements

I would like to thank my advisors Inês Aniceto and Christopher Howls for their guidance and support during the last four years.

I would like to thank Oscar Dias, Christopher Lustri, and Adri Olde Daalhuis for the interesting discussions.

I would like to thank Davide Bufalini, Luigi Bobbio, Enrico Parisini, Alex Davey, Sami Rawash, Federico Capone, Elliot Bridges, Linus Too, Aaron Poole, Michele Santagata, Thomas Celora, Savvas Pitsinigkos, Geraint Evans, Giuseppe Di Nardo, Adam Chalabi, Filip Landgren, and Noam Tamarin for the shared laughter.

I would like to thank my family for having supported me throughout my life.

I would like to thank Alexander Brunbauer, Johann Gehringer, Harprit Singh, Lorenz Steinwender and Lukas Tarra for our joint adventures.

Thesis overview

Asymptotic expansions remain an important tool in the technical repertoire of any applied mathematician today. In mathematical physics, they arise as formal perturbative solutions in many different contexts from correlation functions in quantum field theories to non-linear waves in fluid mechanics, where the complexity of the problems forces one to rely on perturbative methods. In many interesting problems these perturbative expansions are factorially divergent, which means that the coefficients in the expansion diverge as $\sim n!$. In such cases, summing a few terms surprisingly provides very accurate results, but adding extra terms will quickly make the result begin to diverge.

Nevertheless, it is possible to extract analytic information from such divergent expansions, and several techniques such as optimal truncation, hyperasymptotics, Borel summation and transasymptotic summation can be used [7, 8, 9, 10]. The factorial growth of the coefficients in the perturbative expansion indicates that the observable contains non-perturbative sectors that are not captured directly from the perturbative analysis alone. These non-perturbative sectors are asymptotic expansions themselves that come multiplied by non-perturbative functions. Often the non-perturbative terms are decaying exponentials and thus, exponentially smaller than any of the terms in the original perturbative asymptotic series.

Mathematically, the complete formal solution to an asymptotic observable, including both perturbative and non-perturbative sectors, can in many cases be described using a so-called exponential transseries, which typically includes an infinite number of subdominant contributions. The further one moves away from the expansion point, the more significant the decaying exponentials may become. Moreover, the exponentials can change dominance depending on the value of the variable in the non-perturbative

domain, and can give rise to widely different analytic behaviour, from oscillations to pole singularities.

This PhD thesis will explore three different problems for which the asymptotic behaviour is well-known in perturbation theory, and for which capturing non-perturbative contributions is nonetheless crucial to an understanding of important analytic properties. A novel approach in the study of deterministic chaos will be developed which analytically captures the bifurcations in discrete non-linear chaotic systems. Moreover, a new interpretation of the bifurcation phenomenon will be given from the behaviour of the exponential weights in a transseries. In the context of hydrodynamics, a methodology for the interpolation between late and early times based on well-established summation techniques will be developed, and novel global analytic properties will be deduced. The findings of these projects have been published in two publications [2, 4], wherein significant sections of this thesis have been reproduced verbatim.

Chapter 1 will provide an introduction to the non-perturbative methods which will be used throughout this thesis. The importance of non-perturbative phenomena in physics will be explained using the most well-known example of such non-perturbative behaviour,which is that of instantons in quantum mechanics. The resurgent properties of factorially divergent asymptotic series will then be discussed using Borel resummation, and the essential role of exponentially small terms in the analytic continuation in parameter space, also known as the Stokes phenomenon, will be discussed using the language of Écalle's Stokes automorphisms and alien derivatives [7, 11, 12]. The hyperasymptotic summation method will be introduced in the context of WKB expansions in quantum mechanics, and the transasymptotic method will be discussed as a means of accessing a regime where the non-perturbative exponentials contributing to the observable are no longer small. These methods can all be regarded as tools to access the non-perturbative domain of a mathematical/physical problem, and will be used repeatedly in the following Chapters of this thesis.

In Chapter 2 the discrete logistic map will be studied, a non-linear system which contains bifurcations depending on the value of a parameter λ in the equation. The system will be explored both in the case where λ is constant (the static case), and in the case

where the parameter is growing in time (the dynamical case). The bifurcations will be described using an exponential transseries ansatz, and a systematic method to obtain the bifurcations will be presented. The bifurcations themselves will be shown to take place as a consequence of a change in dominance in the exponential weights of the transseries. It will be shown that truncating the transseries after a few exponential terms can never be sufficient to capture the period-doublings, which lie within the non-perturbative domain of the system. The transasymptotic summation method will provide the necessary tool in this case, which will be used to derive an analytic approximation to the period-doublings. Moreover, in the dynamical case, the Borel plane of the perturbative and the first non-perturbative sectors will be studied, complementing the transasymptotic approach and leading to an improved understanding of the non-perturbative domain of the problem.

In Chapter 3, the asymptotics of the time evolution of a conformally invariant relativistic fluid will be studied. The evolution equation is a non-linear first-order ODE which contains an attractor at infinity. The attractor is a solution to which all other physical solutions converge exponentially, a process which can be interpreted as a gradual loss of the information encoded in the initial conditions of the system. This information is never completely lost, but rather encoded in the exponentially decaying amplitudes of the non-perturbative modes. A question that naturally arises is how to interpolate between the late-time regime in which the attractor dominates the behaviour, and the non-perturbative early-time regime in which the different solutions differ significantly depending on the initial value problem. The interpolation problem will be approached using the well-established methods of Borel summation and hyperasymptotic summation, and the value of the non-perturbative amplitudes of the transseries will be numerically computed as a function of a parameter representing the initial data. The non-linear ODE will also be shown to give rise to interesting mathematical properties such as the existence of an infinite number of square-root branch points, as well as different asymptotics at $+\infty$ and $-\infty$ in time. These global properties will be shown to be mathematically related to a change in dominance of the non-perturbative exponentials in the late-time transseries. The transasymptotic summation will again prove to be a useful tool in this case, and it will be used to dervive an analytic approximation to the locations of the branch points as well as the asymptotics at $-\infty$ in time.

In Chapter 4, the non-perturbative regime of a quasinormal-mode equation of a massless charged scalar matter field in a Reissner-Nordström-de Sitter background will be studied. The non-perturbative contributions to the quasinormal mode frequencies contain information about the validity of the so-called strong cosmic censorship conjecture. More specifically, the magnitude of the imaginary part of the frequencies is proportional to the degree of regularity β of generic solutions, and it was found numerically in [6] that β oscillates around the critical value $\beta = 1/2$. These oscillations are non-perturbative in the large charge regime of the scalar field. The work in this chapter aims at understanding the nature of these non-perturbative contributions, and how it arises from the perturbative WKB-expansions for large charges. The WKB approach in [6] implicitly assumes that the perturbative expansions can first be expanded out in the scalar field charge, and then in the radial variable. The validity of this assumption will be confirmed using a multiple scales approach. Moreover, an analytic relationship between the non-perturbative, radially-dependent exponentials of the quasinormal mode wave function and those of the quasinormal mode frequencies will be derived. The methods and some of the results of this project are generic and can be applied to the computation of quasinormal modes of other spacetimes. This project is still ongoing, and further research is needed to gain a complete understanding of the full non-perturbative picture. The last chapter of this thesis is an outlook on ongoing and future work, including how the work presented in this thesis could be used to solve other open physical and mathematical problems.

Chapter 1

Non-perturbative methods

Non-perturbative phenomena are ubiquitous in many areas of physics and mathematics. They arise whenever perturbative expansions (i.e. power series expansions) do not give an accurate mathematical description of a given observable. A function $f(x)$ is called non-perturbative at a point $x = x_0$ if it cannot be described using a perturbative expansion around x_0. An example of such a function is

$$f(x) = \mathrm{e}^{-1/x}\,, \tag{1.1}$$

which cannot be approximated by a power series expansion around $x_0 = 0$. In many cases, a power series which formally solves a given equation (e.g. an ordinary differential equation (ODE), a partial differential equation (PDE), a finite difference equation) can be found, but the naive sum of all terms does not yield a finite result.

In the following non-perturbative phenomena will be introduced using the example of instantons in quantum mechanics (see e.g. [13], [14]). In this thesis instantons per se do not occur in any of the three research projects. Nonetheless, the mathematical foundations behind non-perturbative effects arising from factorially divergent expansions will be the same throughout all the chapters of this thesis, and instantons provide an intuitive physical interpretation for the factorial divergence. The notion of an instanton provides an interpretation for quantum tunneling, an effect responsible for certain observable phenomena such as radioactive decay [15, 16] and certain chemical reactions [17], among other things.

An important tool in the description of non-perturbative phenomena is the transseries expansion (see e.g. [18]), a series expansion of a function $f(x)$ which consists of terms not necessarily proportional to x^n, but for which more complicated expressions such as $e^{1/x}$ or $x^2 \log(x)$ are also permitted as 'basis functions'. Such transseries expansions can be used to account for non-perturbative corrections to asymptotic power series expansions.

It will be seen that the asymptotic perturbative expansion of a function, when it is divergent, can nonetheless contain all the information that is needed to construct the full function. This phenomenon is called resurgence [12]: the non-perturbative contributions to the function appear in the large-order behaviour of the coefficients of the original perturbative series. In fact, there is a multitude of mathematical relationships between the different sectors of the transseries, which will be explored in this chapter.

1.1 An example of a non-perturbative effect: Instantons

In this section certain parts of the treatment of instantons in [19] will be closely followed. Instantons are terms appearing in quantum mechanical computations which are non-perturbative in a small parameter called $\hbar$. In quantum physics, $\hbar$ is called the Planck constant and is a fixed constant of nature. However, in semiclassical calculations, $\hbar$ is treated as a small variable in which observables are expanded. The limit $\hbar \to 0$ represents the classical limit, and all the corrections in perturbation theory are quantum mechanical. The phenomenon of quantum tunneling is purely quantum mechanical, i.e. it does not appear in the classical limit, and is non-perturbative in $\hbar$. The transmission amplitude for particle scattering at a potential barrier is of the form

$$T \sim e^{-S_0/\hbar}, \tag{1.2}$$

where S_0 depends on the shape of the potential barrier.

More formally, Instantons are defined as localised solutions to the equations of motion in so-called Euclidean spacetime which have finite but non-zero action. They often appear in quantum field theory, a relativistic framework in which probability amplitudes can be calculated using a so-called path integral [20]. Path integrals can also be used to

calculate amplitudes in non-relativistic quantum mechanics. Consider a particle in two-dimensional spacetime which starts at the position q_i at time $t_i = -T/2$ and ends at the position q_f at $t_f = +T/2$. The probability amplitude for this process to happen is given by the path integral

$$\mathcal{A}_{i\to f} \;=\; \langle q_i |\, \mathrm{e}^{-\mathrm{i}T\,H/\hbar}\, |q_f\rangle \;=\; N \int \mathcal{D}q\, \mathrm{e}^{\mathrm{i}A[q]/\hbar}\,, \tag{1.3}$$

where the action of the particle is given by

$$A[q] \;=\; \int_{-T/2}^{T/2} \mathrm{d}t \left(\frac{1}{2} \left(\frac{\mathrm{d}q}{\mathrm{d}t} \right)^2 \;-\; V(q) \right)\,, \tag{1.4}$$

where $V(q)$ is the potential energy. The idea behind the path integral (1.3) is that all paths satisfying the boundary conditions contribute to the probabilty amplitude of a process. For a detailed introduction to path integrals see [20]. Each path must be weighted with the factor

$$\mathrm{e}^{\mathrm{i}A[q]/\hbar}\,, \tag{1.5}$$

and the 'sum over all paths' is performed via the path integral (see e.g. [20]). To perform calculations with the path integral it is often more practical to perform a so-called Wick rotation

$$t \to -\mathrm{i}t\,. \tag{1.6}$$

In Wick rotating, the spacetime geometry changes from Minkowski to Euclidean. The new time coordinate after the transformation is referred to as Euclidean time. The exponential (1.5) becomes

$$\mathrm{e}^{-S[q]/\hbar}\,, \tag{1.7}$$

where the Euclidean action $S[q]$ is

$$S[q] \;=\; \int_{-T/2}^{T/2} \mathrm{d}t \left(\frac{1}{2} \left(\frac{\mathrm{d}q}{\mathrm{d}t} \right)^2 \;+\; V(q) \right)\,. \tag{1.8}$$

Now consider a quantum mechanical system with potential $V(q)$. In Euclidean spacetime, the probability amplitude is

$$\mathcal{A}_{i\to f} \;=\; \langle q_i |\, \mathrm{e}^{-T\,H/\hbar}\, |q_f\rangle \;=\; N \int \mathcal{D}q\, \mathrm{e}^{-S[q]/\hbar}\,. \tag{1.9}$$

where the integral is over all paths satisfying the boundary conditions $q(t_i = -T/2) = q_i$, $q(t_f = T/2) = q_f$. The classical paths $q_c(t)$ which leave the Euclidean action stationary are solutions to the Euler-Lagrange equation for a potential $-V(q)$. Wick rotating to Euclidean time thus has the same effect on the stationary paths $q_c(t)$ as inverting the potential $V \to -V$ (the kinetic terms do not change their sign as each time, the derivative picks up a complex factor of i). The quantity of interest is the non-perturbative contribution to the energy of the ground state. By expressing the left-hand side of Eq. (1.9) in a linear combination of a complete set of energy eigenstates $|n\rangle$ for $n \in \mathbb{N}_0$, one finds that in the limit $T \to \infty$ the leading order behaviour is proportional to $\mathrm{e}^{-TE_0/\hbar}$, where E_0 is the energy of the ground state $|n = 0\rangle$. This means that one can compute E_0 to leading order by determining the asymptotic behaviour of the Euclidean path integral. One performs a functional coordinate transformation around the classical background q_c,

$$q(t) = q_c(t) + \sqrt{\hbar}\chi(t), \text{ where } \chi(t_i) = \chi(t_f) = 0\,. \tag{1.10}$$

Now the action ((1.8)) is expanded in powers of $\sqrt{\hbar}$:

$$S[q] \;=\; S[q_c] \;+\; \frac{\hbar}{2}\int \mathrm{d}t_1 \int \mathrm{d}t_2\, \frac{\delta^2 S}{\delta q(t_1)\delta q(t_2)}\,\chi(t_1)\,\chi(t_2) \;+\mathcal{O}(\hbar^{3/2})\,, \tag{1.11}$$

where the terms of order $\mathcal{O}\left(\sqrt{\hbar}\right)$ vanish due to the principle of stationary action, $\delta S[q_c]/\delta q(t) = 0$. The second term can be brought into the form

$$\frac{\hbar}{2}\int \mathrm{d}t\,\chi(t)\left(-\frac{\mathrm{d}^2}{\mathrm{d}t^2} \;+\; V''(q_c(t))\right)\chi(t) \;+\; \mathcal{O}(\hbar^{3/2})\,. \tag{1.12}$$

In the large-T limit and to leading order in $\hbar$ (around the non-perturbative background $\mathrm{e}^{-S_c/\hbar}$), one obtains a Gaussian integral with an infinite dimensional quadratic form in the exponent. For the amplitude (1.9) one finds the following expression:

$$\mathcal{A}_{i\to f} \;=\; \tilde{N}\mathrm{e}^{-S_c/\hbar}\det\left(-\frac{\mathrm{d}^2}{\mathrm{d}t^2} \;+\; V''(q_c(t))\right)^{-1/2}\big(1 \;+\; \mathcal{O}(\hbar)\big)\,, \tag{1.13}$$

where $\tilde{N} \propto N$ is a constant. In the following the special cases of a single-well and a double-well potential will be considered.

1.1.1 Single-well potential

Consider a potential well of the form

$$V(q) = \frac{\omega^2}{2} q^2 + \mathcal{O}(q^3)\,, \tag{1.14}$$

The goal is to compute the energy of the ground state. To calculate the determinant in Eq. (1.13), one uses the following theorem proven in [19]:

Theorem 1.1. *[19] Let $\psi_\lambda^W(t)$ be a solution to the following boundary value problem*

$$\begin{aligned} \left(-\frac{\mathrm{d}^2}{\mathrm{d}t^2} + W\right)\psi(t) &= \lambda\psi(t)\,; \\ \psi(-T/2) &= 0\,; \\ \partial_t\psi(t) &= 1\,. \end{aligned} \tag{1.15}$$

Then the ratio

$$\frac{\det\left(-\frac{\mathrm{d}^2}{\mathrm{d}t^2} + W\right)}{\psi_\lambda^W(-T/2)} \tag{1.16}$$

is independent both of λ and W.

For the harmonic oscillator, $W = \omega^2$ and $\lambda = 0$. A solution is given by

$$\psi_0^{\omega^2}(t) \;=\; \omega^{-1}\sinh\left(\omega(t + T/2)\right)\,. \tag{1.17}$$

Having (1.17), one can use (1.16) to find the value of the determinant in (1.13) up to a constant factor. The solution with the correct normalisation is given by [19]

$$N\,\det\left(-\frac{\mathrm{d}^2}{\mathrm{d}t^2} + \omega^2\right)^{-1/2} \;\sim\; \left(\frac{\omega}{\pi\hbar}\right)^{1/2} \mathrm{e}^{-T\omega/2}\,, \quad T \to \infty\,. \tag{1.18}$$

For $q_i = q_f = 0$ one also has

$$\mathcal{A}_{i\to f} \;=\; \mathrm{e}^{-TE_0/\hbar}\,|\langle q = 0|n = 0\rangle|^2 + \ldots\,, \tag{1.19}$$

where $\langle q = 0|n = 0\rangle$ denotes the scalar product of spatial basis state $|q = 0\rangle$ and the ground state $|n = 0\rangle$. The only function which leaves the action stationary and obeys

$q_i = q_f = 0$ is $q_c(t) = 0$. It follows that $S_c = 0$. Using Eq. (1.18) and Eq. (1.19), one finds

$$E_0 \;=\; \hbar\omega/2\,(1+\mathcal{O}(\hbar))\;. \tag{1.20}$$

Here, the only stationary point of the path integral one had to consider was the trivial solution $q_c(t) = 0$. In general, however, there will be non-trivial instanton contributions.

1.1.2 Double-well potential

Consider now the more interesting case of a double-well potential

$$V(q) \;=\; \frac{V_0}{a^4}(q^2-a^2)^2 \tag{1.21}$$

which is symmetric around the origin and has zeros $V(\pm a) = 0$. The starting point q_i and the endpoint q_f of the path are taken to be $q_f = q_i = \pm a$ and $q_f = -q_i = \pm a$. The objective is to calculate the following probability amplitudes:

$$\begin{aligned}\langle -a|\,\mathrm{e}^{-HT/\hbar}\,|-a\rangle \;&=\; \langle a|\,\mathrm{e}^{-HT/\hbar}\,|a\rangle\;;\\ \langle a|\,\mathrm{e}^{-HT/\hbar}\,|-a\rangle \;&=\; \langle -a|\,\mathrm{e}^{-HT/\hbar}\,|a\rangle\;.\end{aligned} \tag{1.22}$$

Analogous to the case of the single potential well, for $q_i = q_f = \pm a$ a solution is given by $q_c(t) = \pm a$. However, non-trivial solutions need to be taken into account as well. One will see that the solutions for both cases $q_f = \pm q_i$ can be constructed from the trivial solution and the one with $q_f = -q_i$. Consider a particle that starts off at $q_i = -a$ at $t_i = -\infty$, passes by the origin at $t = t_0$ and ends up at $q_f = a$ at $t_f = \infty$. The energy conservation equation in Euclidean time is

$$E = \frac{\dot{q_c}^2}{2} - V(q_c)\,. \tag{1.23}$$

If the particle is at rest at $q_i = -a$, the energy is $E = 0$. Moreover, the trajectory $q_c(t)$ obeys $|a| > |q_c(t)|$ and also $\dot{q}_c(t) > 0$. Hence

$$\begin{aligned} \dot{q_c}(t) &= \sqrt{2V(q_c(t))}\,; \\ t - t_0 &= \int \mathrm{d}q\, \frac{1}{\sqrt{2V(q)}}\,; \\ q_c(t) &= a \tanh\left(\frac{\sqrt{2V_0}}{a}(t - t_0)\right)\,. \end{aligned} \tag{1.24}$$

Note that $\omega \equiv \sqrt{2V_0}/a$ is the frequency of the harmonic oscillator approximation around $q = \pm a$. This solution is plotted in Fig. 1.1. Since $|q_c(t)| - a$ is exponentially small for large $|t|$, $q_c(t)$ is highly localised in the time domain, which justifies the term 'instanton'. Heuristically, the instanton can be thought of as having the size $1/\omega$, the interval in which $|q_c(t)| - a$ is not exponentially small. Using $E = 0$, the instanton action can be calculated from (1.8):

$$S_c = \int_{-a}^{a} \mathrm{d}q \sqrt{2V(q)} = \frac{16aV_0}{15}\,. \tag{1.25}$$

Since the Lagrangian has time-reversal symmetry, the path $q_c(-t)$ is also a solution to the equation of motion. It corresponds to a situation where the particle starts off at $q_i = a$ at $t = -\infty$ and travels to $q_f = -a$ at $t = +\infty$. Since the travel direction is reversed, this solution is denoted an anti-instanton.

Now consider adding an instanton $q_{c,t_1}(t)$ centred around $t = t_1$ to an anti-instanton $\bar{q}_{c,t_2}(t)$ centred around $t = t_2$ in the case where $|t_1 - t_2| \gg 1/\omega$. Since the instanton is exponentially suppressed in the region of the anti-instanton and vice-versa, the sum of the two is a good approximation to a stationary path given that the equations of motion are satisfied up to an exponentially small number. Therefore, one should also take into account sequences of instantons and anti-instantons with 'time centres' t_1, t_2 ... in the expansion of our path integral, where an instanton can only be followed by an anti-instanton and vice-versa. The instantons t_k are time ordered, that is

$$-T/2 < t_1 < t_2 \ldots < t_n < T/2\,. \tag{1.26}$$

The action of such a multi-instanton contribution is $n\,S_c$ up to exponentially small corrections. It can be shown [19] that the determinant-contribution in the amplitude (1.13) must be of the form

$$\left(\frac{\omega}{\pi\hbar}\right)^{1/2} \mathrm{e}^{-\omega T/2}\, K^n\,. \tag{1.27}$$

The first two factors are also present in the single potential well problem, and the factor K^n is the n-instanton contribution, where each instanton/anti-instanton accounts for one factor of K. Integrating over all possible instanton centres t_i gives an additional factor of $T^n/n!$, where the factorial in the denominator accounts for the fact that the t_i are chronologically ordered. In summary, a configuration with n instantons/anti-instantons results in the following contribution to the path integral

$$\left(\frac{\omega}{\pi\hbar}\right)^{1/2} \mathrm{e}^{-\omega T/2} \, \frac{\left(KT\mathrm{e}^{-S_c/\hbar}\right)^n}{n!} \,. \tag{1.28}$$

If one were to sum over all these contributions, the n-dependent part of the above expression would be given by the exponential $\exp\left(KT\mathrm{e}^{-S_c/\hbar}\right)$. However, the boundary conditions for the probability amplitudes Eq. (1.22) only allow for either an even or odd number of instantons and anti-instantons. For the leading order behaviour of the probability amplitudes one obtains

$$\langle \pm a | \, \mathrm{e}^{-HT/\hbar} \, |a\rangle \;\approx\; \left(\frac{\omega}{\pi\hbar}\right)^{1/2} \mathrm{e}^{-\omega T/2} \, \frac{1}{2} \left(\exp\left(KT\mathrm{e}^{-S_c/\hbar}\right) \pm \exp\left(-KT\mathrm{e}^{-S_c/\hbar}\right)\right) \,. \tag{1.29}$$

One can interpret the result in Eq. (1.29) as quantum tunneling. Note that without the instanton contributions, the amplitude $\langle -a | \, \mathrm{e}^{-HT/\hbar} \, |a\rangle$ would vanish and a particle that starts off at $q = -a$ could never overcome the potential barrier to reach $q = +a$. In terms of the energy eigenstates, the first term is associated with the ground state and the second term with the first excited state of the problem. Without the instanton contributions, the energies of these two states would be identical, and the double-well problem would have a degenerate ground state. By multiplying out Eq. (1.29) and adding up the exponents, the ground state/first-excited state energies E_0/E_1 are

$$\begin{aligned} E_0 &= \frac{\omega\hbar}{2} - K\hbar\mathrm{e}^{-S_c/\hbar} + \mathcal{O}(\hbar^2) \,; \\ E_1 &= \frac{\omega\hbar}{2} + K\hbar\mathrm{e}^{-S_c/\hbar} + \mathcal{O}(\hbar^2) \,. \end{aligned} \tag{1.30}$$

Strictly speaking, the term $K\hbar\mathrm{e}^{-S_c/\hbar}$ should not improve the approximation to E_0 since it vanishes more rapidly than the error, which is of order $\mathcal{O}(\hbar^2)$. However, the difference of the two energies is non-perturbative in nature, which is why the additional term is important. The example of the double well potential illustrates a) that perturbation theory is not enough to capture all aspects of our quantum mechanical world, and b)

that instantons are a useful way of describing such quantum mechanical effects.

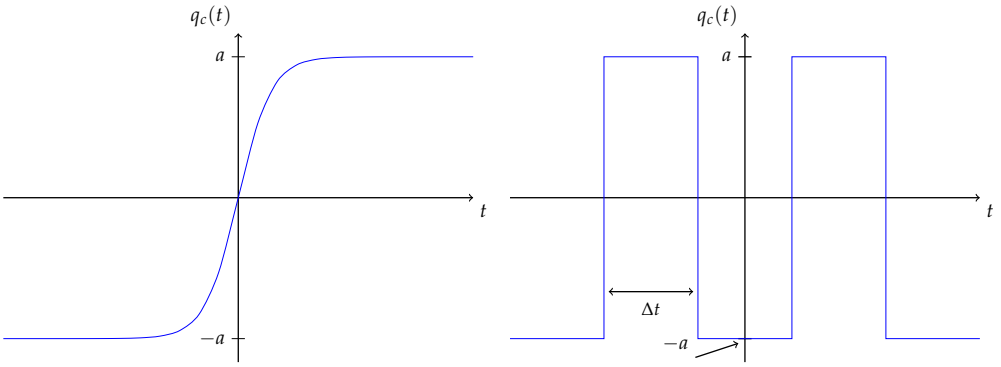

FIGURE 1.1: Left: Plot of the one-instanton solution $q_c(t)$ from Eq. (1.24) for $t_0 = 0$. Right: Approximate solution $q_c(t)$ of a sequence of instantons and anti-instantons in the limit $\sqrt{2V_0}/a \gg \Delta t$, where Δt is the time between an instanton and an anti-instanton (or vice-versa).

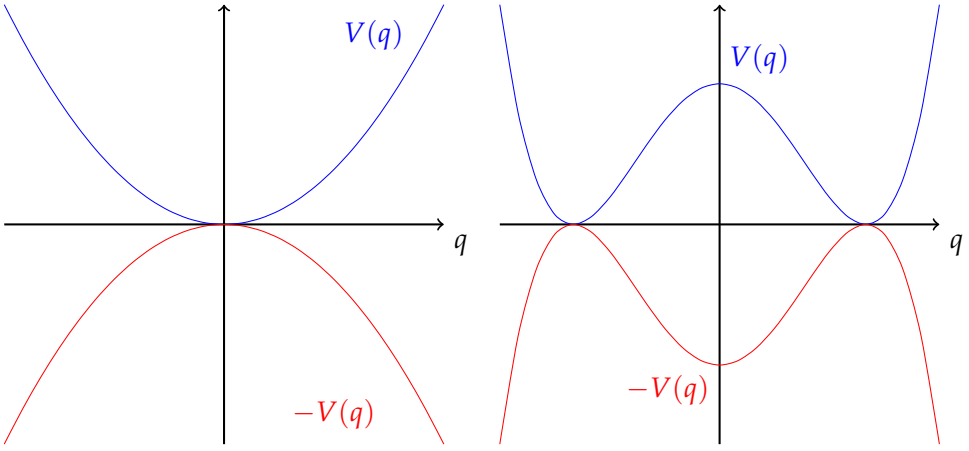

FIGURE 1.2: Left: quadratic potential. Right: quartic double-well potential. The red curves represent the inverted potentials $-V(q)$

1.2 Écalle's resurgence and Borel analysis

It has already been mentioned that the perturbative expansion of a function may contain information about its non-perturbative contributions. In some cases, the full function can be formally constructed as a transseries by including non-perturbative exponentials. The full exponential transseries can be grouped into different non-perturbative sectors, which are related in several ways. Each sector implicitly includes the data of every other sector, and the other different sectors 'resurge' in several mathematical relations. In this section some aspects of this phenomenon will be discussed. Moreover, specific examples

in which resurgence techniques can be used to solve ODEs will be introduced. For a detailed treatment of the theory of resurgent functions see [12].

1.2.1 Borel resummation

In many problems in mathematical physics, one finds that perturbation theory gives rise to series expansions which formally solve the problem locally, but are divergent for all non-vanishing values of the perturbative variable. One defines the notion of an asymptotic series to describe such formal solutions.

Definition 1.2. (Asymptotic series [21]) The power series

$$g(x) \;=\; \sum_{n=0}^{+\infty} a_n (x - x_0)^n \tag{1.31}$$

is said to be asymptotic to the function $f(x)$ at x_0 along the direction $\mathbf{v}$, if for all $N \in \mathbb{N}$

$$\lim_{\substack{x \to x_0 \\ \mathbf{v}}} \frac{f(x) \;-\; \sum_{n=0}^{N} a_n (x - x_0)^n}{(x - x_0)^N} \;=\; 0\,. \tag{1.32}$$

One then writes $f \sim g$ as $x \underset{\mathbf{v}}{\to} x_0$.

In the rest of this chapter $x \to \infty$ will be assumed unless explicitly specified otherwise, and hence $(x - x_0)$ must be replaced by $1/x$ as the variable of expansion. Note that the above definition does not required the series $g(x)$ to be convergent. In the case where the divergence is due to coefficients which grow at most factorially, i.e. $\mathcal{O}(n!)$, one can use the method of Borel resummation to obtain numerical values for the function. Consider the example of the inhomogeneous differential equation [11]

$$y'(x) - y(x) \;=\; -\frac{1}{x}\,. \tag{1.33}$$

A formal perturbative solution to this equation is given by the asymptotic expansion as $x \to \infty$,

$$\tilde{y}(x) \;\equiv\; \sum_{n=0}^{+\infty} (-1)^n \frac{n!}{x^{n+1}}\,, \tag{1.34}$$

which is divergent for finite x. The following identity is important

$$x^{-(n+1)} \;=\; \mathcal{L}\left[\frac{\xi^n}{n!}\right](x) \;=\; \int_0^{+\infty} \mathrm{d}\xi\, \mathrm{e}^{-\xi x}\, \frac{\xi^n}{n!}\,, \quad n \geq 0\,, \tag{1.35}$$

where $\mathcal{L}$ denotes the Laplace transform. One now defines the Borel transform to act on the monomials $(1/x)^{n+1}$ in the same way as an inverse Laplace transform (see Eq. (1.35))

$$\mathcal{B}\left[x^{-(n+1)}\right] \equiv \mathcal{L}^{-1}\left[x^{-(n+1)}\right] = \frac{\xi^n}{n!}\,. \tag{1.36}$$

If one takes the Borel transform of the monomial terms in the expansion $\tilde{y}(x)$ and adds them up one obtains

$$\mathcal{B}[\tilde{y}](\xi) \equiv \sum_{n=0}^{+\infty}(-\xi)^n, \quad \text{in some neighbourhood of } \xi = 0\,. \tag{1.37}$$

For $|\xi| < 1$ this power series is convergent and equals

$$\frac{1}{1+\xi}\,, \tag{1.38}$$

which is analytic on the punctured complex plane $\mathbb{C} \setminus \{-1\}$. One can then define the Borel transform $\mathcal{B}[\tilde{y}](\xi)$ on the domain $\mathbb{C} \setminus \{-1\}$ by setting it equal to (1.38).

$$\mathcal{B}[\tilde{y}](\xi) \equiv \frac{1}{1+\xi} \quad \text{for } \xi \in \mathbb{C} \setminus \{-1\}\,. \tag{1.39}$$

Eq. (1.35) suggests that one take the Laplace transform Eq. (1.39) to return to the x-plane. Indeed, one obtains an integral solution to Eq. (1.33),

$$y_{\text{sol}}(x) \equiv \int_0^{+\infty} \mathrm{d}\xi\, \mathrm{e}^{-\xi x}\, \frac{1}{1+\xi}\,, \quad \text{for } \mathbb{R}e(x) > 0\,. \tag{1.40}$$

To obtain solutions for a larger domain than merely the half-plane $\mathbb{R}e(x) > 0$, one defines the Borel resummation along the angle φ:

Definition 1.3. (Borel resummation [22]) Let Φ be the following power series expansion as $x \to \infty$ with a vanishing zeroth order term

$$\Phi(x) \equiv \sum_{n=0}^{+\infty} \Phi_n x^{-n-1}\,, \tag{1.41}$$

where the coefficients Φ_n are complex numbers. If the series F defined by

$$F(\xi) \equiv \sum_{n=0}^{+\infty} \frac{\Phi_n}{n!}\,\xi^n \tag{1.42}$$

has a finite radius of convergence, the Borel transform $\mathcal{B}[\Phi](\xi)$ is defined as the analytic continuation of F to the largest possible domain. The Borel resummation along the direction $\exp(\mathrm{i}\varphi)$ is defined as

$$\mathcal{S}_\varphi \Phi(x) \;=\; \int_0^{\exp(\mathrm{i}\varphi)\infty} \mathrm{d}\xi\, \mathcal{B}[\Phi](\xi) \mathrm{e}^{-\xi x}, \quad \text{for } \arg(x) \in (-\varphi - \pi/2, -\varphi + \pi/2)\,, \tag{1.43}$$

where the path of integration is a straight line between 0 and $\exp(\mathrm{i}\varphi)\infty$. Note that in the case where the Borel transform $\mathcal{B}[\Phi](\xi)$ has singularities along the angle φ a convention must be specified on how to avoid them.

Due to the exponential decay of the integrand (and therefore a vanishing contribution from an imagined arc closing the path at ∞), it follows from Cauchy's theorem that the Borel resummation is the same for two angles φ_1 and φ_2 provided that the sector which is spanned by those angles contains no singularities. However, the domains for the two resummations are different, and so changing the angle φ provides a way of analytically continuing the Borel resummation to regions other than the right half-plane. In the example Eq. (1.40), this can be done both clockwise and counter clockwise until reaching the angles $\pi \pm \varepsilon$ for small ε, afterwhich one encounters a singularity. Using Cauchy's theorem one obtains

$$(\mathcal{S}_{\pi+\varepsilon} - \mathcal{S}_{\pi-\varepsilon})\, y(x) \;=\; -2\pi\mathrm{i} \exp(x)\,. \tag{1.44}$$

The appearance of the exponential upon crossing a line containing a singularity is a consequence of jumping between two different sheets on a Riemann surface. Any direction along which the Borel transform has singularities is referred to as a Stokes line. The analytic continuation of $\mathcal{S}_0 y(x)$ to the whole Riemann surface $\mathcal{S}y(x)$ can also be interpreted as a multi-valued function on the complex plane. This multi-valuedness is a natural consequence of the singularities in the Borel plane. Whenever one crosses a Stokes line, one or more new exponential contributions are turned on. The most general multi-valued solution to Eq. (1.33) on the complex plane is

$$y(x) \;=\; \mathcal{S}_{-\arg(x)+\varepsilon}\, y(x) \;+\; (c - 2\pi\mathrm{i}\, k) \exp(x) \quad \text{where } \arg(x) \in (-\pi, \pi] \text{ and } k \in \mathbb{Z}\,, \tag{1.45}$$

and c is an integration constant. The summation in Eq. (1.45) is performed along the direction $\exp(-\arg(x))$ because in that way the argument of the exponential function

inside the integral is $-\xi\, x = -|\xi|\,|x|$ and the integral converges. Note that as a consequence the half plane on which a resummation is well-defined rotates in the opposite sense of the direction of resummation. The constant c in 1.45 is an integration constant and one can think of k as the index labelling the sheet of the Riemann surface. One can ask which class of functions is amenable for a treatment with the Borel resummation procedure. Consider the series

$$a(\xi) \;=\; \sum_{n=0}^{+\infty} a_j \xi^j \,. \tag{1.46}$$

If there exists $K,\ A \geq 0$ such that

$$\left|a_j\right| \;\leq\; \frac{K}{A^j}\,, \tag{1.47}$$

one obtains the upper bound

$$\left|a(\xi)\right| \;\leq\; K \sum_{n=0}^{+\infty} \left|\frac{\xi}{A}\right|^n , \tag{1.48}$$

which is convergent for $\xi < A$ and so A is a lower bound for the radius of convergence of $a(\xi)$. By setting $a(\xi) = \tilde{\Phi}(\xi)$ for the Borel transform from Eq. (1.42) one arrives at the condition

$$\left|\Phi_n\right| \;\leq\; K\,\frac{n!}{A^n}, \quad \text{for some } K,\ A > 0\,. \tag{1.49}$$

If this condition holds, then the Borel transform of the series $\Phi(x)$ from Eq. (1.41) is guaranteed to converge in some neighbourhood of the origin. It is useful to introduce the following definitions:

Definition 1.4. (1-Gevrey formal series [22]) The expansion $\varphi(x) = \sum_{n=0}^{+\infty} \varphi_n\, x^n$ is called a 1-Gevrey formal series if there exist $K,\ A > 0$ such that $\left|\varphi_n\right| \leq K n!/A^n$ for all $n \in \mathbb{N}_0$. In that case one writes $\varphi \in \mathbb{C}[[z^{-1}]]_1$

Definition 1.5. (Small power series, minor [11]) Let $\varphi(x) = \sum_{n=0}^{+\infty} \varphi_n\, x^n$. One defines

$$\breve{\varphi}(x) \;\equiv\; \varphi(x) - \varphi_0\,. \tag{1.50}$$

The power series φ is said to be a small power series if $\varphi = \breve{\varphi}$, i.e. $\varphi_0 = 0$. The Borel transform of $\breve{\varphi}$, $\mathcal{B}[\breve{\varphi}]$, is called the minor of φ.

1.2.2 Simple resurgent functions and Stokes automorphism

Écalle's theory of resurgence deals with the class of simple resurgent functions:

Definition 1.6. (Simple resurgent function [11]) Let $\Phi \in \mathbb{C}[[x^{-1}]]_1$. The minor of Φ, $\mathcal{B}[\breve{\Phi}](\xi)$, is said to have a simple singularity at $\xi = \omega$ if

$$\mathcal{B}[\breve{\Phi}](\xi)\Big|_{\xi\sim\omega} = \frac{a_\omega}{2\pi\mathrm{i}(\xi-\omega)} + \frac{g_\omega(\xi-\omega)}{2\pi\mathrm{i}}\log(\xi-\omega) + h_\omega(\xi-\omega)\,, \tag{1.51}$$

where a_ω is a constant, and g_ω and h_ω are holomorphic functions in some neighbourhood of the origin. If all the singularities of $\mathcal{B}[\breve{\Phi}](\xi)$ are simple, then Φ is denoted a simple resurgent function and one writes $\Phi \in^+ \mathcal{R}(1)$.

The interesting thing about simple resurgent functions is their behaviour when a line in the Borel resummation integral is crossed. This is called a Stokes line and comes with a discontinuity in the resummation. Assume that the only singularity of $\mathcal{B}[\breve{\Phi}](\xi)$ occurs at $\xi = \omega$. If the function g_ω is written as the Borel transform of a small formal power series

$$\breve{\Psi} \in x^{-1}\mathbb{C}[[x^{-1}]]\,, \tag{1.52}$$

where Ψ has the zeroth order term $\Psi_0 = a_\omega$, i.e. $g_\omega = \mathcal{B}[\breve{\Psi}]$, and define $\theta \equiv \arg(\omega)$, the resummation discontinuity can be written as

$$\begin{aligned}
\left(\mathcal{S}_\theta^+ - \mathcal{S}_\theta^-\right)\breve{\Phi}(x) &= -\left(a_\omega + \mathcal{S}_\theta\breve{\Psi}(x)\right)\exp(-\omega\,x)\,;\\
\left(\mathcal{S}_\theta^+ - \mathcal{S}_\theta^-\right)\Phi(x) &= -\left(\Psi_0 + \mathcal{S}_\theta\breve{\Psi}(x)\right)\exp(-\omega\,x)\,;\\
&= -\,\mathcal{S}_\theta\left(\Psi(x)\,\exp(-\omega\,x)\right)\,.
\end{aligned} \tag{1.53}$$

where it is assumed that $\mathcal{B}[\breve{\Psi}](\xi)$ has no singularities in the direction θ the so-called lateral resummations

$$\mathcal{S}_\theta^\pm \equiv \mathcal{S}_{\theta\pm\varepsilon}, \quad \text{for some small } \varepsilon. \tag{1.54}$$

have been introduced. The corresponding integration paths in the Borel plane are visualised in Fig.

It should be noted that the resummation operator $\mathcal{S}$ leaves the non-perturbative exponentials untouched and acts trivially on the zeroth-order terms. The proof of Eq. (1.53) is straightforward and involves the application of Cauchy's theorem as well an appropriate

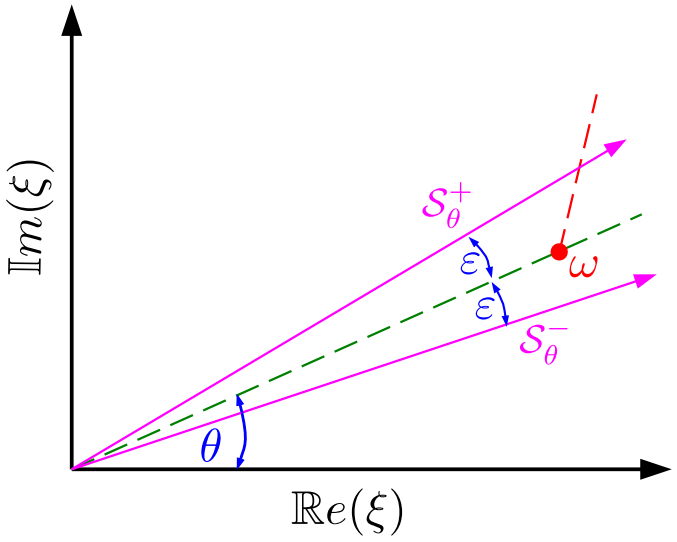

FIGURE 1.3: Purple: the integration paths of the resummations $\mathcal{S}_\theta^+$ and $\mathcal{S}_\theta^-$ in the Borel plane of $\breve{\Phi}$. Red: the branch point singularity at $\xi = \omega$ together with the branch cut. The difference between the two resummation integral is non-perturbative in x and associated with Ψ, The location of the singularity ω becomes the exponential weight of the non-perturbative sector through the exponential factor within the Laplace integral.

choice of the integration contour for the logarithmically singular term [1]. Eq. (1.53) can be interpreted as follows. Consider the analytic continuation of $\mathcal{S}_0\Phi(x)$, $\mathcal{S}\Phi(x)$. The presence of singularities in the Borel plane causes the domain of $\mathcal{S}\Phi$ to be a Riemann surface with several sheets. On the simply connected set

$$U \equiv \mathbb{C} \setminus \{\lambda \exp(-\mathrm{i}\theta) | \lambda \in \mathbb{R}\} \tag{1.55}$$

one can write $\mathcal{S}\Phi(x) = \mathcal{S}_{-\arg(x)}\Phi(x)$ for $x \in U$. To analytically continue across the Stokes line while moving in the clockwise sense in the x-plane (and thus in anti-clockwise sense in the Borel plane), one can use the resummation $\mathcal{S}_{\theta-\varepsilon}\Phi(x)$. However, this only works up to the point where $\arg(x) = -(\theta + \pi/2 - \varepsilon)$ since the resummation integral needs to converge. To go further, one can use Eq. (1.53) to express $\mathcal{S}_\theta^-\Phi(x)$ as a function of $\mathcal{S}_\theta^+\Phi(x)$. Hence Eq. (1.53) tells us that when a Stokes line is crossed, an exponentially decaying contribution is picked up,

$$\mathcal{S}_\theta^-\Phi(x) = \mathcal{S}_\theta^+\left(\Phi(x) + \Psi(x)\exp(-\omega x)\right). \tag{1.56}$$

It has been seen that a perturbative expansion can turn on non-perturbative sectors when a Stokes line is crossed due to the singularities in the Borel plane. To include all non-perturbative exponentials in the asymptotic description of a function, the one uses

an exponential transseries (see [18] for an introduction for more general transseries). In what follows, an (exponential) transseries with k parameters $\sigma_1, \ldots, \sigma_k$ will denote an expansion of the form

$$\mathcal{R}(x, \sigma_1, \ldots, \sigma_k) \;=\; \sum_{n_1=0}^{+\infty} \ldots \sum_{n_k=0}^{+\infty} \sigma_1^{n_1} \ldots \sigma_k^{n_k}\, \mathrm{e}^{-(n_1 A_1 + \cdots + n_k A_k)\, x}\, \Phi_{n_1,\ldots,n_k}(x)\,. \tag{1.57}$$

For each transseries parameter σ_j there is an exponential weight $A_j \in \mathbb{C}$ as well as a formal power series $\Phi_{n_1,\ldots,n_k}(x) \in \mathbb{C}[[x^{-1}]]_{\mathbf{1}}$. The terms of a given polynomial order in the σ_j belong to the same non-perturbative sector. In the case of linear differential equations, the set of solutions is a vector space and the transseries is just a linear combination, whereas in non-linear problems all the polynomial orders of the σ_j are needed in general to describe the solution. The purpose of the transseries parameters σ_j is to parametrise the space of solutions on the one hand, and on the other hand to encode information about the sheet of the Riemann surface and the behaviour on a Stokes line. In the example (1.33), a linear two-parameter transseries $\mathcal{F}$ was used to encode the fact that the domain is larger that the complex plane $\mathbb{C}$.

$$\mathcal{F}(x, \sigma_1, \sigma_2) \;=\; \sigma_1\, \Phi(x) \;+\; \sigma_2 \Psi(x) \exp(-\omega x)\,. \tag{1.58}$$

From Eq. (1.56) it follows that if one starts off with $\mathcal{S}_{-\arg(x)}\mathcal{F}(x, 1, 0)$ for some x with $-\arg(x) < \theta$ and cross the line at the angle θ moving to a point $\tilde{x}$ with $-\arg(\tilde{x}) > \theta$, the transseries parameters must be changed to obtain the correct analytic continuation at $\tilde{x}$, $\mathcal{S}\Phi(\tilde{x}) = \mathcal{S}_{-\arg(\tilde{x})}\mathcal{F}(\tilde{x}, 1, 1)$. Since after crossing the Stokes line the transseries also contains a Ψ-term, one needs to take into account the singularities of the Ψ-sector as well to analytically continue further. Typically, $\mathcal{B}[\breve{\Psi}]$ will have a simple singularity as defined in Def. (1.51) at $\xi = -\omega$, and therefore there will be another Stokes line at the angle $-\arg(x) = \theta + \pi$.

Examples of functions which can be described using a linear two-parameter transseries are the Airy function [1] and the partition function of a quartic potential [7], as both are solutions to a second order linear ODE. At each Stokes line the transseries parameters which correspond to the correct analytic continuation will change, $\sigma_i \mapsto \sigma_i + \Delta\sigma_i$. This shift is induced by the so-called Stokes automorphism $\underline{\mathfrak{S}}_\varphi$ defined as

$$\mathcal{S}_\varphi^+ \mathcal{F}(x, \sigma_1, \sigma_2) \;=\; \mathcal{S}_\varphi^- \circ \underline{\mathfrak{S}}_\varphi\, \mathcal{F}(x, \sigma_1, \sigma_2)\,. \tag{1.59}$$

The Stokes automorphism acts trivially at all angles φ without a Stokes line. In terms of the discontinuity

$$\mathcal{S}_\varphi^- \circ \mathrm{Disc}_\varphi \mathcal{F} \equiv -\left(\mathcal{S}_\varphi^+ - \mathcal{S}_\varphi^-\right)\mathcal{F}\,, \tag{1.60}$$

the Stokes automorphism can be written as

$$\underline{\mathfrak{S}}_\varphi = \mathbf{1} - \mathrm{Disc}_\varphi\,. \tag{1.61}$$

By now two distinct aspects of resurgence have been encountered: a) the Borel transform of the perturbative series encodes information about the non-perturbative contributions in the form of its behaviour near the singularities in the Borel plane; b) if one starts off with the perturbative series alone at some $x = x_i \in \mathbb{C}$ and continuously varies x in the complex plane, the non-perturbative sectors emerge after crossing a Stokes line.

1.2.3 Alien derivatives and Bridge equations

The Stokes automorphism has already been defined in Eq. (1.59). In what follows a method will be given to calculate it. It relies on the formalism of Alien calculus developed by Ećalle [12] (see also e.g. [23], [24], [22]). The general idea is to write the Stokes automorphism as the exponential of a derivation operator $\underline{\Delta}_\varphi$ [11]

$$\underline{\mathfrak{S}}_\varphi = \exp\left(\underline{\Delta}_\varphi\right)\,. \tag{1.62}$$

The operator $\underline{\Delta}_\varphi$ acts on the algebra of simple resurgent functions ${}^+\mathcal{R}(1)$ and satisfies the Leibniz rule. Just as the translation operator $T_\varepsilon : x \mapsto x + \varepsilon$ induces a change in the variable x when acting on a function $f(x)$, the Stokes automorphism induces a change in the transseries parameters. Note that T_ε may also be written as the exponential of a derivative ∂_x

$$T_\varepsilon f(x) = \exp(\varepsilon\partial_x) f(x) = f(x+\varepsilon)\,, \tag{1.63}$$

and ∂_x plays a similar role in ordinary calculus as the derivation operator $\underline{\Delta}_\varphi$ in Alien calculus. The derivation operator can be split into a sum of so-called dotted alien derivatives

$$\dot{\Delta}_\omega \equiv \exp(-\omega x)\Delta_\omega. \tag{1.64}$$

The alien derivative vanishes unless the minor of the function it acts upon has a singularity at $\xi = \omega$. This can be illustrated using the example of the partition function $Z(u)$ of a quartic potential taken from [7], where $Z(u)$ is expanded around $u = 0$. Note that one could just as well define $u = 1/x$ and expand around $x \to \infty$ as was done in the previous section. $Z(u)$ satisfies the second-order differential equation

$$16u^2 Z''(u) + (32u - 24)Z'(u) + 3Z(u) = 0\,. \tag{1.65}$$

A general solution to the ODE can be found with the ansatz

$$Z(u) = \exp(-\omega/u)\Phi(u)\,, \tag{1.66}$$

where Φ is a power series. One finds that there are two solutions $\omega \in \{0, 3/2\}$. If

$$A \equiv 3/2\,, \tag{1.67}$$

the linear transseries for this problem is of the form

$$\mathcal{Z}(u, \sigma_0, \sigma_1) = \sigma_0 \Phi_0(u) + \sigma_1 \Phi_1(u) \exp(-A/u)\,, \tag{1.68}$$

where the $\Phi_i(u)$ are power series in u. The problem is linear and so the $\Phi_i(u)$ are only defined up to a multiplicative constant by Eq. (1.65). In [7] the ODE is derived from an integral representation which fixes $\Phi_i(0)$. It can be shown that the minor of Φ_0 has a logarithmic singularity at A, while Φ_1 has one at $-A$[7]. This is a typical pattern of simple resurgent functions. The relative positions of the exponential weights in the transseries 'resurge' as singularities in the Borel plane of the different power series (with the exception of the origin of the Borel plane, at which the power series is analytic). In our example, Eq. (1.68), the exponential weights are 0 and A, and the relative positions therefore A and $-A$. By considering the behaviour of the Borel transforms $\mathcal{B}\left[\widetilde{\Phi_0}\right](\xi)$ and $\mathcal{B}\left[\widetilde{\Phi_1}\right](\xi)$ near $\xi = A$ it can be shown that [7]

$$\begin{aligned}
\mathcal{B}[\check{\Phi}_0](\xi) &= (+2) \times \frac{\Phi_{1,0}}{2\pi\mathrm{i}(\xi - A)} + (+2) \times \mathcal{B}[\check{\Phi}_1](\xi - A)\, \frac{\log(\xi - A)}{2\pi\mathrm{i}} + \text{holomorphic}\,; \\
\mathcal{B}[\check{\Phi}_1](\xi) &= (-1) \times \frac{\Phi_{0,0}}{2\pi\mathrm{i}(\xi + A)} + (-1) \times \mathcal{B}[\check{\Phi}_0](\xi + A)\, \frac{\log(\xi + A)}{2\pi\mathrm{i}} + \text{holomorphic}.
\end{aligned} \tag{1.69}$$

The multiplicative constants $(+2)$ and (-1) are called (the sign-reversed) Stokes constants. They determine the how the alien derivatives act on the power series appearing in the transseries. By expanding out the Stokes automorphism (1.62) and comparing it to the discontinuity obtained by Borel resumming the expressions in (1.69) above and below the singularity one obtains [7]

$$\begin{aligned} \Delta_A \Phi_0 &= (-2)\Phi_1 \,; \\ \Delta_{-A} \Phi_1 &= (+1)\Phi_0 \,; \\ \Delta_A \Phi_1 &= 0 \\ \Delta_{-A} \Phi_0 &= 0 \,. \end{aligned} \tag{1.70}$$

Since there is only one singularity along each ray (at the angles 0 and π) one can write

$$\begin{aligned} \underline{\Delta}_{\arg(A)} &= \underline{\Delta}_0 \equiv \dot{\Delta}_A ; \\ \underline{\Delta}_{\arg(-A)} &= \underline{\Delta}_\pi \equiv \dot{\Delta}_{-A} \,. \end{aligned} \tag{1.71}$$

This is a very simple example. Due to the linearity of the ODE (1.65) the transseries is linear in the parameters σ_0, σ_1 and so the whole non-perturbative behaviour is fully described by only two power series Φ_0 and Φ_1. In this case, the Stokes automorphism $\underline{\mathfrak{S}}_\theta$ induces the change in the transseries parameters

$$\begin{aligned} \underline{\mathfrak{S}}_0 : \begin{pmatrix} \sigma_0 \\ \sigma_1 \end{pmatrix} &\mapsto \begin{pmatrix} \sigma_0 \\ -2\sigma_0 + \sigma_1 \end{pmatrix} ; \\ \underline{\mathfrak{S}}_\pi : \begin{pmatrix} \sigma_0 \\ \sigma_1 \end{pmatrix} &\mapsto \begin{pmatrix} \sigma_0 + \sigma_1 \\ \sigma_1 \end{pmatrix} , \end{aligned} \tag{1.72}$$

which can be shown by acting with the Stokes automorphism on the general solution (1.68). This can be done by using the Borel transforms (1.69) and to calculate the resummation discontinuity along the angles 0 and π and expressing the result as a linear combination of $\Phi_0(u)$ and $\mathrm{e}^{-A/u}\Phi_1(u)$. The derivation operator is equal to a single alien derivative at each Stokes line because there is only one singularity along each line. Since higher powers of the alien derivative vanish, the Stokes constants appear explicitly in (1.72). The knowledge of the Stokes automorphism at all the Stokes lines also allows one to deduce the monodromy. If one starts at $u \equiv r\exp(\mathrm{i}\varepsilon)$ for $r > 0$ and some small ε, and walks in circles around the origin of $\mathbb{C}$ in the clockwise sense, the direction

of resummation must be rotated clockwise as well so as to obtain convergence of the resummation integral. Whenever a Stokes line is crossed, the Stokes automorphism must be applied one the transseries. A full 2π-rotation corresponds to the operator

$$R \equiv \underline{\mathfrak{S}}_{\pi} \circ \underline{\mathfrak{S}}_{0} \,. \tag{1.73}$$

By representing $\underline{\mathfrak{S}}_{\pi}$ and $\underline{\mathfrak{S}}_{0}$ using the matrices (1.72) it is easy to show that $R^2 = -\mathbf{1}$ by performing the corresponding matrix multiplication. As a consequence, the operator R is a fourth root of the identity. Hence the solution to the ODE (1.65) has a Riemann surface with four sheets as its natural domain. Had one started with a non-linear problem, an ansatz proportional to $\exp(-A/u)$ would not work since the non-linear terms of the equation would generate terms with higher powers $\exp(-nA/u)$ (for $n > 1$). As described in [7], a non-linear model can be obtained by considering at the free energy $F = \log(Z)$ of the partition function Z from (1.69) The ODE one obtains is

$$16u^2F''(u) \,+\, 16u^2\left(F'(u)\right)^2 \,+\, (32u-24)\,F'(u) \,+\, 3 \,=\, 0\,. \tag{1.74}$$

This equation is non-linear. Moreover, notice that there is no $F(u)$ term, and so this is actually equivalent to a first order ODE for the function $F'(u)$. Therefore, there will only be one instead of the previous two transseries parameters. The 'lost' degree of freedom is given by the possibility to add an arbitrary constant to $F(u)$. An ansatz for $F(u)$ which accounts for higher powers of $\exp(-A/u)$ is

$$\mathcal{F}(u,\sigma) \,=\, \sum_{n=0}^{+\infty} \sigma^n \exp(-nA/u)\, u^{n\beta}\Psi_n(u) \,=\, \sum_{n=0}^{+\infty} \left(\sigma u^{\beta}\exp(-A/u)\right)^n \Psi_n(u)\,. \tag{1.75}$$

By substituting this ansatz into our ODE (1.74) and matching equal powers of σ one finds [7]

$$A \,\in\, \{0,\, 3/2\}\,; \qquad \beta \,=\, 0\,. \tag{1.76}$$

The trivial weight $A = 0$ describes the perturbative sector, and hence

$$A \equiv 3/2 \tag{1.77}$$

will be set. There is one important subtlety. Since the ODE is of second order in $F(u)$ (albeit only dependant on $F'(u)$), there are strictly speaking two transseries parameters.

Even though at the level of the transseries this second transseries parameter just corresponds to an additive constant, it does lead to corrections in the action of the alien derivatives. To simplify things, those corrections will not be taken into account here (see [7] for the more details). The interesting thing about the non-linear case is the different singularity structure of the minors $\mathcal{B}[\breve{\Psi}_n](\xi)$, which are located at the positions

$$\xi_{\text{sing},n} \in \{-nA, -(n-1)A, \dots, -A, A\}\,. \tag{1.78}$$

In this example, the minors of all the sectors $\Psi_n(z)$ only have purely logarithmic singularities

$$\mathcal{B}[\breve{\Psi}_n](\xi)\Big|_{\xi\sim kA} = \mathrm{S}_{k\to n+k} \times \mathcal{B}[\breve{\Psi}_{n+k}](\xi - kA)\frac{\log(\xi - ka)}{2\pi\mathrm{i}} + \text{holomorphic}\,. \tag{1.79}$$

In [7] it is shown that the alien derivatives Δ_{kA} act on the on the power series Ψ_n by shifting the index by k

$$\begin{aligned} \Delta_{kA}\Psi_n &= (n+k)\mathrm{S}_k\,\Psi_{n+k} && \text{for } k \leq 1 \text{ and } k \neq 0\,; \\ \Delta_{kA}\Psi_n &= 0 && \text{for } k > 1\,. \end{aligned} \tag{1.80}$$

where S_k are the Stokes constants. The calculation of the Stokes constants S_k is beyond the scope of this introduction and can be found in [7]. Note that although they are closely related, for non-linear problems the Borel residues $\mathrm{S}_{n\to n+k}$ are not merely equal to the Stokes constants S_k up to a minus sign as it was the case in the linear example above.

One can derive Eq. (1.80) using the so-called Bridge equations. It is useful to note that the dotted alien derivatives $\dot{\Delta}_\omega$ commute with the u-derivative ∂_u [1]

$$[\dot{\Delta}_\omega, \partial_u] = 0\,. \tag{1.81}$$

It is clear from the structure of the transseries (1.75) that the u-derivative also commutes with the σ-derivative

$$[\partial_\sigma, \partial_u] = 0\,. \tag{1.82}$$

If a first-order ODE of the unknown function $\mathcal{F}(u,\sigma)$ is acted upon with some derivation operator δ which commutes with ∂_u and which satisfies the chain rule, this results in a

homogeneous linear ODE of the function $\delta\mathcal{F}$. As a result both $\dot{\Delta}_\omega\mathcal{F}$ and $\partial_\sigma\mathcal{F}$ satisfy the same linear homogeneous first-order ODE in the variable u. The set of solutions of this linear ODE must form a one-dimensional vector space and thus any two solutions must be proportional. This statement is expressed through the so-called Bridge equations

$$\dot{\Delta}_\omega\mathcal{F}(u,\sigma) \;=\; \mathrm{S}_\omega(\sigma)\partial_\sigma\mathcal{F}(u,\sigma)\,, \tag{1.83}$$

where $\mathrm{S}_\omega(\sigma)$ is some function of σ and ω. The structure of Eq. (1.83) restricts the form of $\mathrm{S}_\omega(\sigma)$ in the following way. Consider the weight $w = m + n$ of a transseries term multiplied by $\sigma^n \mathrm{e}^{mA/u}$. Then

$$\partial_\sigma : \; w \mapsto w - 1\,; \qquad \dot{\Delta}_{kA}\,.w \mapsto w - k\,. \tag{1.84}$$

Since for all the terms in the transseries $\mathcal{F}$ $m = -n$ and therefore $w = 0$, it follows that for $\omega = kA$, the weight of the left-hand side of (1.83) is $-k$ and the weight of the right-hand side is -1. Hence the weight of S_{kA} must be equal to $1 - k$ to be consistent with the Bridge equation. One can therefore set

$$\mathrm{S}_{kA}(\sigma) \;\equiv\; \mathrm{S}_k\sigma^{1-k}\,. \tag{1.85}$$

Since both $\dot{\Delta}_\omega\mathcal{F}$ and $\partial_\sigma\mathcal{F}$ are regular functions of σ and generically do not vanish at $\sigma = 0$, $\mathrm{S}_\omega(\sigma)$, it follows that $S_k = 0$ for all $k > 1$. The bridge equations (1.83) then become

$$\dot{\Delta}_{kA}\mathcal{F}(u,\sigma) \;=\; \mathrm{S}_k\sigma^{1-k}\,\partial_\sigma\mathcal{F}(u,\sigma) \qquad \text{for } k \leq 1,\, k \neq 0\,. \tag{1.86}$$

By writing out the transseries $\mathcal{F}(u,\sigma)$ and matching equal powers of σ, one obtains the previous definition of the Stokes constants, Eq. (1.80). Eq. (1.86) implies that even in the non-linear case, the action of the Stokes takes the form of a transformation of the transseries parameter σ. One has [7]

$$\begin{aligned} \underline{\mathfrak{S}}_0\mathcal{F}(u,\sigma) \;&=\; \exp\big(\dot{\underline{\Delta}}_0\big)\mathcal{F}(u,\sigma) \;=\; \exp\big(\dot{\Delta}_A\big)\mathcal{F}(u,\sigma) \\ &=\; \exp(\mathrm{S}_1\partial_\sigma)\mathcal{F}(u,\sigma) \;=\; \mathcal{F}(u,\sigma+S_1)\,, \end{aligned} \tag{1.87}$$

and so at the angle $\theta = 0$, the transseries parameters transform according to $\underline{\mathfrak{S}}_0 : \sigma \mapsto \sigma + S_1$, which is a translation. At the line with $\theta = \pi$, the story is more complicated

since there is more than one non-vanishing Alien derivative.

$$\begin{aligned}\underline{\mathfrak{S}}_\pi \mathcal{F}(u,\sigma) &= \exp\left(\dot{\underline{\Delta}}_\pi\right)\mathcal{F}(u,\sigma) = \exp\left(\sum_{n=1}^{+\infty}\dot{\Delta}_{-nA}\right)\mathcal{F}(u,\sigma)\\ &= \exp\left(\sum_{n=1}^{+\infty}\mathrm{S}_{-n}\sigma^{n+1}\partial_\sigma\right)\mathcal{F}(u,\sigma)\\ &\equiv \exp\left(\underline{\mathrm{S}}_\pi(\sigma)\partial_\sigma\right)\mathcal{F}(u,\sigma) \equiv \mathcal{F}(u,\underline{\mathrm{S}}_\pi(\sigma))\,.\end{aligned} \tag{1.88}$$

In the last line $\underline{\mathrm{S}}_\pi(\sigma)\partial_\sigma$ is a vector field parametrised by σ and $\underline{\mathrm{S}}_\pi(\sigma)$ function of σ representing the parameter change induced by the Stokes automorphism. The function $\underline{\mathrm{S}}_\pi(\sigma)$ is given by the exponentiation of the vector field vector field $\underline{\mathrm{S}}_\pi(\sigma)\partial_\sigma$. Therefore $\underline{\mathrm{S}}_\pi(\sigma)$ is the image of the flow $\phi^t(\sigma)$ (t being the parameter parametrising the flow and the argument σ representing the starting point) of the vector field $\underline{\mathrm{S}}_\pi(\sigma)\partial_\sigma$ at $t=1$ (see e.g. [25, 26, 27]):

$$\begin{aligned}\partial_t\phi^t(\sigma) &= \underline{\mathrm{S}}_\pi(\phi^t(\sigma))\,;\\ \phi^0(\sigma) &\equiv \sigma\,;\\ \underline{\mathrm{S}}_\pi(\sigma) &= \phi^1(\sigma)\,.\end{aligned} \tag{1.89}$$

The question is now how to compute the Stokes constants. In the case of the partition function this was easy to do because the transseries was linear and only contained two power series. One way of computing the Stokes constants, which is discussed in detail in [7], is to take the logarithm of the transseries and compare this with the transseries $\mathcal{F}$. However, not every problem is that easy, and sometimes Stokes constants can only be obtained numerically using the so-called large-order relations.

1.2.4 The large-order relations

The large order relations describe how the coefficients of the different sectors Φ_k of some transseries behave in the limit $k \to \infty$. They rely on the fact that using Cauchy's integral formula, a function $G(u)$ with an asymptotic expansion around $u=0$ can be rewritten in terms of its discontinuities $\mathrm{Disc}_{\theta_j}G(u)$. For a transseries sector $\Phi_k(u)$, the discontinuities are sums containing the other sectors $\Phi_{l\neq k}$ of the transseries. For the sake of simplicity, consider the case where $G(u)$ only has one Stokes line at the angle θ, with Borel singularities at the locations A, $2A$, $3A\ldots$ in the Borel plane. If one takes

loop encircling u and deforms the integration contour in an appropriate manner (see [1])), Cauchy's integral formula becomes

$$G(u) \;=\; -\frac{1}{2\pi \mathrm{i}} \int_0^{\mathrm{e}^{\mathrm{i}\theta}\infty} \mathrm{d}w \, \frac{\mathrm{Disc}_\theta G(w)}{w-u} \,. \tag{1.90}$$

Now consider the partition function Z from (1.65) and its transseries $\mathcal{Z}(u)$ with the two sectors $\Phi_0(u)$ and $\Phi_1(u)$. If one sets $G(u) = \Phi_0(u)$, the angle of the only Stokes line is $\theta = 0$ and the integral (1.90) becomes

$$\sum_{n=0}^{+\infty} \Phi_{0,n} \, u^n \;=\; +\frac{1}{2\pi \mathrm{i}} \int_0^{+\infty} \mathrm{d}w \, \frac{\mathrm{S}_1}{w-u} \mathrm{e}^{-A/w} \sum_{k=0}^{+\infty} \Phi_{1,k} w^k \,. \tag{1.91}$$

If $u < w$, then

$$\frac{1}{w-u} \;=\; \frac{1}{w} \sum_{\ell=0}^{+\infty} \left(\frac{u}{w}\right)^\ell \,. \tag{1.92}$$

Since the w-integration starts at $w = 0$, there are always values of w for which $u > w$. Nonetheless, using Eq. (1.92) leads to a useful formula which is valid asymptotically. One obtains

$$\begin{aligned} \sum_{\ell=0}^{+\infty} u^\ell \Phi_{0,\ell} \;&=\; \frac{\mathrm{S}_1}{2\pi \mathrm{i}} \sum_{\ell=0}^{+\infty} \sum_{k=0}^{+\infty} u^\ell \Phi_{1,k} \left(\int_0^\infty \mathrm{d}w \, \mathrm{e}^{-A/w} \, w^{k-\ell-1} \right), \qquad k < l \\ &=\; \frac{\mathrm{S}_1}{2\pi \mathrm{i}} \sum_{\ell=0}^{+\infty} u^\ell \left(\sum_{k=0}^{+\infty} \frac{\Gamma(\ell-k)}{A^{\ell-k}} \Phi_{1,k} \right) . \end{aligned} \tag{1.93}$$

By matching equal powers of u^ℓ one obtains the large-order relations for $n \gg 1$ [1]

$$\begin{aligned} \Phi_{0,n} \;&\sim \frac{\mathrm{S}_1}{2\pi \mathrm{i}} \sum_{k=0}^{+\infty} \Phi_{1,k} \frac{\Gamma(n-k)}{A^{n-k}} \\ &\sim \frac{\mathrm{S}_1}{2\pi \mathrm{i}} \frac{\Gamma(n)}{A^n} \sum_{k=0}^{+\infty} \Phi_{1,k} \, A^k \left(\prod_{m=1}^{k} \frac{1}{n-m} \right) \\ &\sim \frac{\mathrm{S}_1}{2\pi \mathrm{i}} \frac{\Gamma(n)}{A^n} \left[\Phi_{1,0} + \Phi_{1,1} \frac{A}{n} + \frac{A}{n^2} \left(\Phi_{1,1} + A \Phi_{1,2} \right) + \dots \right] . \end{aligned} \tag{1.94}$$

In [7], the large-order relations are discussed for the free energy $F = \log Z$ of the partition function Z from (1.65). The basic idea is the same. However, in the non-linear problem there is an infinite number of transseries sectors which contribute to the large-order relations. In that case all but one transseries sector are exponentially supressed as $n \to \infty$. One can use (1.94) in order to compute the Stokes constants S_1 numerically if

the coefficients $\Phi_{0,n}$ and $\Phi_{1,0}$ are known. The sequence

$$a_n \equiv \frac{2\pi \mathrm{i}}{\Phi_{1,0}} \frac{A^n}{\Gamma(n)} \Phi_{0,n} \tag{1.95}$$

converges toward the Stokes constant $a_n \to \mathrm{S}_1$. However, the convergence is quite weak, since $a_n - \mathrm{S}_1 \in \mathcal{O}(n^{-1})$. In order to accelerate this convergence, one can use the so-called Richardson extrapolation method (see e.g. [28]). Take a (possibly asymptotic) series $S(n)$ of the form

$$S(n) = s_0 + \frac{s_1}{n} + \frac{s_2}{n^2} + \dots . \tag{1.96}$$

The Richardson transform $\mathrm{RT}_S(\ell, n, N)$ denotes the following sequence in n with the properties $\mathrm{RT}_S(\ell, n, N) - s_0 \in \mathcal{O}(n^{-(N+1)})$ and $\lim_{n\to\infty} \mathrm{RT}_S(\ell, n, N) = s_\ell$ [1, 21, 28]:

$$\begin{aligned} S_\ell(n) &= S(n) - \sum_{k=0}^{\ell-1} \frac{s_k}{n^k} ; \\ \mathrm{RT}_S(\ell, n, 0) &\equiv S_\ell(n) ; \\ \mathrm{RN}_S(\ell, n, N) &\equiv \mathrm{RT}_S(\ell, n+1, N-1) \\ &\quad + \frac{n}{N} \left(\mathrm{RT}_S(\ell, n+1, N-1) - \mathrm{RT}_S(\ell, n, N-1) \right) , \\ &\quad N \geq 1 . \end{aligned} \tag{1.97}$$

Increasing the parameter $N \to N+1$ results in the cancellation of another order in the large n expansion of $S_\ell(n)$.

1.2.5 The Borel-Padé approximation

Sometimes one is unable to find closed-form expressions for all the sectors in a transseries summation and one has to rely on numerical approximations [29, 30, 31]. It is very typical for divergent asymptotic series that the magnitude of the first few coefficients in the power series decrease very quickly. Given an asymptotic power series $\Phi(x)$ which is asymptotic to some function $F(x) \sim \Phi(x)$ as $x \to \infty$, one way of approximating $F(x)$ is to truncate the series $\Phi(x)$ just before the term with the smallest order of magnitude. The truncation condition is

$$\left| \frac{\Phi_n}{x^{n+1}} \right| \leq \left| \frac{\Phi_{n-1}}{x^n} \right| . \tag{1.98}$$

and therefore for the last term in the optimal truncation has the index $N_{\text{op}}(x)$ given by

$$N_{\text{op}}(x) \;=\; \max\left\{ n \in \mathbb{N} \,\middle|\, \frac{|\Phi_n|}{|\Phi_{n-1}|} \leq |x| \right\} . \tag{1.99}$$

The optimally truncated series F_{op} of F is then defined as (see e.g. [21])

$$F_{\text{op}}(x) \;\equiv\; \sum_{n=0}^{N_{\text{op}}(x)} \frac{\Phi_n}{x^{n+1}} \tag{1.100}$$

Another method is to Borel-resum the series $\Phi(x)$ approximately by first approximating the minor $\mathcal{B}[\breve{\Phi}](\xi)$. In practical applications one only calculates a finite number of terms of the series $\Phi(x)$. Therefore the minor $\mathcal{B}[\breve{\Phi}](\xi)$ is also only known to a finite order in some neighbourhood of the origin of the Borel plane, where the series converges. The minor $\mathcal{B}[\breve{\Phi}](\xi)$ can be approximated using so-called Borel-Padé approximants $\text{BP}_{n,m}[\breve{\Phi}](\xi)$ (see e.g. [7]). These are rational functions

$$\text{BP}_{n,m}[\breve{\Phi}](\xi) \;=\; \frac{P_m[\breve{\Phi}](\xi)}{Q_n[\breve{\Phi}](\xi)} , \tag{1.101}$$

where $P_m[\breve{\Phi}](\xi)$, $Q_n[\breve{\Phi}](\xi)$ are polynomials of order n and m and $\mathcal{B}[\breve{\Phi}](\xi)$ is the function which is approximated. The requirement which fixes $P_m[\breve{\Phi}](\xi)$ and $Q_n[\breve{\Phi}](\xi)$ is that the perturbative expansion of $\text{BP}_{n,m}[\breve{\Phi}](\xi)$ at the origin must agree with the perturbative expansion of $\mathcal{B}[\breve{\Phi}](\xi)$ to order $m+n$. Consider a symmetrical Padé approximant where $m = n$, which will be denoted by $\text{BP}_{2m}[\breve{\Phi}](\xi)$. One defines:

Definition 1.7. Borel-Padé resummation For $M \in 2\mathbb{N}$ and $\Phi \in \mathbb{C}[[x^{-1}]]$ the Borel-Padé resummation $\mathcal{S}_\varphi^{(M)}\Phi$ along the angle φ is defined as

$$\mathcal{S}_\varphi^{(M)}\Phi(x) \;=\; \int_0^{\mathrm{e}^{\mathrm{i}\varphi}\infty} \mathrm{d}\xi \mathrm{e}^{-x\xi}\, \text{BP}_M[\breve{\Phi}](\xi) \tag{1.102}$$

where $\text{BP}_M[\Phi](\xi)$ is the Borel-Padé approximant of order M. Note that because $\text{BP}_M[\breve{\Phi}](\xi)$ is an approximation and includes poles at locations where there are none in the Borel transform it approximates, it is necessary to avoid them carefully by slightly altering the integration path in any numerical implementation.

In practice, one should always check whether the Borel-Padé approximant is indeed a good approximation to a given function. In certain special cases, the convergence of the

Borel-Padé approximant can be shown rigorously if the denominator polynomial is fixed to be a Chebyshev polynomial and the all the information about the function is encoded in the numerator [32]. However, a Padé approximant which is generated by a fixed denominator polynomial like in [32] is not suitable for an analysis of the singularity structure, as all the information about the singularities is encoded in the denominator.

1.3 Further into resurgence and summation techniques

In the previous section it has been shown that the non-perturbative contributions in a transseries can be calculated using Borel resummation. In this section two further resummation techniques, transasymptotics and hyperasymptotics, will be introduced. Moreover, the WKB method will be used in the context of the Schrödinger equation.

1.3.1 Stokes phenomena from steepest-descent

In the case where the non-perturbative contributions are small, the first few terms of a transseries will already yield a good approximation. However, this is not always the case. For example, in the case of a one-parameter transseries, $-A\,x$ is pure imaginary at certain angles in the complex x-plane. Hence the exponential e^{-Ax} will be of order one, and higher orders of the exponential factor are no longer negligible. In that case, all the exponential orders in the transseries become important. This is called an anti-Stokes line. The condition for the presence of an anti-Stokes line is

$$\mathbb{R}\mathrm{e}(xA) = 0\,. \tag{1.103}$$

On the other hand, the condition for the presence of a Stokes line is

$$\mathbb{I}\mathrm{m}(xA) = 0\,. \tag{1.104}$$

At a Stokes line, the different exponential orders in the transseries differ maximally since the exponent $-x\,A$ is purely real. Upon crossing a Stokes line a Stokes phenomenon takes place, and the terms in the transseries are reshuffled by the Stokes automorphism. In some cases, Stokes and Anti-Stokes lines can be intuitively understood in terms of

the connectivity of saddle points in the integration paths of an integral representation. Assume the function of interest $F(x)$ admits a complex-line-integral representation

$$F(x) \;=\; \int_{\Gamma} \mathrm{d}z\, \mathrm{e}^{-x\phi(z)} g(z) \tag{1.105}$$

where $g(z)$ and $\phi(z)$ are holomorphic functions on the complex plane and Γ some path of integration with a given 'ingoing direction' θ_{in} and an 'outgoing direction' θ_{out} in the complex plane. The anti-Stokes and Stokes conditions (1.103) and (1.104) can be understood with the method of steepest descent-curves [21]. The idea is that the path of integration can be deformed in such a way that it a) passes through a saddle-point z_* of $\phi(z)$ and b) has a constant phase $\mathbb{I}\mathrm{m}(\phi(z))\big|_{z\in\Gamma} = \text{const}$. The points of Γ which lie in a small open ball around the saddle z_* will then dominate the line integral in the limit $x \to +\infty$.

At the level of the transseries, this phenomenon manifests in the presence of a non-perturbative exponential sector of the type

$$\mathrm{e}^{-A\,x} = \mathrm{e}^{-\phi(z_*)\,x} \tag{1.106}$$

At a Stokes line different saddles have the same phase, and the integration path passes through more than one saddle. Upon crossing the Stokes line the topology of the configuration changes, and the set of saddle points through which a given line of steepest descent Γ passes changes at a Stokes line. This change of topology is visualised in Fig. 1.4. Since each saddle corresponds to one exponential order in the transseries, the fact that the set of saddles of Γ changes means that new contributions are picked up at a Stokes line. This provides an explanation of why the Stokes automorphism induces a transformation in the transseries parameters. On the other hand, anti-Stokes lines are values of x at which two different saddles start to contribute at the same exponential order, which happens when the real parts the exponential weights of two different terms in the transseries are equal. A more detailed explanation of the saddle point interpretation of Stokes phenomena can be found in [33, 7, 1].

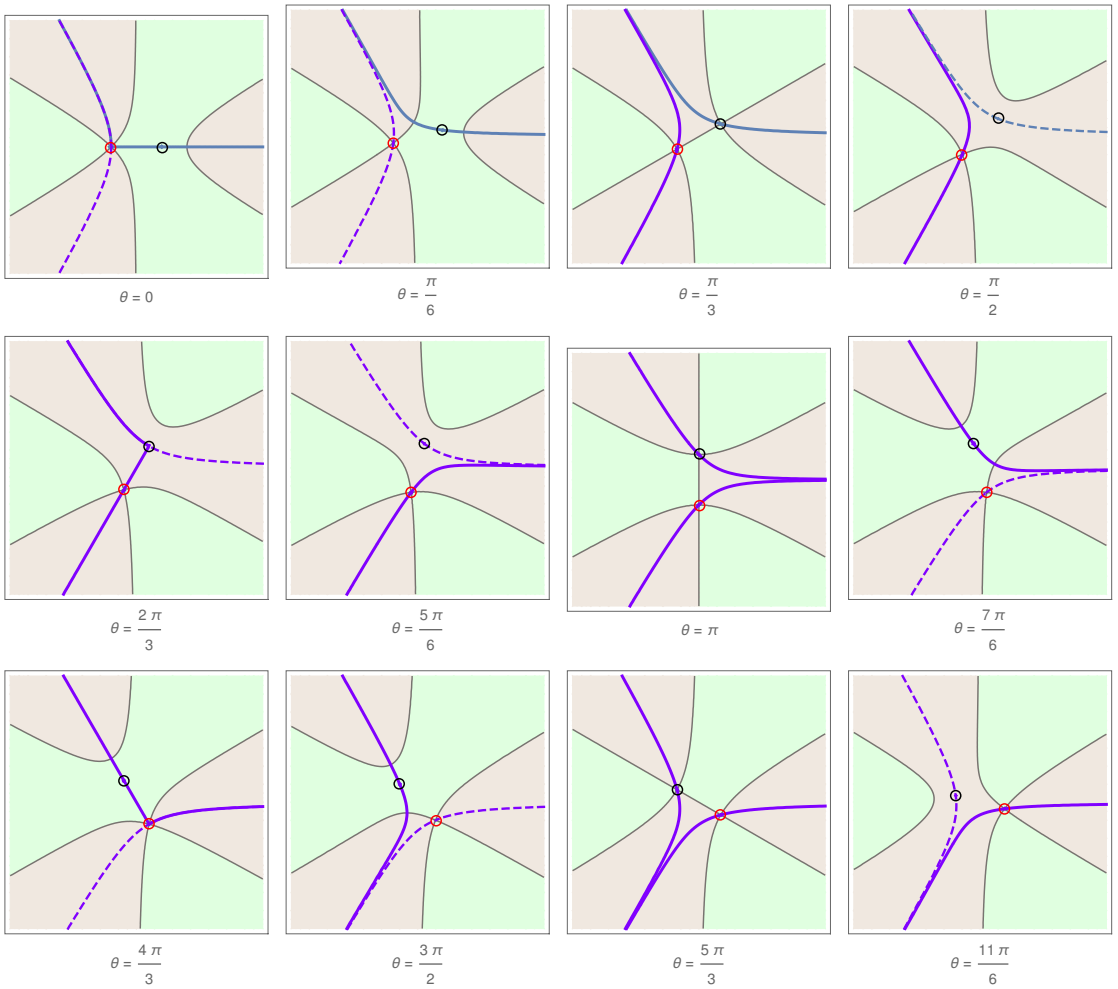

FIGURE 1.4: The steepest descent paths in the complex z-plane for the case of a line integral of type (1.105) with $\phi(z) = -z$ and $g(z) = \mathrm{e}^{-z^3/3}$. It is the integral representation of the Airy function. Each plot corresponds to a different angle $\theta = \arg(x)$ in the complex x-plane ($|x| = 1$). The saddle points are represented as black and red dots. Notice how the topology of the integration paths changes at the Stokes lines $\theta = 0,\ 2\pi/3,\ 4\pi/3$. Adapted from [1].

1.3.2 Transasymptotic summation

The following is a short introduction to the so-called transasymptotic summation developed in [9]. Consider a transseries $\mathcal{F}(y, x, \sigma)$ which depends on an additional parameter y:

$$\mathcal{F}(y, x, \sigma) \;=\; \sum_{n=0}^{\infty} \left(\sigma\, x^{\beta} \mathrm{e}^{-A(y)x}\right)^n \Phi_n(y, x)\,. \tag{1.107}$$

One defines a new variable τ

$$\tau(y, x) \;\equiv\; \sigma x^{\beta} \mathrm{e}^{-A(y)x}\,. \tag{1.108}$$

At an anti-Stokes line, $|\tau|$ is of order one and all the terms in the transseries become non-negligible, and after crossing an anti-Stokes line, the variable τ may even grow exponentially in x.

In such cases, one may no longer assume that τ is small, and truncating the transseries after the first few exponential sectors will not yield a good approximation to the $\mathcal{F}$. At the same time, expanding out terms in the variable x^{-1} around $x = \infty$ poses no problem. Therefore, one can obtain approximations to $\mathcal{F}$ by first expanding out the $\Phi_n(y, x)$ in $1/x$. and then summing over all orders of τ.

$$\begin{aligned} \mathcal{F}(y, \tau, \sigma) &= \sum_{n=0}^{+\infty} \tau^n \sum_{k=0}^{+\infty} \Phi_{n,k}(y) x^{-k} = \sum_{k=0}^{+\infty} x^{-k} \sum_{n=0}^{+\infty} \tau^n \Phi_{n,k}(y) \\ &\equiv \sum_{k=0}^{+\infty} x^{-k} f_k(y, \tau) \,. \end{aligned} \tag{1.109}$$

In (1.109), all the τ-dependence has been absorbed into the transasymptotic coefficient functions $f_k(y, \tau)$. This method of summing over all the exponentials is called orthogonal or transasymptotic summation [9]. To understand how powerful this approach can be, consider the function

$$f(\tau) = \frac{\tau}{\tau + 1} = \frac{1}{1 + \tau^{-1}} \,. \tag{1.110}$$

To obtain the transseries representation of $f(\tau)$, the function must be expanded in τ around $\tau = 0$:

$$f(\tau)\Big|_{\tau \sim 0} = \tau - \tau^2 + \tau^3 \cdots = \sum_{n=1}^{+\infty} (-1)^{n+1} \tau^n \,. \tag{1.111}$$

If $f(\tau)$ is to be evaluated in a regime where τ is exponentially growing in x , any truncation of the sum in (1.111) after a finite amount of terms will give a bad approximation of $f(\tau)$ since the partial sums of (1.111) converge to $f(\tau)$ in the limit $\tau \to 0$. This is because the transseries representation corresponds to expanding $f(\tau)$ in the wrong regime. However, with the transasymptotic summation, the expansion (1.111) is summed and the resulting expression,

$$\frac{1}{1 + \tau^{-1}} \,, \tag{1.112}$$

can be evaluated at large τ, far beyond the radius of convergence of (1.111), which is $|\tau| = 1$. The function $f(\tau)$ is not a good example in terms of asymptotics since there is no explicit x-dependence in it and as a consequence $f(\tau)$ has no resurgent properties, but it does illustrate how the transasymptotic summation can in principle be used to

study asymptotic regimes which are completely inaccessible from the perspective of the original transseries.

1.3.3 Hyperasymptotics and the WKB-method

Hyperasymptotics [8, 33, 10] is a resummation technique which generalises the method of optimal truncation displayed in Eq. (1.100). The method consists of finding an approximation for the exponentially small remainder as a finite sum using Borel resummation in combination with resurgent properties. The remainder of the improved approximation can then again be approximated by a truncated sum, and so on. A general, systematic way of calculating hyperasymptotic summations of any order can be found in [10]. In the following introduction, the approach in [8] will be closely followed. Consider the following second-order Schrödinger-type ODE:

$$x^{-2}\,\frac{\mathrm{d}^2 y}{\mathrm{d}z^2} - V(z)y(z,x) \;=\; 0\,, \tag{1.113}$$

where z is a complex variable and x is a parameter which will be taken to be large. In a quantum mechanics problem x^{-1} would be proportional to the Planck constant $\hbar$, while $V(z,x)$ would be proportional to the potential energy. Eq. (1.113) can be solved using the WKB method. The idea is to assume an ansatz of the form

$$y(z) \sim \mathrm{e}^{-x\,S_{\pm}(z)} \sum_{n=0}^{+\infty} y_{\pm,k}(z)\, x^{-n} \tag{1.114}$$

and calculate the coefficients $y_k(z)$ using the ODE. One finds

$$S_{\pm} = \pm \int_{z^*}^{z} \mathrm{d}\xi \sqrt{V(\xi)}\,. \tag{1.115}$$

In the context of quantum mechanics, the WKB method is a powerful tool to solve scattering problems. The exponential in (1.114) can be interpreted as a wave with phase $\mathbb{I}\mathrm{m}\,(-xS(z))$. Since Eq. (1.113) is a second-order ODE, there are two linearly independent solutions corresponding to the signs $(+)$ and $(-)$ in (1.114). In a scattering problem, one of the two solutions corresponds to the ingoing wave, while the other solution represents the outgoing wave (see [21, 24]). In the case of the Schrödinger equation (1.113), the asymptotic WKB expansion (1.114) can be written in a simpler and

more practical form in terms a new variable F defined by

$$F(z) \equiv 2\,x \int_{z^*}^{z} \mathrm{d}\xi \sqrt{V(\xi)}\,. \tag{1.116}$$

$F(z)$ is the difference between the two exponents in (1.114),

$$F(z) = x(S_+(z) - S_-(z))\,. \tag{1.117}$$

Assuming that $\mathbb{R}\mathrm{e}\,(F) > 0$, the subdominant solution which is exponentially small for large positive x can be written as

$$y(z) = \frac{\mathrm{e}^{-F/2}}{F^{1/4}}\,Y(F)\,. \tag{1.118}$$

One may expand the re-scaled function $Y(F)$ in powers of x^{-1} in the following way

$$Y(F) = \sum_{r=0}^{+\infty} (-1)^r\,Y_r(F), \;\text{ where } Y_r \sim x^{-r}\,. \tag{1.119}$$

Substituting (1.119) into the Schrödinger equation yields the following recursion relation

$$Y'_{r+1}(F) = -Y''_r(F) + \frac{(V(F)^{1/4})''}{V(F)^{1/4}} Y_r(F)\,. \tag{1.120}$$

Using this recursion relation, the following resurgence relation can be derived [8, 34]:

$$Y = S_0 + \sum_{r=0}^{+\infty} Y_r\,(-F)^r \sum_{s=N_0}^{+\infty} (-1)^s\,\frac{(s-r-1)!}{2\pi F^s}\,, \tag{1.121}$$

where S_0 represents the optimal truncation of Y, that is,

$$S_0 \equiv \sum_{r=0}^{N_0-1} (-1)^r Y_r\,. \tag{1.122}$$

Eq. (1.121) has the remarkable property that the remainder of the optimal truncation is expressed as an asymptotic sum which depends on the terms Y_r of the original expansion of $Y(F)$ as well as on powers of F^{-1}. This is a manifestation of the underlying resurgence structure of the problem. One can apply the Borel resummation to regulate the divergence arising from the factorial growth of the factorial coefficients in (1.121).

The calculation performed in [8] yields

$$Y = S_0 + \sum_{r=0}^{+\infty} (-1)^r Y_r \, K_{r1}, \tag{1.123}$$

where

$$K_{r1} = \frac{(-1)_0^N}{2\pi F^{N_0 - r}} \int_0^{+\infty} \mathrm{d}\xi \mathrm{e}^{-\xi} \frac{\xi^{N_0 - r - 1}}{1 + \xi/F} \, . \tag{1.124}$$

Note that now the remainder of S_0 in (1.123) is again an asymptotic series which can be optimally truncated. This yields

$$Y = S_0 + S_1 + \sum_{r=0}^{+\infty} Y_r \, (-F)^r \sum_{s=N_1}^{+\infty} (-1)^s \, \frac{(s - r - 1)!}{2\pi F^s} \, K_{s1} \, , \tag{1.125}$$

where S_1 is the optimal truncation

$$S_1 \equiv \sum_{r=0}^{N_1 - 1} (-1)^r Y_r K_{r1} \, , \tag{1.126}$$

and N_1 is the index of the least term. This process can be repeated

$$Y = S_0 + S_1 + S_2 + \ldots \, . \tag{1.127}$$

Including only S_0 in the sum (1.127) is called level-0 hyperasymptotic summation, if one includes the terms S_0 and S_1 this is called the level-1 hyperasymptotic summation, and so on. In this formulation of hyperasymptotics S_0 is the optimal truncation consisting of N_0 terms. It can be shown that at each additional level that is included, the number of terms in the optimal truncations for the hyperasymptotic levels S_r is approximately halved:

$$N_r = \left\lfloor \frac{N_0}{2^r} \right\rfloor \, . \tag{1.128}$$

The analysis in [8] reveals that the index of optimal truncation is given by

$$N_0 = \lfloor |F| \rfloor \, . \tag{1.129}$$

which corresponds to an exponential weight Hence there is a hyperasymptotic sector $r = r_{\max}$ for which $N_{r_{\max}} = 1$, and the hyperasymptotic summation (1.127) terminates after a finite number of terms. The minimal error which was given in [8] for this

procedure is of exponential order

$$\begin{aligned} |\Delta Y| &\sim \exp\Big(-(1+2\log(2))\,|F|\Big) \\ &\approx \exp\big(-2.386\,|F|\big)\,. \end{aligned} \tag{1.130}$$

In the later work [10] it was shown that the error estimate (1.130) is non-optimal and can be further improved with a new method. In fact, in [10] it was proven that by including enough hyperasymptotic levels in the summation and choosing appropriate truncation indices at each level, the approximation can be made arbitrarily precise. In [35] the results from [10] obtained for linear ODEs were applied to a non-linear Ricatti equation. This was possible since the validity of the proofs in [36] only depends on the singularity structure of the Borel plane. Hence the assumption of linearity is not needed for the method to work [35]. In Chapter 3, a non-linear ODE for the function $f(w)$ in the variable w will be discussed. In this problem, the function f has Borel singularities located at the positions A, $2A$, $3A$, ... on the positive real line of the Borel plane. In that case, the hyperasymptotic summation method devoloped in we [36] results in an error of exponential order

$$|\Delta f| \sim \mathrm{e}^{-r|Aw|}\,, \tag{1.131}$$

where r is the highest hyperasymptotic level (the analogue of the term S_r in the sum (1.127)). A detailed discussion of the hyperasymptotic method developed in [36] would exceed the scope of this introduction. The formulas (3.31), (3.32), and (B.1) used in Chapter 3 are obtained by applying the theorems in [36] to the function in question, $f(w)$.

1.4 Summary

The asymptotic methods presented here will be used throughout this thesis, in the analysis of non-perturbative phenomena which arise in the different problems that will be studied.

The non-perturbative objects that will appear in the next chapters will have different interpretations from the instantons introduced here, but their semi-classical WKB-like

interpretation will have completely analogous properties. Instantons, as the prototypical non-perturbative objects in quantum physics, provide an intuitive physical interpretation of non-perturbative effects, which will appear in several different contexts throughout this thesis.

Finally, the different asymptotic methods that were just introduced will play crucial roles in the unravelling of non-perturbative phenomena in the problems to come, and their analytic properties beyond the local perturbative analysis that is usually accessible in the study of such complex problems.

Chapter 2

Delayed bifurcations in the discrete logistic equation

Large parts of this chapter have been published verbatim in [2]. The research presented in this chapter is my own. It was developed under the guidance of my supervisors, Inês Aniceto and Christopher Howls, and in collaboration with Christopher Lustri. The error analysis presented in Section 2.3.2 was done by Christopher Lustri.

In this chapter the discrete logistic equation (DLE) is studied from the perspective of asymptotics. The solution to the DLE is a sequence which is either convergent or oscillating between a finite set of limit points depending on an underlying parameter. At certain values of said parameter each limit point splits into two, which is known as a period doubling bifurcation. When the parameter is itself slowly varied (in the literature this is known as a "slow-fast system"), a phenomenon known as delayed bifurcations or "canards" occurs. They have been studied widely in systems of ordinary differential equations (see, for example, [37]). In this case the solution of the singularly perturbed variant of the DLE stays at the first metastable branch for some time before jumping to the stable branch. In other words, the solution remains near an unstable solution for a significant amount of time after stability has been lost and then jumps to the new stable solution.

There has been a significant volume of work studying the asymptotic behaviour of canards in continuous settings, see for example, using composite asymptotic expansions in [38, 39, 40], steepest descent analysis [41], and Borel summation methods in [42]. Borel

summation methods are closely connected to transseries resummation methods (see [7]), and have been used to study discrete problems, as in [43]. This motivates the idea that transseries resummation methods could be a useful technique for studying delayed bifurcation behaviour. In the present study, the focus will be on delayed bifurcations appearing in discrete systems, and in particular, singularly perturbed variants of the logistic map.

It will be shown that period doubling bifurcations depend on the interaction between different exponential factors, and it is therefore advantageous to represent them explicitly using transseries. By expanding in the asymptotic limit, one may determine terms in the algebraic power series to determine the initially stable non-periodic solution. The next step will be to reorder the transseries terms and perform a transasymptotic resummation, which will produce an accurate description of the doubling phenomena. This approach has the additional advantage that it allows one to determine further subdominant exponential scales in the transseries explicitly which dictate subsequent doubling bifurcations present in the solution.

By incorporating a multiple scales ansatz into the transseries expression, it will be shown that transseries resummation – which was developed to describe continuous behaviour – can be used to calculate discrete variation without any further analysis to the transseries method.

Here two variants of the following ubiquitous (and generic) standard logistic map are studied:

$$Y_{n+1} = \lambda Y_n \left[1 - Y_n\right], \qquad 0 < Y_0 < 1, \tag{2.1}$$

where λ is a dimensionless bifurcation parameter $0 < \lambda \leq 4$.

This system contains a period-doubling route to chaos, found by allowing the parameter λ to vary. In the range $1 < \lambda \leq 3$, this system tends to a stable equilibrium without periodic effects. In the range $3 < \lambda \leq 1 + \sqrt{6}$, the system tends to a 2-periodic stable equilibrium. Increasing λ beyond $1 + \sqrt{6}$ produces systems that tend to stable equilibria with higher periodicity.

The earliest study of the delayed bifurcations in the slowly-varying logistic map is [44], who applied renormalisation methods to derive asymptotic scaling laws for the delays

between period doubling, and performed analysis and numerical experiments to determine the location of the bifurcation points. In addition to establishing specific results about the slowly-varying logistic map, this study established that delayed bifurcations can play an essential role in the behaviour of discrete systems. Similar methods were used to study delayed bifurcations in more general unimodal maps [45], as well as discrete maps with noise [46, 47, 48].

Further studies of this system appeared in subsequent years. In [49, 50, 39], the existence of canard solutions was rigorously proven in general classes of discrete maps that include the slowly-varying logistic map. Further discussions of canard solutions to both discrete continuous and discrete dynamical systems are given in [51, 52].

In more recent years, this system was studied using matched asymptotic expansions and multiple scales methods [3]. The purpose of this previous work was to show that the method of multiple scales could be used to combine a "fast" discrete timescale with a slow time variable that could be treated as continuous, while still capturing the essentially discrete-scale behaviour present in the problem. By carefully balancing terms, it is possible to identify the bifurcation points and produce accurate asymptotic approximations to the solution behaviour on both sides of the delayed bifurcation. In the works described here, the slowly-varying logistic equation has provided a useful testing ground for treatments of discrete systems, due to the complicated behaviour that it produces.

In addition to the slowly-varying logistic equation, multiple scales-based approaches which describe a system in terms of a fast discrete timescale and a slow continuous timescale have been used to study asymptotic effects in a number of other discrete systems. This includes the study of Stokes Phenomena in discrete Painlevé equations [53, 54, 55], Frenkel-Kontorova models [56], and discrete variants of the Korteweg-de Vries equation [57] and nonlinear Schrödinger equation [58].

It has been shown in [59] that transseries approaches may be used to improve upon asymptotic results obtained using matched asymptotic expansions. In that study, transseries resummation methods were used to obtain a uniform approximation to a continuous problem that had been previously solved using multiple scales methods. The transseries approach was able to naturally incorporate higher exponential terms, and thereby improve on the accuracy of the results, even for values of the perturbation

parameter that were not extremely small. Motivated by this result, it will be shown that transseries resummation can be used to improve on existing multiple scales results in discrete systems.

2.1 Motivation from population dynamics

In order to gain an intuitive understanding of Eq. (2.1), the equation will be regarded as a model describing the evolution of a population [60]. One may think of an isolated population of some animal species without migration. If there are no obstacles to reproduction (e.g. a shortage of food), one expects the growth rate of the population to be proportional to the number of individuals at any given time. If the number of individuals in a population at the time t is denoted $y(t)$, then in this simple model without obstacles one has

$$\frac{\mathrm{d}y}{\mathrm{d}t} = r\,y(t)\,. \tag{2.2}$$

The solution is exponential growth $y(t) = y(0)\exp(r\,t)$. Clearly this does not describe real populations because resources are always finite and hence infinite growth is not sustainable. For small y one expects exponential growth, whereas for large y the growth rate has to be negative to reflect a decrease of the population (e.g. due to competition or starvation). The simplest model which is consistent with these two observations is a

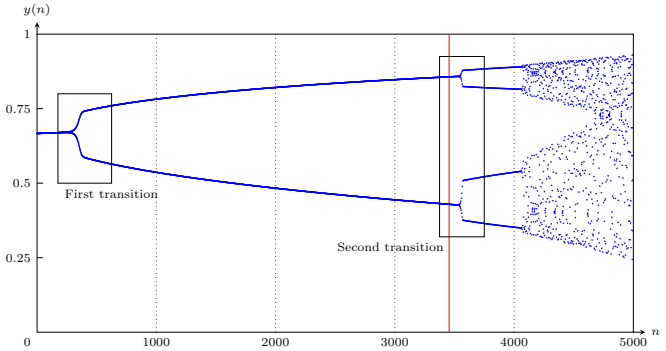

FIGURE 2.1: Solution to logistic equation 2.1, where $\lambda = 3 + \varepsilon n$ with $\varepsilon = 0.012^2$. The period-doubling cascade is apparent; the transition between non-periodic and 2-periodic behaviour is visible, as is the transition between 2-periodic and 4-periodic behaviour. As the solution continues, it eventually becomes chaotic. The 2-periodic behaviour in the solution begins to contribute immediately, but is not immediately visibly apparent due to the delay in the bifurcation behaviour. The red line shows the point at which the 2-period solution becomes unstable according to the analysis in this work. Taken from [2].

linear dependence of r on y, $r(y) = a - b\,y$, giving

$$\frac{\mathrm{d}y}{\mathrm{d}t} \;=\; (a - b\,y)\;y\,. \tag{2.3}$$

This so-called continuous logistic model is a bit more complicated, but still easy to solve. By separating $\mathrm{d}y$ and $\mathrm{d}t$, performing a partial fraction expansion and integrating one obtains the closed form expression

$$y(t) \;=\; \frac{1}{\beta - (\beta - 1/y(0))\mathrm{e}^{-at}}\,. \tag{2.4}$$

where $\beta = b/a$. The behaviour of this equation depends on whether the product $\beta\,y(0)$ is greater, equal to or smaller than 1. The limit as $t \to \infty$ is $1/\beta$. Note that it does not depend on the initial value $y(0)$. If $y(0) < 1/\beta$, then the solution grows monotonically, whereas for $y(0) > 1/\beta$ it is monotonically decreasing. For $y(0) = 1/\beta$ the population size stays constant. In order to discretise the continuous model Eq. (2.3) one has to choose some time interval ε and define

$$y_n \;\equiv y(t = n\varepsilon); \tag{2.5}$$

$$\lambda \;\equiv 1 \,+\, a\varepsilon\,. \tag{2.6}$$

Eq. (2.3) then becomes

$$y_{n+1} \;=\; \lambda y_n \left(1 - \frac{\beta a\varepsilon}{\lambda} y_n\right)\,. \tag{2.7}$$

To obtain the logistic equation Eq. (2.1), one can perform a re-scaling

$$Y_n \;=\; \frac{\beta a\varepsilon}{\lambda}\, y_n\,. \tag{2.8}$$

Assuming that the solution tends to some well defined limit Y_∞, one obtains (for $Y_0 > 0$) $Y_\infty = (\lambda - 1)/\lambda$. In terms of the original y_n this corresponds to $y_\infty = 1/\beta$, which is exactly what is expected from the above considerations. The difference to the continuous equation is that the fixed point is only stable in a certain range of parameters. As shall be seen, the solutions of the discrete logistic equation display an oscillatory behaviour for $\lambda > 3$. In terms of population dynamics, the limiting value $1/\beta$ has an intuitive explanation. The larger the initial growth rate $r(y = 0) = a$ and the smaller the growth rate of the obstacles b, the larger the maximum size that the population will reach. Note

that the logistical model is local since it is of the form

$$Y_{n+1} = F(Y_n)\,. \tag{2.9}$$

This means that the system has no memory. If ε is interpreted as the lifetime of one generation, then the size of a given generation only depends on the size of the previous one and not on the size of any of the generations which lived before.

2.2 The static logistic equation

The static logistic equation is given by

$$Y_{n+1} = (3+\varepsilon)Y_n\left[1-Y_n\right], \qquad Y_0 = 2/3. \tag{2.10}$$

The solution will be written as a continuous transseries in terms of $\varepsilon > 0$ and an asymptotic expansion is produced in the limit $0 < \varepsilon \ll 1$. The transseries approach will be used to extend this result to produce an accurate approximation for $\varepsilon = \mathcal{O}(1)$. It will then be shown that this continuous transseries is capable of capturing discrete period-doubling effects seen in this system, and approximating higher periodicity behaviour for values of ε that lead to 2-, 4- and even 8-periodic solutions.

In [3], the authors studied the asymptotic behaviour of this system for small ε using multiple scales methods. This showed the manner in which the behaviour approached the 2-periodic stable manifold associated with $\lambda > 3$. Using transseries methods, this approach can be extended to consider systems in which ε is not asymptotically small, and demonstrate the manner in which the solution approaches the stable solution for higher periodicities. In order to first determine the non-periodic and 2-periodic solutions, the initial condition will be ignored and (2.10) will be solved with the condition that $Y_{n+2} = Y_n$. This gives three unique solutions. One solution is non-periodic, and is given by

$$Y_n = \frac{2+\varepsilon}{3+\varepsilon}. \tag{2.11}$$

The remaining two solutions are 2-periodic, and are given by

$$Y_n = \frac{4+\varepsilon \pm (-1)^n\sqrt{\varepsilon(4+\varepsilon)}}{2(3+\varepsilon)}. \tag{2.12}$$

For $\varepsilon > 0$, the non-periodic solution is unstable. For $0 < \varepsilon < \sqrt{6} - 2$, the 2-periodic solution is stable. If ε exceeds $\sqrt{6} - 2$, the 2-periodic solution is unstable, and the stable solution to the system becomes 4-periodic, and can be identified by solving $Y_{n+4} = Y_n$, however this solution cannot be expressed in closed form. Continuing to increase ε leads to the periodicity of the stable solution increasing until chaotic behaviour is eventually obtained.

2.2.1 Static 2-period solution

Since the first bifurcation of the discrete model happens for $\lambda > 3$, this threshold value is perturbed by some small positive number ε:

$$\lambda(\varepsilon) \;=\; 3 + \varepsilon\,. \tag{2.13}$$

In order to solve (2.10) for this choice of λ, the discrete variable n will be transformed into the continuous variable

$$x \equiv n\,\varepsilon \tag{2.14}$$

and the following ansatz will be used:

$$R(x,\varepsilon) \;=\; \sum_{k=0}^{+\infty} \sigma_0^k \mathrm{e}^{-kA(x)/\varepsilon} R_k(x,\varepsilon)\,. \tag{2.15}$$

Then (2.10) becomes

$$R(x+\varepsilon,\varepsilon) \;=\; (3+\varepsilon) R(x,\varepsilon)\;\left(1 - R(x,\varepsilon)\right)\,. \tag{2.16}$$

The relationship between R and Y_n is then

$$\begin{aligned} R(n\varepsilon,\varepsilon) \;&= Y_n\,; \\ R(0,\varepsilon) \;&\equiv Y_0 \;= \frac{2}{3}. \end{aligned} \tag{2.17}$$

This series takes into account non-perturbative contributions by including powers of $e^{A(x)/\varepsilon}$. The parameter σ_0 is fixed by the initial condition. One obtains

$$\sum_{k=0}^{+\infty} \sigma_0^k e^{-k\,A(x+\varepsilon)/\varepsilon}\, R_k(x+\varepsilon,\varepsilon) = (3+\varepsilon) \sum_{k=0}^{+\infty} \sigma_0^k\, e^{-k\,A(x)/\varepsilon} \Bigg[R_k(x,\varepsilon) - \sum_{j=0}^{+\infty} R_j(x,\varepsilon)\, R_{k-j}(x,\varepsilon) \Bigg]. \tag{2.18}$$

For $\sigma_0 = 0$ this gives

$$R_0(x+\varepsilon,\varepsilon) \;=\; (3+x) R_0(x,\varepsilon)\,(1 - R_0(x,\varepsilon))\;. \tag{2.19}$$

Eq. (2.19) can be solved with the x-independent function

$$R_0(x,\varepsilon) \;=\; R_0(\varepsilon) \;=\; \frac{2+\varepsilon}{3+\varepsilon}\,. \tag{2.20}$$

In order to find $A(x)$, one needs to use Eq. (2.20) and consider the equation at order σ_0^1

$$e^{-(A(x+\varepsilon)-A(x))/\varepsilon} R_1(x+\varepsilon,\varepsilon) \;=\; -(1+\varepsilon) R_1(x,\varepsilon)\,. \tag{2.21}$$

It turns out that it is possible to put all the x-dependence into the $A(x)$. This comes at the price of allowing $A(x)$ to depend also on ε. This is done by defining the functions $\overline{R}_n(\varepsilon)$ and redefining $A(x,\varepsilon)$ through

$$e^{-n\,A(x,\varepsilon)/\varepsilon} \overline{R}_n(\varepsilon) \;=\; e^{-n\,A(x)/\varepsilon} R_n(x,\varepsilon)\,. \tag{2.22}$$

Substituting Eq. (2.22) into Eq. (2.21) and expanding

$$A(x+\varepsilon,\varepsilon) = A(x,\varepsilon) + \varepsilon \partial_x A(x,\varepsilon) + \frac{\varepsilon^2}{2} \partial_x^2 A(x,\varepsilon) + \mathcal{O}(\varepsilon^3) \tag{2.23}$$

gives

$$\left[e^{-\partial_x A(x,\varepsilon)} \left(1 + \frac{\varepsilon}{2} \partial_x^2 A(x,\varepsilon) + \mathcal{O}(\varepsilon^2) \right) + (1+\varepsilon) \right] \overline{R}_1(\varepsilon)\,. \tag{2.24}$$

If one can solve Eq. (2.24) with the ansatz $A(x,\varepsilon) = xB(\varepsilon)$ to linear order in ε, then one can solve it to all orders in ε (since all higher-oder derivatives $\partial_x^j A(x,\varepsilon) = 0$ for $j > 1$).

This is indeed possible and one obtains

$$A(x,\varepsilon) \;=\; -x\,(\mathrm{i}\pi(2p+1)+\log(1+\varepsilon))\;, \tag{2.25}$$

where p is some integer.

In what follows, $p=0$ will be set. Plugging Eq. (2.25) back into Eq. (2.18) while using Eq. (2.20) and matching equal powers of σ_0 one obtains the recursion equation

$$\overline{R}_n(\varepsilon) \;=\; \frac{-(3+\varepsilon)}{(1+\varepsilon)\,(1-(-1)^{n-1}(1+\varepsilon)^{n-1})}\sum_{j=1}^{n-1}\overline{R}_j(\varepsilon)\,\overline{R}_{n-j}(\varepsilon) \tag{2.26}$$

for $n>1$. The function $\overline{R}_1(\varepsilon)$ is unconstrained since $A(x,\varepsilon)$ is chosen in such a way that it solves Eq. (2.21) independently of $\overline{R}_1(\varepsilon)$. This is not surprising since any ε-dependent re-scaling of $\overline{R}_1(\varepsilon)$ corresponds to a redefinition of σ_0. Here $R_1(\varepsilon)=\varepsilon$ is chosen. For the first few $\overline{R}_n(\varepsilon)$ one obtains

$$\begin{aligned}
\overline{R}_1(\varepsilon) \;&=\varepsilon\,;\\
\overline{R}_2(\varepsilon) \;&=\;-\frac{(\varepsilon+3)}{(\varepsilon+1)(\varepsilon+2)}\,\varepsilon^2\,;\\
\overline{R}_3(\varepsilon) \;&=\;-\frac{2(\varepsilon+3)^2}{(\varepsilon+1)^2(\varepsilon+2)^2}\,\varepsilon^2\,;\\
\overline{R}_4(\varepsilon) \;&=\;-\frac{(\varepsilon-4)(\varepsilon+3)^3}{(\varepsilon+1)^3(\varepsilon+2)^3\,(\varepsilon^2+\varepsilon+1)}\,\varepsilon^3\,;\\
\overline{R}_5(\varepsilon) \;&=\frac{2(\varepsilon+3)^4\,\left(2\varepsilon^2+\varepsilon+6\right)}{(\varepsilon+1)^4(\varepsilon+2)^4\,(\varepsilon^2+\varepsilon+1)\,(\varepsilon^2+2\varepsilon+2)}\,\varepsilon^3\,.
\end{aligned} \tag{2.27}$$

The pattern is

$$\overline{R}_n(\varepsilon) \;\sim\; \varepsilon^{\lfloor n/2\rfloor+1}\sum_{k=0}^{+\infty}\overline{R}_{n,k}\varepsilon^k\,. \tag{2.28}$$

For the leading order coefficients there are the following simple expressions

$$\overline{R}_{2n+1,0} \;=\; \frac{(-9)^n\Gamma(n+\frac{1}{2})}{\Gamma(n+1)}\,;\qquad \overline{R}_{2n,0}=\frac{(-9)^n}{6}\,. \tag{2.29}$$

2.2.2 Computing the terms for the static case

The knowledge of the special form of the $\overline{R}_n(\epsilon)$ can now be used to derive an expression for the transseries. The idea is to first sum up all the exponentials:

$$\begin{aligned} R(x,\varepsilon) \;&=\; \sum_{n=0}^{+\infty} \sigma_0^n \, \mathrm{e}^{-n\,A(x,\varepsilon)/\varepsilon}\, \overline{R}_n(\varepsilon) \\ &= R_0(\varepsilon) \;+\; \sum_{\substack{n \text{ odd} \\ n\geq 1}} \Big(\sigma_0\, \mathrm{e}^{-A(x,\varepsilon)/\varepsilon)}\Big)^n \; \varepsilon^{n/2+1/2} \sum_{k=0}^{+\infty} \overline{R}_{n,k}\, \varepsilon^k \\ &\quad + \sum_{\substack{n \text{ even} \\ n\geq 2}} \Big(\sigma_0\, \mathrm{e}^{-A(x,\varepsilon)/\varepsilon)}\Big)^n \; \varepsilon^{n/2+1} \sum_{k=0}^{+\infty} \overline{R}_{n,k}\, \varepsilon^k \\ &= R_0(\varepsilon) \;+\; \sqrt{\varepsilon} \sum_{k=0}^{+\infty} \varepsilon^k \sum_{\substack{n \text{ odd} \\ n\geq 1}} \overline{R}_{n,k} \, \Big(\sigma_0\, \mathrm{e}^{-A(x,\varepsilon)/\varepsilon)} \sqrt{\varepsilon}\Big)^n \\ &\quad + \varepsilon \sum_{k=0}^{+\infty} \varepsilon^k \sum_{\substack{n \text{ even} \\ n\geq 2}} \overline{R}_{n,k} \, \Big(\sigma_0\, \mathrm{e}^{-A(x,\varepsilon)/\varepsilon)} \sqrt{\varepsilon}\Big)^n \,, \end{aligned} \tag{2.30}$$

$$R(x,\varepsilon) \equiv\; R_0(\varepsilon) \;+\; \sqrt{\varepsilon} \sum_{k=0}^{+\infty} \varepsilon^k\, \Omega_{o,k}(\tau_0) \;+\; \varepsilon \sum_{k=0}^{+\infty} \varepsilon^k \Omega_{e,k}(\tau_0)\,. \tag{2.31}$$

In the last line, the new variable

$$\tau_0 \;=\; \sqrt{\varepsilon}\, \sigma_0\, \mathrm{e}^{-A_\varepsilon(x)/\varepsilon} \tag{2.32}$$

was introduced, as well as the analytic functions $\Omega_{o,k}$ and $\Omega_{e,k}$ which are odd and even respectively and vanish at $\tau_0 = 0$ (any constant term in the expansion can be absorbed into the $R_0(\varepsilon)$ term). From $-A(x+\varepsilon,\varepsilon)/\varepsilon \;=\; -A(x,\varepsilon)/\varepsilon + \mathrm{i}\pi + \log(1+\varepsilon)$ it follows that

$$\tau_0(x+\varepsilon) \;=\; -(1+\varepsilon)\tau_0\,. \tag{2.33}$$

This property becomes useful in combination with our split of R into even and odd functions of τ_0 since

$$\begin{aligned} \Omega_{o,k}(-(1+\varepsilon)\tau_0) \;&=\; -\,\Omega_{o,k}(\tau_0+\varepsilon\tau_0) \;=\; -\sum_{j=0}^{+\infty} \frac{(\varepsilon\tau_0)^j}{j!}\, \Omega_{o,k}^{(j)}(\tau_0)\,; \\ \Omega_{e,k}(-(1+\varepsilon)\tau_0 \;&=\; +\,\Omega_{e,j}(\tau_0+\varepsilon\tau_0) \;=\; +\sum_{j=0}^{+\infty} \frac{(\varepsilon\tau_0)^j}{j!}\, \Omega_{e,k}^{(j)}(\tau_0)\,. \end{aligned} \tag{2.34}$$

If the ansatz is written in the form

$$R(\tau_0,\varepsilon) \;=\; R_0(\varepsilon) \;+\delta R(\tau_0,\varepsilon)\,, \tag{2.35}$$

the logistic equation Eq. (2.3) becomes

$$\delta R(-(1+\varepsilon)\tau_0,\varepsilon) \;=\; \delta R(\tau_0,\varepsilon)(1+\varepsilon) \;+\; \delta R(\tau_0,\varepsilon)^2(3+\varepsilon)\,. \tag{2.36}$$

Using Eq. (2.34) the terms in Eq. (2.36) can be written as (all the Ωs and their derivatives are evaluated at argument τ_0)

$$\begin{aligned}
\delta R(-(1+\varepsilon)\tau_0) \;&=\; -\sqrt{\varepsilon}\sum_{n=0}^{+\infty}\varepsilon^n\sum_{j=0}^{n}\frac{\tau_0^j}{j!}\,\Omega_{o,n-j}^{(j)} \;+\sum_{n=1}^{+\infty}\varepsilon^n\sum_{j=0}^{n-1}\frac{\tau_0^j}{j!}\,\Omega_{e,n-1-j}^{(j)}\,;\\
3\delta R(\tau_0)^2 \;&=3\sum_{n=1}^{+\infty}\varepsilon^n\sum_{j=0}^{n-1}\Omega_{o,j}\,\Omega_{o,n-1-j} \;+\;3\sum_{n=2}^{+\infty}\varepsilon^n\sum_{j=0}^{n-2}\Omega_{e,j}\,\Omega_{e,n-2-j}\\
&\quad+\;6\sqrt{\varepsilon}\sum_{n=1}^{+\infty}\varepsilon^n\sum_{j=0}^{n-1}\Omega_{o,j}\,\Omega_{e,n-1-j}\,;\\
\delta R(\tau_0)^2 \;&=\sum_{n=2}^{+\infty}\varepsilon^n\sum_{j=0}^{n-2}\Omega_{o,j}\,\Omega_{o,n-2-j} \;+\sum_{n=3}^{+\infty}\varepsilon^n\sum_{j=0}^{n-3}\Omega_{e,j}\,\Omega_{e,n-3-j}\\
&\quad+\;2\sqrt{\varepsilon}\sum_{n=2}^{+\infty}\varepsilon^n\sum_{j=0}^{n-2}\Omega_{o,j}\,\Omega_{e,n-2-j}\,;\\
\delta R(\tau_0) \;&=\sqrt{\varepsilon}\sum_{n=0}^{+\infty}\varepsilon^n\,\Omega_{o,n} \;+\;\varepsilon\sum_{n=1}^{+\infty}\varepsilon^n\,\Omega_{e,n-1}\,;\\
\varepsilon\delta R(\tau_0) \;&=\sqrt{\varepsilon}\sum_{n=1}^{+\infty}\varepsilon^n\,\Omega_{o,n-1} \;+\sum_{n=2}^{+\infty}\varepsilon^n\,\Omega_{e,n-2}\,.
\end{aligned} \tag{2.37}$$

Substituting these expressions back into Eq. (2.36) gives an infinite tower of recursively solvable differential equations which together with the choice for $\overline{R}_1(\varepsilon)$ determine the $\Omega_{o,k}$ and $\Omega_{e,k}$ uniquely. The first four of these functions will be computed. The

differential equations which need to be solved are

$$\begin{aligned}
0 &= 2\Omega_{e,0}(\tau_0) + 3\Omega_{o,0}(\tau_0)^2\,;\\
0 &= \left(6\Omega_{e,0}(\tau_0)+1\right)\Omega_{o,0}(\tau_0) - \tau_0\Omega'_{o,0}(\tau_0)\,;\\
0 &= 6\Omega_{e,1}(\tau_0)\Omega_{o,0}(\tau_0) + 2\Omega_{e,0}(\tau_0)\left(\Omega_{o,0}(\tau_0) + 3\Omega_{o,1}(\tau_0)\right)\\
&\quad - \frac{1}{2}\tau_0^2\Omega''_{o,0}(\tau_0) - \tau_0\Omega'_{o,1}(\tau_0) + \Omega_{o,1}(\tau_0)\,;\\
0 &= \frac{1}{2}\tau_0^2\Omega''_{e,0}(\tau_0) + \tau_0\Omega'_{e,1}(\tau_0) + \Omega_{e,0}(\tau_0)^2 + 6\Omega_{e,0}(\tau_0)\Omega_{e,1}(\tau_0)\\
&\quad + \Omega_{e,1}(\tau_0) + 2\Omega_{e,2}(\tau_0) + 3\Omega_{o,1}(\tau_0)^2 + 2\Omega_{o,0}(\tau_0)\Omega_{o,1}(\tau_0) +\\
&\quad 6\Omega_{o,0}(\tau_0)\Omega_{o,2}(\tau_0)\,.
\end{aligned} \tag{2.38}$$

These equations are solved by

$$\begin{aligned}
\Omega_{o,0}(\tau_0) &= \frac{\tau_0}{\sqrt{c_1+9\tau_0^2}}\,;\\
\Omega_{e,0}(\tau_0) &= -\frac{3\tau_0^2}{2\left(c_1+9\tau_0^2\right)}\,;\\
\Omega_{o,1}(\tau_0) &= \frac{\tau_0\left(c_1\left(33\log\left(c_1+9\tau_0^2\right)+14\right)-8c_2-45\tau_0^2\right)}{24\left(c_1+9\tau_0^2\right)^{3/2}}\,;\\
\Omega_{e,1}(\tau_0) &= \frac{\tau_0^2\left(-33c_1\log\left(c_1+9\tau_0^2\right)+8c_2+36\tau_0^2\right)}{8\left(c_1+9\tau_0^2\right)^{2}}\,.
\end{aligned} \tag{2.39}$$

In order to determine the integration constants c_1 and c_2, one needs to compare the orthogonal resummation containing Eq. (2.39) with our original transseries obtained by choosing $\overline{R}_1(\varepsilon)=\varepsilon$. One obtains (note that $R_0(\epsilon)$ cancels):

$$\begin{aligned}
0 &= \sum_{n=1}^{+\infty}\left(\frac{\tau_0}{\sqrt{\varepsilon}}\right)^n \overline{R}_n(\varepsilon) - \sqrt{\varepsilon}\sum_{n=0}^{+\infty}\Omega_{o,n}(\tau_0)\,\varepsilon^n - \varepsilon\sum_{n=0}\Omega_{e,n}(\tau_0)\,\varepsilon^n\\
&= \left[\left(\frac{1}{\sqrt{c_1}}-1\right)\sqrt{\epsilon} + \frac{\left(14c_1 - 8c_2 + 33c_1\log(c_1)\right)}{24c_1^{3/2}}\,\epsilon^{3/2} + \mathcal{O}(\epsilon^2)\right]\tau_0 + \mathcal{O}(\tau_0^2)\,.
\end{aligned} \tag{2.40}$$

Requiring Eq. (2.40) to vanish at the orders which have been computed fixes the constants

$$c_1 = 1\,; \qquad c_2 = \frac{7}{4}\,. \tag{2.41}$$

With this choice of integration constants the four Ω-functions become

$$\begin{aligned}
\Omega_{o,0}(\tau_0) &= \frac{\tau_0}{\sqrt{9\tau_0^2+1}}\,;\\
\Omega_{e,0}(\tau_0) &= -\frac{3\tau_0^2}{18\tau_0^2+2}\,;\\
\Omega_{o,1}(\tau_0) &= \frac{11\tau_0\log\left(9\tau_0^2+1\right)-15\tau_0^3}{8\left(9\tau_0^2+1\right)^{3/2}}\,;\\
\Omega_{e,1}(\tau_0) &= \frac{\tau_0^2\left(36\tau_0^2-33\log\left(9\tau_0^2+1\right)+14\right)}{8\left(9\tau_0^2+1\right)^2}\,.
\end{aligned} \tag{2.42}$$

2.2.3 The static initial value problem

Let the n-th order transasymptotic summation be defined as

$$R_n(\tau_0,\varepsilon) \equiv R_0(\varepsilon) + \sqrt{\epsilon}\sum_{k=0}^{n-1}\varepsilon^k\,\Omega_{o,k}(\tau_0) + \varepsilon\sum_{k=0}^{n-1}\varepsilon^k\Omega_{e,k}(\tau_0)\,. \tag{2.43}$$

Having computed R_2, one can now approximately solve the initial value problem for different values of ε and determine the parameter $\sigma_0(\varepsilon)=\sigma_{0,0}+\sigma_{0,1}\varepsilon+\sigma_{0,2}\varepsilon^2+\mathcal{O}(\varepsilon^3)$ to second order in ε. One requires $R(\tau_0(x=0),\varepsilon)=R(\sqrt{\varepsilon}\sigma_0,\varepsilon)=2/3$, and expands

$$0 = R_2(\tau_0.\varepsilon)-\frac{2}{3} = \left(\sigma_{0,0}+\frac{1}{9}\right)\varepsilon+\ldots\,. \tag{2.44}$$

One finds

$$\sigma_{0,0} = -\frac{1}{9}\,;\quad \sigma_{0,1} = \frac{4}{81}\,;\quad \sigma_{0,2} = -\frac{19}{648}\,. \tag{2.45}$$

The approximation is relatively accurate, with a relative error of at most $\sim 10^{-5}$. In Fig. 2.2, both $R_2(n)$ and its relative error w.r.t. the solution Y_n to the DLE are displayed as a function of n.

2.2.4 The static 4-period solution from map-iteration

It has been seen how the static problem can be solved using a transasymptotic summation approach. This method can be generalised to get solutions for higher periods. The trick is to iterate the logistic map $Y_{n+1}=F(Y_n)$ several times. To obtain the 4-period solution, one considers the equation $Y_{n+2}=F\circ F(Y_n)$. As before, a transseries ansatz of

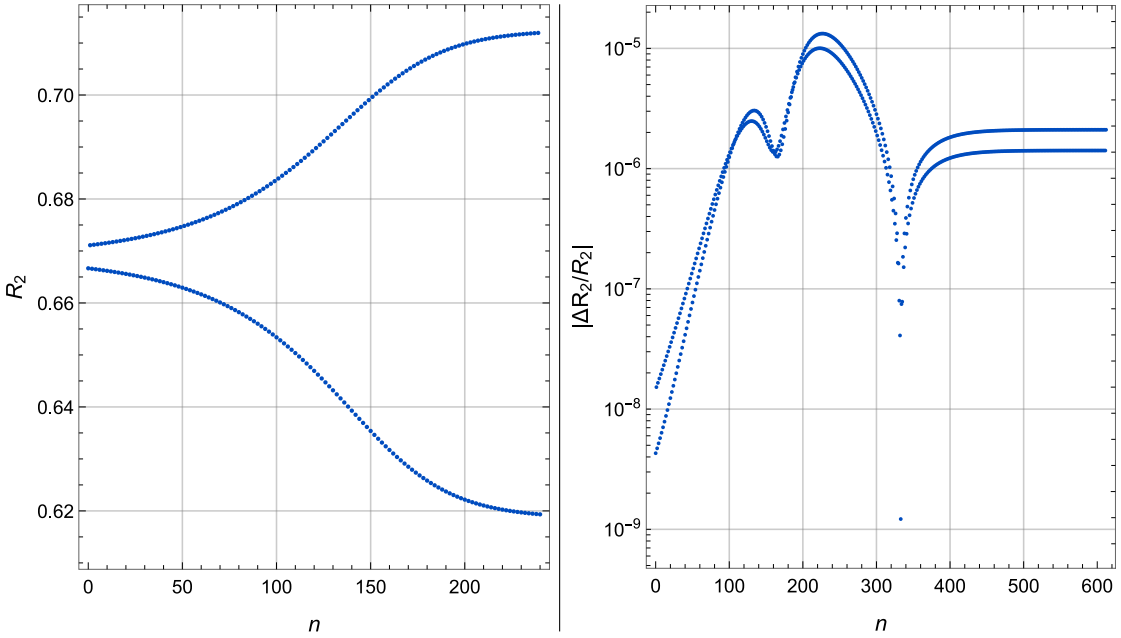

FIGURE 2.2: Left: Second order transasymptotic summation R_2 as a function of n for $\epsilon = 2/100$. Right: Relative error of transasymptotic summation $R_2(n)$ with respect to solution Y_n of DLE (obtained numerically).

the form (2.15) is used:

$$R(x,\varepsilon) \;=\; R_0(\varepsilon) \;+\; \sum_{n=1}^{+\infty} \sigma_2^n \mathrm{e}^{-nC(x,\varepsilon)/\varepsilon}\, \overline{R}_n(\varepsilon)\,. \tag{2.46}$$

In terms of $R(x,\varepsilon)$, one obtains the following equation (the ε and σ_2 dependence are dropped to keep the notation simple)

$$R\left(x+2\varepsilon\right) = (3+\varepsilon)^3 R(x)\left(1-R(x)\right)\left(1-(3+\varepsilon)R(x)\left(1-R(x)\right)\right)\,. \tag{2.47}$$

By expanding this equation in σ_2 and matching the zeroth-order terms one finds three solutions for $R_0(\varepsilon)$

$$\begin{aligned} R_{0,\text{1-period}}(\varepsilon) \;&=\frac{2+\varepsilon}{3+\varepsilon}\,; \\ R_{0,\pm}\left(\varepsilon\right) \;&=\frac{4+\varepsilon \pm \sqrt{\varepsilon\left(4+\varepsilon\right)}}{2(3+\varepsilon)}\,. \end{aligned} \tag{2.48}$$

The solutions $R_{0,\pm}(\varepsilon)$ correspond to the two values between which the 2-period solution oscillates in the limit $n \to \infty$. If the transasymptotic summation $R_2(\tau, x, \sigma)$ is expanded,

$$\begin{aligned} R_2(\tau, \varepsilon; \sigma) &\sim R_{0,\text{1-period}}(\varepsilon) + \frac{\sqrt{\varepsilon}}{3}\frac{\tau}{|\tau|} - \frac{\varepsilon}{6} - \frac{45}{648}\frac{\tau}{|\tau|}\varepsilon^{3/2} + \frac{36}{648}\varepsilon^2 + \mathcal{O}(\varepsilon^{5/2}); \\ &\sim \frac{2}{3} + \frac{\sqrt{\varepsilon}}{3}\mathrm{e}^{\pi\mathrm{i}\frac{x}{\varepsilon}} - \frac{\varepsilon}{18} - \frac{45}{648}\mathrm{e}^{\pi\mathrm{i}\frac{x}{\varepsilon}}\varepsilon^{3/2} + \frac{\varepsilon^2}{54} + \mathcal{O}(\varepsilon^{5/2}). \end{aligned} \tag{2.49}$$

To this order, the expansion agrees with $R_{0,\pm}(\varepsilon)$ The term linear in σ_2 in our equation allows one to deduce the exponential weight $C(x, \varepsilon)$

$$C(x, \varepsilon) = -\frac{x}{2}\log\left(1 - \varepsilon(4 + \varepsilon)\right) + \text{constant}. \tag{2.50}$$

This is not the same as the weight which was obtained for the non-iterated static logistic equation. Notice that the argument of the logarithm decreases with ε and reaches 0 for $\varepsilon = -2 + \sqrt{5}$, and the logarithm is singular there. If ε is further increased, the argument of the logarithm picks up a factor of -1. $C(x, \varepsilon)$ can be written as

$$C(x, \varepsilon) = -\frac{\pi\mathrm{i}}{2}x - \frac{x}{2}\log\left(\varepsilon(4 + \varepsilon) - 1\right). \tag{2.51}$$

The term $-\mathrm{i}\frac{\pi}{2}$ is responsible for an oscillatory behaviour once $\varepsilon > -2 + \sqrt{5}$ since a shift $n \mapsto n + 2$ flips the sign of the transasymptotic variable τ_2. However, as long as $a(\varepsilon) \equiv \varepsilon(4 + \varepsilon) - 1 < 1$, the real part of $-C(x, \varepsilon)$ will be negative and hence $|\tau_2| \to 0$ exponentially in the limit $n \to \infty$. Hence the oscillatory behaviour is exponentially suppressed. It is only when $a(\varepsilon) > 1$, and therefore $\varepsilon > -2 + \sqrt{6}$, when $|\tau_2| \to \infty$ for $n \to \infty$ and the solution will display a 4-period behaviour. The above reasoning motivates the introduction of a new set of variables

$$(\bar{x}, \delta) \equiv \left(\frac{x\delta}{2\varepsilon}, \varepsilon - \varepsilon_0\right), \tag{2.52}$$

where $\varepsilon_0 = -2 + \sqrt{6}$. A shift $x \mapsto x + 2\varepsilon$ corresponds to $\bar{x} \mapsto \bar{x} + \delta$. The new exponential scale τ_2 is then defined as

$$\tau_2(\bar{x}, \delta) = \sqrt{\delta}\,\sigma_2\,\mathrm{e}^{-C(\bar{x},\delta)/\delta}. \tag{2.53}$$

The transasymptotic summation ansatz which is used is of the same form as in our previous 2-period calculation

$$R_{\pm}\left(\tau_2, \delta; \sigma_2\right) = R_{0,\pm}\left(\delta\right) + \sqrt{\delta} \sum_{k\geq 0} \delta^k \Omega_{o,k}^{(\pm)}\left(\tau_2\right) + \delta \sum_{k\geq 0} \delta^k \Omega_{e,k}^{(\pm)}\left(\tau_2\right) . \tag{2.54}$$

Substituting (2.54) into (2.47) leads to a set of differential equations for the $\Omega^{(\pm)}$-functions, which can be solved recursively. Solving for the functions $\Omega_{o,0}^{(\pm)}$ and $\Omega_{e,0}^{(\pm)}$ yields

$$\begin{aligned} \Omega_{o,0}^{(\pm)}(\tau_2) &= \frac{\tau_2}{\sqrt{1+\frac{5}{6}\left(14 \pm 7\sqrt{2} \pm 4\sqrt{3} + 4\sqrt{6}\right)\tau_2^2}}; \\ \Omega_{e,0}^{(\pm)}(\tau_2) &= -\frac{\frac{1}{2}\left(2 \pm 6\sqrt{3} + \sqrt{6\left(7 \pm 4\sqrt{3}\right)}\right)\tau_2^2}{1+\frac{5}{6}\left(14 \pm 7\sqrt{2} \pm 4\sqrt{3} + 4\sqrt{6}\right)\tau_2^2}. \end{aligned} \tag{2.55}$$

The initial value problem is given by

$$R_{\pm}(x=0) = R_{0,\pm}\left(\varepsilon_0\right) = \frac{1}{5}\left(2 \pm \sqrt{3} + \sqrt{2 \pm \sqrt{3}}\right) . \tag{2.56}$$

As before, it is solved by expanding out the transseries parameter $\sigma_2(\delta)$ in powers of δ, which allows one to expand $R_{\pm}(x=0)$ in terms of δ

$$\sigma_{2,\pm} = -\frac{1}{25}\left(6 \pm 8\sqrt{3} - \sqrt{78 \pm 21\sqrt{3}}\right) - \frac{21 \mp 108\sqrt{2} \mp 65\sqrt{3}}{76 + 36\sqrt{6}}\,\delta + \cdots . \tag{2.57}$$

The method of iterating the logistic map several times can also be used to obtain higher-period solutions, and the values ϵ_b at which a bifurcation occurs can be determined from the exponential weight $C(x, \varepsilon)$ as demonstrated above. Each ε_b will be the zeros of some polynomial.

2.2.5 Static 4-period solution from the original equation

2.2.5.1 Transseries ansatz

To obtain the 4-periodic solution requires an adaptation of the previous process. One now takes a four-periodic perturbation about the 2-periodic solution obtained in (2.44). This allows to form a transseries that can be used to capture solutions which tend to a

four-periodic stable manifold. In [3], this would have required solving a challenging multiple scales problem, as the asymptotic solution obtained therein is only valid for small ε. Using the transseries approach, a significantly more general result is obtained.

The solution is written as a perturbation around the non-period behaviour and the 2-periodic behaviour captured by the transseries expression (2.31), in terms of the variable τ_0, here written as $\hat{R}(\tau_0, \varepsilon)$.

$$R(x,\varepsilon) = R_0(\varepsilon) + \sqrt{\varepsilon}\sum_{k=0}^{\infty}\varepsilon^k\Omega_{o,k}(\tau_0) + \varepsilon\sum_{k=0}^{\infty}\varepsilon^k\Omega_{e,k}(\tau_0) + S(x,\varepsilon) = \hat{R}(x,\varepsilon) + S(x,\varepsilon). \tag{2.58}$$

It will then be shown that this perturbation starts contributing for values of ε large enough. It can be seen by direct substitution into (2.16) that

$$S(x+\varepsilon,\varepsilon) = (3+\varepsilon)(1-2\hat{R}(\tau_0,\varepsilon) - S(x,\varepsilon))S(x,\varepsilon). \tag{2.59}$$

In order to identify the correct scaling for $S(x)$, note the form of the 2-periodic manifold, given in (2.12). The 2-periodic behaviour is represented in terms of the continuous variable x by writing $(-1)^n$ as $\alpha = \text{sign}(\cos(\pi x/\varepsilon))$, such that

$$\hat{R}(\tau_0,\varepsilon) = \frac{4+\varepsilon-\alpha\sqrt{\varepsilon(4+\varepsilon)}}{2(3+\varepsilon)} + \mathcal{O}(\tau_0^{-1}) \quad \text{as} \quad x\to\infty, \tag{2.60}$$

where the asymptotic order of this expression can be obtained by rewriting (2.44) in powers of τ_0^{-1} and equating terms. One may now follow similar methods to the 2-periodic case, and formulate an ansatz for the solution in terms of ε and a new transseries parameter, denoted σ_1. Motivated by (2.22), one chooses the ansatz

$$S(x,\varepsilon) = \sum_{m=1}^{\infty}\sigma_1^m \mathrm{e}^{-mB(x,\varepsilon)/\varepsilon}S_m(\varepsilon), \tag{2.61}$$

noting that ε dependence on the exponential scale is now allowed. The exponential scaling $B(x,\varepsilon)$ may then be determined by considering the large-x behaviour. This is convenient, as the form for $R(x)$ in this limit has already been given in (2.60), and it is known from the asymptotic order of this expression that the solution approaches this limit exponentially as x becomes large. Using (2.60) in (2.59) and matching powers of ε

in an identical fashion to (2.24) gives

$$\frac{\partial}{\partial x}B(x,\varepsilon) = -\pi\mathrm{i} - \log\left(1 - \alpha\sqrt{\varepsilon(4+\varepsilon)}\right). \tag{2.62}$$

This may be solved to give

$$B(x,\varepsilon) = f(\varepsilon)x - \varepsilon g(x,\varepsilon), \tag{2.63}$$

where

$$f(\varepsilon) = -\tfrac{1}{2}\log(1-\varepsilon(4+\varepsilon)) - \pi\mathrm{i}, \tag{2.64}$$

and $g(x,\varepsilon)$ is a bounded function that vanishes for $x = \varepsilon n$ for $n \in \mathbb{Z}$, given by

$$g(x,\varepsilon) = \alpha\left(\frac{x}{2\varepsilon} - \frac{1}{2}\left\lfloor\frac{x}{\varepsilon} + \frac{1}{2}\right\rfloor\right)\log\left(\frac{1-\sqrt{\varepsilon(4+\varepsilon)}}{1+\sqrt{\varepsilon(4+\varepsilon)}}\right). \tag{2.65}$$

As $g(n\varepsilon,\varepsilon) = 0$ for $n \in \mathbb{Z}$, this expression could be ignored and the result will still give the correct value of $B(x,\varepsilon)$, and hence the correct exponential scaling, on $x = \varepsilon n$. This therefore suggests that one can capture the 4-periodic solution by defining a new variable τ_1, such that

$$\tau_1(x,\varepsilon) = \sigma_1\sqrt{\varepsilon}\mathrm{e}^{-B(x,\varepsilon)/\varepsilon}. \tag{2.66}$$

In subsequent analysis, it will be useful to have a convenient expression for the value of τ_1 at $x+\varepsilon$ and $x+2\varepsilon$. Through direct substitution, one finds that

$$\tau_1(x+\varepsilon,\varepsilon) = -\mathrm{i}(\varepsilon(4+\varepsilon)-1)^{1/2}\mathrm{e}^{-2g(x,\varepsilon)}\tau_1(x,\varepsilon), \tag{2.67}$$

$$\tau_1(x+2\varepsilon,\varepsilon) = -(\varepsilon(4+\varepsilon)-1)\,\tau_1(x,\varepsilon). \tag{2.68}$$

2.2.5.2 Exponential weights

The form of $B(x,\varepsilon)$ provides insight into the behaviour of the solution as ε increases outside of the range of validity of the original small-ε transseries. The behaviour of this term is shown in Figure 2.3, which identifies three distinct ranges of ε which must be considered separately.

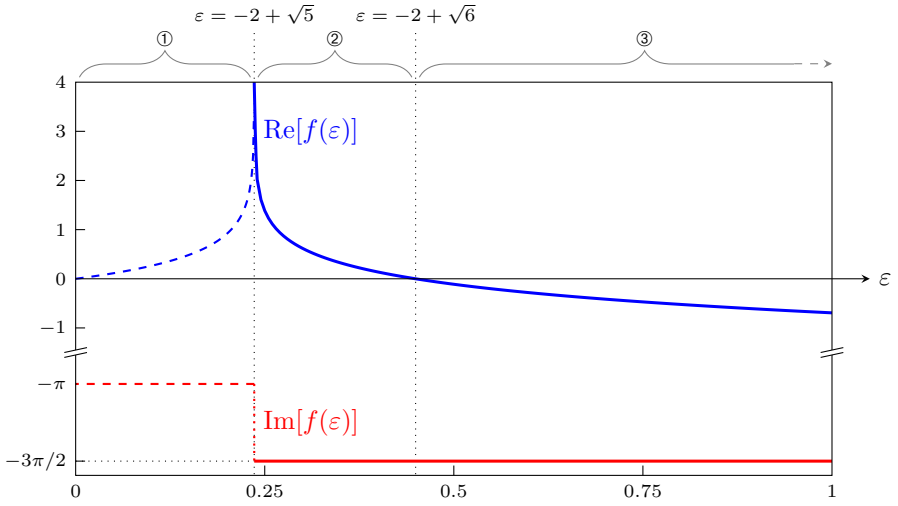

FIGURE 2.3: This figure shows the real and imaginary parts of $f(\varepsilon) = -\frac{1}{2}\log(1-\varepsilon(4+\varepsilon)) - \pi\mathrm{i}$, where the exponential weight $B(x)$ is given in (2.63). If $\mathrm{Re}[f(\varepsilon)] > 0$, the 4-periodic exponential contribution is exponentially small in ε, while if $\mathrm{Re}[f(\varepsilon)] < 0$, the contribution is large, and must be incorporated into any approximation in order to accurately describe the system behaviour. In parameter regime ①, this exponential contribution is not present in the transseries, and is therefore denoted as a dashed curve. In regime ②, the 4-periodic exponential terms appear, but are exponentially small. In regime ③, the exponential contributions become large, and 4-periodic behaviour becomes apparent in the solution. The 4-periodicity of the solution arises due to $\mathrm{Im}[f(\varepsilon)]$. This represents a multiplicative factor in $B(x)$ of $-\mathrm{i}$, corresponding to 4-periodic behaviour in the exponential term. Taken from [2].

From the form of (2.66), it is seen that $B(x,\varepsilon)$ is the exponential controlling factor for S, and therefore determines how this series will contribute as x grows. If $\mathrm{Re}[B] > 0$, corresponding to $\mathrm{Re}[f(\varepsilon)] > 0$, the exponential contribution will decay as x grows, while if $\mathrm{Re}[B] < 0$, corresponding to $\mathrm{Re}[f(\varepsilon)] < 0$, the exponential part will grow and become the most significant contribution for large x.

This change in sign occurs at $\varepsilon = -2+\sqrt{6}$. At this point, $\mathrm{Re}[f(\varepsilon)]$ becomes negative, and the exponentials in (2.61) therefore grow as x becomes large, rather than decaying. This means that in Region ③ the S term is no longer a small decaying perturbation around $\hat{R}$, but rather plays a significant role in the limiting behaviour as $x \to \infty$. If S is ignored, this behaviour is not captured in the transseries, and the resultant expression for R is an inaccurate description of the solution behaviour.

Note that $\mathrm{Im}[f(\varepsilon)] = -3\pi/2$ for $\varepsilon > -2+\sqrt{5}$. This has the effect of making τ_1^m 4-periodic in $m \in \mathbb{Z}^+$, due to having a factor of $-\mathrm{i}$, rather than the 2-periodic behaviour associated with a factor of -1. Hence, this exponential behaviour represented by $B(x,\varepsilon)$ corresponds to 4-periodic effects in the solution.

In order to include this behaviour in the transseries expression, one cannot simply expand the solution about $\varepsilon = 0$. One must instead expand S about some point ε_0 such that the 4-periodic behaviour is present in the expansion. This requirement suggests that $\varepsilon_0 = -2 + \sqrt{6}$ is a sensible choice, as 4-periodic effects are apparent in the solution at this value.

Finally, the region in which the series terms obtained by expanding about ε_0 are valid must be considered. If the behaviour of $B(x, \varepsilon)$ is examined for $\varepsilon > \varepsilon_0$, it is seen that the real part of $f(\varepsilon)$ becomes infinite as $\varepsilon \to -2 + \sqrt{5}$. This corresponds to the exponentials disappearing, as every exponential term tends to zero. The series expansion about ε_0 is not valid for ε smaller than this value. Consequently, region ② contains exponentially small 4-periodic behaviour, while no such behaviour exists in region ①. In Figure 2.3 $f(\varepsilon)$ has been represented in region ① as a dashed curve, to indicate that it does not have any effect on the transseries.

Consequently, simply by studying $B(x, \varepsilon)$, it is possible to describe the onset of 4-periodicity in the solution. In region ①, there are no 4-periodic effects present. In region ②, there are 4-periodic effects caused by the appearance of new exponential terms, but they are exponentially subdominant compared to the 2-periodic behaviour. In region ③, these effects grow to become the most significant effect in the solution behaviour. Note that the switching of the 4-period exponentials is independent of the initial data, the latter only determines how quickly they grow to dominate the solution. For higher values of ε, there must be values for which higher-periodicity behaviour appears. The onset of 8-periodic behaviour is discussed in Section 2.2.7.

Finally, note that the change in exponential contribution has a parallel with a Borel transform approach to asymptotic expansions. Borel transforms encode the different exponential weights of an asymptotic series as singularities in a complex domain known as the "Borel plane". There, a change in the number of exponential contributions corresponds to singularities moving across a branch cut onto a different Riemann sheet of the Borel plane, giving rise to behaviour known as the "Stokes phenomenon" [61] as the number of exponential contributions in an asymptotic series abruptly changes. A similar, but not identical, behaviour occurs in this system at $\varepsilon = -2 + \sqrt{5}$, where $\mathrm{Re}[f(\varepsilon)]$ becomes infinite and $\mathrm{Im}[f(\varepsilon)]$ changes instantaneously, corresponding to a branch point in the f-plane.

2.2.5.3 Static computation of resummed transseries

Writing an appropriate form for the 4-periodic ansatz is slightly more involved than in the 2-periodic case, given in (2.31). Recall from Section 2.2.5.2 that the significant change in the behaviour of the exponential contribution occurs for values of ε greater than $\varepsilon_0 = -2 + \sqrt{6}$. Therefore a new series variable $\sqrt{6}\eta = \varepsilon - \varepsilon_0$ is defined, where the $\sqrt{6}$ term is included for subsequent algebraic convenience.

In analogous fashion to (2.31), the ansatz is again devided up into separate power series. In the 2-periodic case, it was clear from the form of the previously calculated terms that splitting the odd and even powers of τ_0 would capture the discrete variation effectively. From the analysis in Section 2.2.5.2, one finds the power series for the 4-periodic solution should instead be split into four parts, such that

$$S(\tau_1,\eta) = \sqrt{\eta}\sum_{k=0}^{\infty}\eta^k\sum_{m=0}^{\infty}\tau_1^{4m+1}S_{4m+1,k} + \eta\sum_{k=0}^{\infty}\eta^k\sum_{m=0}^{\infty}\tau_1^{4m+2}S_{4m+2,k} + \sqrt{\eta}\sum_{k=0}^{\infty}\eta^k\sum_{m=0}^{\infty}\tau_1^{4m+3}S_{4m+3,k} + \eta\sum_{k=0}^{\infty}\eta^k\sum_{m=0}^{\infty}\tau_1^{4m+4}S_{4m+4,k}. \quad (2.69)$$

Consequently, each split power series is now written as functions $\Theta_{j,k}$, $j = 1,2,3,4$, giving

$$S(\tau_1,\eta) = \sqrt{\eta}\sum_{k=0}^{\infty}\eta^k\Theta_{1,k}(\tau_1) + \eta\sum_{k=0}^{\infty}\eta^k\Theta_{2,k}(\tau_1) + \sqrt{\eta}\sum_{k=0}^{\infty}\eta^k\Theta_{3,k}(\tau_1) + \eta\sum_{k=0}^{\infty}\eta^k\Theta_{4,k}(\tau_1). \quad (2.70)$$

Noting that each series consists only of powers τ_1^m with the same $m \mod 4$, and comparing this with the expression for τ_1 in (2.66), this indicates that the functions $\Theta_{j,k}$ for $j = 1,\ldots,4$ must have the symmetries

$$\Theta_{1,k}(-\mathrm{i}\tau_1) = -\mathrm{i}\Theta_{1,k}(\tau_1), \qquad \Theta_{2,k}(-\mathrm{i}\tau_1) = -\Theta_{2,k}(\tau_1), \quad (2.71)$$

$$\Theta_{3,k}(-\mathrm{i}\tau_1) = \mathrm{i}\Theta_{3,k}(\tau_1), \qquad \Theta_{4,k}(-\mathrm{i}\tau_1) = \Theta_{4,k}(\tau_1). \quad (2.72)$$

At this stage, it might be expected that one should express the governing equation (2.59) in terms of η, and perform an expansion in this variable; however, a comparison of the terms in (2.67) and (2.68) suggests that iterating the map once leads to a simplification.

Writing the x dependence explicitly, the equation becomes:

$$S(x+2\varepsilon,\varepsilon) = (3+\varepsilon)^2[1-2\hat{R}(x+\varepsilon,\varepsilon)-(3+\varepsilon)(1-2\hat{R}(x,\varepsilon)-S(x,\varepsilon))S(x,\varepsilon)] \times (1-2\hat{R}(x,\varepsilon)-S(x,\varepsilon))S(x,\varepsilon), \tag{2.73}$$

This expression does not contain any $S(x+\varepsilon,\varepsilon)$ terms, and instead only contains the double iteration term, $S(x+2\varepsilon,\varepsilon)$. This is convenient, as the expression for $\tau_1(x+2\varepsilon,\varepsilon)$ is substantially simpler than $\tau_1(x+\varepsilon,\varepsilon)$, as it does not contain $g(x,\varepsilon)$. This simplifies significantly the subsequent analysis.

Expressing the left-hand term in (2.73) in terms of τ_1 and η gives

$$S(x+2\varepsilon,\varepsilon) = S(-(\varepsilon(4+\varepsilon)-1)\,\tau_1,\varepsilon) = S(-(1+12\eta+6\eta^2)\tau_1,\eta). \tag{2.74}$$

Rewriting (2.73) in terms of τ_1 and η therefore gives

$$\begin{aligned} S(-(1+12\eta+6\eta^2)\tau_1,\eta) = S(\tau_1,\eta)\Big(1-\alpha\sqrt{2+12\eta+6\eta^2}+(1+\sqrt{6}(1+\eta))S(\tau_1,\eta)\Big) \\ \times\Big(1+\alpha\sqrt{2+12\eta+6\eta^2}-(1+\sqrt{6}(1+\eta))^2S(\tau_1,\eta)^2 \\ -S(\tau_1,\eta)(1+\sqrt{6}(1+\eta))\Big(1-\alpha\sqrt{2+12\eta+6\eta^2}\Big)\Big). \end{aligned} \tag{2.75}$$

Analogously to the analysis of the 2-periodic case in Appendix A.1, the next step is to expand this expression as a power series in η, and apply the series expression for $S(\tau_1,\eta)$ given in (2.69). Matching powers of $\eta^{j/2}$ for $j=1,\dots 4$ produces a system of four equations – two of these equations are algebraic, and two are nonlinear ordinary differential equations in τ_1. These four equations may be simplified using the symmetry relations in (2.71)–(2.72), resulting in the following system of equations

$$\Theta_{4,0}(\tau_1) = 2a\Theta_{1,0}(\tau_1)\Theta_{3,0}(\tau_1), \tag{2.76}$$

$$\Theta_{2,0}(\tau_1) = a\Theta_{1,0}(\tau_1)^2 + a\Theta_{3,0}(\tau_1)^3, \tag{2.77}$$

$$\tau_1\Theta'_{1,0}(\tau_1) = \Theta_{1,0}(\tau_1) - b(\Theta_{3,0}(\tau_1)^3 + 3\Theta_{1,0}(\tau_1)^2\Theta_{3,0}(\tau_1)), \tag{2.78}$$

$$\tau_1\Theta'_{3,0}(\tau_1) = \Theta_{3,0}(\tau_1) - b(\Theta_{1,0}(\tau_1)^3 + 3\Theta_{3,0}(\tau_1)^2\Theta_{1,0}(\tau_1)), \tag{2.79}$$

where

$$a = \frac{1}{2}\left(2 + 2\sqrt{6} - 3\alpha(\sqrt{2} + 2\sqrt{3})\right), \qquad b = \frac{5}{6}\left(14 + 4\sqrt{6} - \alpha(7\sqrt{2} + 4\sqrt{3})\right). \quad (2.80)$$

By substituting the power series (2.69) into the governing equation (2.75), it can be seen at leading order as $\eta \to 0$ and $\tau_1 \to 0$ that $S_{1,0} = -S_{3,0}$, providing one initial condition for the system (2.76)–(2.79). The second initial condition may be chosen arbitrarily, as this choice may be absorbed into the expression for σ_1, in the same manner as the constant c_1 in (2.39). For algebraic convenience, and without loss of generality, one fixes $S_{1,0} = 1$. These conditions are sufficient to uniquely solve (2.76)–(2.79). The solution to this system is given by

$$\Theta_{1,0}(\tau_1) = \frac{\alpha\tau_1}{\sqrt{2 - 2b^2\,\tau_1^4}}\sqrt{1 + \sqrt{1 - b^2\tau_1^4}}, \qquad \Theta_{2,0}(\tau_1) = -\frac{a\tau_1^2}{1 - b^2\tau_1^4}, \quad (2.81)$$

$$\Theta_{3,0}(\tau_1) = -\frac{\alpha b\tau_1^3}{\sqrt{2 - 2b^2\,\tau_1^4}}\left(\sqrt{1 + \sqrt{1 - b^2\tau_1^4}}\right)^{-1}, \qquad \Theta_{4,0}(\tau_1) = \frac{ab\tau_1^4}{1 - b^2\tau_1^4}. \quad (2.82)$$

In principle, one can match the expansion of (2.75) at higher powers of η in order to obtain $\Theta_{j,k}$ for $j = 1, \ldots 4$ with $k > 0$. For the purposes of this example, however, the first four terms of the series will produce a useful approximation for the solution behaviour.

The final step is to determine the behaviour of the transseries parameter σ_1. This is slightly more complicated than in the 2-periodic problem, as the behaviour of $\hat{R}(x, \varepsilon)$ must be incorporated into the calculations. The details of this process are found Appendix A.2, where it is shown that

$$\sigma_1 = -\frac{1}{50}\left(3\sqrt{2} - 16\sqrt{3} - 7\sqrt{6} + 12\right) + \frac{\eta}{500}\left(297\sqrt{2} - 709\sqrt{3} - 189\sqrt{2} + 399\right) + \mathcal{O}(\eta^2), \quad (2.83)$$

Now determined enough transseries terms have been determined to accurately approximate the solution behaviour in the 4-periodic regime.

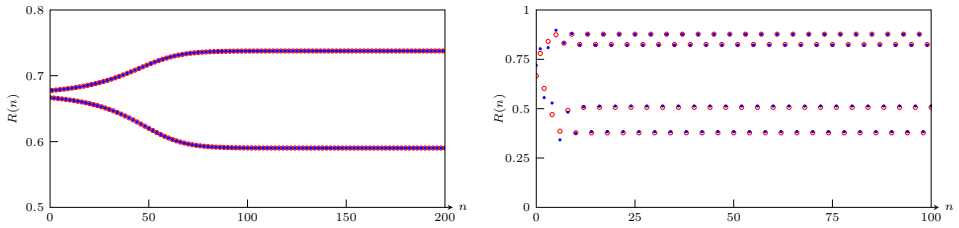

(A) Exact solution (red circles) and 2-periodic approximation (blue dots) for $\varepsilon = 0.05$.

(B) Exact solution (red circles) and 4-periodic approximation (blue dots) for $\varepsilon = 0.51$.

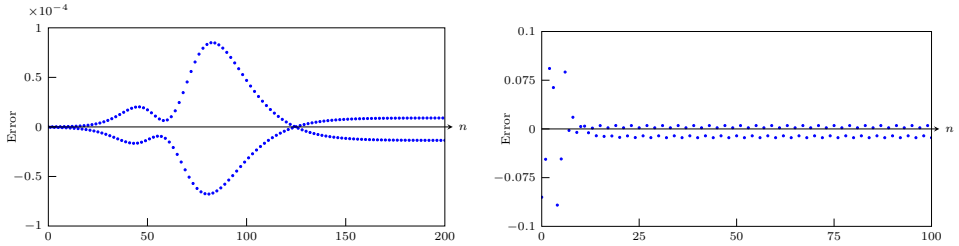

(C) 2-periodic approximation error for $\varepsilon = 0.05$.

(D) 4-periodic approximation error for $\varepsilon = 0.51$

FIGURE 2.4: The plot in (a) compares the 2-periodic approximation $R_{2,\text{app}}$, from (2.84), against the exact solution for $\varepsilon = 0.05$. The plot in (b) compares the 4-periodic approximation $R_{4,\text{app}}$, from (2.86), against the exact solution for $\varepsilon = 0.51$, or $\sqrt{6\eta} \approx 0.0605$. The approximation errors, given by the difference between the exact solution $R(x)$ and the approximations are shown in (c) and (d). The 2-periodic approximation has maximum error in the region just before reaching the 2-periodic steady solution. The 4-periodic approximation has maximum error in the initial region; this is to be expected, as the initial condition was obtained directly from the 2-periodic solution, and is not expected to be highly accurate in the 4-periodic regime. Taken from [2].

2.2.6 Error comparison

As a consequence of the preceding analysis, it is possible to derive an approximation for the solution to the logistic equation in the 2-periodic and 4-periodic parameter regimes, which is denoted as $R_{2,\text{app}}(x)$ and $R_{4,\text{app}}(x)$ respectively. Combining (2.32), (2.31), and (2.42), it is found that in the 2-periodic parameter regime

$$R(x) \approx R_{2,\text{app}}(x) = \frac{2+\varepsilon}{3+\varepsilon} + \varepsilon^{1/2}\Omega_{o,0}(\tau_0) + \varepsilon\Omega_{e,0}(\tau_0) + \varepsilon^{3/2}\Omega_{o,1}(\tau_0) + \varepsilon^2\Omega_{e,1}(\tau_0), \quad (2.84)$$

where τ_0 and σ_0 are approximated as

$$\tau_0 = \sigma_0\varepsilon^{1/2}\mathrm{e}^{-x(\pi\mathrm{i}+\log(1+\varepsilon))/\varepsilon}, \qquad \sigma_0 \approx -\frac{1}{9} + \frac{4\varepsilon}{81} - \frac{19\varepsilon^2}{648}. \quad (2.85)$$

A comparison of the exact solution against the approximation is shown for $\varepsilon = 0.05$ in Figure 2.4(a). The exact solution is shown as red circles, while the approximation is shown as blue dots. The two curves are visually indistinguishable. The approximation

error is shown in Figure 2.4(c). It is clear from this figure that the error has a peak at the end of the transition region, just before the solution settles into the stable 2-periodic behaviour.

In the 4-periodic parameter regime $\varepsilon > -2 + \sqrt{6}$, the approximated transseries is given combining the expressions in (2.66), (2.81)–(2.83), and the previous approximation (2.84), to give

$$R(x) \approx R_{4,\text{app}}(x) = R_{2,\text{app}}(x) + \sqrt{\eta}(\Theta_{1,0}(\tau_1)+\Theta_{3,0}(\tau_1)) + \eta(\Theta_{2,0}(\tau_1) + \Theta_{4,0}(\tau_1)), \tag{2.86}$$

where τ_1 and σ_1 are approximated as

$$\tau_1 = \sigma_1 \varepsilon^{1/2} \mathrm{e}^{x(\log(1-\varepsilon(4+\varepsilon))/2+\pi\mathrm{i})/\varepsilon}, \tag{2.87}$$

$$\sigma_1 \approx -\frac{1}{50}\left(3\sqrt{2} - 16\sqrt{3} - 7\sqrt{6} + 12\right) + \frac{\eta}{500}\left(297\sqrt{2} - 709\sqrt{3} - 189\sqrt{2} + 399\right). \tag{2.88}$$

Note that the term containing $g(x,\varepsilon)$ in $B(x,\varepsilon)$ from (2.63) is not included. This term disappears for integer values of n, and therefore can be omitted at this stage without altering the approximation.

In Figure 2.5(a), the approximation error for a range of values of ε is shown, where the error is measured as the maximum difference between the exact solution and the transseries approximation, shown as a blue curve. This error measure was chosen to allow for direct comparison with equivalent results from [3], which are shown as a red curve. The transseries approximation is more accurate than the multiple scales approximation in this parameter regime, and the error decays faster in the limit that $\varepsilon \to 0$. The reason for this behaviour is that the transseries approach allowed for higher-order exponential corrections to be easily computed and retained. The maximum approximation error occurs at the end of the transition region between non-periodic and 2-periodic behaviour, where the exponential contributions contribute significantly to the solution behaviour. Computing these exponential corrections using multiple scales methods would be an algebraically significantly more demanding task, requiring matched asymptotic expansions to be applied at higher orders of the expansion.

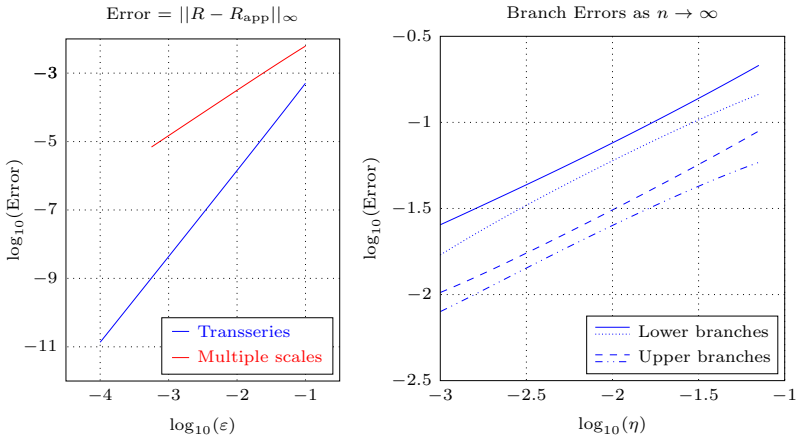

(A) Error for 2-Periodic Approximation

(B) Error for 4-Periodic Approximation

FIGURE 2.5: The plot in (a) shows the resummed transseries approximation error in blue, corresponding to the maximum difference between the approximated and exact value. This measure of the error was chosen to be consistent with the error measure provided in [3]; this error is shown as a red curve. Due to the ease with which the transseries method captures higher-order exponential behaviour, which plays an important role in the transition region between non-periodic and 2-periodic behaviour, it outperforms the multiple scales approximation. In (b), the error of the four solution branches as $n \to \infty$ is shown, approximated by taking $|R - R_{4,\text{app}}|$ on each of the four branches for a value of n sufficiently large that the error is not visibly changing. For each of the four branches, the error decreases as $\eta \to 0$, as would be expected. Taken from [2].

2.2.7 8-periodic solution

This process may be continued to understand the emergence of the next period doubling bifurcation. It will be shown that the exponential factor can be used to identify the appearance of 8-periodic stable solutions as ε is increased further.

The method from Section 2.2.5 can be applied again in order to obtain approximations for solutions with even higher periodicity. One can now write the next term in the transseries such that $R(x,\varepsilon) = \hat{R}(x,\varepsilon) + S(x,\varepsilon) + T(x,\varepsilon)$. The quantity $T(x,\varepsilon)$ is defined in terms of a new transseries parameter σ_2 to be

$$T(x,\varepsilon;\sigma_2) = \sum_{m=1}^{\infty} \sigma_2^m \mathrm{e}^{-mF(x,\varepsilon)/\varepsilon} T_m(\varepsilon). \tag{2.89}$$

The transseries terms $\hat{R} + S$ capture the 4-periodic solution behaviour, and therefore must tend to the 4-periodic solution in the limit that τ_0 and τ_1 become large. This solution is denoted as $R_4(\varepsilon)$. Hence, the expression $R(x,\varepsilon) = R_4(\varepsilon) + T(x,\varepsilon)$ is applied

to the governing equation (2.16) an expression for the exponential weights is found, in similar fashion to the process for obtaining (2.25) or (2.62).

The exponential weights may again be written in the form $F(x,\varepsilon) = f(\varepsilon)x + \varepsilon g(x,\varepsilon)$, where g disappears on $n \in \mathbb{Z}$. The behaviour of $f(\varepsilon)$ is illustrated in Figure 2.6. A very similar set of inferences may be drawn from this image as for Figure 2.3. In region ①, the 8-periodic behaviour does not contribute to the solution, as discussed for the 4-periodic case in Section 2.2.5.2. This 8-periodic contribution appears in the transseries as ε moves into region ②. In this range of ε, there are 8-periodic contributions to the solution, but they are smaller than the 4-periodic solution contribution, as the exponential term is relatively small compared to those in $S(x,\varepsilon)$, decaying exponentially as $x \to \infty$. Finally, in region ③, the 8-periodic solution grows exponentially, and the behaviour of $T(x,\varepsilon)$ dominates the solution behaviour.

It is therefore clear that the onset of these higher periodicity solutions can be explained by explicitly studying the exponential weights of the transseries solution; while the algebraic complexity of the process increases after each doubling, the steps for identifying this behaviour remain essentially the same. The resummed transseries therefore provides a systematic approach to studying bifurcations even for larger values of the bifurcation parameter, where classical asymptotic methods typically fail.

2.3 Dynamical Logistic Equation

In the previous section, the classical logistic equation has been studied, and it has been shown that the higher periodicity solutions may be obtained directly using a transseries approach. In this section, a more complicated variant of this problem is considered, known as the slowly-varying logistic equation.

$$Y_{n+1} = (\lambda_0 + \varepsilon n)\, Y_n\, (1 - Y_n)\,, \qquad 0 < Y_0 < 1, \tag{2.90}$$

with $\varepsilon > 0$. The bifurcation parameter is given by $\lambda = \lambda_0 + \varepsilon n$, and in this case, it changes slowly over time. In previous studies [51, 52, 49], this has been shown as an example of a "canard" solution, in which the behaviour appears to remain near the unstable solution for an extended period of time, before rapidly jumping to approach the stable

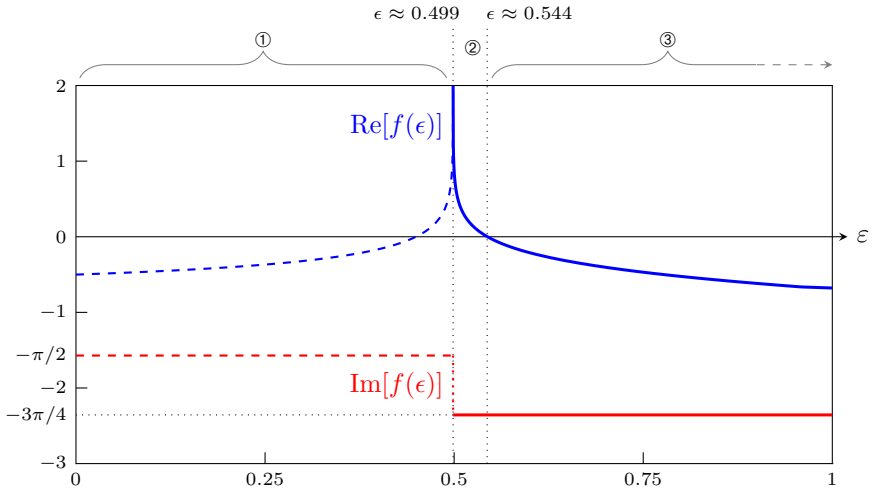

FIGURE 2.6: This figure shows the real and imaginary parts of $f(\varepsilon)$, where $F(x,\varepsilon) = f(\varepsilon)x + \varepsilon g(x,\varepsilon)$. The behaviour of the transseries depends on both the real and imaginary part of this quantity, in the same fashion as Figure 2.3. The exponential contribution is not present in the transseries in parameter regime ①. In regimes ② and ③ the contribution is present, and must be 8-periodic, due to the value of $\mathrm{Im}[f(\varepsilon)]$ in these regimes. In regime ②, the 8-periodic contribution is small, due to the positive sign of $\mathrm{Re}[f(\varepsilon)]$, and this contribution becomes significant in regime ③, as the sign of $\mathrm{Re}[f(\varepsilon)]$ becomes negative. Taken from [2].

solution with higher periodicity. As n increases, this parameter will pass through values across which the solution stability is known to change. When $\lambda_0 + \varepsilon n = 3$, the 1-periodic equilibrium becomes unstable, and the 2-periodic equilibrium becomes stable. As n increases further, eventually λ exceeds $1 + \sqrt{6}$, and the 2-periodic equilibrium becomes unstable, with the 4-periodic equilibrium becoming stable. This process continues until the bifurcation parameter becomes sufficiently large that the solution becomes chaotic. For the problem studied here, $\lambda_0 = 3$ and $y(0) = 2/3$ will be set.

In [3], it was shown that a discrete multiple scales approach can be used to describe this behaviour asymptotically. This approach required balancing several different timescales, and using asymptotic matching to connect the solutions in each different asymptotic region.

In this section, it will be shown that this process can be described using a transseries approach, with the resulting expansion to be valid even as the solution behaviour changes dramatically, and increases in periodicity. It will now be shown that transseries provide a systematic and generally more accurate approach than the multiple scales procedure of [3] in describing the solution behaviour as it transitions from an unstable

to a stable manifold; this will demonstrate that transseries expansions can be used to effectively capture canard behaviour in discrete systems.

The first stability transition will be shown in detail. Subsequently an outline of how this method can be extended to describe the second transition will be provided, together with some results.

2.3.1 2-periodic solution

2.3.1.1 Transseries ansatz

The difference from (2.16) above is that in the prefactor of the r.h.s. the perturbative parameter ε is replaced now by x. Again one begins by applying a multiple scales ansatz, and expanding as a transseries in a continuous variable x. Setting $x = \varepsilon n$ and $R(x) = y(n)$ gives

$$R(x+\varepsilon) = (3+x)\,R(x)\,(1-R(x))\,, \qquad R(0) = \tfrac{2}{3}. \tag{2.91}$$

An ansatz for the solution in terms of ε and a transseries parameter σ_0 is again formulated. The ansatz is identical to that given in (2.15), but has been included below for convenience:

$$R(x,\varepsilon;\sigma_0) = \sum_{m=0}^{\infty} \sigma_0^m \mathrm{e}^{-mA(x)/\varepsilon} R_m(x,\varepsilon), \qquad R_m(x,\varepsilon) \simeq \varepsilon^{\beta_m} \sum_{k=0}^{\infty} \varepsilon^k R_{m,k}(x), \tag{2.92}$$

where β_m will again be chosen such that $R_{m,0}$ takes nonzero value.

It is straightforward to compute the first few terms of the algebraic portion of the series expression, corresponding to $m = 0$ in (2.92), which gives a power series expression for the non-periodic manifold. The recursion relation is given obtained by expanding $R(x+\varepsilon)$ using a power series in ε, and matching powers of ε in the resultant expression. This process gives

$$R_{0,0}(x) = \frac{2+x}{3+x}, \tag{2.93}$$

$$R_{0,k}(x) = -\frac{1}{(2+x)}\left[\sum_{n=1}^{k} \frac{1}{n!} R_{0,k-n}^{(n)}(x) + (3+x)\sum_{n=1}^{k-1} R_{0,n}(x) R_{0,k-n}(x)\right], \qquad k \geq 1. \tag{2.94}$$

The first few iterations of this recurrence relation give

$$\begin{aligned} R_{0,1}(x) &= -\frac{1}{(x+2)(x+3)^2}, \\ R_{0,2}(x) &= \frac{x^2+x-4}{(x+2)^3(x+3)^3}, \\ R_{0,3}(x) &= -\frac{x^4-2x^3-28x^2-33x+24}{(x+2)^5(x+3)^4}. \end{aligned} \tag{2.95}$$

This process may be continued indefinitely in order to continue calculating terms in the power series for the non-periodic manifold. This process will not, however, capture the transition to the 2-periodic manifold. In order to obtain an approximation for this behaviour, one must consider the terms in the ansatz (2.92) with $m \neq 0$. Continuing to the next order in σ_0, one finds that

$$\mathrm{e}^{-[A(x+\varepsilon)-A(x)]/\varepsilon} R_1(x+\varepsilon,\varepsilon) = (3+x) R_1(x,\varepsilon)[1-2R_0(x,\varepsilon)]. \tag{2.96}$$

As before, the argument of the exponential may be determined by expanding R_1 as a power series in ε, as well as expanding $A(x+\varepsilon) = A(x) + \varepsilon A'(x) + \cdots$. At leading order in ε, this gives the differential equation

$$\mathrm{e}^{-A'(x)} = -(x+1) = \mathrm{e}^{-(2p+1)\pi\mathrm{i}+\log(x+1)}, \qquad p \in \mathbb{Z}. \tag{2.97}$$

Hence, one obtains

$$A(x) = (2p+1)\pi\mathrm{i}\, x + x - (x+1)\log(x+1), \tag{2.98}$$

where the same reasoning as in the analysis used to determine (2.25) is followed, and one absorbs the constant into the series parameter. Note that in principle it is possible to have several exponential weights at the same time. In that case a multiple-parameter transseries approach would be necessary. In Appendix A.3 it is proven that it is always possible to reduce the multiple parameter transseries to a transsummation of a single variable. From a practical perspective, it is enough to note that for $x = n\,\varepsilon$, the value of the exponential $\exp(-A(x)/\varepsilon)$ is a real number and does not depend on the choice of the integer p in (2.98). Hence without loss of generality $p = 0$ is set. Once $A(x)$ has been determined, it is possible to obtain a recurrence relation for $R_m(x)$ by applying the first ansatz expression in (2.92) to the governing equation (2.91), and matching powers

of the transseries parameter σ_0. This gives

$$(-1)^m(1+x+\varepsilon)^m \,\mathrm{e}^{m((1+x)\log(1+\varepsilon/(1+x))/\varepsilon-1)}R_m(x+\varepsilon,\varepsilon) \\ =(3+x)R_m(x,\varepsilon)[1-2R_0(x,\varepsilon)]-(3+x)\sum_{n=1}^{m-1}R_n(x,\varepsilon)R_{m-n}(x,\varepsilon). \tag{2.99}$$

It is now possible to apply the second part of the ansatz in (2.92) and to match powers of ε in this expression. By direct substitution, one finds that $\beta_m = m$ gives the result that $R_{m,0}$ is nonzero. By subsequently matching terms which are $\mathcal{O}(\varepsilon)$ in the small ε limit, it is possible to generate an equation for $R_{1,0}$ and a recurrence relation for $R_{m,0}$ for $m \geq 2$. One finds that

$$(x+1)R'_{1,0}(x) = -\left(\frac{2}{x+2}-\frac{2}{x+3}+\frac{1}{2}\right)R_{1,0}, \tag{2.100}$$

The initial condition in (2.100) may be chosen arbitrarily, as this choice may be absorbed into the transseries parameter. Choosing $R_{1,0}(0) = 1$ gives

$$R_{1,0}(x) = \frac{3(x+2)^2}{4(x+1)^{3/2}(x+3)}. \tag{2.101}$$

The recurrence relation for subsequent terms is given by

$$\left[(-1)^m(1+x)^m+(1+x)\right]R_{m,0}(x) = -(3+x)\sum_{n=1}^{m-1}R_{n,0}(x)R_{m-n,0}(x), \qquad m \geq 2. \tag{2.102}$$

Continuing to match higher powers of ε allows for the direct computation of terms further terms such as $R_{m,k}$, obtained by matching terms which are $\mathcal{O}(\varepsilon^k)$ in the small ε limit. The direct computation of further terms is not required for the present analysis.

2.3.1.2 Computing terms in the resummed transseries

Motivated by the analysis of the static system, and in particular the form of (2.15), the order of summation in the transseries (2.92) is switched, writing it as

$$R(x,\varepsilon;\sigma_0) \simeq \sum_{k=0}^{\infty}\varepsilon^k\sum_{m=0}^{\infty}\left(\sigma_0\varepsilon\mathrm{e}^{-A(x)/\varepsilon}\right)^m R_{m,k}. \tag{2.103}$$

A main difference from the static one is that the expansion in powers of ε is asymptotic, while the sum over the exponentials ($m \geq 0$) is convergent. Thus (2.103) is a formal expansion.

As for the static system, a new series parameter τ_0 is defined, and new quantities $\Omega_k(\tau_0)$ such that

$$\tau_0 = \sigma_0 \varepsilon \mathrm{e}^{-A(x)/\varepsilon}, \qquad \Omega_k(\tau_0) = \sum_{m=0}^{\infty} \tau_0^m R_{m,k}. \tag{2.104}$$

It will be helpful later to note that

$$\tau_0(x+\varepsilon) = \mathrm{e}^{-(A(x+\varepsilon)-A(x))/\varepsilon}\tau_0(x) = \tau_0(x)\left[\mathrm{e}^{-A'(x)} + \mathcal{O}(\varepsilon)\right] \quad \text{as} \quad \varepsilon \to 0. \tag{2.105}$$

The transseries expression in (2.103) is now given by

$$R(\tau_0, \varepsilon) \simeq \sum_{k=0}^{\infty} \varepsilon^k \Omega_k(\tau_0). \tag{2.106}$$

This expression can now be applied to (2.91) and match orders of ε. At leading order, one finds that

$$\Omega_0\left(\mathrm{e}^{-A'(x)}\tau_0\right) = (3+x)\Omega_0(\tau_0)(1-\Omega_0(\tau_0)), \tag{2.107}$$

where (2.105) was used to obtain the leading-order on the left-hand side. At this stage, one could mechanically obtain the function Ω_0 as a Taylor series in τ_0, which is convergent, with some finite radius of convergence. It happens, however, that there exists a particularly convenient variable transformation that converts the right-hand side from a dilation to a translation. If a new variable y is defined such that $y = -x\log(\tau_0)/A'(x)$, the expression in (2.107) becomes (see Appendix A.3.1)

$$\Omega_0(y+x) = (3+x)\Omega_0(y)(1-\Omega_0(y)). \tag{2.108}$$

This expression has the same form as the static logistic map equation, given in (2.16), with x in place of ε. The equation for $\Omega_1(y)$ is also derived in Appendix A.3.1. Furthermore, since $x = \varepsilon n$, it is valid to apply the asymptotic solution derived for this expression in Section 2.2.1. As the goal is to capture the first transition, across which the solution switches from having no periodic component to having a 2-periodic component, the transseries expression for the 2-periodic solution given in (2.31) can directly be applied.

In order to take into account the form of (2.108), one must replace ε and x with x and

y respectively in (2.31). The τ_0 in this expression must also be replaced with a new transseries parameter $\overline{\tau}_0$, in which ε and x are again replaced with x and y respectively. This gives

$$\overline{\tau}_0(y,x) = \overline{\sigma}_0\sqrt{x}\mathrm{e}^{-\mathrm{i}\pi y/x + y\log(1+x)/x} = \overline{\sigma}_0\sqrt{x}\mathrm{e}^{(\mathrm{i}\pi+\log(1+x))\log(\tau_0)/A'(x)} = \overline{\sigma}_0\sqrt{x}\tau_0, \tag{2.109}$$

where $\overline{\sigma}_0$ is a new transseries parameter that remains to be determined. Making the appropriate substitutions in (2.31) now gives the form of $\Omega_0(y)$ as

$$\Omega_0(y) = \frac{2+x}{3+x} + \sqrt{x}\sum_{k=0}^{\infty} x^k\Omega_{o,k}(\overline{\tau}_0) + x\sum_{k=0}^{\infty} x^k\Omega_{e,k}(\overline{\tau}_0), \tag{2.110}$$

where $\Omega_{o,k}$ and $\Omega_{e,k}$ are defined in (2.32), and $\Omega_{o,k}$ and $\Omega_{e,k}$ for $k=0$ and $k=1$ are given explicitly in (2.42) respectively.

In a typical problem of this form, $\overline{\sigma}_0$ would be determined using the fact that $\Omega_0 = 2/3$ at $y=0$; however, this is enforced by the transformation $y = -x\log(\tau_0)/A'(x)$, which forces x to be zero if $y=0$. Consequently, the initial condition cannot be used to determine $\overline{\sigma}_0$. This is to be expected, as the the initial condition will instead be used to determine the original transseries parameter σ_0.

Instead, the expression in (2.110) is expanded as a Taylor series about $x=0$ using the form of $\Omega_{o,0}$ and $\Omega_{e,0}$ given in (2.42). This gives

$$\Omega_0(y) = \frac{2+x}{3+x} + \overline{\sigma}_0 x\tau_0 - \frac{3}{2}(\overline{\sigma}_0 x\tau_0)^2 + \ldots, \tag{2.111}$$

where the omitted terms are $\mathcal{O}(x^3\tau_0^2)$. One may now match powers of τ_0 with (2.103) to determine that $x\overline{\sigma}_0 = R_{1,0}$, which was explicitly calculated in (2.101). Therefore one finds that

$$\overline{\sigma}_0 = \frac{3(x+2)^2}{4x(x+1)^{3/2}(x+3)}. \tag{2.112}$$

2.3.1.3 Initial Condition

All of the required quantities for the transseries approximation have now been explicitly calculated except for σ_0, which must be determined from the initial condition at $x=0$. At $x=0$, it follows that $\tau_0 = \sigma_0\varepsilon$. Consequently, the initial condition is given by $R(\tau_0 = \sigma_0\varepsilon, x=0) = 2/3$, which is applied to the first expression in (2.92). Then σ_0 is

expressed as a power series in ε, where the series terms are functions of $R_{m,k}$ for various values of m and k, giving

$$\sum_{m=0}^{\infty} \sigma_0^m R_m(0,\varepsilon), \quad \text{where} \quad \sigma_0 = \sum_{j=0}^{\infty} \varepsilon^j \sigma_{0,j}. \tag{2.113}$$

Using the second expression from (2.92) and matching powers of ε allows to compute $\sigma_{0,j}$. Enough $R_{m,k}$ terms have been obtained to solve for $\sigma_{0,0}$, giving

$$\sigma_0 = -R_{0,1} + \mathcal{O}(\varepsilon) = \frac{1}{18} + \mathcal{O}(\varepsilon). \tag{2.114}$$

Computing subsequent series terms for σ_0 requires values of $R_{m,k}$ that are not presented in this study, as even this first order approximation is sufficiently accurate as will be shown.

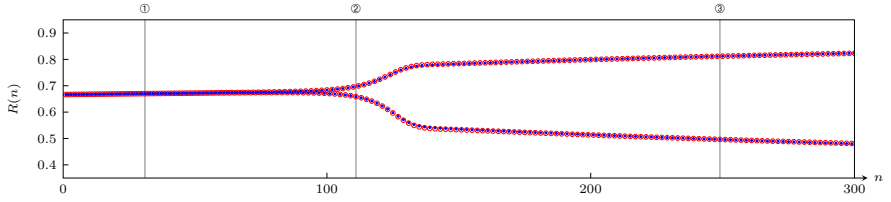

(A) Exact solution (red circles) and transseries approximation (blue dots) for $\varepsilon = 0.001$.

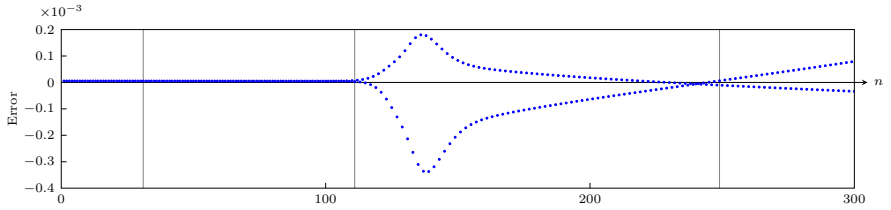

(B) Approximation error for $\varepsilon = 0.001$.

FIGURE 2.7: The plot in (a) shows the approximation (2.115) and exact solution of (2.90) for $\varepsilon = 0.001$. The difference between these is shown in (b). The points labeled ①, ② and ③ will be referenced below in Figure 2.8. It is seen that the error reaches a maximum at the start of the 2-periodic regime. It then decreases, although will eventually increase as n grows, due to the increasing influence of the 4-periodic region which was not computed. Note that the small error at the point labelled ③ corresponds to the value where the approximation crosses the exact solution. This occurs at some point in the 2-periodic region for any choice of ε, and therefore does not signify a special parameter choice. It is an artifact of the error calculation. Taken from [2].

2.3.2 Error comparison

As a consequence of the preceding analysis, it is possible to derive an approximation for the solution to the slowly-varying logistic equation (2.91), which is denoted R_{app}. Combining (2.32), (2.104), (2.109), (2.110), (2.112) and (2.114), one finds an approximation for the transseries solution

$$R(x) \approx R_{\text{app}}(x) = \frac{2+x}{3+x} + x^{1/2}\Omega_{o,0}(\overline{\tau}_0) + x\Omega_{e,0}(\overline{\tau}) + x^{3/2}\Omega_{o,1}(\overline{\tau}_0) + x^2\Omega_{e,1}(\overline{\tau}_0), \tag{2.115}$$

where

$$\overline{\tau}_0 \approx \frac{\epsilon(x+2)^2 \mathrm{e}^{-(\pi \mathrm{i} x + x - (x+1)\log(x+1))/\varepsilon}}{24x^{1/2}(x+1)^{3/2}(x+3)}. \tag{2.116}$$

The most useful feature of this approximation is that it is valid before, during, and after the transition region in the slowly-varying logistic equation. An example comparison is illustrated in Figure 2.7(a), corresponding to $\varepsilon = 0.001$. The approximation is shown as blue dots, and overlaid on top of the exact solution, shown as red circles. The two solutions are visually almost indistinguishable.

The approximation error for this example is shown in Figure 2.7(b), calculated by $y(n) - R_{\text{app}}(\varepsilon n)$. The error reaches a peak following the transition region, at the beginning of the stable 2-periodic behaviour. The error does grow in this region as n becomes large, and continues to do so until the transition to 4-periodic behaviour occurs. This behaviour is not depicted in Figure 2.7(b).

In order to obtain a more complete picture of the accuracy of the transseries approximation, the approximation error was determined at three selected values of n. These values were tested in [3] relative to other methods, to obtain representative computations of the approximation error in important parts of the solution domain. The first point is $n = \lfloor 1/\sqrt{\varepsilon} \rfloor$. This point is found in the early non-periodic region before the transition from non-periodic behaviour to 2-periodic behaviour occurs. It is labelled ① in the example solution from Figure 2.7.

For comparison, the remaining representative points used in [3] need to be identified, which required the computation of an intermediate quantity K, satisfying

$$K = \sqrt{\log K - \tfrac{3}{2}\log(\varepsilon)}. \tag{2.117}$$

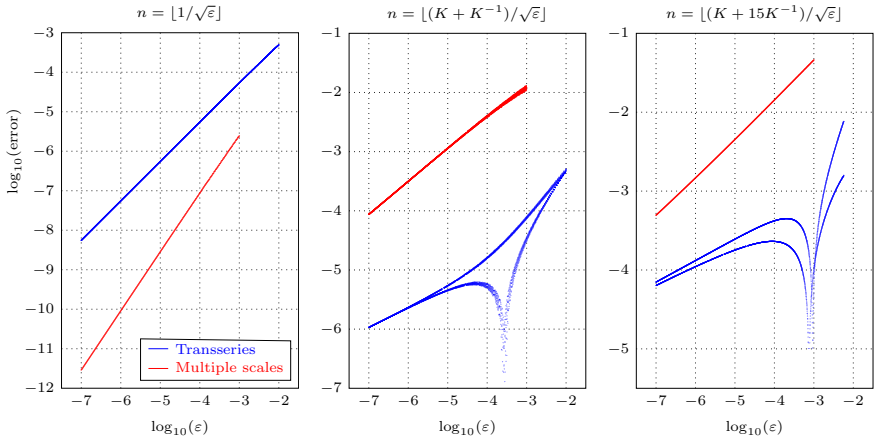

(A) Non-periodic region ①

(B) Transitional region ②

(C) 2-periodic region ③

FIGURE 2.8: This figure shows the error in the dynamic system at the three points identified in [3] as belonging to the inner region, transition region, and outer region, shown as points ①, ② and ③ in Figure 2.7. In each case, the error is shown as a blue curve. This curve becomes smaller as ε decreases. The point at which the error dips is an artifact of the observation that the approximation crosses the exact solution at the identified point for this choice of ε, and does not represent any significant phenomenon within the transseries approximation. The cause of this behaviour is explained in more detail within the description of Figure 2.7. A similar range of small parameter as in the analysis in [3] has been chosen, shown in red. The transseries outperforms the multiple scales method in both the transition region and the outer region, in which the exponential terms play an important role in describing the solution behaviour. These terms are more naturally captured using transseries methods, leading to an improved approximation. Taken from [2].

This quantity was derived in [3] although it has been adjusted to take into account the slightly different form for the slowly-varying logistic equation considered here. The second point falls within the transition region between the non-periodic unstable manifold and the 2-periodic stable manifold, and is given by $n = \lfloor K + K^{-1}/\sqrt{\varepsilon} \rfloor$. This point is labelled ② in the example solution from Figure 2.7. Finally, the error at a point in the region where the solution has completed its transition to 2-periodic stable behaviour is also determined. This point is given by $n = \lfloor K + 15K^{-1}/\sqrt{\varepsilon} \rfloor$, and is labelled ③ in the example solution from Figure 2.7. The error for each of these three points was studied in [3] allowing for direct comparison between the transseries approximation and the multiple scales approximation errors.

The error for each of the three representative points over a range of ε values may be seen in Figure 2.8, shown in blue. The error for the approximation from the multiple scales approximation in [3] is shown in red for each point. In each region, both approximations are relatively accurate. In the non-periodic region, the multiple scales approximation

outperforms the transseries approximation, while in the transition and 2-periodic region, the transseries approximation is substantially more accurate.

This outcome is sensible; the transseries approximation tracks the contribution of exponentials in the solution, and accurately incorporates them into the solution behaviour. In the non-periodic region, the solution is best represented by an algebraic power series in ε. The multiple scales approach involves calculating this power series to several terms, while our transseries approximation relies only on the leading-order behaviour of this series. In the transition and 2-periodic region, however, these exponential contributions become more significant, and this corresponds to the transseries approximation becoming more accurate than the multiple scales approximation. While the multiple scales approximation is able to capture some of the exponential behaviour, the transseries approximation is able to incorporate several exponential corrections in a straightforward fashion, producing greater accuracy in the solution regions where these corrections play an important role. Furthermore, increasing the accuracy of the transseries approximation in the non-periodic region can be done systematically by including higher corrections in ε.

Finally, note that there are points in Figure 2.8(b)–(c) where the error appears to drop to zero. This corresponds to a coincidental crossing between the approximation and actual solution occurring at this value of n. The crossing may be seen in the example solution from 2.7 at $n \approx 250$. Any solution with a reasonable amount of accuracy will have some value of n where this crossing occurs; this does not provide any added insight into the accuracy of the approximation.

2.3.3 4-periodic solution

From Figure 2.1, one sees that as n increases, eventually the bifurcation parameter becomes sufficiently large that the solution becomes 4-periodic. As discussed in Section 2.2.5.2, this higher periodicity must be encoded in the transseries solution as the weights of new exponential scales. These exponential weights do, in fact, predict the emergence of stable behaviour with higher periodicity.

A new term with transseries parameter σ_1 is included, and the analysis suggests that it is natural to define a new scaled variable $z = 2n\varepsilon$. This new contribution to the transseries,

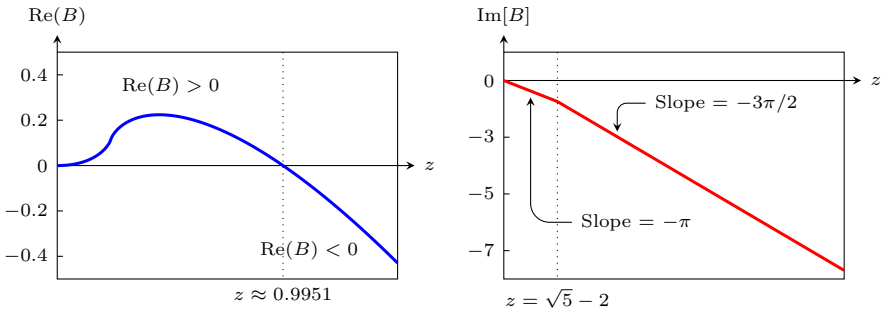

(A) Real part of $B(z)$ (B) Imaginary part of $B(z)$

FIGURE 2.9: This figure shows the real and imaginary parts of $B(z)$, corresponding to the exponential weight from (2.119). The periodicity of this contribution may be determined by identifying the slope of the imaginary part, corresponding to $\mathrm{Im}[B'(z)]$. For $z < \sqrt{5}-2$, the weight $B(z)$ contains an imaginary term $-\pi\mathrm{i}$, which corresponds to 2-periodic behaviour. After z exceeds $\sqrt{5}-2$, the slope of the imaginary term changes to $-3\pi\mathrm{i}/2$, which leads to the appearance of 4-periodic behaviour. This behaviour is not immediately apparent, as the contribution is exponentially small if $\mathrm{Re}[z] > 0$, corresponding to $z < z_0$, where $z_0 \approx 0.9951$. For $z > z_0$, the 4-periodic terms become significant in the solution behaviour. Note that, due to the bifurcation delay, this behaviour is not immediately visibly apparent in the solution; however, a careful analysis of the corresponding transseries terms will identify the transition between 2-periodic and 4-periodic behaviour. Taken from [2].

denoted $S(z,\varepsilon;\sigma_1)$, is given by

$$S(z,\varepsilon;\sigma_1) = \sum_{m=0}^{\infty} \sigma_1^m \mathrm{e}^{-mB(z)/\varepsilon} S_m(z,\varepsilon). \tag{2.118}$$

By adding S as a perturbation to the 2-period solution approximated by (2.115) and balancing terms in (2.91) in a similar fashion to Section 2.3.1.1, one obtains an equation for $B(z)$ that gives

$$\begin{aligned} B(z) = -\pi\mathrm{i}z + z - \frac{z}{2}\log(1-z(4+z)) + (\sqrt{5}-2)\log\left(\frac{\sqrt{5}-2}{\sqrt{5}-2-z}\right) \\ - (\sqrt{5}+2)\log\left(\frac{\sqrt{5}+2}{\sqrt{5}+2+z}\right), \end{aligned} \tag{2.119}$$

where the constant of integration is picked to set $B(0) = 0$ for convenience, though this choice may be absorbed into the parameter σ_1. The behaviour of $B(z)$ is depicted in Figure 2.9. There are two significant conclusions that may be drawn from this figure. In Figure 2.9(b), it is seen that

$$\mathrm{Im}[B'(z)] = \begin{cases} -\pi & z < \sqrt{5}-2 \\ -3\pi/2 & z > \sqrt{5}-2 \end{cases} \tag{2.120}$$

Noting the format of (2.118), it is seen that this exponent changes from 2-periodic behaviour to 4-periodic behaviour when crossing the value $z = \sqrt{5} - 2$. This change in exponent gives rise to 4 different branches in the solution, and therefore explains the onset of 4-periodic behaviour in the solution to the dynamical logistic equation.

The second important observation is that this 4-periodicity is not immediately apparent in the solution, due to the behaviour of $\mathrm{Re}[z]$. In Figure 2.9(a), it is seen that there is a value of z, denoted z_0 and located at $z_0 \approx 0.9951$, at which the real part of $B(z)$ changes sign from positive to negative. From the form of (2.118), one sees that this corresponds to the 4-periodic transseries contribution being exponentially small for $z < z_0$, before growing to have a significant impact on the solution behaviour for $z > z_0$.

This value of z_0 corresponds to 4-periodic behaviour becoming apparent at $n \approx 0.4975/\varepsilon$. For example, in Figure 2.1, one would expect that 4-periodic solution to become significant at $n \approx 3455$, which is consistent with the appearance of the second transition region in this image.

A more detailed transseries analysis would permit to calculate a series approximation for the 4-periodic behaviour; however, as is expected from the transseries approach, a straightforward analysis of the exponential weights in the transseries is sufficient to explain the onset of the higher periodicity, and identify the location in z (and hence, in n) where this transition to dominant 4-periodic behaviour takes place.

Finally, note that the points where the periodicity changes correspond to values of n where the real part of the exponential weights changes sign, or z_0 in Figure 2.9. In asymptotic analysis, this corresponds to the crossing of a curve known as an anti-Stokes curve. This suggests that the Stokes phenomenon plays a role in this system behaviour, in a similar fashion to the continuous delayed bifurcations in [41]. In fact, the solution does contain Stokes curves that are responsible for appearance of exponential factors in the solution; however, finding these Stokes curves requires continuing the solution in the negative-n direction, and was therefore not presented here. Nonetheless, the study the Stokes phenomenon in the dynamic logistic map is an interesting and rich subject which is beyond the scope of the present work.

2.3.4 Asymptotic analysis of the perturbative sector R_0

Remember that the perturbative sector of the transseries of the dynamical logistic equation (2.91) is given by

$$R_0(\epsilon, x) \;=\; \sum_{k=0}^{\infty} R_{0,k}(x)\epsilon^k \,. \tag{2.121}$$

The coefficients $R_{0,k}$ can be calculated using the recursion relations (2.93). The expected leading asymptotic behaviour of the coefficients $R_{0,k}$ of the asymptotic expansion for a problem with a single exponential weight A is

$$R_{0,k} \;\sim\; S\frac{\Gamma(k+\beta)}{A^{k+\beta}} \quad \text{as } k \to \infty, \tag{2.122}$$

where S is the Stokes constant up to a factor and β is a complex number yet to be determined. (2.122) is just the leading contribution of the large order relation for the perturbative sector. The reason one allows for the parameter β is that in general the non-perturbative sectors R_n may have a factor of $\varepsilon^{n\beta}$ multiplied with the power series. The prefactor $1/(2\pi\mathrm{i})$ found in the more common form of the large order relations has been absorbed into constant S in Eq. (2.122). Eq. (2.98) indicates which exponential weights $A(x)$ are theoretically possible. In order to find the constant p from (2.98), the minor of $R_0(x,\varepsilon)$ can be computed, $\mathcal{B}[\widehat{R}_0](\xi)$, and analyse its singularities on the Borel plane. One has

$$\mathcal{B}[\widehat{R}_0](\xi) \;=\; \sum_{n=0}^{+\infty} \frac{R_{0,n+1}(x)}{n!}\,\xi^n \,. \tag{2.123}$$

The singularities of $\mathcal{B}[\widehat{R}_0](\xi)$ which are nearest to the origin will are the exponential weights of the problem. In Fig. (2.10) the singularities of the Pade approximant $\mathrm{BP}_{200}[\widehat{R}_0](\xi)$ are displayed for different values of x. By comparing the singularities of $\mathrm{BP}_{200}[\widehat{R}_0](\xi)$ with the expression in (2.98) one finds that there are two exponential weights $A(x)$ and $\bar{A}(x)$. The weight $A(x)$ is given by

$$A(x) \;=\; A_{-2}(x) \;=\; x + i\pi(x+1) - (x+1)\log(x+1) + 2\,, \tag{2.124}$$

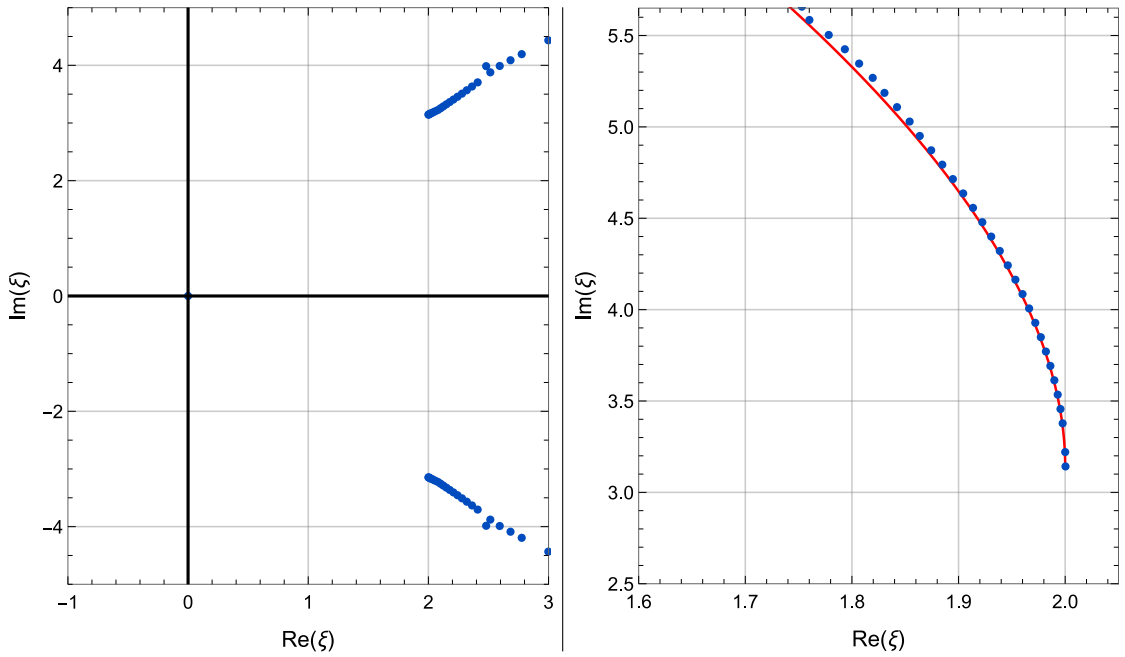

FIGURE 2.10: Left: The dots are the singularities of the Pade approximant $\mathrm{BP}_{200}[\widehat{R}_0](\xi)$ in the Borel plane for $x = 1/1000$. The points which is nearest to the origin are the positions of logarithmic singularities and the 'lines of dots' which start there represent the branch cuts. Right: The numerically computed singularities in the upper half of the Borel plane as a function of x (blue) and the function $A(x)$ from (2.124) (red).

where $A_{-2}(x)$ denotes the exponential weight (remember that from the equations it is only defined up to an additive constant) satisfying

$$A_{-2}(-2) = 0\,. \tag{2.125}$$

Since the solutions of the logistic equation are real, one expects the following asymptotic behaviour of $R_{0,k}$ (whether the real or imaginary part is chosen does not matter since a factor of i can be absorbed into the phase of S):

$$R_{0,k} \sim \mathbb{I}\mathrm{m}\left(S\frac{\Gamma(k+\beta)}{A^{k+\beta}}\right)\,. \tag{2.126}$$

By writing $S = |S|\mathrm{e}^{\mathrm{i}\alpha_S}$, $S = |A|\mathrm{e}^{\mathrm{i}\alpha_A}$ and $\beta = \beta_r + \mathrm{i}\beta_i$ Eq. (2.126) can be brought into the form

$$R_{0,k} \sim \frac{|S|\mathrm{e}^{\alpha_A\beta_i}}{|A|^{k+\beta_r}}\mathbb{I}\mathrm{m}\Big(\Gamma(k+\beta)\exp\left[\mathrm{i}\left(\alpha_S - \alpha_A(k+\beta_r) + \beta_i\log|A|\right)\right]\Big)\,. \tag{2.127}$$

Assume the $R_{0,k}$ have been calculated numerically for $k \leq N$. If N is sufficiently large, one should be able to obtain a reasonable approximation for the β by fitting the expected

asymptotic behaviour in Eq. (2.127) to the numerical data of the $R_{0,k}$. Note that due to the large growth in k of the function $|\Gamma(k+\beta)/A^{(k+\beta)}|$, the $R_{0,k}$ will vary across several orders of magnitude. This makes the fitting procedure more difficult. Therefore, first a reasonable estimate $\beta_r \approx \beta_{\text{est}}$ is found using trial and error (here $\beta_{est} = 0.672$ is used) and the function f_k is fitted to a set of redefined coefficients $\overline{R}_{0,k}$, where f_k and $\overline{R}_{0,k}$ are given by

$$f_k \equiv |S| e^{\alpha_A \beta_i} \frac{|A|^{\beta_{\text{est}}-\beta}}{\Gamma(k+\beta_{\text{est}})} \mathbb{I}\text{m}\Big(\Gamma(k+\beta)\exp\left[\text{i}\left(\alpha_S - \alpha_A\beta_r + \beta_i \log|A|\right)\right]\Big); \tag{2.128}$$

$$\overline{R}_{0,k} \equiv \frac{|A|^{k+\beta_{\text{est}}}}{\Gamma(k+\beta_{\text{est}})} R_{0,k}\,. \tag{2.129}$$

The function f_k was fitted to the coefficients $\overline{R}_{0,k}$ for $130 \leq k \leq 200$, where the four unknown real parameters which have to be determined are $(|S|, \alpha_S, \beta_r, \beta_i)$. One finds that the fit parameter β has a slight x-dependence and that the fits approximate the $\overline{R}_{0,k}$ very well. In Fig. 2.11 it is seen that the computed $\beta(x)$ stays within the complex region $[0.672,\ 0.686] + \text{i}[0.065, 0.085]$ as x is varied within the interval $[0,\ 0.2]$. However, it turns out that if one chooses coefficients $\overline{R}_{0,k}$ with larger k for the fit, the range of values across which the fit parameter β varies decreases. This seems to indicate that the x-dependence vanishes in the limit $k \to \infty$, which is the only limit for which our formula Eq. (2.126) is supposed to hold in any case. To see this, it is instructive to do the β-fits for a range of indices $[k,\ k+30]$ and compute $|\delta\beta|(k) = |\beta(0) - \beta(0.1)|(k)$. By plotting $\log(\delta\beta)$ as a function of $\log(k)$, one sees that as for large k, the dependence approximates a straight line with slope $\alpha \approx -0.71$, which hints toward a power law convergence $|\delta\beta|(k) \sim 1/k^{\alpha}$ as $k \to \infty$.

This is illustrated in Fig. 2.12. Note that previously it was assumed that the m-th sector of the transseries comes multiplied with a factor ε^m, and hence $\beta_m = m\beta = m$. Hence one might expect that $\beta = 1$. However, note that from the equations β_m is not determined and hence in this case the β that is found from the asymptotic analysis does not need to be equal to the β that was chosen to fix the factor ε^{β_m}. The exact value of β is not important. However, the results in this asymptotic analysis indicate that the β parameter is not dependent on x, which confirms that choosing a constant β in the transseries ansatz is justified.

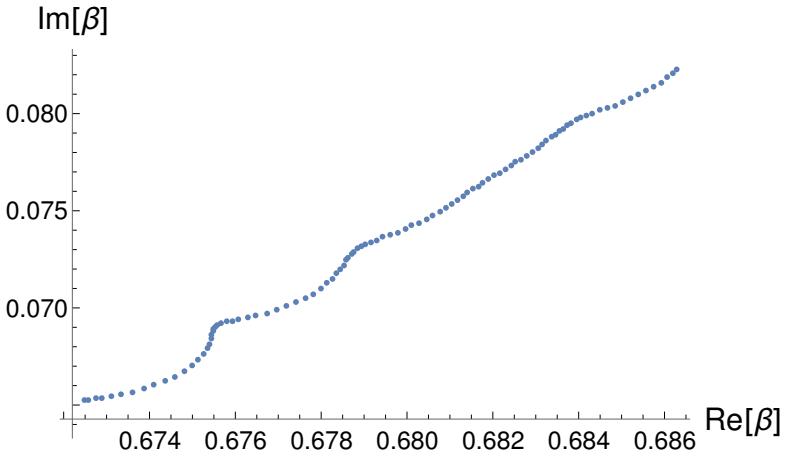

FIGURE 2.11: The fit parameter $\beta(x)$ plotted in the complex plane for different values of $x \in [0, 0.2]$. For the fitthe coefficients $\{R_{0,k}(x) \,|\, 130 \leq k \leq 200\}$ were used and the fit function f_k. At $x = 0$, β lies in the bottom left corner. β moves towards the top right corner as x increases. The values of x have been chosen by dividing the interval $[0, 0.2]$ into $N = 100$ equidistant steps with increasing x.

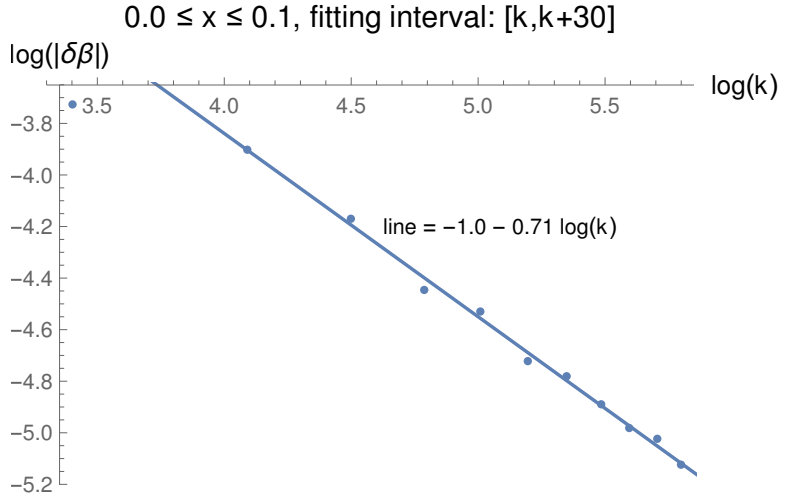

FIGURE 2.12: A double logarithmic plot of $|\delta\beta|(k)$ as a function of the first fit index k, where the coefficients $\overline{R}_j$ for $j \in [k, k+30]$ have been used as the fit data for the fit function f_k. The line is drawn to illustrate that the approximate behaviour is $|\delta\beta|(k) \sim \frac{1}{k^\alpha}$ for $\alpha \sim 0.71$ as k becomes large.

2.3.5 Asymptotic analysis of the first non-perturbative sector R_1

In this section the asymptotic behaviour of the transseries sector R_1 will be analysed. The first step is to compute the coefficients $R_{1,k}$. The following notation is introduced to factor out the prefactor β_n such that the Ψ_n are asymptotic power series in ε with x-dependent coefficients:

$$R_n(x, \varepsilon) \equiv \varepsilon^{\beta_n} \Psi_n(x, \varepsilon)\,. \tag{2.130}$$

By substituting this into Eq. (A.44) the same equation for $\Psi_n(x,\varepsilon)$ is obtained since the factor ε^{β_n} appears on both sides of the equation. The equation for Ψ_1 is

$$-(1+x)\eta(x,\varepsilon)\Psi_1(x+\varepsilon,\varepsilon) \;=\; (3+x)\Big[\,\Psi_1(x,\varepsilon)\,(1-\Psi_0(x,\varepsilon))\,\Big]\,. \tag{2.131}$$

One finds

$$\begin{aligned}\Psi_n(x,\varepsilon) \;&=\; \sum_{k=0}^{+\infty} R_{n,k}(x)\varepsilon^k\,; \quad \Psi_n(x+\varepsilon,\varepsilon) \;=\; \sum_{k=0}^{+\infty}\varepsilon^k\left(\sum_{j=0}^{k}\frac{1}{j!}\mathrm{d}_x^j R_{n,k-j}(x)\right)\,;\\ \eta(x,\varepsilon) \;&=\; \sum_{k=0}^{+\infty}\eta_k(x)\varepsilon^k\,.\end{aligned} \tag{2.132}$$

The coefficients η_k can be easily calculated by expanding Eq. (A.45). After substituting these expressions into Eq. (2.131) one is left with the following equations for the coefficients $R_{1,k}$:

$$-(1+x)\sum_{\ell=0}^{k}\eta_{k-\ell}\sum_{j=0}^{\ell}\frac{1}{j!}\mathrm{d}_x^j R_{1,\ell-j} \;=\; (3+x)\left[R_{1,k}-2\sum_{j=0}^{k}R_{1,k}R_{0,j}\right]\,. \tag{2.133}$$

It turns out that the $R_{1,k}$-terms in Eq. (2.133) cancel. One obtains an equation for $R_{1,k}$ by performing a shift $k\mapsto k+1$:

$$\begin{aligned}&-(1+x)\mathrm{d}_x R_{1,k}-\left(\frac{1}{2}+\frac{2}{(2+x)(3+x)}\right)R_{1,k}\\ &=\;(1+x)\left[\eta_1\sum_{j=1}^{k}\frac{1}{j!}\mathrm{d}_x^j R_{1,k-j}+\sum_{\ell=0}^{k-1}\eta_{k+1-j}\sum_{j=0}^{\ell}\frac{1}{j!}\mathrm{d}_x^j R_{1,\ell-j}+\sum_{j=2}^{k+1}\frac{1}{j!}\mathrm{d}_x^j R_{1,k+1-j}\right]\\ &\quad-\;2(3+x)\sum_{j=2}^{k}R_{1,k+1-j}R_{0,j}\,.\end{aligned} \tag{2.134}$$

This expression can be put into the form

$$\mathrm{d}_x R_{1,k}+F(x)R_{1,k}=G_k(x)\,, \tag{2.135}$$

where

$$F(x) = \frac{1}{1+x}\left(\frac{1}{2}+\frac{2}{(2+x)(3+x)}\right) = -\frac{2}{x+2}+\frac{1}{x+3}+\frac{3}{2(x+1)}\,; \tag{2.136}$$

$$\begin{aligned} G_k(x) &= -\left[\eta_1\sum_{j=1}^{k}\frac{1}{j!}\mathrm{d}_x^j R_{1,k-j} + \sum_{\ell=0}^{k-1}\eta_{k+1-\ell}\sum_{j=0}^{\ell}\frac{1}{j!}\mathrm{d}_x^j R_{1,\ell-j} + \sum_{j=2}^{k+1}\frac{1}{j!}\mathrm{d}_x^j R_{1,k+1-j}\right] \\ &\quad + \frac{2(3+x)}{1+x}\sum_{j=2}^{k+1} R_{1,k+1-j}R_{0,j}\,; \\ &= -\sum_{j=0}^{k-1}\left[\frac{\eta_1}{(j+1)!}\mathrm{d}_x^{j+1}R_{1,k-1-j} + \frac{1}{(j+2)!}\mathrm{d}_x^{j+2}R_{1,k-1-j}\right. \\ &\quad \left. + \eta_{k+1-j}\sum_{\ell=0}^{j}\frac{1}{\ell!}\mathrm{d}_x^{\ell}\,R_{1,j-\ell} - \frac{2(3+x)}{1+x}R_{1,k-1-j}R_{0,j+2}\right]. \end{aligned} \tag{2.137}$$

For simplicity of notation, the following definition is introduced

$$R_{1,k} \equiv Y_k\,. \tag{2.138}$$

The equation for Y_k is then

$$\begin{aligned} &LY_k(x) = G_k(x)\,; \\ &L \equiv \mathrm{d}_x + F(x)\,. \end{aligned} \tag{2.139}$$

For each k a linear differential equation of first order is obtained. First one determines the solution to the homogeneous equation

$$LY_{\mathrm{hom}}(x) = 0\,. \tag{2.140}$$

The equation can be integrated, giving

$$Y_{\mathrm{hom}}(x) = Y_0(x) = \frac{3(2+x)^2}{4(1+x)^{3/2}(3+x)}Y_{\mathrm{hom}}(0)\,, \tag{2.141}$$

where $Y_{\mathrm{hom}}(0)$ is the integration constant. Note that the result for Y_{hom} is consistent with the previous result for $R_{1,0}$, Eq. (A.53), since $G_0(x) = 0$ (in Eq. (2.137) the convention $\sum_{j=0}^{-1} = 0$ is used). Before proceeding with approximations, $Y_1(x) = R_{1,1}(x)$ is calculated

exactly. The equation for $Y_1(x)$ is

$$LY_1(x) = G_1(x)\,, \tag{2.142}$$

where

$$\begin{aligned} G_1(x) &= -\frac{1}{2}\mathrm{d}_x^2 R_{1,0}(x) - \eta_1(x)\mathrm{d}_x R_{1,0} - \eta_2(x)R_{1,0}(x) + \frac{2(3+x)}{1+x}R_{1,0}(x)R_{0,2}(x) \\ &= -\frac{x^5+12x^4+69x^3+302x^2+672x+480}{16(x+1)^{7/2}(x+2)(x+3)^3}\,, \end{aligned} \tag{2.143}$$

where the expression for $R_{1,0}$ in Eq. (A.53) was used as well as

$$R_{0,2}(x) = \frac{x^2+x-4}{(x+2)^3(x+3)^3}\,, \tag{2.144}$$

which was determined from the recursion equation Eq. (2.93). For $Y_1(x)$ one finds the following expression:

$$\begin{aligned} Y_1(x) =& Y_0(x)\Bigg[\left(Y_1(0)+\frac{1}{4}\right) \\ &- \frac{1}{4}\left(\frac{8}{(x+2)^2}+\frac{4}{x+2}-\frac{27+x}{3(x+1)(x+3)}+2\log\left(3\frac{x+1}{x+3})\right)\right)\Bigg]\,. \end{aligned} \tag{2.145}$$

The integration constant $Y_1(0)$ may be chosen freely. The solutions for any two different choices of $Y_1(0)$ differ by some multiple of the homogeneous solution $Y_{\mathrm{hom}}(x)$, which is also evident from Eq. (2.145). This is due to the linearity of L and a general feature of all the $Y_k(x)$.

Now the singularity structure of Ψ_1 in the Borel plane will be analysed. Ψ_1 has been computed as an approximation by truncating the series at order $\bar{k}+1$:

$$\Psi_1(x,\varepsilon) \approx \sum_{k=0}^{\bar{k}} \varepsilon^k Y_k(x)\,. \tag{2.146}$$

The algorithm for the computation of the coefficients $Y_k(x)$ can be found in Appendix A.4. The $Y_k(x)$ are given to order $\tilde{n}-k$ in x and satisfy the initial conditions.

$$Y_k(x=0) = \begin{cases} 1, & k=0 \\ 0, & \text{else} \end{cases}\,. \tag{2.147}$$

This allows one to write down an approximation for the Borel transform $\mathcal{B}[\Psi_1](\xi)$ (the x-dependence in our notation is dropped):

$$\mathcal{B}[\widehat{\Psi}_1](\xi) \approx \sum_{k=0}^{\bar{k}-1} \frac{Y_{k+1}}{\Gamma(k+1)} \xi^k . \tag{2.148}$$

To get an approximation for the analytic continuation of this series and get an insight into the pole structure, the Pade approximant $\mathrm{BP}_N[\Psi_1]$ is computed. The branch cut singularities of $\mathcal{B}[\Psi_1](\xi)$ manifest as the condensation of the poles of $\mathrm{BP}_N[\Psi_1]$ into a line. The computation has been carried out for the parameters $x = 1/1000$, $\bar{k} = 250$, $n = 40$, $N = 220$ with a numerical precision of 200 digits using Mathematica. The pole structure of the Pade approximant is displayed in Fig. 2.13.

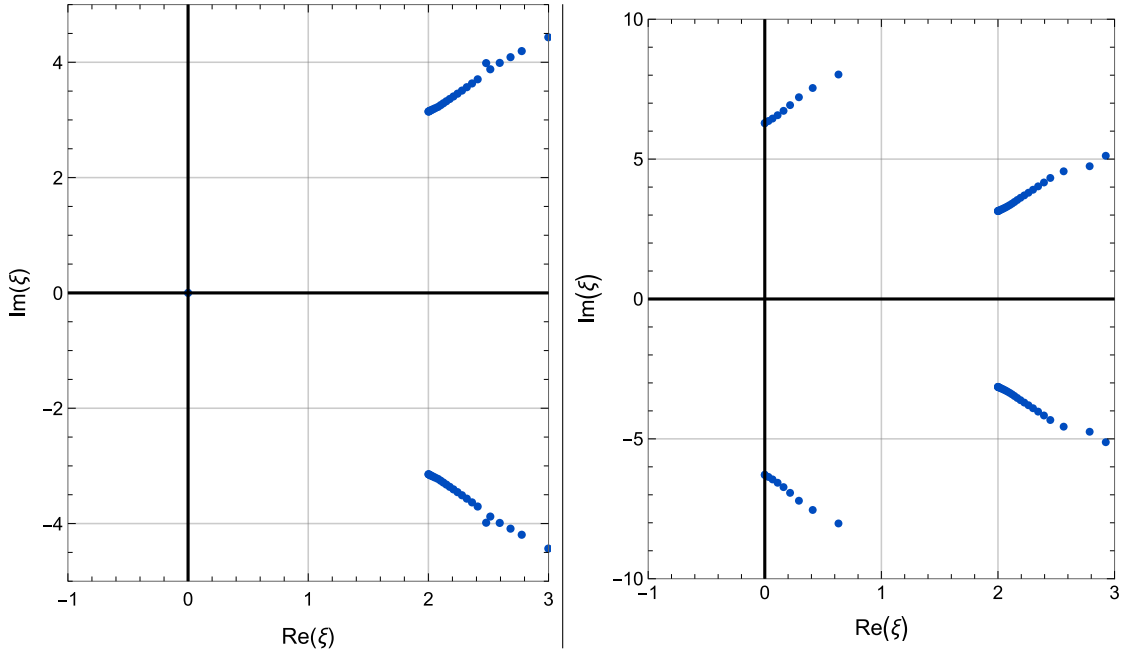

FIGURE 2.13: Singularities of the Borel-Pade approximants in the Borel plane of $\mathrm{BP}_{200}[\widehat{\Psi}_0](\xi)$ (left) and $\mathrm{BP}_{220}[\widehat{\Psi}_1](\xi)$ (right) for $x = 1/1000$.

To a very high precision the branch cut singularities for $x = 1/1000$ are given by $\xi_1 \equiv 2 + \pi\,\mathrm{i}$ and $\xi_2 \equiv 2\,\pi\mathrm{i}$, as well as their complex conjugates $\bar{\xi}_1$, $\bar{\xi}_2$. It is known that for a resurgent function the singularities are expected to be given by the relative positions of the exponential weights in the transseries. It is also known that $\mathcal{B}[\widehat{\Psi}_0](\xi)$ has singularities at $\xi = A$ and $\xi = \bar{A}$ and is expected to have additional singularities at $\xi = 2A, 3A \ldots$ and $\xi = 2\bar{A}, 3\bar{A} \ldots$ which are difficult to 'see' in the Borel-Pade approximation. Since the sector Ψ_1 corresponds to the weight A, poles at the relative positions $\bar{\xi}_2 = \bar{A} - A$ and $\xi_1 = 2A - A = A$ are expected , which is exactly what is

found. As for the other two singularities, they follow from the fact that the expansion of $\mathcal{B}[\widehat{\Psi}_1](\xi)$ around the origin has only real coefficients and therefore

$$\overline{\mathcal{B}[\widehat{\Psi}_1](\xi)} = \mathcal{B}[\widehat{\Psi}_1](\bar{\xi}), \tag{2.149}$$

from which it follows that the set of singularities is invariant under complex conjugation.

2.4 Discussion

Transasymptotic approximations for the solutions to both the standard and slowly varying logistic equation have been obtained. In each case, the results calculated in [3] using multiple scales asymptotic methods were not only reproduced, but also improved and extended.

As, *a priori*, transseries methods allow for the straightforward calculation of higher-order exponentials, the transseries approximation was able to represent the solution more accurately than the multiple scales method both during and after the delayed bifurcation, as seen in Figure 2.8; during and after the birfurcation, the initially subdominant exponentials contribute significantly to the solution, so it should be expected that the transseries approximation would be particularly accurate compared to other methods in these regions.

Furthermore, the transseries approach can still provide a useful approximation when the parameter ε is not particularly small, as the solution can simply be re-scaled to determine the next asymptotic weight.

The dynamic logistic equation with $\varepsilon > 0$ was considered, producing a cascade of delayed bifurcations. If $\varepsilon < 0$, causing the bifurcation parameter to decrease rather than increase, bifurcations appear earlier than the solution stability would suggest, rather than later [44]. A transseries approach could be used in almost identical fashion to the present study in order to approximate these accelerated bifurcations; however, that analysis is beyond the scope of this study.

There are several significant and general advantages to the transseries resummation approach. The first is that the method which has been described can be applied in systematic fashion to a wide range of problems, including both discrete and continuous

systems. Whilst such advantages have already been seen elsewhere, in the context of the logistic equation it has been instructive to compare this to the multiple scales approach from [3], which required the careful comparison of asymptotic terms up to several orders. In order to capture the fast discrete scale, as well as both the inner and outer continuous scales near the bifurcation, asymptotic matching was performed through three scales.

The transseries approach here was able to reproduce this behaviour by resumming the series in order to ensure that the transasymptotic approximation contained behaviour encoded in the subdominant exponentials; this behaviour contained all of the information found using asymptotic matching methods. Furthermore, improving approximation accuracy by computing more terms of a multiple scales expansion requires comparing the asymptotic behaviour of more terms and checking to determine when the relative dominance of terms changes, while obtaining a more accurate transseries expression simply requires the systematic calculation of further series terms in the transseries. While these calculations can prove challenging, the steps required to obtain the subdominant exponentials, and the associated solution behaviour, follow the same consistent process at each stage at which it is applied.

Computing the subdominant exponentials is not valuable simply in that it produces a more accurate approximation. In fact, a second major advantage of the transseries method is that the exponential weights have a significant effect on the system behaviour, and computing just these weights can tell one the form of the solution as parameters in the problem vary. In this analysis of the standard logistic map, it was shown that 2-, 4-, and 8-periodic behaviour can be determined simply by carefully studying the subdominant weights. This explains the appearance of higher periodicities in the solution, and suggests that if this process is continued, it can be used to study further bifurcations in the period doubling process.

In the subsequent analysis of the period doubling cascade found in the slowly varying logistic equation, the onset of 2-periodic and 4-periodic behaviour in the solution was predicted, simply by studying the relative size of the exponential weights associated with the 2- and 4-periodic contributions. It would be particularly interesting to continue to investigate how the full period doubling cascade is encoded in the exponential weights of this system, and whether this can provide (at least theoretically) further insight into the period doubling route to chaos.

Transseries methods have been used to study Stokes Phenomenon in a wide range of continuous problems. Given that multiple scales methods have been used to study Stokes Phenomenon in discrete problems [58, 53, 57, 54, 55, 56], it is likely that the transseries approach described here could be used to provide new insight into discrete variants of Stokes Phenomenon.

Finally the full analysis of the movements of exponential contributions between Riemann sheets, seen in the dynamic logistic map, also merits further investigation. Examples of such phenomena have been observed recently in novel features of aeroacoustic flows [62, 63]. Initial explorations appear to suggest this is commonly found in other physical and mathematical contexts.

The application of the transasymptotic summation introduced in Chapter 1 method in this work made it possible to obtain approximations when the dominance of the exponential terms changes. In Chapter 3, this approach will be applied to deduce global analytical properties in the context of a non-linear first order ODE and infer the relationship between the asymptotics of the solution in different regions.

Chapter 3

The late to early time behaviour of an expanding plasma

Large parts of this chapter have been published verbatim in [4]. The research presented in this chapter is my own. It was developed under the guidance of my supervisor Inês Aniceto, and in collaboration with Adri Olde Daalhuis. The numerical computation of the branch point locations presented in Fig. 3.4 and Tab. 3.1 was done by Adri Olde Daalhuis.

The purpose of this project is to apply exponential asymptotics techniques to a matching problem in hydrodynamics. The time evolution of an expanding conformally invariant fluid will be considered and the late-time behaviour of the fluid will be linked to the behaviour at early times. The expansion is modelled via the so-called pressure anisotropy $f(w)$, which is given as a function of the timelike variable w. The differential equation which describes the evolution is

$$wf(w)f'(w) + 4f(w)^2 + f(w)\left(-8 + Aw\right) + \left(4 - \beta - Aw\right) = 0\,, \tag{3.1}$$

where A and β are constants which will be introduced later.

The reason this problem is both interesting and important from a physics perspective is its applicability in the modelling of strongly coupled Quark-Gluon-Plasmas (QGPs) created in high-energy ion collisions. The time-dependent evolution arising from the microscopic theory of Quantum Chromodynamics (QCD) can be modelled by macroscopic

hydrodynamics models after a short period of time, even in a regime far-away from thermodynamic equilibrium [64, 65, 66, 67]. This is somewhat surprising, considering that hydrodynamics is classically thought of as a framework which is only valid at thermodynamic equilibrium or at least very close to it. Under the additional symmetry assumption of boost invariance (Bjorken flow) [68], all the information in our model is encoded in the time evolution of a single observable - the effective temperature.

The pressure anisotropy satisfies a first order ODE with interesting dynamical properties such as the existence of a late-time attractor [69]. Mathematically, this attractor manifests as an exponentially fast convergence of a family of solutions to the (resummed) asymptotic and divergent hydrodynamic series. This process is known as hydrodynamisation (see *e.g.* [70]).

From a physical perspective, the information stored in the initial state of the system dissipates, and at large times near equilibrium our physical observables no longer depend on their history up to exponentially small corrections. The perturbative expansion around infinity in the time variable is called the hydrodynamic mode because it corresponds to the regime where near-equilibrium viscous hydrodynamics is a valid approximation. The exponentially decaying corrections can be described by a transseries in which each exponential comes multiplied with a divergent power series, and in which all the exponentials are powers of a basis exponential. These contributions are called the non-hydrodynamic modes.

Unlike many of their convergent counterparts, it is well known that these asymptotic expansions converge to their expected results quite quickly before eventually diverging – in fact keeping just a few terms provides a very precise approximation, which can be extended far beyond the original expansion point, in our case large time (see *e.g.* [71]).

The work layed out in this chapter consists in using the well-established techniques Borel resummation, hyperasymptotics and transasymptotics (see *e.g.* [7, 9, 72]) to retrieve the exponentially small information at late times (see also [73, 74, 75]) and match it to the correct initial conditions (the initial value problem) at early times. The techniques will also be used to interpolate the observable between the two regimes of early- and late-times. Our approach is generic and can be used to solve any interpolation problem as long as it can be described with a local asymptotic transseries expansion and a solution is known at a single point in a region far away from the expansion point. It will also be

shown how the transasymptotic resummation can be used to deduce global analytical properties of the solutions using the methods in [9, 72, 76, 77]. In particular, it will be shown how to calculate the locations of the square-root branch points and to link asymptotic expansions around different points to each other.

3.1 The hydrodynamic model

The basis for our macroscopic hydrodynamic model is a conformal fluid. The stress energy tensor of the system is

$$T^{\mu\nu} = \mathcal{E} u^\mu u^\nu + \mathcal{P}(\mathcal{E})(g^{\mu\nu} + u^\mu u^\nu) + \Pi^{\mu\nu}, \tag{3.2}$$

where u^μ is the relativistic flow velocity of the fluid, $\mathcal{E}$ is the energy density,

$$\mathcal{P}(\mathcal{E}) = \frac{\mathcal{E}}{3} \tag{3.3}$$

is the pressure of the perfect fluid part of $T^{\mu\nu}$ and $\Pi^{\mu\nu}$ is the shear-stress tensor representing the dissipative terms describing the deviation from thermodynamic equilibrium. The evolution of the system is dictated by the conservation equation

$$\nabla_\mu T^{\mu\nu} = 0\,. \tag{3.4}$$

A condition for the hydrodynamic frame must be imposed (see e.g. [78]) - here the Landau frame is chosen, i.e. the shear stress tensor is transverse to the flow as in [30]:

$$u_\mu \Pi^{\mu\nu} = 0\,. \tag{3.5}$$

To exploit the conformal symmetry in our calculation the so-called Weyl-derivative is useful. The formalism makes use of the derivative operator $\mathcal{D}_\mu$ defined through the connection

$$\mathcal{A}_\mu = u^\lambda \nabla_\lambda u_\mu - \frac{1}{3}\nabla_\lambda u^\lambda u_\mu, \tag{3.6}$$

Following [30], the derivative along the flow is defined as

$$\mathcal{D} \equiv u^\mu \mathcal{D}_\mu, \tag{3.7}$$

and

$$\sigma^{\mu\nu} = \mathcal{D}^{\mu}u^{\nu} + \mathcal{D}^{\nu}u^{\mu}, \quad \omega^{\mu} = \mathcal{D}^{\mu}u^{\nu} - \mathcal{D}^{\nu}u^{\mu}. \tag{3.8}$$

According to the Landau-Lifschitz formulation of relativistic viscous thermodynamcs the stress energy tensor is given by

$$\Pi^{\mu\nu} = -\eta\sigma^{\mu\nu}\,. \tag{3.9}$$

However, Landau-Lifschitz theory is acausal (and the initial value problem is ill-posed) since signal propagation is unbounded by the speed of light (see [69] and references therein). The ill-posedness is a consequence of ultraviolet divergences at short distances where hydrodynamics does not apply, and it is necessary to introduce a prescription to regulate these divergences. The approach taken here is called Müller-Israel-Stuart (MIS) causal hydrodynamics [79, 80, 81, 82], where the shear-stress tensor $\Pi^{\mu\nu}$ is regarded as a dynamical field satisfying a relaxation type differential equation (see [69, 31, 30]). In a first step, all the terms up to second order the derivatives of $\Pi^{\mu\nu}$ are included as long as they are allowed by the symmetry, yielding [30]

$$\begin{aligned}\Pi^{\mu\nu} =& -\eta\sigma^{\mu\nu} + \eta\tau_{\Pi}\mathcal{D}\sigma^{\mu\nu} + \lambda_1\sigma^{<\mu}{}_{\lambda}\sigma^{\nu>\lambda} + \lambda_2\sigma^{<\mu}\omega^{\omega>\lambda} \\ &+ \lambda_3\omega^{<\mu}{}_{\lambda}\omega^{2>\lambda}\,,\end{aligned} \tag{3.10}$$

where the brackets $< ... >$ denote symmetrisation followed by subtraction of the trace, and τ_{Π} and λ_i are the second order transport coefficients. If the microscopic theory is known and one can calculate the transport coefficients from it, the macroscopic fluid dynamical model can be used to study the hydrodynamisation process. For example, the transport coefficients of an $\mathcal{N} = 4$ SYM plasma have been obtained using the AdS/CFT correspondence. If the term which comes multiplied by τ_{Π} in (3.10) is replaced by $\tau_{\Pi}\mathcal{D}\Pi^{\mu\nu}$ (up to second-order in $\mathcal{D}$ they are the same), one obtains [30]

$$\begin{aligned}(\tau_{\Pi}\mathcal{D}+1)\,\Pi^{\mu} =& -\eta\sigma^{\mu} + \frac{\lambda_1}{\eta^2}\Pi^{<\mu}_{\lambda}\Pi^{\nu>\lambda} - \frac{\lambda_2}{\eta}\Pi^{<\mu}_{\lambda}\omega^{\nu>\lambda} \\ &+ \lambda_3\omega^{<\mu}{}_{\lambda}\omega^{\nu>\lambda}\,.\end{aligned} \tag{3.11}$$

As an additional symmetry, boost-invariance of the flow will be imposed on the system. This is called Bjorken flow [68]. In a quark-gluon-plasma created by ion collisions, the plasma is created between two thin Lorentz contracted sheets of the nuclei. Since

they move away from each other close to the speed of light, the initial conditions are approximately boost invariant, and hence Bjorken flow is a good approximation to describe the evolution. Since the system is homogeneous in the transverse plane to the collision axis, it can be described using the two Minkowski coordinates z and t. Due to boost-invariance it is useful to use the coordinate system defined by proper time τ and rapidity ξ [31]:

$$\begin{aligned} &t = \tau \cosh\zeta, \quad z = \tau \sinh\zeta \Leftrightarrow \tau = \sqrt{t^2 - z^2}, \\ &\zeta = \tanh^{-1}(t/z)\,. \end{aligned} \tag{3.12}$$

In the (τ, ξ) coordinate system the conservation equation (3.4) and the relaxation-type equation for the shear-stress tensor become [30]

$$\begin{aligned} \tau\dot{\epsilon} &= -\frac{4}{3}\epsilon + \phi, \\ \tau_\Pi\dot{\phi} &= \frac{4\eta}{3\tau} - \frac{\lambda_1\phi^2}{2\eta^2} - \frac{4\tau_\Pi\phi}{3\tau} - \phi, \end{aligned} \tag{3.13}$$

where the dot denotes the derivate with respect to proper time and

$$\phi \equiv -\Pi^y_y\,, \tag{3.14}$$

the only independent component of the shear-stress tensor. The transport coefficients can be expressed in terms of the dimensionless constants $C_{\tau\Pi}$, C_{λ_1} and C_η:

$$\tau_\Pi = \frac{C_{\tau\Pi}}{T}, \quad \lambda_1 = C_{\lambda_1}\frac{\eta}{T}, \quad \eta = C_\eta s, \tag{3.15}$$

where T is the effective temperature (note that the system is not at equilibrium) which is related to $\mathcal{E}$ through

$$\mathcal{E} \sim T^4\,. \tag{3.16}$$

in a conformal theory, and s is the entropy density. In this work the C_{λ_1} is chosen to vanish.

$$C_{\lambda_1} = 0\,, \tag{3.17}$$

since this leads to a very interesting mathematical structure. Instead of using the proper time τ and describe the evolution of the system through the function, the approach in [30, 31] is followed and the following variables are used [1]:

$$w = T\tau; \qquad f = \frac{3\tau}{2w}\frac{\mathrm{d}w}{\mathrm{d}\tau}, \tag{3.18}$$

where f is the pressure anisotropy up to addition of a constant and re-scaling [2]. One obtains

$$wf(w)f'(w) + 4f(w)^2 + f(w)\left(-8 + Aw\right) + \left(4 - \beta - Aw\right) = 0, \tag{3.19}$$

where

$$A = \frac{3}{2C_{\tau\Pi}}, \quad \beta = \frac{C_\eta}{C_{\tau\Pi}}. \tag{3.20}$$

Note that (3.19) is the same as (3.1) from the introduction. In this analysis the following values for A and β are chosen (as in [69]) [3]:

$$A = \frac{3\pi}{2 - \log(2)}; \qquad \beta = \frac{1}{2(2 - \log(2))}. \tag{3.21}$$

However, note that our analysis is generic and can be carried out in the same way for any other choice of parameters.

3.2 Solutions of the evolution equation

Consider the solutions of Eq. (3.19). In the solutions plot shown in Fig. 3.1 the real solutions along the real axis are displayed.

There are two distinct solutions, represented by the red and black curves in Fig. 3.1, which are finite at the origin. The solution represented by the black curve is called

[1] Our definition of $f(w)$ in (3.18) differs from the convention in [69] by $f_{\text{ours}} = \frac{3}{2} f_{\text{theirs}}$. Nonetheless this normalisation is chosen because it leads to simpler equations.

[2] The pressure anisotropy $\mathcal{A}$ is related to f by $\mathcal{A} = 8\,(f-1)$ [83].

[3] There are three phenomenological parameters defining the second-order transport coefficients which are relevant for the MIS dynamics: $C_{\tau\Pi}$, C_{λ_1} and C_η. Assuming the microscopic theory is $\mathcal{N} = 4$ SYM, these parameters have been derived using holography and are given by [84, 85]:

$$C_{\tau\Pi}^{(\text{SYM})} = \frac{2 - \log 2}{2\pi}; \quad C_{\lambda_1}^{(\text{SYM})} = \frac{1}{2\pi}; \quad C_\eta^{(\text{SYM})} = \frac{1}{4\pi};$$

The ODE (3.19) is obtained by setting $C_{\lambda_1} = 0$. The other two phenomenological parameters are chosen as $C_{\tau\Pi} = C_{\tau\Pi}^{(\text{SYM})}$, $C_\eta = C_\eta^{(\text{SYM})}$, leading to (3.21). Note that Eq. (3.19) is only correct in the case $C_{\lambda_1} = 0$.

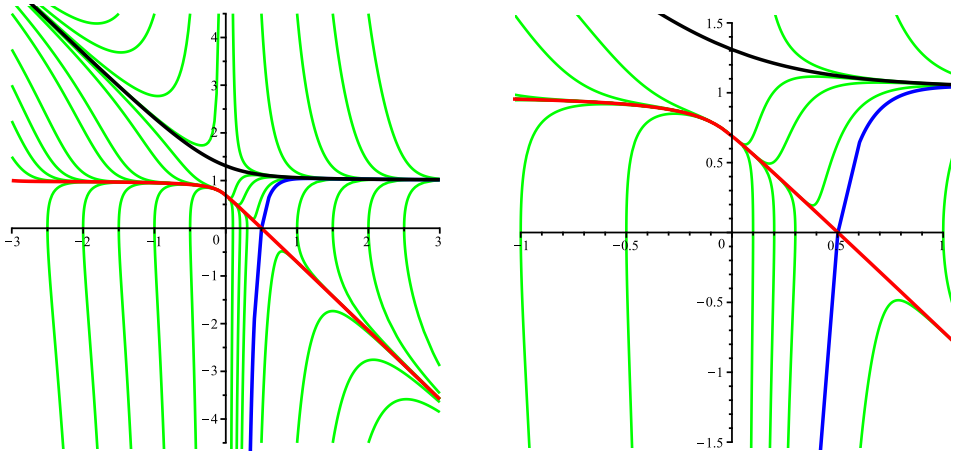

FIGURE 3.1: The real graph $(w, f(w))$ plane. The figure on the right is a zoom-in around the origin of the figure on the left. The red and blue curves are the only two solutions with a regular zero. The red curve representing $f_-(w)$ and black curve representing $f_+(w)$ are the only two solutions with finite values at the origin. Taken from [4].

f_+, and the one represented by the red curve f_-. The functions f_+ and f_- are special solutions because they are attractors at $w = +\infty$, and f_+ (respectively f_-) is the attractor (respectively repellor) at $w = -\infty$. This means that all other solutions, represented by green curves in Fig. 3.1, become exponentially close to either $f_+(w)$ or $f_-(w)$ as $w \to +\infty$. An important feature of the solutions is the presence of square root branch points, whose locations are denoted by w_s. It can be shown that Eq. (3.19) admits solutions of square root type, and admits the following analytic expansion in powers of $(w - w_s)^{1/2}$:

$$\begin{aligned} f(w) &= \sum_{n=1}^{\infty} h_n(w_s)\,(w - w_s)^{n/2}\,, \\ \text{with } h_1^2(w_s) &= \frac{2Aw_s + 2\beta - 8}{w_s},\ h_2(w_s) = \frac{16 - 2Aw_s}{3w_s},\ \cdots . \end{aligned} \tag{3.22}$$

The locations w_s of the branch points depend on the initial conditions imposed on $f(w)$. The presence of these square root branch points implies that the natural domain of $f(w)$ is a non-trivial Riemann surface. Note that the summation in (3.22) starts at $n = 1$, hence, $f(w)$ is zero at the branch points. It is easy to check that the only possible regular zero for solutions of (3.19) is at $w = (4 - \beta)/A \approx 0.5$, the point of intersection of red and blue curve in Fig. 3.1. In the following, the relationship between the real solutions will be analysed considering their expansions around the origin and around infinity.

3.2.1 Solutions around the origin

Around $w = 0$ there are the following convergent expansions:

(a) Two finite solutions at the origin

$$f_{\pm}(w) = (1 \pm \sqrt{\beta}/2) + \mathcal{O}(w), \quad w \to 0, \tag{3.23}$$

(b) A one-parameter family of solutions diverging at the origin

$$f_C(w) = Cw^{-4} + 2 + \mathcal{O}(w), \quad w \to 0. \tag{3.24}$$

Consider the solutions $f_C(w)$ and their relation to $f_+(w)$. In the solutions plot of Fig. 3.1 the green curves above the graph of $f_+(w)$ (in black) correspond to $f_C(w)$ for $C > 0$. As C becomes smaller, the green curves in Fig. 3.1 approach $f_+(w)$. In the limit $C \to 0^+$, $f_C(w)$ converges pointwise to $f_+(w)$ for $w \neq 0$. Hence $f_+(w)$ can be understood as the $C \to 0^+$ limit of $f_C(w)$, in which the divergence at the origin disappears. For $0 > C > C_{\text{split}} \approx -0.0874$, $f_C(w)$ has a square root branch point on the positive real axis. At $C = C_{\text{split}}$ this square root singularity splits into two singularities, one above and one below the real axis. The corresponding function $f_{C_{\text{split}}}(w)$ is represented by the blue curve in Fig. 3.1. For $C < C_{\text{split}}$, the function $f_C(w)$ has no square root branch points along the real axis and admits a real solution for all $w > 0$. These solutions are represented by the green curves in the bottom right corner of Fig. 3.1.

3.2.2 Solutions around infinity

Around $w = \infty$ there are two distinct expansions, depending on whether the solutions converge or diverge at infinity.

(a) *Solutions of finite limit:* the solutions which converge to the hydrodynamic attractor $f_+(w)$ as $w \to +\infty$ can be described with the following transseries expansion [69]

$$\mathcal{F}(w, \sigma) = \sum_{n=0}^{\infty} \sigma^n w^{\beta n} \mathrm{e}^{-nAw} \Phi^{(n)}(w). \tag{3.25}$$

The transseries $\mathcal{F}$ describes a one-parameter family of solutions converging to the finite value $\mathcal{F} \to 1$ as $w \to +\infty$. Hence all the green curves in Fig. 3.1 which approach the black curve $f_+(w)$ have a transseries parameter σ assigned to them. The parameter σ is not determined by the equation and has to be matched with the early-time behaviour of $f(w)$ around $w = 0$, where all the solutions are known as convergent series expansions (3.23) and (3.24). The value of σ corresponding to the black and blue curves in Fig. 3.1 are approximately $\sigma_+ = -0.3493 + 0.0027\mathrm{i}$ and $\sigma_{\text{blue}} = -14.4111 + 0.0027\mathrm{i}$, respectively. The particular form of (3.25) implies that the amplitudes of all the non-perturbative modes are known once the transseries parameter σ is given. The $\Phi^{(n)}(w)$ is the divergent, asymptotic series of the n^{th} non-perturbative sector

$$\Phi^{(n)}(w) = \sum_{k=0}^{\infty} a_k^{(n)} w^{-k}. \tag{3.26}$$

The coefficients $a_k^{(n)}$ above can be determined from recurrence equations obtained by substituting the ansatz (3.25) into the MIS ODE (3.19) and matching equal powers of σ.

The convention $a_0^{(1)} = 3/2$ is used. [4] The perturbative sector $\Phi^{(0)}(w) = 1 + \frac{\beta}{A} w^{-1} + \mathcal{O}\left(w^{-2}\right)$ describes the hydrodynamic series and defines the attractor at $w \to +\infty$. Due to the factor e^{-nAw} multiplying the non-hydrodynamic series $\Phi^{(n)}(w)$, $n \geq 1$, the convergence of the solutions to the attractor is exponentially fast.

(b) *Growing solutions:* the solutions which are linearly growing to leading order and asymptotically approximate $f_-(w)$ as $w \to +\infty$ admit the following transseries expansion [5]

$$\Psi(p_4, w) = \sum_{k=-1}^{3} p_k\, w^{-k} + \sum_{k=4}^{9} w^{-k} \left(p_k + q_k \log w\right) + \sum_{k=10}^{14} w^{-k} \left(p_k + q_k \log w + r_k \log^2 w\right) + \ldots, \tag{3.27}$$

[4] With this convention our Stokes constant and transseries-parameter normalisation is the same as in [69, 31, 30], and choosing a different value for $a_0^{(1)}$ corresponds to a re-scaling of σ.

[5] Note that the transseries Ψ from Eq. (3.27) is constructed from the basis monomials w^{-1} and $\log w$, whereas $\mathcal{F}$ is constructed from the basis monomials w^{-1} and e^{-Aw}. This is novel compared with the transseries which appeared in the previous Chapters 1 and 2.

with $p_{-1} = -A/5$. The first four coefficients, $n = -1,\ 0,\ 1,\ 2,\ 3,\ 4$, are uniquely determined by the MIS equation (3.19) alone. The coefficient p_4 is not determined by (3.19), and all other coefficients generically depend non-linearly on the coefficient p_4. Hence the transseries Ψ from (3.27) represents a one-parameter family of solutions. The red curve in Fig. 3.1, that is f_-, corresponds to $p_4 = -0.3474942558$. In Fig. 3.1 it can be seen that as $w \to -\infty$ the regular solutions have a transseries expansion of the form (3.27).

The current work concerns the solutions of finite limit, also known as attractor solutions, given by the transseries (3.25). This transseries can be regarded as an expansion with a two-scale structure, the perturbative variable w^{-1}, as well as an exponential variable

$$\tau \equiv \sigma\, w^{\beta} \mathrm{e}^{-Aw}. \tag{3.28}$$

In general, the transseries (3.25) is formally written such that the outer sum is performed over powers of τ, with coefficients $\Phi^{(n)}(w)$ depending on the variable w^{-1}. In this work different summation approaches of the asymptotic functions $\Phi^{(n)}(w)$ will be presented. Moreover, an alternative way of summing the transseries (3.25) called transasymptotic summation will be explored, in which the order of summation is reversed [72], such that the coefficients in the w^{-1}-expansion are then functions of τ (defined by a convergent Taylor series in τ). Thus the divergence of the transseries is not caused by the large-order behaviour of the exponential scales, but instead by the divergent asymptotic expansions at each order of the non-perturbative exponential. Although the transseries (3.25) is an expansion around $w = +\infty$, the transasymptotic approach allows one to access different regimes where τ is no longer small.

3.3 Interpolation between late-times and early-times

In the previous section the the behaviour of the solutions to the MIS equation (3.19) was described both for early- and late-times. It was found that there exists a one-parameter family of solutions with a finite limit at late times ($w \to +\infty$). These solutions converge exponentially fast to a hydrodynamic attractor described by a perturbative series. It was seen that this series could be upgraded to the transseries (3.25) by including decaying

exponential terms at large times. The transseries parameter σ from (3.25) was identified as a proxy for the amplitudes of the non-perturbative exponential modes. In the early-time regime near the origin, another representation of said family of solutions (3.24) was found, labelled by the leading-order coefficient C of their Laurent expansion around the origin. Linking the magnitude of the non-perturbative modes of the late-time asymptotic transseries to the early-time behaviour can be very useful, and has previously been done by numerical fitting [86, 87]. However, the fitting approach does not exploit the vast possibilities arising from the rich late time asymptotics of the solutions. In particular, the difficulty with the fitting method lies in the exponential proximity of any two distinct solutions at late times, and hence a significant deviation from the desired solution is weakly penalised at late times, while at early times the function is not accurately captured by the fit model due to the finite truncation of the transseries (3.25). Fortunately, given that the solution at late times is divergent asymptotic, there is a range of tools to do the matching, whose exponential accuracy provides a way to differentiate the behaviour of the different solutions. The matching between late and early times will be achieved in three main steps:

(i) The factorial divergent expansion at late times will be summed, using exponentially accurate methods, keeping not only the perturbative series but also a non-perturbative, exponentially small part (effectively keeping the exponential accuracy). This sum will then be evaluated at a finite but large enough time w_0.

(ii) The solution at the origin will be analytically continued to the same value w_0.

(iii) The two approximations that will be found depend on their respective parameters (C representing early times and σ late times) and their relation can be obtained via direct comparison.

After having found the transseries parameter for a given solution at early times, the asymptotic summation methods can be used to find exponentially accurate interpolations in the regime between early-times and late-times.

3.3.1 Hyperasymptotic summation

Hyperasymptotics is a resummation method which exploits the asymptotic properties of the transseries to approximate the value of a function by truncated sums [74, 88, 75, 89]. In order to compute an approximation for the solution $f(w_0)$ to the MIS ODE (3.19) at a finite "matching time" w_0, terms up to linear order in the parameter σ will be kept from the late time transseries solution (3.25). This corresponds to calculating level-one hyperasymptotics, for which terms of the transseries sectors $\Phi^{(0)}(w)$ and $\Phi^{(1)}(w)$ from (3.25) have to be computed for the computation). In level-one hyperasymptotics, the optimal number of terms N_{Hyp} at which the series expansions must be truncated is a function of the resummation point w at which transseries is being resummed [90]

$$N_{\text{Hyp}}(w) = 2\left\lfloor \left| Aw \right| \right\rfloor, \tag{3.29}$$

where $\lfloor \cdots \rfloor$ is the floor function. Thus the terms of the power series $\Phi^{(0)}(w)$ and $\Phi^{(1)}(w)$ have to be computed to sufficiently high order (A maximum of 100 terms were used [6]for all our approximations).

The level-one hyperasymptotic summation is then given by [10] [7]

$$f_{\text{Hyp}}(w_0) = f_{\text{Hyp},0}(w_0) + \sigma\, f_{\text{Hyp},1}(w_0), \tag{3.30}$$

where the hyperasymptotic summations for the perturbative sector and the first non-perturbative sector are given by

$$\begin{aligned} f_{\text{Hyp},0}(w_0) =& \sum_{m=0}^{N_{\text{Hyp}}(w_0)-1} a_m^{(0)} w_0^{-m} \\ &+ w_0^{1-N_{\text{Hyp}}(w_0)} \frac{S_1}{2\pi \mathrm{i}} \sum_{m=0}^{N_{\text{Hyp}}(w_0)/2-1} a_m^{(1)} F^{(1)}\left(w_0; \begin{matrix} N_{\text{Hyp}}(w_0)+\beta-m \\ -A \end{matrix} \right); \\ f_{\text{Hyp},1}(w_0) =& \mathrm{e}^{-Aw_0} w_0^{\beta} \sum_{m=0}^{N_{\text{Hyp}}(w_0)/2-1} a_m^{(1)} w_0^{-m}. \end{aligned} \tag{3.31}$$

[6] Using 200 terms allows to use the hyperasymptotic approximation with optimal precision up to $w = 7$.

[7] $f_{\text{Hyp},0}(w_0)$ is not the same as the level-0 hyperasymptotics or optimal truncation, since the number of terms at which the perturbative series is truncated must be increased as more non-perturbative sectors are included in the calculation.

The function $F^{(1)}$ in (3.31) is called hyperterminant and defined in terms of incomplete gamma functions via [91]

$$F^{(1)}\left(w;\begin{matrix}M\\a\end{matrix}\right) = \mathrm{e}^{aw+i\pi M} w^{M-1}\,\Gamma(M)\Gamma(1-M,aw). \tag{3.32}$$

The quantity S_1 in (3.31) is the Stokes constant, which may be defined as the change in the transseries parameter σ of (3.25) upon crossing the Stokes line, which in our case is the positive real axis. The constant S_1 has been calculated in previous work [31, 30] (see also Appendix B.1) and is given by

$$S_1 \approx 5.4703 \times 10^{-3}\,\mathrm{i}. \tag{3.33}$$

This Stokes constant can also be determined using hyperasymptotics, see Appendix B.1, where the Stokes constant S_1 is also given with more precision. Note that contributions of order $\mathcal{O}\left(\sigma^2\right)$ and above in the transseries (3.25) are not included in level-one hyperasymptotics. The error in (3.31) is therefore of order $\mathrm{e}^{-2|Aw_0|}$ [90].

In order to match the late time approximation with the early time solution, the solution at early times (Eqs. (3.23) and (3.24)) has to be brought to the finite value w_0. This is done by analytical continuation with the numerical Taylor series method. The numerical approximation obtained for $f(w_0)$ is denoted as [8]

$$\begin{aligned} f_{\mathrm{ac}}(w_0) \quad &:= \quad \text{numerical analytic continuation of } f(w) \text{ from the origin,} \\ &\qquad\quad \text{evaluated at the time } w_0. \end{aligned} \tag{3.34}$$

By requiring $f_{\mathrm{ac}}(w_0) = f_{\mathrm{Hyp}}(w_0)$, the following approximation is obtained for σ:

$$\sigma \approx \frac{f_{\mathrm{ac}}(w_0) - f_{\mathrm{Hyp},0}(w_0)}{f_{\mathrm{Hyp},1}(w_0)}. \tag{3.35}$$

By decreasing the step size and increasing the order of the Taylor expansions in the calculation of $f(w_0)$, arbitrary accuracy can be achieved, such that the error in the approximation (3.35) is determined by limitations of the hyperasymptotic approximation. Hence the parameter σ in (3.35) is accurate up to an error of order $\mathrm{e}^{-|Aw_0|}$.

[8] Note that $f_{\mathrm{ac}}(w_0)$ depends on which solution is picked around the origin from the set $\{f_+, f_-, f_C | C \in \mathbb{C}\}$.

Do note that the approximation for $f(w_0)$ from the late-time transseries solution can easily be extended to higher orders in the transseries parameter σ, by computing more non-hydrodynamic sectors $\Phi^{(n)}(w)$ in (3.25). In Fig. 3.2 the results of the early-to-late-time matching $C \leftrightarrow \sigma$ are plotted for $C > 0$. Our results are consistent with the observation in Section 3.2 that as $(C, \sigma) \to (0^+, \sigma_+ = -0.349261 + 0.00273515\mathrm{i})$, the solutions $f_C(w)$ converge pointwise to the solution $f_+(w)$, which is finite at the origin. The function $\sigma(C)$ in Fig. 3.2 is roughly linear (left plot) except for a tiny region around the origin $C = 0$, where the convergence towards σ_+ is very slow and is best visualised on a log-linear plot.

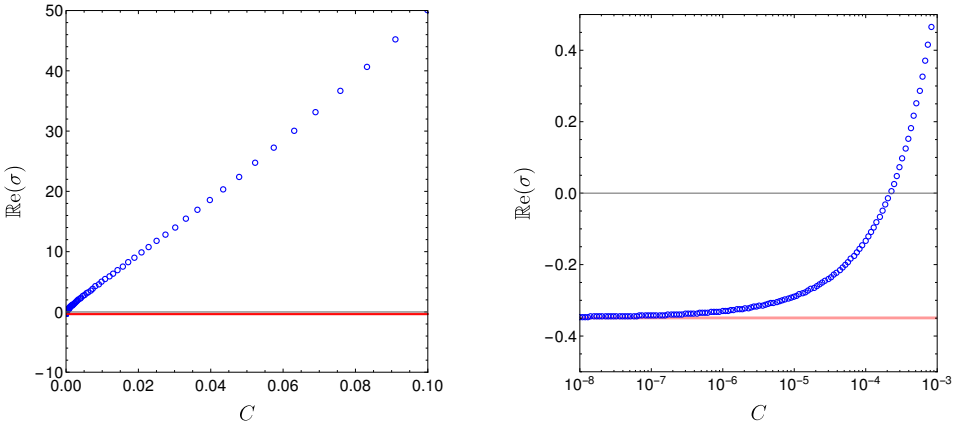

FIGURE 3.2: The real part of the matched late-time transseries parameter σ from (3.25) as a function of the early-time solution $f(w \sim 0)$, displayed in a linear plot (left) and a log-linear plot (right). Note that the range of values on the horizontal axis is different in each plot. The blue dots represent the matched solution $f_C(w)$ from (3.24) for $C > 0$, and the red line corresponds to the value $\mathbb{R}\mathrm{e}(\sigma)$ when matched to the solution $f_+(w)$ from (3.23).The imaginary part of σ is always given by $\mathbb{I}\mathrm{m}(\sigma) = \mathbb{I}\mathrm{m}(\frac{S_1}{2})$. The convergence $\sigma(C) \to \sigma_+$ as $C \to 0$ shows the pointwise convergence $f_C(w) \to f_+(w)$. Taken from [4].

3.3.2 The Borel resummation

Another way of approximating $f(w_0)$ is through Borel resummation (see *e.g.* [7] for a review). The Borel transform of a series $\Phi(w) = \sum_{j\geq 0} a_j\, w^{-j}$ is given by[9]

$$\mathcal{B}\left[\Phi\right](\xi) = a_0\, \delta(\xi) + \sum_{j=0}^{+\infty} \frac{a_{j+1}}{j!} \xi^j. \tag{3.36}$$

[9] As usual with Borel transforms, any finite number of powers w^j, $j \geq 0$ need to be addressed separately, see *e.g.* [7].

The series in (3.36) is truncated after N_0 terms [10] and its Padé approximant $\mathrm{BP}_{N_0}[\Phi]$, *i.e.* The resulting truncated sum is approximated by a rational function $\mathrm{BP}_{N_0}[\Phi]$ with a numerator/denominator of order $\lfloor N_0/2 \rfloor$.

The Borel-Padé resummation method then consists of taking the inverse Borel transform of $\mathrm{BP}_{N_0}[\Phi]$, which is given by the Laplace transform

$$\mathcal{S}_{N_0,\theta}\Phi(w) = a_0 + \int_0^{\mathrm{e}^{\mathrm{i}\theta}\infty} \mathrm{d}\xi\, \mathrm{e}^{-w\xi}\mathrm{BP}_{N_0}[\Phi](\xi). \tag{3.37}$$

The resurgence properties of the transseries (3.25) directly translate to the existence of pole singularities of the Padé approximant $\mathrm{BP}_{N_0}[\Phi](\xi)$ in Eq. (3.37) along the positive real axis – the Stokes line – and these singularities reflect the branch cuts of the Borel transform (3.36), starting at all $\xi = nA,\ n \in \mathbb{N}$ (one for each exponential in the transseries). Thus $\mathcal{S}_{N_0,\theta}\Phi(w)$ cannot be resummed along the positive real axis, and the integration contours need to be chosen such that the angle θ is slightly away from this axis, either above or below. Although this ambiguity in the choice of integration contour gives rise to an imaginary contribution for each summed sector $\mathcal{S}_{N_0,\theta}\Phi^{(n)}(w)$, there is a natural way of summing the resurgent transseries (3.25) such that the final result is unambiguous and real for real positive values of w – this summation procedure it the the so-called *median summation* [92, 93]. To do a small negative angle $\theta = -\varepsilon < 0$ is picked for the integration (3.37), and require the imaginary value of σ in the following way (see Appendix B.1 for some more details):

$$\mathrm{i}\,\mathbb{I}\mathrm{m}(\sigma) = \frac{S_1}{2}. \tag{3.38}$$

This way an approximation for $f(w_0)$ to first order in the transseries parameter σ is obtaineds [11], given by

$$f_{\mathrm{B}}(w_0) \equiv \mathcal{S}_{N_0,-\varepsilon}\Phi^{(0)}(w_0) + \sigma w^{\beta}\,\mathrm{e}^{-Aw_0}\mathcal{S}_{N_0,-\varepsilon}\Phi^{(1)}(w_0). \tag{3.39}$$

[10] Here $N_0 = 100$ was used, which allows one to perform the Borel resummation with optimal accuracy up to $w = 7$.

[11] The transseries (3.25) is used and all the terms of order $\mathcal{O}(\sigma^2)$ and above are thrown away.

In analogy to (3.35), using the Borel resummation method results in the following expression for σ:

$$\sigma \approx \frac{f_{\text{ac}}(w_0) - \mathcal{S}_{N_0,-\varepsilon}\Phi^{(0)}(w_0)}{w^\beta \, \mathrm{e}^{-Aw_0} \, \mathcal{S}_{N_0,-\varepsilon}\Phi^{(1)}(w_0)}. \tag{3.40}$$

Notice that for both Eq. (3.35) and (3.40) only terms up to linear order in σ were included in the approximation of $f(w_0)$. To obtain more accurate results, higher powers of σ can be included, which amounts to including additional exponential orders [12]. For the Borel summation method the integrals (3.37) for the higher-order hydrodynamic sectors $\Phi^{(n)}(w)$ would only have to be numerically computed in (3.25), while the generalisation of the hyperasymptotic summation is a bit less straightforward. It can nonetheless be done [75, 89, 90, 35]. However, one can obtain the same accuracy if instead of increasing the number of exponentials/powers of sigma, one would just increase the value of the matching time w_0.

Once the parameter σ has been matched to a given initial condition,[13] the transseries (3.25) can be used to find an approximation of $f(w)$ everywhere, via a summation technique such as hyerasymptotics and Borel summation described above. The hyperasymptotic method does not require computing numerical integrals, but has the disadvantage of yielding discontinuous approximations to the summed transseries: it provides a piecewise analytic approximation (which is clear from the left plot of Fig. 3.3). On the other hand, the Borel summation integrals (3.37) must be computed as numerical approximations at each evaluation point, but the method has the advantage of giving a continuous function of w_0.

In Fig. 3.3, It can be seen how different resummation methods compare with each other. In terms of accuracy the hyperasymptotic summation and the Borel resummation method are equivalent outside of a very small region near the origin, both giving an exponentially small error of approximately $\sim \mathrm{e}^{-2|Aw|}$ (the order of the first exponential which was neglected). It can also clearly be seen that the approximations given by each summation method are still accurate at very early times, even though only included a single exponential mode has been included – to obtain accurate results at earlier times

[12] A similar matching was already done in [69] for the solution f_+ using Borel resummation with two exponentials.

[13] This initial condition was either the value of $f_+(0)$, or the value of C for the divergent solutions at the origin $f_C(w)$.

one would need to include further exponentials and their respective asymptotic expansions from (3.25). Also in Fig. 3.3 one can find results corresponding to a transasymptotic resummation, which will be discussed in the next Section 3.4.

Let us also briefly mention the optimal truncation method, which consists of truncating the power series of the perturbative sector before the least term [14]

$$f_{\text{opt}}(w) = \sum_{n=0}^{N_{\text{opt}}(w)-1} a_n^{(0)} w^{-n}, \quad \text{where} \quad N_{\text{opt}}(w) = \lfloor |Aw| \rfloor . \tag{3.41}$$

The accuracy of this optimal truncation is approximately $\sim \mathrm{e}^{-|Aw|}$, in agreement with the plots in Fig. 3.3.

Now that the interpolation between late and early times has been discussed using Borel resummation and hyperasymptotics, the next section will be devoted to the transasymptotic summation method.

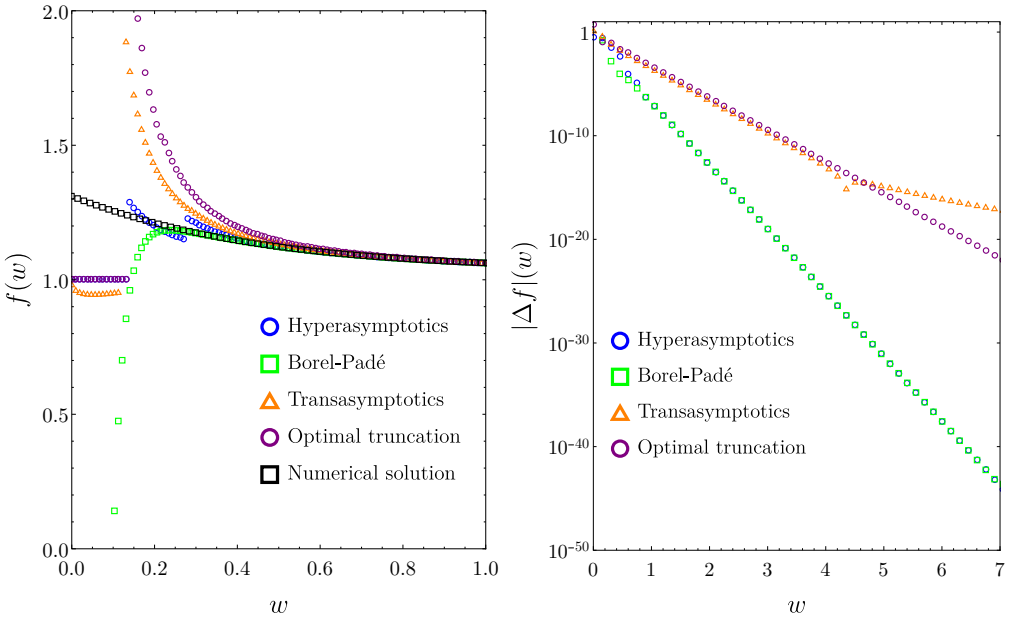

FIGURE 3.3: Left: approximations of $f(w)$ using different resummation methods for the transseries parameter $\sigma_+ = -0.3493 + 0.0027\mathrm{i}$, corresponding to the function $f_+(w)$ (3.23). The numerical solution is given by the black curve on the left. Right: the absolute value of the error of the different methods, which has been computed by comparing the resummations to the numerical solution. The kink in the error plot of the transasymptotic summation appears due to the limited number of coefficient functions which have been calculated and is expected to disappear if enough orders are calculated. Taken from [4].

[14] The formula for N_{opt} in (3.41) is a good approximation for the least term.

3.4 Transasymptotic summation

In Section 3.3 it was seen that approximating the transseries (3.25) by keeping only the perturbative and the first non-perturbative sectors gives excellent approximations of exponential accuracy for the function $f(w)$ outside a small region near the origin. However, one can only truncate the transseries in this way if the exponential factors are small. Along the negative axis, the exponential monomial $\tau \sim \mathrm{e}^{-Aw}$ defined in (3.28) grows arbitrarily large, and thus one cannot truncate the transseries (3.25) at any exponential order, since all orders of τ will contribute significantly towards the sum in that regime. This raises the question of whether the transseries can be used in regions where the exponential monomial is large enough. This is indeed the case. One can exploit the fact that the divergent behaviour in the transseries comes only from large orders of the perturbative variable w^{-1}, whereas the large order behaviour of the exponential variable τ is convergent. All that needs to be done is change the order of summation in (3.25):

$$\mathcal{F}(\tau, w) = \sum_{n\geq 0}\sum_{r\geq 0} \tau^n a_r^{(n)} w^{-r} = \sum_{r\geq 0}\left(\sum_{n\geq 0} a_r^{(n)}\tau^n\right) w^{-r} \equiv \sum_{r\geq 0} F_r(\tau) w^{-r}. \tag{3.42}$$

The coefficient functions $F_r(\tau)$ are analytic at $\tau = 0$, and it will be seen that it is possible to systematically calculate them in closed form. This approach is called the transasymptotic summation [9, 72], and has been shown to be a powerful tool in the study of non-linear problems [76, 2, 86]. This summation procedure allows us to probe regimes where $|w| \to \infty$ but the exponentials are no longer small.

The special form of (3.42) allows us to compute the functions $F_r(\tau)$ by treating τ and w as independent variables. Let us start with the first order approximation

$$\mathcal{F}(\tau, w) = F_0(\tau) + \mathcal{O}\left(w^{-1}\right), \quad w \to \infty. \tag{3.43}$$

Then F_0 obeys the ODE

$$-1 + F_0(\tau)\left(1 - \tau F_0'(\tau)\right) = 0, \tag{3.44}$$

which is solved by $F_0(\tau) = 1 + W(\frac{3}{2}\tau)$ [15], where W stands for the branch W_0 of the

[15] The general solution to (3.44) is $F_0(\tau) = 1 + W(c\tau)$. The integration constant c is found by matching the transasymptotic expansion to the transseries (3.25), and depends on the choice for $a_0^{(1)}$. Our choice was $a_0^{(1)} = 3/2$.

Lambert-W function (see Appendix B.5). One can go further and calculate all $F_r(\tau)$ recursively. For $r \geq 1$ one finds the following differential equations for F_r:

$$\begin{aligned} A\left(\tau F_0(\tau)F_r'(\tau) + \left(\tau F_0'(\tau) - 1\right)F_r(\tau)\right) =& (4-\beta)\delta_{r,1} - 8F_{r-1}(\tau) + \\ &+ \frac{9-r}{2}\sum_{k=0}^{r-1} F_k(\tau)F_{r-1-k}(\tau) + \beta\tau\sum_{k=0}^{r-1} F_k(\tau)F_{r-1-k}'(\tau) - A\tau\sum_{k=1}^{r-1} F_k(\tau)F_{r-k}'(\tau). \end{aligned} \tag{3.45}$$

Note that in (3.45) all the derivative terms come multiplied by the variable τ, and that the variable τ does not appear other than as a multiplier of the derivatives. This motivates the convenient variable transformation $\tau \to W = W(\frac{3}{2}\tau)$. The derivatives transform as

$$\tau\frac{\mathrm{d}}{\mathrm{d}\tau} = \frac{W}{1+W}\frac{\mathrm{d}}{\mathrm{d}W}. \tag{3.46}$$

With the transformation (3.46) it is possible to rewrite the original recursive set of ODEs (3.45) and integrate them exactly. The details of this calculation as well as the method of fixing the integration constants are given in Appendix (B.3). It turns out that all the F_r are rational functions in W and can be computed exactly (see also [94, 95]). Let us now see how the functions $F_r(\tau)$ can be used to solve the interpolation problem between early and late times.

3.4.1 Interpolation with transasymptotics

The objective is to find an approximation for the transseries parameter σ corresponding to a given solution around the origin ((3.24) or (3.23)) using the transasymptotic summation (3.42). The first step of our approach is the same as in Section 3.3 – using numerical analytical continuation from the origin to the matching point $w = w_0$ to obtain the numerical approximation $f_{\mathrm{ac}}(w_0)$ (see (3.34)). Next, an approximation for $\tau(w_0)$ is computed, from which the transseries parameter σ can directly be calculated using the definition of $\tau(w_0)$, Eq. (3.28). The idea is to solve for the function $\gamma(w)$ obeying

$$\mathcal{F}(\gamma(w), w) = \sum_{n\geq 0} F_r\left(\gamma(w)\right) w^{-r} = f_{\mathrm{ac}}(w_0) = \text{constant, for } w \gg 1, \tag{3.47}$$

which will be equal to $\tau(w_0)$ when evaluated at the point w_0, *i.e.* $\gamma(w_0) = \tau(w_0)$. The function $\gamma(w)$ satisfying (3.47) admits a perturbative, divergent asymptotic expansion

in w^{-1}:

$$\gamma(w) = \sum_{k=0}^{+\infty} \gamma_k \, w^{-k}, \tag{3.48}$$

and determining $\gamma(w)$ will correspond to finding the coefficients γ_k. Truncating the above expansion at its first term $\gamma(w) = \gamma_0 + \mathcal{O}\left(w^{-1}\right)$, one finds from (3.47) that up to leading order

$$1 + W\left(\frac{3}{2}\gamma_0\right) = f_{\text{an}}(w_0). \tag{3.49}$$

Then $\gamma_0 = \tau(w_0)$ (up to leading order in w_0^{-1}), and using the definition of $\tau(w)$ (3.28) one finds

$$\sigma(w_0) = \left(f_{\text{ac}}(w_0) - 1\right) w_0^{-\beta} \, \mathrm{e}^{f_{\text{ac}}(w_0) - 1 + A w_0} \left(1 + \mathcal{O}\left(w_0^{-1}\right)\right). \tag{3.50}$$

This result can be easily extended to higher orders in w_0^{-1} by including higher orders in the ansatz (3.48) and matching powers of w^{-1} in (3.47).

The transasymptotic summation (3.42) can also be used to re-sum the transseries by truncating the series at the term of least magnitude. The difference with respect to the classical optimal truncation is that coefficients $F_r(\tau(w))$ vary with w. The result is displayed in Fig. 3.3, where it can be seen that this approach slightly outperforms optimal truncation. Note that only the coefficient functions $F_r(w)$ up to $r = 15$ have been calculated, and so the calculation is no longer optimal after the kink in the logarithmic error plot of Fig. 3.3. Furthermore, the kink happens at a higher value of w than one would expect from the resummation point w_0 corresponding to 15 terms with classical optimal truncation given by (3.41).

3.4.2 Analytic results: branch points and global behaviour

Transasymptotics can also be used to describe *global properties* of the function $f(w)$ from (3.19), such as zeros, poles and branch points, or to link distinct expansions in different asymptotic regimes. This is quite remarkable given that the transasymptotic summation was derived as a *local expansion* around the point $w = +\infty$.

Notice that in the solutions plot found in Fig. 3.1, the locations w_{s} of the square root branch points depend on the initial value problem for $f(w)$ (given by $f(0)$ for convergent solutions at the origin, or by the value of the continuous continuation of $w^4 f(w)$ at $w = 0$ for the divergent solutions). From the perspective of late-time asymptotics, this

means that the locations w_s are functions of the transseries parameter σ. As already mentioned, all the coefficient functions $F_r(\tau)$ in the transasymptotic summation (3.42) can be expressed as rational functions of the Lambert-W function $W(\frac{3}{2}\tau)$, which has a square-root branch point at $\tau = -\frac{2}{3}e^{-1}$. This branch point in the τ-plane translates to an infinite number of branch points in the w-plane, once one substitutes $\tau = \tau(w)$ as in (3.28). Since the Lambert-W function appears in all the coefficient functions in the transasymptotic summation (3.42), one expects the function $f(w)$ to have an infinite number of square root branch points as well. The analytic information about the non-perturbative exponentials encoded in the coefficient functions $F_r(\tau)$ can be used to provide an approximation for the locations w_s.

All zeros of $f(w)$ are square root branch point singularities (see the expansions in Eq. (3.22)) with the exception of a potential regular zero at $w = (4-\beta)/A \approx 0.502$. Hence one can solve for the branch points w_s by solving the equation

$$\mathcal{F} = \sum_{n=0}^{\infty} w^{-k} F_k(\tau) = 0 \tag{3.51}$$

for $w = w_s(\sigma)$, where $\mathcal{F}$ is the transasymptotic summation in Eq. (3.42). This can be done by first expanding τ around the branch point of the Lambert-W function $W(\frac{3}{2}\tau)$, i.e. $\tau_0 = -\frac{2}{3e}$ in some power of w,

$$\varepsilon = w^{\alpha}, \tag{3.52}$$

$$\tau = \tau_0 + \tau_1\varepsilon + \tau_2\varepsilon^2 + \mathcal{O}\left(\varepsilon^3\right) . \tag{3.53}$$

The idea now is to choose the expansion of τ (3.53) in such a way that the sum (3.51) vanishes for all values of w. In the second step the expression of τ from the expansion (3.53) is set equal to the original definition of τ, (3.28), and this allows to solve for the value of w at which the full transasymptotic sum (3.51) has a branch point. The zeroth order coefficient function F_0 can then be expanded in ε in the following way

$$F_0(\varepsilon) = a_1\sqrt{\varepsilon} + a_2\varepsilon + \mathcal{O}\left(\varepsilon^{3/2}\right) , \tag{3.54}$$

where $a_1 = \sqrt{3e\tau_1}$. One finds that the leading order in the ε-expansions of the $F_k(\varepsilon)$ behave as

$$
\begin{aligned}
F_1(\varepsilon) &= -\frac{2\left(\beta^2+5\beta-2\right)}{3Aa_1}\,\varepsilon^{-1/2}+\mathcal{O}\left(\varepsilon^0\right);\\
F_2(\varepsilon) &= -\frac{4\left(\beta^2+5\beta-2\right)^2}{27A^2a_1^3}\,\varepsilon^{-3/2}+\mathcal{O}\left(\varepsilon^{-1}\right);\\
F_3(\varepsilon) &= -\frac{16\left(\beta^2+5\beta-2\right)^3}{243A^3a_1^5}\,\varepsilon^{-5/2}+\mathcal{O}\left(\varepsilon^{-2}\right);\\
&\cdots\\
F_k(\varepsilon) &= -\left(\frac{3(-2+5\beta+\beta^2)}{2Aa_1^2}\right)^k a_1\,\frac{2^k}{3^{k-1}}C_{k-1}\varepsilon^{-\frac{2k+1}{2}}+\mathcal{O}\left(\varepsilon^{-2k}\right),
\end{aligned}
\tag{3.55}
$$

where C_{k-1} is the $(k-1)$-th Catalan number. From now on it will be assumed that $\varepsilon = w^{-1}$, corresponding to $\alpha = 1$ in (3.52). All other choices of α can be excluded through a consistency analysis. The expression that was found for the $F_k(\varepsilon)$ in (3.55) allows one to sum up the leading order expression of the transasymptotic summation (3.42), giving

$$
\sum_{k=0}^{\infty} w^{-k}F_k \sim \frac{a_1}{2}\sqrt{9-\frac{16}{3}\left(\frac{3(-2+5\beta+\beta^2)}{2Aa_1^2}\right)}w^{-1/2}+\mathcal{O}\left(w^{-1}\right). \tag{3.56}
$$

The expression (3.56) must vanish, from which one obtains

$$
a_1 = \pm\frac{2\sqrt{c}}{\sqrt{3}}. \tag{3.57}
$$

It was already found that $a_1 = \sqrt{3\mathrm{e}\tau_1}$. Together with (3.57) this implies

$$
\tau_1 = \frac{4c}{9\mathrm{e}}. \tag{3.58}
$$

To find a leading order approximation for the position of the branch points the next step is to use the definition of τ, (3.28) and solve

$$
\tau_0 + \tau_1 w^{-1} = \sigma w^{\beta}\,\mathrm{e}^{-Aw}. \tag{3.59}
$$

Now define

$$
y = A\,w. \tag{3.60}
$$

Then

$$\tau_0 + (\tau_1 A)\, y^{-1} = \frac{\sigma}{A^\beta} y^\beta \, \mathrm{e}^{-y}\,, \tag{3.61}$$

and after taking the logarithm:

$$y - \beta \log y = \log\left(\frac{\sigma}{\tau_0 A \beta}\right) + 2\pi \mathrm{i} n - \log\left(1 + \frac{\tau_1 A}{\tau_0} y^{-1}\right), \quad n \in \mathbb{Z}\,. \tag{3.62}$$

One only needs to include terms up to order w^{-1} since our original approximation (3.59) is only correct up to that order, and by expanding out the logarithm one obtains

$$y - \beta \log y = \underbrace{\log\left(\frac{3\sigma \mathrm{e}}{2A^\beta}\right) + \pi \mathrm{i}(1+2n)}_{\equiv t(n,\sigma)} - \frac{\tau_1 A}{\tau_0} y^{-1} + \mathcal{O}\left(y^{-2}\right)\,. \tag{3.63}$$

This equation is can be solved for y up to (and including) order y^{-1} and t^{-1}, and one obtains

$$y = t + \beta \log t + \frac{1}{t}\left(\beta^2 \log t + \beta^2 - 5\beta - \frac{3}{A}\right). \tag{3.64}$$

Hence one arrives at the following formula for the location of the branch points, w_s:

$$w_{\mathrm{s}}(t) \simeq w_{\mathrm{s}}^{(\mathrm{approx})}(t) = \frac{t}{A} + \frac{\beta}{A}\,\log t + \frac{1}{A\,t}\left(\beta^2\,\log t + \beta^2 - 5\beta - \frac{3}{A}\right), \quad \text{as } t \to \infty, \tag{3.65}$$

where

$$t = t(n,\sigma) = \log\left(\frac{3\sigma \mathrm{e}}{2A^\beta}\right) + \pi \mathrm{i}(1+2n), \qquad n \in \mathbb{Z}. \tag{3.66}$$

The integer n in (3.66) parameterises the sequence of branch points. Note that (3.65) is the partial sum of a divergent asymptotic expansion in t, and thus Eq. (3.65) is only a good approximation for the branch points/zeros of $f(w)$ when $|t|$ is large enough. In particular, $w^{(\mathrm{approx})}(t)$ becomes more accurate for large values of the discrete parameter n, because the auxiliary variable t grows as an affine function of n. Since the leading order approximation $w^{(\mathrm{approx})}(t)$ from Eq. (3.65) grows linearly in t, the branch points which lie far from the origin are the ones best approximated by $w^{(\mathrm{approx})}(t)$.

Numerically, the zeros of $f(w)$ can be computed by initially guessing the position of the branch point using (3.65) [16] and then using a contour integral to find an approximation for the exact location. One starts by choosing a value for the transseries parameter σ and using the hyperasymptotic approximation Eq. (3.31) to find $f(w_0)$ (at *e.g.* $w_0 = 10$).

[16] I could also have used Padé approximants for the initial guess.

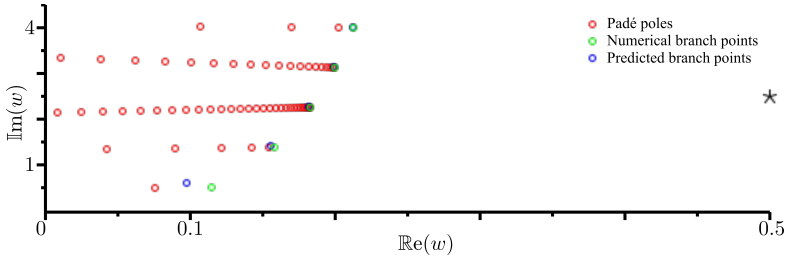

FIGURE 3.4: Branch cuts of the $f(w)$ for the case $\sigma = \frac{2}{3}$. Green dots: numerically computed branch-points. Blue dots: approximations (3.65) to the locations of the branch points obtained from the transasymptotic summation of the late time solution $\mathcal{F}(w)$ (3.25) (compare Table 3.1). Red dots: poles for the Padé approximant (about $w = \frac{1}{2} + \frac{5}{2}$i, shown as $\star$) representing the branch cuts of the solution. It can be seen that the further the singularities are the more accurate the approximations become. Taken from [4].

Then one analytically continues $f(w)$ from w_0 to a point in the vicinity of our prediction (3.65) using the Taylor series method, $w_1 = w_{\mathrm{s}}^{(\mathrm{approx})}(t) + \varepsilon$ (*e.g.* $\varepsilon = 0.3$). Next one analytically continues again to compute the data on the circle $|w - w_{\mathrm{s}}^{(\mathrm{approx})}(t)| = \varepsilon$. Using the trapezoidal rule [96] one evaluates the contour integral of $\frac{wf'(w)}{f(w)}$ to obtain the zeros of $f(w)$ [17]. The approximate locations obtained with Eq. (3.65) as well as the numerical results are listed in Table 3.1, and plotted in Fig. 3.4.

	approx. (3.65)	numerical
$n = 0$	$0.0975 + 0.6040$i	$0.1147 + 0.5076$i
$n = 1$	$0.1555 + 1.416$i	$0.1580 + 1.384$i
$n = 2$	$0.1817 + 2.276$i	$0.1827 + 2.257$i
$n = 3$	$0.1991 + 3.143$i	$0.1997 + 3.129$i
$n = 4$	$0.2122 + 4.012$i	$0.2125 + 4.001$i

TABLE 3.1: Approximations for the locations of the square-root branch points of (3.65) versus their numerically computed values for $\sigma = \frac{2}{3}$. Taken from [4].

3.5 Linking the two infinities

There is yet another powerful application of transasymptotics, which is that it can be used to correctly predict the different asymptotic behaviour of our solutions in separate regions of the w-plane. Consider the attractor f_+ in the solutions plot of Fig. 3.1 (the black curve). At large, positive w, $f_+(w)$ converges to a finite value, while at large, negative w the same solution grows linearly with w. Therefore there are two different asymptotic expansions, the transseries (3.25) at large positive w and the linearly growing expansion

[17] Due to the square root singularity (see (3.65)), the branch point must be encircled twice.

(3.27) at large negative w (which is also a transseries, but with $\log w$-monomials instead of exponentials e^{-Aw}, see [18]). This is not surprising given the presence of square root branch points in the domain of our solutions. But it also raises an interesting question: can two expansions somehow be related to one another? The answer is yes, the great power of the transasymptotic approach lies in the possibility of analytically accessing regions in which the non-perturbative exponentials are no longer small. While the large, positive w limit corresponds to exponentially small values of $\tau \sim e^{-Aw}$, the large, negative w limit is associated with exponentially large values of τ. Thus when one flips the sign $w \to -w$, the powers of w^{-1} in the transasymptotic summation (3.42) do not change size, while the exponential variable $\tau \sim e^{-Aw}$ becomes exponentially large instead of exponentially small.

3.5.1 Matching the coefficient functions for large exponentials

The goal is to analytically continue across the anti-Stokes line along the positive imaginary axis in the z-plane. It has already been found that there are two different asymptotic expansions around $w = \infty$. If one starts off at $w = +\infty$ with the finite-valued solution, moves across the anti-Stokes line and then to $w = -\infty$, but now along some path in the second quadrant, then there will be a change in the asymptotic behaviour. This change corresponds to a switching from the asymptotic expansion of order $\mathcal{O}\left(z^0\right)$ to the growing expansion with leading order $\mathcal{O}\left(z\right)$. This behaviour is visualised in Fig. 3.5

However, there is only a single expression for the transasymptotic summation, and both expansions must be encoded in that same transasymptotic series, and hence there must be a correspondence between the two free parameters σ and p_4. The role that σ plays in the transasymptotic summation is known as an exact expression for τ in terms of σ has been given. It is also known that all the coefficient functions

$$F_k(\tau) \equiv G_k(F_0(\tau)) \tag{3.67}$$

are known functions $G_k(F_0)$ of the 'zeroth' coefficient function

$$F_0(\tau) = (1 + W(\frac{3}{2}\tau))\,, \tag{3.68}$$

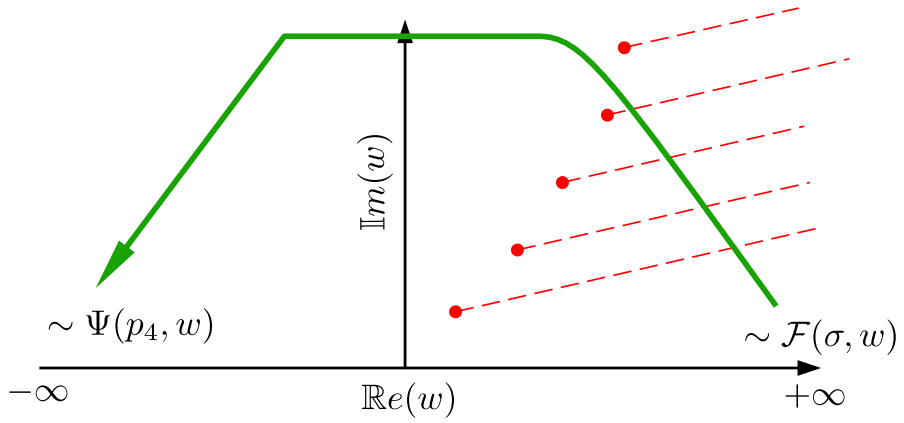

FIGURE 3.5: A schematic illustration of the correspondence between the asymptotic expansions in two different regions of the w-plane. If one starts off at $w = +\infty$ with the exponential transseries $\mathcal{F}(\sigma, w)$ and analytically continues across the green line to $w = -\infty$, one obtains the logarithmic transseries $\Psi(p_4, w)$, where both σ and p_4 parametrise the solutions. The red dots represent square root singularities and the dotted red lines the associated branch cuts. Since there is an infinite tower of singularities whose imaginary parts become arbitrarily large, it is impossible to circumvent all of them by choosing a suitable path in the complex plane. The solution $\Psi(p_4, w)$ and the parameter p_4 one obtains at $w = -\infty$ from this procedure is ambiguous and dependent upon the exact path taken (green line).

Hence the problem can be decomposed into two steps, (1) to expand W (and hence F_0) for large z with negative real part (hence large τ), and (2) to find the coefficients $F_{k,j}$ in the expansion of F_k in powers of F_0^{-1}. For convenience, the following notation is introduced

$$E \equiv F_0^{-1}\,, \tag{3.69}$$

The function W can be expanded in the following way [97]:

$$W = L_1 - L_2 + \sum_{k=0}^{\infty}\sum_{m=1}^{\infty} C_{km} L_1^{-(k+m)}\, L_2^m\,, \tag{3.70}$$

where

$$\begin{aligned} L_1 &= \log(\tau)\,; \\ L_2 &= \log\log(\tau)\,; \\ C_{km} &= \frac{(-1)^{k+m+1}}{m!} s(k+m, k+1)\,. \end{aligned} \tag{3.71}$$

Here, $s(k+m,k+1)$ denotes a Stirling circle number of the first kind. Remember that τ has been defined before in (3.28). Using

$$\begin{aligned} \tau &= \sigma\, w^{\beta}\, \exp(-Aw)\,; \\ c &= \log(\sigma) + 2\pi \mathrm{i}\, n, \quad n \in \mathbb{Z}\,, \end{aligned} \tag{3.72}$$

one can write down the following expansions for L_1 and L_2:

$$\begin{aligned} L_1 &= -Aw + \beta \log(w) + c\,; \\ L_2 &= \log(-Aw) - \sum_{n=1}^{+\infty} \frac{1}{n} \left(\frac{\beta \log(z) + c}{Aw} \right)^n . \end{aligned} \tag{3.73}$$

Using the above, one finds an expansion for $E(w)$:

$$E(w) = -\frac{1}{A}\, w^{-1} - \frac{(1 + c + \beta \log(w))}{A^2}\, w^{-2} + \ldots . \tag{3.74}$$

Now the transasymptotic summation is expanded $\mathcal{F}$ in the following way:

$$\mathcal{F} = \sum_{n \geq 0} G_n(E)\, w^{-n} = \sum_{n \geq 0} \sum_{k \geq -\widetilde{k}} G_{n,k} E(w)^k\, w^{-n}\,; \tag{3.75}$$

The notation $\widetilde{k}$ denotes the following discrete function:

$$\widetilde{k} = \begin{cases} (k+1) & \text{for } k \leq 4 \\ k & \text{for } k \geq 5 \end{cases} . \tag{3.76}$$

The first power $k = -\widetilde{k}$ has been found by considering the first few G_k ($k \leq 18$) and expanding in E. One further defines

$$Z_r = \frac{W}{1+W} F_r\,, \tag{3.77}$$

The task is now to expand Z_k in powers of E and to match those powers to derive recursive equations for $Z_{k,j}$, where j denotes the j-th power coefficient in the E-expansion of $Z_k(E)$. Note that just as $G_k(E)$, this expansion also starts with the negative power $-\widetilde{j}$, the re-scaling factor θ by which the two quantities has an expansion which starts with a

constant. It is useful to expand $Z_r(E)$ in powers of E in the following way:

$$Z_r(E) = E^{-\widetilde{r}} \sum_{m=0}^{\infty} Z_{r,m}\, E^m = Z_{r,0} E^{-\widetilde{r}} + Z_{r,1} E^{-\widetilde{r}+1} + \ldots ; \tag{3.78}$$

The differential equation can be brought into the following form (note that Y_r and Z_r are functions of different variables):

$$\begin{aligned} & E^{\widetilde{r}+1} Z_r' + \delta_{r,1} \frac{E^{\widetilde{r}}(4-\beta)}{A(1-E)^2} + \left(\frac{-8E^{\widetilde{r}}}{A(1-E)} \right) \\ + \sum_{k=0}^{r-1} \Bigg\{ & \left(-\frac{E}{A} \right)^{\widetilde{r}} \left((k-4) - \beta E^2 \right) Z_k\, Z_{r-k-1} \\ & - g_{1,k}\, E^{\widetilde{r}+2}\, Z_k\, Z_{r-k} \\ & - \frac{\beta}{A}(1-E)\, E^{\widetilde{r}+2}\, Z_k\, Z_{r-k-1}' \\ & + (1-E)\, E^{\widetilde{r}+2}\, g_{1,k}\, Z_k\, Z_{r-k}' \Bigg\} \\ & = 0\,, \end{aligned} \tag{3.79}$$

where in the expression (3.79) the following notation has been introduced

$$g_{\ell,k} \equiv \begin{cases} 0 & \text{for } k < \ell \\ 1 & \text{for } k \geq \ell \end{cases} . \tag{3.80}$$

The next step is to subsitute the ansatz (3.78) into the recursion equation for Z_r, Eq. (3.79) and match equal powers of E. For $\widetilde{r} \neq m$ one obtains an explicit recursion relation for coefficients of the E-expansion of $Z_r(E)$, $Z_{r,m}$, which can be found in Appendix B.7. One still has to fix the coefficients $Z_{r,\widetilde{r}}$. These are just the integration constants to the family of first order ODEs (3.79). The next step is to compute the coefficients for large r for the first few orders in m. Since the closed-form expressions for $Z_r(E)$ for $r \leq 15$ have been computed, these constants can be found by expanding the $Z_r(E)$ and reading off the coefficient $Z_{r,\widetilde{r}}$. The coefficients $Z_{r,m}$ for $m \leq 14$ and arbitrarily high r can be calculated using this method.

3.5.2 Summing the series

The next step is to sum the series using the coefficient in the large w expansion for $\mathbb{R}\mathrm{e}\,(w) < 0$. Remember that the relationship between G_n and Z_n is given by (3.77).

$$\begin{aligned}\mathcal{F} &= \sum_{n=0}^{\infty} G_n(E) w^{-n}\,; \\ &= \sum_{r\geq 0}\sum_{m\geq 0} (1-E) Z_{r,m} E^{-\widetilde{r}+m} w^{-r}\,.\end{aligned} \tag{3.81}$$

It has already been shown how to use the known asymptotic expansion of the Lambert-W function to expand E. This can be expressed as

$$E = E(w^{-1},\xi) \equiv -\frac{1}{Aw}\left(1 + w^{-1}\eta(w^{-1},\xi)\right); \qquad \xi = -\log(w), \tag{3.82}$$

where $\eta(w^{-1},\xi)$ is an analytic function of both w^{-1} and ξ whose leading order is a constant. Its Taylor expansion in these variables can be calculated to arbitrary order using (3.70). Finally one obtains

$$\mathcal{F} = \sum_{r=0}^{\infty}\sum_{m=-1}^{\infty} h_{r,m}(w^{-1},\xi) w^{-m}\,, \tag{3.83}$$

where

$$\begin{aligned}h_{r,m}(w^{-1},\xi) \equiv\ g_{\alpha(r),m}\, Z_{r,m-\alpha(r)}\ (-A)^{\alpha(r)+\widetilde{r}-m}\,(1-E(w^{-1},\xi))\times \\ \times \left(1 + w^{-1}\eta(w^{-1},\xi)\right)^{m-\alpha(r)-\widetilde{r}}\,,\end{aligned} \tag{3.84}$$

and

$$\alpha(r) \equiv -1 + \Theta(r-4)\,. \tag{3.85}$$

Now one expands further

$$\begin{aligned}\mathcal{F} &= \sum_{r=0}^{\infty}\sum_{m=-1}^{\infty}\sum_{j=0}^{\infty} h_{m,r,j}(\xi) w^{-m+j} \\ &= \sum_{n=-1} w^{-n}\left(\sum_{m=-1}^{n}\sum_{r=0}^{\infty} h_{m,r,n-m}(\xi)\right) \equiv \sum_{n=-1}^{\infty} w^{-n} K_n(\xi),\end{aligned} \tag{3.86}$$

where $h_{m,r,j}(\xi)$ denotes the j-th coefficient in the Taylor expansion of $h_{m,r}(w^{-1}, \xi)$ in the variable w^{-1}. By summing up to $r = 400$, one finds that K_n converges to the coefficients of the asymptotic expansion Eq. (3.27) for $n \leq 3$. For $n = 4$, the series K_n diverges, which makes it impossible to calculate p_4. The reason for the breakdown of the calculation of p_4 can be interpreted as a natural consequence of the ambiguity of the value of p_4 due to the existence of an infinite amount of branch points. Regardless of how large one chooses the radius for the path of analytic continuation linking $w = +\infty$ to $w = \infty$, there will always be branch points and the result must therefore depend on the exact path taken. [98].

3.6 Discussion

This work has focused on solving the problem of late-time to early-time matching for arbitrary solutions of the nonlinear ODE (3.19). One finds a one-parameter family of solutions in two different regions of our domain, both at early and late times. At late times, the ODE (3.19) admits formal, asymptotic transseries solutions consisting of a hydrodynamic perturbative sector as well as non-hydrodynamic sectors weighed by positive integer powers of the non-perturbative exponentials e^{-Aw} (with variable w representing time). In the early time regime $w \sim 0$ there is also a one-parameter family of divergent solutions which behave asymptotically as $\sim w^{-4}$, as well as two finite solutions which are special limits of the one-parameter family (see solution plots in Fig. 3.1). The exponentially small contributions appearing at late times can be expected to be the leading contributions at early times. Beyond the MIS case, one expects to find similar transseries solutions in other hydrodynamic systems which observe a factorially divergent late time behaviour (see *e.g.* [99])

The results obtained in the previous sections were based on the well-established resummation methods of hyperasymptotics, Borel-Padé summation and transasymptotics. Nevertheless, previous work did not exploit their strengths to do the parameter-matching and relied instead on less accurate procedures such as numerical least square fits [86, 87]. An analysis of said methods has been carried out, and it has been shown that they are very effective tools for the parameter-matching. In terms of accuracy, the hyperasymptotic approach and the Borel resummation perform best. Both give an exponentially small error $\sim \mathrm{e}^{-2|Aw|}$.

The hyperasymptotic approximation has discontinuities since the number of terms which are included in the series varies with w, but requires no intricate numerical computations other than determining the series coefficients of the perturbative and first non-perturbative sectors. On the other hand, the Borel resummation is a continuous function of w. However, the calculation of the Laplace transform (3.37) in going from the Borel-plane to the complex w-plane requires the numerical computation of an integral. As a consequence, Borel resummation is more computationally expensive than the hyperasymptotic summation, especially since said integral must be computed to exponential accuracy e^{-Aw} for the method to perform as well as the level-1 hyperasymptotic summation.

The summation methods can be made arbitrarily accurate by increasing the number of non-perturbative modes included in the approximation, as both resummation methods can be extended to include an arbitrary number of exponentials. But while the extension of Borel-summation methods to include higher exponentials is straightforward, the generalisation of hyperasymptotics beyond level-1 quickly becomes impractical.

The transasymptotic summation was originally used very effectively in the analysis of solutions of non-linear ODEs [72]. While the transasymptotic summation is less accurate in performing the interpolation, giving an error of $\sim \mathrm{e}^{-|Aw|}$ (as opposed to $\mathrm{e}^{-2|Aw|}$ for the methods mentioned above), it is an extremely useful tool in the study of the *global* analytic properties of the solutions. The power of the transasymptotic approach lies in encoding the behaviour of the non-perturbative exponentials in analytic closed-form expressions, which provide analytic continuations beyond the validity of the original transseries expansion. A systematic way of calculating these functions has been provided and the functions have been used to derive general analytic results such as analytic approximations to the locations of the square-root branch points as well as a way of linking distinct asymptotic expansions in two different regions of the w-plane.

The matching procedure which was used is quite general and can be used beyond relativistic hydrodynamics. In fact, one can apply it to any interpolation problem between two different regions (e.g. late-time to early-time, strong/weak coupling, large charge to small charge), where the solutions in one region are described by resurgent, asymptotic perturbative expansions, and where the behaviour in the other regime is known analytically (*e.g.* [100, 101, 86, 102, 103, 104, 105]).

From a mathematical standpoint, the asymptotic methods introduced in Chapter 1 were used to obtain the global behaviour of the time-dependent energy density of a strongly coupled fluid. It was seen that the exponential terms become relevant and how that translates to a widely different behaviour of the energy density at early times, as well as the existence of branch points for complex time. This is similar to the bifurcation phenomenon uncovered in the previous chapter, which was seen to be directly connected to a change in dominance of the exponential terms in the transseries. This was explicitly shown by using transasymptotic summation to effectively perform analytic continuation.

The next chapter will to take this idea further, using the same asymptotic methods to analyse a perturbative expansion of the so-called quasinormal modes of a black hole, to uncover the non-perturbative 'instanton-like' phenomena that must be included in a transseries formulation, and potentially use the same summation techniques to understand the full non-perturbative picture of these modes.

Chapter 4

Quasinormal modes and strong cosmic censorship

The on-going research presented in this chapter is my own. It was developed under the guidance of my supervisor Inês Aniceto.

General relativity is the best theory of gravity available at the moment. While in the Newtonian picture gravity is a force which acts on matter proportional to its mass, general relativity postulates that gravity is essentially a geometric phenomenon. Space and time are no longer to be thought of as separate from each other, but rather as unified in one curved four-dimensional spacetime manifold. In this picture matter has the effect of causing the spacetime to curve, and particles under the influence of gravity naturally follow geodesics - the natural generalisation of a straight line in flat space - in the curved geometry. The geometry of the spacetime is uniquely determined by the metric tensor, which dictates how distances and angles are to be measured locally. The metric tensor can be calculated using Einstein's equations, a system of 10 coupled, non-linear PDEs. These equations admit very interesting solutions, among which are the famous black holes containing event horizons and space-time singularities.

Some black hole solutions such as the Reissner-Nordstrom-(de Sitter) spacetimes [106] contain a so-called Cauchy-Horizon within the black hole instead of a spacelike singularity like in the Schwarzschild spacetime. The Cauchy horizon marks the boundary of the range of validity of the Cauchy problem - the generalisation of the initial value problem for geometries.. Mathematically one can perform an analytical continuation beyond the

Cauchy horizon and write down exact solutions containing regions with unphysical attributes like the existence of timelike singularities [107]. However, these extended regions beyond the Cauchy horizon cannot be obtained by evolving the Einstein equations from some initial conditions since the Cauchy problem is no longer well-posed beyond the Cauchy horizon. This means that if an observer is able to cross the Cauchy-Horizon, the theory cannot predict what will happen after the crossing. If, however, the spacetime curvature becomes strong enough to destroy any physical observer before they can cross the Cauchy-Horizon, general relativity is deterministic in the sense that the theory can predict any event in the future given the precise initial conditions (since the region beyond the Cauchy horizon would not exist physically and therefore not belong to the future).

The requirement that one cannot continue the metric solution in a physically meaningful way beyond the Cauchy horizon is called the Strong Cosmic Censorship conjecture (SCC) [108, 109, 110, 111, 112]. Some spacetimes such as the Reissner-Nordström-(de Sitter) solution describing a charged black hole can be analytically continued across the Cauchy horizon [107]. However, to conclude that a certain spacetime violates the SCC conjecture, the violation must be generic, that is, it must not depend on a fine-tuning of the initial data. To check whether a 'candidate spacetime' for a potential violation of the SCC conjecture actually does violate it, one must consider perturbations of the initial data and check whether the solutions for the perturbed data violate the conjecture generically. In the following, the perturbations will be assumed to be smooth. However, rough perturbations have also been discussed in the literature [113, 5]. Depending on what one considers to be a 'physically meaningful' way of continuation, there are several versions of the SCC conjecture. In other words, the question is how regular the metric is required to be at the Cauchy horizon for the solution to be a meaningful description of a physical spacetime.

Historically different versions of SCC have been discussed, among which are the C^0-version (the metric must not be continuous), the C^2-version (the metric must not be twice continuously differentiable), and the Christodoulou version, where the metric must not belong to the Sobolev space H^1_{loc} (corresponding to so-called weak solutions of the Einstein equations, see [112]) for the SCC conjecture to hold. For certain black hole spacetimes there exists a mathematical criterion of determining the behaviour of smooth linear perturbations and hence the validity of the SCC which relies on examining the

strength of decay of the quasinormal mode (QNM) frequencies [114, 115]. Each matter field can be decomposed into quasinormal modes at late times with complex frequencies, the real part of which determines the period of the oscillation whereas the complex part determines the decay rate [116].

Within the event horizon, two effects are competing for the energy of a given mode. The decay of the mode decreases the energy, while the blueshift effect causes an increase in the energy density. If the blueshift effect is strong enough to cause an energy blow-up at the Cauchy horizon despite the decay, the backreaction of the matter field on the metric destroys the horizon and SCC is preserved. If, on the other hand, the decay of the mode is strong the energy blow-up does not happen, a physical observer can pass through the horizon, and the SCC conjecture is violated [114]. It is possible to examine the validity of the SCC by considering the QNM of a given matter field with the weakest decay rate and checking whether it surpasses a critical value. Strictly speaking, it would be necessary to consider a matter model including all the known fields of the Standard Model, evolve the Cauchy data with the full non-linear Einstein equations and check the regularity of the resulting metric at the Cauchy horizon. However, here it is assumed that the SCC conjecture is valid if and only if it is valid for the linearised version of the Einstein equations, that is, it is assumed that non-linear effects do not matter qualitatively in what concerns the regularity of the metric. This assumption needs to be verified for each spacetime of interest. Nonetheless, for the sake of gaining an improved understanding of the regularity of perturbations in different matter models and the SCC problem in general, the approach taken here is justified.

The basis of the ongoing work presented in this chapter is [6], where the QNM frequencies of a charged scalar field in a Reissner-Nordström-de Sitter background have been calculated numerically to study the validity of the SCC conjecture. For this spacetime massless uncharged scalar perturbations had already been found to violate the SCC conjecture for certain near-extremal values of the parameters even when the non-linear backreaction on the spacetime was included [117, 118]. Later, massless pure Einstein-Maxwell theory (classical electromagnetism coupled to linearised gravity) was studied [5], and an even worse violation of SCC was found as for certain near-extremal black holes perturbations can be continued across the Cauchy horizon in an arbitrarily smooth manner. Both Einstein-Maxwell and massless scalar theory have in common that it is not possible to form the black hole. In the Kerr-dS case, it was found that both massless

scalar and linearised gravitational perturbations respect SCC [119]. As opposed to the RNdS black hole, the Kerr-dS black hole can be formed via gravitational collisions. The difference between the massless scalar and Einstein-Maxwell perturbations in RNdS and the massless scalar and linearised gravitational perturbations in Kerr-dS spacetime with respect to the possibility of forming the black hole motivates studying massless charged scalar perturbations in RNdS, as in that case the black hole can be formed via collapse in this case. In [6] it was found that for certain near extremal parameters, SCC is violated.

The violation of SCC in charged massless scalar theory on an RNdS background is very interesting from an asymptotics perspective because it is linked to an oscillatory behaviour of the decay rate of the QNMs with respect to variations of the field charge. The QNMs are asymptotic in the field charge, and one can hope to perform a similar analysis as in the previous chapters to check for SCC. For near extremal values of the spacetime parameters, the asymptotic value of the smallest decay rate of all the QNM frequencies (the criterion to be considered for SCC) lies just below the critical value, indicating that SCC is satisfied in the large-charge limit. However, for smaller values of the field, the non-perturbative sectors contribute in such a way as to oscillate around the critical value, which means that for certain points in the parameter space SCC is violated. For a discussion of the physical significance of this result how SCC can be rescued by allowing rough initial data see [6, 119].

The summation of asymptotic results going beyond the asymptotic regime would allow to perform an analytic analysis of the previous numerical results in [6], and provide ways of calculating calculating the QNM frequencies which do not rely on computationally expensive numerics. This approach could in principle also be applied to other spacetimes.

The work presented here builds onto the WKB approach of [6], and thus a summary of their WKB analysis will be presented, so that it can be generalised from the perspective of resurgence and summation. The results in this chapter are preliminary and part of an ongoing project.

4.1 The charged massless scalar field model in RNdS

In this section the mathematical models for the spacetime and the massless scalar field will be presented and the linear ODE for the quasinormal modes will be derived following [6]. Consider a system containing a charged, massive scalar field Φ with mass μ and charge q in an RNdS background spacetime with mass M and charge Q. The RNdS-action is

$$S = \frac{1}{16\pi G}\int \mathrm{d}^4x\,\sqrt{-g}\left(R - 2\Lambda - F^{\mu\nu}F_{\mu\nu}\right), \tag{4.1}$$

where $\Lambda = 3/L^2$ is the cosmological constant, R is the Ricci scalar and $F = \mathrm{d}A$ is the electromagnetic field tensor with a one-form potential A. The solution which leaves the action S stationary is

$$\begin{aligned} g_{\mu\nu}\mathrm{d}x^\mu\mathrm{d}x^\nu &= \mathrm{d}s^2 = -f(r)\,\mathrm{d}t^2 + \frac{1}{f(r)}\,\mathrm{d}r^2 + r^2\mathrm{d}\Omega_2^2, \\ \text{where } f(r) &\equiv 1 - \frac{2M}{r} + \frac{Q^2}{r^2} - \frac{r^2}{L^2} \\ \text{and } \mathrm{d}\Omega_2^2 &\equiv \mathrm{d}\theta^2 + \sin^2(\theta)\mathrm{d}\varphi^2; \\ A &= -\frac{Q}{r}\mathrm{d}t\,. \end{aligned} \tag{4.2}$$

$f(r)$ has four zeros, out of which three are positive and correspond to the Cauchy horizon r_-, the black hole horizon r_+ and the cosmological horizon r_c. The Penrose diagram for the RNdS spacetime is shown in Fig. 4.1

The function $f(r)$ can be factorised as

$$f(r) = -\frac{(r-r_-)\,(r-r_+)\,(r-r_c)\,(r+r_c+r_-+r_+)}{r^2\left(r_-\,(r_c+r_+)+r_c^2+r_+r_c+r_-^2+r_+^2\right)}\,. \tag{4.3}$$

By expanding out this expression and comparing it with the one in Eq. (4.2) one finds that the black hole the black hole charge is a function of the three horizons, $Q = Q(r_-, r_+, r_c)$. The extremal charge Q_{ext} can then be easily obtained by setting $r_- = r_+$, which gives

$$Q_{\text{ext}} = r_c\,y_+\sqrt{\frac{2y_+ + 1}{3y_+^2 + 2y_+ + 1}}\,, \tag{4.4}$$

where $y_j = r_j/r_c$ for $j \in \{-, +, c\}$. Another important quantity is the surface gravity $\kappa_j = \left|f'(r_j)\right|/2$ at the horizon r_j with $f(r_j) = 0$. The function $f(r)$ obeys the following

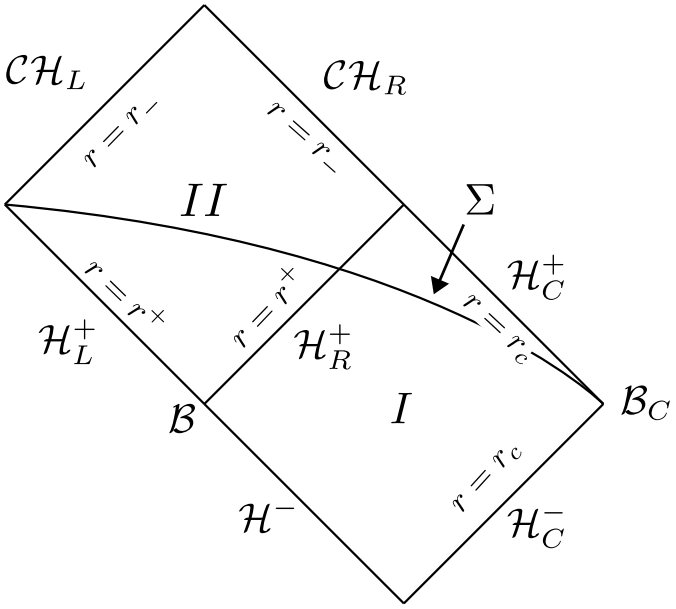

FIGURE 4.1: The Penrose diagram of the two physical regions I and II of the RNdS spacetime. Each point on the diagram represents a spatial two-sphere in the spacetime. Curves in the diagram whose tangents form an angle of less than 45 deg with the vertical axis are timeline, lines parallel to the diagonals in the diagrams are null, and curves which form an angle of less than 45 deg with the horizontal axis are spacelike. $\mathcal{CH}_L$ and $\mathcal{CH}_R$ together form the Cauchy horizon. $\mathcal{H}_C^+$ is the cosmological horizon, $\mathcal{H}_R^+$ is the black hole event horizon, and $\mathcal{B}_C$ is the de Sitter-analogue of spatial infinity. The spacelike hypersurface defined by Σ is an example of a Cauchy surface. Initial data specified on a Cauchy surface uniquely determines the behaviour of the system in the union of the regions I and II. Adapted from [5].

identity:

$$f(r)^{-1} = \frac{-1}{2\kappa_c(r-r_c)} + \frac{1}{2\kappa_+(r-r_+)} - \frac{1}{2\kappa_-(r-r_-)} + \frac{1}{2\kappa_{\text{neg}}(r-r_{\text{neg}})}\,. \tag{4.5}$$

The surface gravities at $r = r_+$ and $r = r_c$ are given by:

$$\begin{aligned} \kappa_+ &= \frac{1}{2r_c}\frac{(1-y_+)\,(y_+-y_-)\,(y_-+2y_++1)}{y_+^2\,\left(y_-^2+y_+y_-+y_-+y_+^2+y_++1\right)}\,; \\ \kappa_c &= \frac{1}{2r_c}\frac{(1-y_-)\,(1-y_+)\,(y_-+y_++2)}{\left(y_-^2+y_+y_-+y_-+y_+^2+y_++1\right)}\,. \end{aligned} \tag{4.6}$$

The RNdS background will be taken as fixed without taking into account the backreaction of the field Φ on the spacetime. The action of the scalar field is

$$S_\Phi = \int \mathrm{d}^4x\,\sqrt{-g}\,\left[-\frac{1}{2}\mathcal{D}_\mu\Phi\,\left(\mathcal{D}^\mu\Phi\right)^* - \frac{1}{2}\mu^2\Phi\,\Phi^*\right], \tag{4.7}$$

where $\mathcal{D}_\mu \equiv \nabla_\mu - \mathrm{i}qA_\mu$. Applying the principle of stationary action, $\delta S_\Phi = 0$, leads to the equation of motion

$$\left(\mathcal{D}^2 - \mu^2\right)\Phi \;=\; 0\,. \tag{4.8}$$

To obtain the quasinormal modes, one makes the ansatz

$$\Phi(t,r,\theta,\varphi) \;=\; \mathrm{e}^{\mathrm{i}\omega t}\, Y_{\ell m}(\theta,\varphi)\,\widehat{\Phi}(r)\,, \tag{4.9}$$

where $Y_{\ell m}$ are the spherical harmonics satisfying

$$\Delta_\Omega\, Y_{\ell m} \;=\; -\ell(\ell+1)\, Y_{\ell m}\,, \tag{4.10}$$

where

$$\Delta_\Omega f(\theta,\varphi) \;\equiv\; \frac{1}{\sin(\theta)}\partial_\theta\big(\sin(\theta)\partial_\theta f(\theta,\varphi)\big) \;+\; \frac{1}{\sin^2(\theta)}\partial_\varphi^2 f(\theta,\varphi)\,. \tag{4.11}$$

for a function f defined on the unit-sphere S^2. Plugging Eq. (4.9) into Eq. (4.8) leads to the ODE in the variable r (Eq. (3.3) in [6])

$$\left(r^2 f\widehat{\Phi}'\right)' \;+\; \left[\frac{r^2}{f}\left(\omega \;-\; \frac{qQ}{r}\right)^2 - \ell(\ell+1) - r^2\mu^2\right]\widehat{\Phi} \;=\; 0\,. \tag{4.12}$$

in addition to satisfying Eq. (4.12), the quasinormal modes must satisfy boundary conditions at the black hole horizon r_+ and the cosmological horizon r_c

$$\Phi \;\sim\; \begin{cases} \text{outgoing wave}, & r \to r_c \\ \text{ingoing wave}, & r \to r_+ \end{cases}\,. \tag{4.13}$$

Physically, the boundary conditions can be justified by noting that at the black hole horizon, all matter must fall into the black hole, while the boundary condition at the cosmological horizon means that no matter should enter the horizon from outside since even an inward travelling photon has a monotonically increasing r-coordinate along its trajetory for $r > r_c$. For the rest of this work, the scalar field will be taken to be massless, hence $\mu = 0$. For the only quasinormal mode which is relevant with regards to the SCC conjecture one has $\ell = 0$ [6]. In that case Eq. (4.12) becomes

$$\left(r^2 f\widehat{\Phi}'\right)' \;+\; \frac{r^2}{f}\left(\omega \;-\; \frac{qQ}{r}\right)^2 \widehat{\Phi} \;=\; 0\,. \tag{4.14}$$

4.2 Probing the SCC conjecture with QNMs

As already stated, the purpose of this work is to use asymptotic techniques to understand the numerical results from [6]. The analyis therein relies on the computation of a 'regularity value'

$$\beta = \frac{\alpha}{\kappa_-}, \tag{4.15}$$

where α is the so-called spectral gap defined as the minimum decay rate $-\mathbb{I}\mathrm{m}\,(\omega)$ over all the QNM frequencies ω. The value β is tied to the regularity of generic linear perturbations of smooth initial data at the Cauchy horizon [5, 115]. In particular, according to the arguments in [115], the scalar field is an element of the Sobolev space (see e.g. [120] for an introduction to Sobolev spaces)

$$H^{1/2+\beta}_{\mathrm{loc}} \tag{4.16}$$

at the Cauchy horizon. As was already mentioned in the introduction, there are several versions of the SCC conjecture depending on the amount of regularity that one imposes for the possibility of continuing the metric beyond the Cauchy horizon. A detailed review would be beyond the scope of this thesis and can be found in [121]. The so called Christodoulou formulation is the most appropriate one according to the current state of research. It requires that the scalar fields not be elements of the Sobolev space $H^{1+\varepsilon}_{\mathrm{loc}}$ for some small positive ε for SCC to hold. This leads to following requirement for the regularity value β:

$$\beta \leq \frac{1}{2}. \tag{4.17}$$

If (4.17) is satisfied, then the SCC conjecture holds for smooth linear perturbations of the initial data. It was shown that for RNdS and a massless charged scalar field there is a violation of SCC for some parameters (Q, q) in the parameter space. In the limit of an uncharged scalar field, $q = 0$, there are three families of modes, called de-Sitter, photon sphere and near-extremal modes. The families which are important in this context emerge from the photon-sphere modes when a charge is introduced. We will follow [6] and refer to them as 'black-hole' and 'cosmological' modes. In the the near-extremal region, the black-hole family merges with the near extremal family in the limit $q \to \infty$ (see Fig. 9 in [6]) and determines the validity of SCC. The non-perturbative 'wiggles' in the regularity value β around the critical value $\beta_{\mathrm{crit}} = 1/2$ as a function of q in the

near-extremal region were numerically determined in [6]. The authors of [6] found the following relationship for the relevant black-hole mode (called ω_+)

$$-\frac{\mathrm{Im}(\omega_+)}{\kappa_-} = \frac{1}{2} - \frac{r_c^2 + 2r_c r_+ - r_+^2}{(r_c - r_+)(r_c + 3r_+)}\,\sigma + \mathcal{O}(\sigma^2) + \mathcal{O}(1/q) + \text{non-perturbative terms} \tag{4.18}$$

where $\sigma \equiv 1 - \frac{r_-}{r_+}$ represents the deviation from extremality (the Cauchy horizon r_- and the black hole horizonr_+ merge) and so $\sigma \to 0$ in the limit of $Q \to Q_{\text{ext}}$ if Q_{ext} is the extremal black hole charge. Since the factor in front of the term linear in σ is negative, this means that for any non-extremal value of σ there will be some $\widehat{q}$ such that for all $q > \widehat{q}$ we have $\beta = \inf\{-\mathrm{Im}(\omega)/\kappa_-\} < 1/2$ and so for all values of Q there exist (large) charges q for which SCC is respected. However, apart from being exponentially decaying, the non-perturbative terms are also oscillatory in q and as a consequence one can always find some neighbourhood of extremality in which $\beta > 1/2$ for certain values of q (the crests of the oscillation) and hence SCC is violated.

4.3 Asymptotic analysis at large charge: set-up

As already mentioned, previous analysis in [6] has shown numeric evidence of a violation of SCC for certain points in the parameter space. In [6] it was also seen that from a large charge perspective one could analyse the QNMs asymptotically, and this was done via a WKB approach. Of course, one would like to take this further and use asymptotic methods including summations that were used in the previous chapters to go beyond the large q behaviour and recover the smaller q results from the asymptotics. To do so one needs to have an in-depth asymptotic analysis of the problem, which will follow, both at the perturbative level (in this section) and to determine non-perturbative contributions so one can write a complete solution to the QNMs which one can then sum. An analysis of the expected non-perturbative contributions can be found in Sections 4.5 and , and a discussion of the ongoing work can be found in Section 4.6.

4.3.1 Fixing the boundary conditions

Here we review the analysis done in [6]. To fix the correct boundary conditions at the black hole horizon r_+ and the cosmological horizon r_c, the QNMs will be represented

as asymptotic WKB expansions at large charge q. These calculations have already been done in [6]. In order to calculate the perturbative expansion of the QNM frequencies, one must expand the scalar field of the BH mode around the BH horizon r_+. Hence both $r - r_+ \to 0$ and $1/q \to 0$. This gives rives to a boundary layer problem which will be analysed from the perspective of multiple scales in Section 4.3.3. It is instructive to carry out a Frobenius analysis on Eq. (4.12) in order to understand the behaviour near the horizons. Since the solution of interest is inside the radial interval $[r_+, r_c]$, it is natural to work with the variable

$$z \;=\; \frac{r - r_+}{r_c - r_+}\,, \tag{4.19}$$

and define $\psi(z(r)) = \widehat{\Phi}(r)$. The ODE Eq. (4.12) (multiplied by r_c^2) becomes

$$C_0(z)\psi(z) \;+\; C_1(z)\psi'(z) \;+ C_2(z)\psi''(z) \;=\; 0\,, \tag{4.20}$$

where the coefficients $C_j(z)$ are

$$\begin{aligned}
C_0(z) \;=& -\mu^2 r_c^2 - \frac{l(l+1)}{(-y_+ z + y_+ + z)^{\,2}} \\
&- \frac{\left(y_-^2 + (y_+ + 1)\, y_- + y_+^2 + y_+ + 1\right)\left(\omega r_c \left(y_+(z-1) - z\right) + qQ\right)^2}{(y_+ - 1)^{\,2}(z-1)z\left(-y_+(z-2) + y_- + z + 1\right)\left(y_+(z-1) + y_- - z\right)}\,; \\
C_1(z) \;=& \frac{-y_+\left(8z^3 - 12z^2 + 2z + 1\right) + y_-^2(1 - 2z) + 4z^3 - 2z}{\left(y_-^2 + (y_+ + 1)\, y_- + y_+^2 + y_+ + 1\right)(-y_+ z + y_+ + z)^{\,2}}\,; \\
&+ \frac{2y_+^2\left(2z^3 - 6z^2 + 5z - 1\right) - y_-\,(y_+ + 1)\,(2z - 1)}{\left(y_-^2 + (y_+ + 1)\, y_- + y_+^2 + y_+ + 1\right)(-y_+ z + y_+ + z)^{\,2}}\,; \\
C_2(z) \;=& \frac{(z-1)z\left(y_+(z-2) - y_- - z - 1\right)\left(y_+(z-1) + y_- - z\right)}{\left(y_-^2 + (y_+ + 1)\, y_- + y_+^2 + y_+ + 1\right)(-y_+ z + y_+ + z)^{\,2}}\,.
\end{aligned} \tag{4.21}$$

4.3.1.1 Black hole horizon $r = r_+$

Since one can always choose the leading order coefficient of our Frobenius series to unity, w.l.o.g. the Frobenius series around $r = r_+$ is

$$\psi_+(z) \;=\; z^p\,\left(1 \;+\; \psi_{+,1} z \;+\; \psi_{+,2} z^2 \;+\; \ldots\right)\,. \tag{4.22}$$

To leading order, the equation Eq. (4.20) becomes

$$0 \;=\; \frac{1}{z}\,\frac{\frac{p^2(y_- - y_+)(y_- + 2y_+ + 1)}{y_+^2} \;-\; \frac{\left(y_-^2 + y_+ y_- + y_- + y_+^2 + y_+ + 1\right)^2 (qQ - \omega y_+ r_c)^2}{(y_+ - 1)^2 (y_+ - y_-)(y_- + 2y_+ + 1)}}{\left(y_-^2 + y_+ y_- + y_- + y_+^2 + y_+ + 1\right)} \;+\; \mathcal{O}(z^0)\,. \tag{4.23}$$

Requiring the leading order to vanish fixes the Frobenius exponent p up to a sign. The two solutions are

$$p \;=\; \pm \mathrm{i}\, \frac{y_+ \left(y_-^2 + y_+ y_- + y_- + y_+^2 + y_+ + 1\right) (\omega y_+ r_c - qQ)}{(y_+ - 1)\,(y_+ - y_-)\,(y_- + 2y_+ + 1)}\,. \tag{4.24}$$

This can be rewritten using the surface gravity κ_+ from (4.6):

$$\begin{aligned} p \;&=\; \pm \mathrm{i}\, \alpha_+\,; \\ \alpha_+ \;&=\; \frac{1}{2 r_c \kappa_+} \left(r_c \omega - \frac{qQ}{y^+}\right)\,. \end{aligned} \tag{4.25}$$

4.3.1.2 Cosmological horizon $r = r_c$

One can follow the same procedure at the cosmological horizon, only that now one must expand around $z = 1$ corresponding to $r = r_c$:

$$\psi_c(z) \;=\; (1-z)^p \,\left(1 \,+\, \psi_{1,c}(1-z) \,+\, \psi_{2,c}(1-z)^2 \,+\, \ldots\right)\,. \tag{4.26}$$

By expanding out the ODE Eq. (4.20) in powers of $(1 - z)$ and requiring the leading order coefficient to vanish as before, one obtains

$$\begin{aligned} p \;&=\; \pm\, \mathrm{i}\, \frac{\left(y_-^2 + y_+ y_- + y_- + y_+^2 + y_+ + 1\right) (\omega r_c - qQ)}{(y_- - 1)\,(y_+ - 1)\,(y_- + y_+ + 2)} \\ &=\; \pm\, \mathrm{i}\, \alpha_c\,; \\ \alpha_c \;&=\; \frac{1}{2 r_c \kappa_c}\,(r_c \omega - qQ)\,. \end{aligned} \tag{4.27}$$

4.3.1.3 Boundary conditions

There are two possible Frobenius exponents at each horizon, they are $\pm \mathrm{i}\, \alpha_+$ at $r = r_+$ and $\pm \mathrm{i}\, \alpha_c$ at $r = r_c$. The boundary conditions determine the correct sign of the leading power law exponent dictating the behaviour of the quasinormal mode at each horizon. By reinstating the time dependence of the mode and analysing the behaviour of the phase as $r \to r_+$ and $r \to r_c$ respectively, one can compare the behaviour of each Frobenius solution with the desired boundary condition (4.13). It can be shown that the negative sign must be chosen in p at both $r = r_c$ and $r = r_+$ (in Eq. (4.25) and Eq. (4.27)). The next

step in the large charge analysis will be to consider perturbations around $q = \infty$ and analyse the leading order behaviour of the modes.

4.3.2 Perturbative analysis at leading order

In this section a review of the perturbative calculation in [6] is presented. The previous Frobenius analysis has shown that the field $\widehat{\Phi}(r)$ is not smooth at $r = r_+$ and $r = r_c$ (otherwise the Frobenius exponent would be a non-zero integer). To perform calculations it is therefore convenient to re-scale $\widehat{\Phi}(r)$ in such a way that the solution satisfying the correct boundary conditions is smooth. The 'small' variable ε is introduced as the inverse of 'large' q':

$$\varepsilon \equiv \frac{1}{q}\,. \tag{4.28}$$

Following closely the treatment in [6], the ansatz

$$\widehat{\Phi}(r) \;=\; \left(\frac{r}{r_+}-1\right)^{-\mathrm{i}\,\beta_+(\varepsilon)/\varepsilon} \left(1-\frac{r}{r_c}\right)^{-\mathrm{i}\,\beta_c(\varepsilon)/\varepsilon} \mathrm{e}^{-A(r)/\varepsilon}\,\phi(r,\varepsilon) \tag{4.29}$$

is used for the re-scaling, where the notation $\alpha_j(\varepsilon) = \beta_j(\varepsilon)/\varepsilon$ has been introduced to emphasise that the leading order behaviour of $\alpha_j(\varepsilon)$ is $\mathcal{O}\left(\varepsilon^{-1}\right)$. The re-scaled field $\phi(r,\varepsilon)$ from (4.29) is expanded in powers of ε:

$$\phi(r,\varepsilon) \;=\; \phi_0(r) \,+\, \phi_1(r)\varepsilon \,+\, \phi_2(r)\varepsilon^2 \,+\, \ldots\,. \tag{4.30}$$

Here an important point must be noted. Eq. (4.30) is an expansion of the field in the charge parameter for small ε. Later in the calculation the fields $\phi_j(r)$ will be expanded out in the variable r around the black hole horizon. Hence both ε and $r - r_+$ are small variables. The question then arises whether the results of the calculation depend on the order of expansion, i.e. are the results the same if one first expanded the field $\phi(r)$ in small ε as in (4.30) as they would be had one started with the expansion in $r - r_+$? The answer seems to be yes, but there are interesting mathematical subtleties to this problem which will later be explored in a multiple scales analysis. The leading order of $\omega(\varepsilon)$ is $\mathcal{O}\left(\varepsilon^{-1}\right)$ and hence one defines

$$\omega(\varepsilon) \equiv \frac{\lambda(\varepsilon)}{\varepsilon}\,, \tag{4.31}$$

where $\lambda(\varepsilon)$ admits the series expansion

$$\lambda(\varepsilon) \;=\; \lambda_0 \,+\, \lambda_1\varepsilon \,+\lambda_2\varepsilon^2 \,+\, \ldots \,+\, \text{non-perturbative}\,. \tag{4.32}$$

In terms of λ the exponents β_+ and β_c are given by

$$\begin{aligned}\beta_+ &= \frac{\lambda - \frac{Q}{r_+}}{2\kappa_+};\\ \beta_c &= \frac{\lambda - \frac{Q}{r_c}}{2\kappa_c}\,.\end{aligned} \tag{4.33}$$

By substituting the re-scaling ansatz (4.29) into (4.12) one obtains the equation

$$0 \;=\; C_0(r,\varepsilon)\phi(r,\varepsilon) \,+\, C_1(r,\varepsilon)\partial_r\phi(r,\varepsilon) \,+\, +C_2(r,\varepsilon)\partial_r^2\phi(r,\varepsilon)\,. \tag{4.34}$$

with some coefficient functions $C_j(r,\varepsilon)$. To leading order ε^{-2}, the equation is

$$\begin{aligned}0 \;=&\phi_0(r)\Bigg[\frac{(Q-\lambda_0 r)^{\,2}}{r^2 f(r)} + \frac{1}{4}f(r)\Bigg\{4A'(r)\left(\frac{\mathrm{i}\,(\lambda_0 r_c - Q)}{\kappa_c\,(r-r_c)\,r_c} + \frac{\mathrm{i}\,(\lambda_0 r_+ - Q)}{\kappa_+\,(r-r_+)\,r_+}\right) + 4A'(r)^2\\ &- \frac{2\,(Q-\lambda_0 r_+)\,(Q-\lambda_0 r_c)}{\kappa_c\kappa_+\,(r-r_+)\,r_+\,(r-r_c)\,r_c} - \frac{(Q-\lambda_0 r_c)^{\,2}}{\kappa_c^2\,(r-r_c)^{\,2}r_c^2} - \frac{(Q-\lambda_0 r_+)^{\,2}}{\kappa_+^2\,(r-r_+)^{\,2}r_+^2}\Bigg\}\Bigg]\varepsilon^{-2} \,+\, \mathcal{O}(\varepsilon^{-1})\end{aligned} \tag{4.35}$$

Assuming that $\phi_0(r) \neq 0$, the term between the brackets needs to vanish in order for the equation to be satisfied to leading order, which can be done by an appropriate choice of $A'(r)$. The solutions to the quadratic algebraic equation in $A'(r)$ are

$$\begin{aligned}A'_{\mathrm{sgn}}(r) \;=\; -\,\mathrm{i}\Bigg(&-\frac{\mathrm{sgn}\,(\lambda_0\,(r_c+r_-+r_+)+Q)}{2\,(r_c+r_-+r_+)\,(r_c+r+r_-+r_+)\,\kappa_{\mathrm{neg}}} + \frac{(\mathrm{sgn}+1)\,(\lambda_0 r_c - Q)}{2\kappa_c\,(r-r_c)\,r_c} +\\ &\frac{\mathrm{sgn}\,(\lambda_0 r_- - Q)}{2\kappa_-\,(r-r_-)\,r_-} + \frac{(1-\mathrm{sgn})\,(\lambda_0 r_+ - Q)}{2\kappa_+\,(r-r_+)\,r_+}\Bigg)\end{aligned} \tag{4.36}$$

where

$$\begin{aligned} &\mathrm{sgn} \in \{+1, -1\}; \\ &\kappa_{\mathrm{neg}} = |f'(r_{\mathrm{neg}})|/2; \\ &r_{\mathrm{neg}} = -(r_+ + r_- + r_c)\,. \end{aligned} \tag{4.37}$$

Integrated, this expression results in the exponential weight

$$\begin{aligned} A_{\mathrm{sgn}}(r) \;=\; -\,\mathrm{i}\Bigg(&-\frac{\mathrm{sgn}\log\left(r_c + r + r_- + r_+\right)\left(\lambda_0\left(r_c + r_- + r_+\right) + Q\right)}{2\left(r_c + r_- + r_+\right)\kappa_{\mathrm{neg}}} \\ &+ \frac{(\mathrm{sgn}+1)\log\left(r - r_c\right)\left(\lambda_0 r_c - Q\right)}{2\kappa_c r_c} + \frac{\mathrm{sgn}\log\left(r - r_-\right)\left(\lambda_0 r_- - Q\right)}{2\kappa_- r_-} \\ &+ \frac{(1-\mathrm{sgn})\log\left(r - r_+\right)\left(\lambda_0 r_+ - Q\right)}{2\kappa_+ r_+}\Bigg) \end{aligned} \tag{4.38}$$

The coefficients in front of the logarithmic singularities at $r = r_+$ and $r = r_c$ in the $A(r)$ must vanish. Otherwise, $\widehat{\Phi}(r)$ would not satisfy the correct boundary conditions (and not be regular) since they have already been included in the pre-factor of Eq. (4.29). There are two ways to achieve this

$$\begin{aligned} \lambda_0^{(+)} &= \frac{Q}{r_+}, \quad \mathrm{sgn} = -1\,; \\ \lambda_0^{(c)} &= \frac{Q}{r_c}, \quad \mathrm{sgn} = 1\,. \end{aligned} \tag{4.39}$$

These choices correspond to two different families of quasinormal modes. In [6] they are called the black hole family and the cosmological family. For the question of SCC only the BH family is important with $\lambda_0 = \lambda_0^{(+)}$. To get $\lambda_1^{(+)}$ one considers the leading order ε^{-1} (remember that the terms of order ε^{-2} vanish after having fixed the exponential weight $A(r)$) of Eq. (4.34) and expands in r around $r = r_+$. The resulting expression has an overall factor of $\phi_0(r_+)$. Assuming that $\phi_0(r_+)$ does not vanish (remember that any non-constant leading order behaviour has already been absorbed into the Frobenius factor) one obtains an equation in λ_1 which is solved by

$$\lambda_1^{(+)} \;=\; -\mathrm{i}\frac{\kappa_+}{2} \tag{4.40}$$

Now the equation of order ε^{-1} can be solved, which is a first order ODE in $\phi_0(r)$. The solution is

$$\phi_0(r) = c_0 \exp\left(-\frac{1}{2}\log(r) - \frac{\kappa_+}{4\kappa_-}\log(r-r_-) + \frac{\kappa_+}{4\kappa_{\text{neg}}}\log(r+r_++r_-+r_c)\right), \tag{4.41}$$

where c_0 is an integration constant. Now that the leading order behaviour in ε of the relevant BH-QNM has been found exactly by calculating λ_0, λ_1 and $\phi_0(r)$, the next step is to go towards higher orders to be able to do an analysis of the asymptotics of the series $\lambda(\varepsilon)$.

4.3.3 Multiple scales analysis

As already mentioned, the problem of multiple scales arises due to two small variables in which the QNM solution is expanded:

$$\varepsilon = 1/q\,, \text{ around } q = 0\,; \tag{4.42}$$

$$x = r - r_+, \text{ around } x = 0\,. \tag{4.43}$$

So far only the case has been considered where the ε expansion is performed before the x-expansion. To understand why this approach might be problematic, it is necessary analyse Eq. (4.14) and consider whether there are terms which are singular in either ε or x.

4.3.3.1 Introducing multiple scales

In terms of $\varepsilon = 1/q$ and $\lambda = \varepsilon\omega$, Eq. (4.12) is given by

$$\varepsilon^2\left(f(r)r^2\widehat{\Phi}'(r)\right)' + \frac{r^2}{f(r)}\left(\lambda - \frac{Q}{r}\right)\widehat{\Phi}(r) = 0\,. \tag{4.44}$$

If one expands out (4.44) and divide by $f(r)r^2$ one obtains

$$\varepsilon^2\,\widehat{\Phi}''(r) + \varepsilon^2\left(\partial_r\log(f(r)) + \frac{2}{r}\right)\widehat{\Phi}'(r) + \left(\frac{\lambda - \frac{Q}{r}}{f(r)}\right)^2\widehat{\Phi}(r) = 0\,. \tag{4.45}$$

One could of course multiply Eq. (4.45) by any power of ε. The reason the form in Eq. (4.45) is chosen is because often a problem of multiple scales can be solved by a re-scaling of the dependent variable by a 'small parameter', in this case ε. The two derivatives each bring out a factor of ε^{-1} after the variable transform, which cancels out the factor ε^2. This approach also works for Eq. (4.45) as will be seen. The term multiplying the first derivative $\widehat{\Phi}'(r)$ in (4.45) is just a sum of simple poles at each of the horizons, i.e. the zeros of $f(r)$:

$$\partial_r \log(f(r)) + \frac{2}{r} = \frac{1}{r-r_+} + \frac{1}{r-r_c} + \frac{1}{r-r_m} + \frac{1}{r-(-r_+-r_c-r_-)}\,; \tag{4.46}$$

In particular, this means that there is a term with a factor of

$$\frac{\varepsilon^2}{r-r_+} \tag{4.47}$$

multiplying $\widehat{\Phi}'(r)$ in Eq. (4.45). When one takes the limits $\varepsilon \to 0$, $r \to r_+$, this factor will either vanish or blow up depending on which limit is taken first. What is more, the factor multiplying $\widehat{\Phi}(r)$ in (4.45) suffers from a similar problem. Consider an expansion around $r = r_+$ using the dimensionless variable

$$x = \frac{r}{r_+ - 1}. \tag{4.48}$$

For the sake of simplicity one further introduces the following definitions:

$$g(x) = \frac{f(r_+(1+x))}{Qx}; \quad \widetilde{\lambda} = \frac{r_+}{Q}\varepsilon\omega = \frac{r_+}{Q}\lambda = \widetilde{\lambda}_0 + \varepsilon\widetilde{\rho}; \tag{4.49}$$

The point of defining $g(r)$ is that its Taylor expansion around $r = r_+$ starts at order $\mathcal{O}\left((r-r_+)^0\right) = \mathcal{O}(1)$, whereas

$$f(r_+(1+x)) = 2\kappa_+ r_+ x + \mathcal{O}\left(x^2\right) \tag{4.50}$$

starts at order $\mathcal{O}((r-r_+)) = \mathcal{O}(x)$. By writing things in terms of $g(x)$ the singular behaviour near $r = r_+$, i.e. $x = 0$ is straightforward to see. The quantity $\widetilde{\rho}$ in (4.49) has a perturbative expansion in ε starting at order $\varepsilon^0 = 1$. In terms of the near-BH-horizon

variable x, our ODE (4.45) can be written as

$$\begin{aligned}&\varepsilon^2\,\widetilde{\Phi}''(x)+\varepsilon^2\left(\frac{1}{x}+\frac{1}{1-\frac{r_c}{r_+}+x}+\frac{1}{1-\frac{r_-}{r_+}+x}+\frac{1}{1-\frac{(-r_+-r_c-r_-)}{r_+}+x}\right)\widetilde{\Phi}'(x)\\&+\left(\frac{1}{g(x)(1+x)}+\frac{\widetilde{\lambda_0}-1}{xg(x)}+\varepsilon\frac{\widetilde{\rho}}{xg(x)}\right)^2\widetilde{\Phi}(x)=0\,.\end{aligned}\tag{4.51}$$

The mode of interest is the BH-mode for which

$$\widetilde{\lambda}_0=1\,.\tag{4.52}$$

For the BH-mode one obtains

$$\begin{aligned}&\varepsilon^2\widetilde{\Phi}''(x)+\varepsilon^2\left(\frac{1}{x}+\frac{1}{1-\frac{r_c}{r_+}+x}+\frac{1}{1-\frac{r_-}{r_+}+x}+\frac{1}{1-\frac{(-r_+-r_c-r_-)}{r_+}+x}\right)\widetilde{\Phi}'(x)\\&+\left(\frac{1}{g(x)(1+x)}+\varepsilon\frac{\widetilde{\rho}}{xg(x)}\right)^2\widetilde{\Phi}(x)=0\,.\end{aligned}\tag{4.53}$$

Now a multiple scale analysis can be performed. One introduces a boundary-layer variable

$$y=\frac{x}{\delta}\,,\tag{4.54}$$

where δ is small. In the limit $\delta\to 0$, y varies across the intervall $[0,+\infty)$ as we vary x in the interval $[0,r_c/r_+-1)$. Further one defines

$$\Psi(y)\equiv\widetilde{\Phi}(\delta y=x)\,.\tag{4.55}$$

The derivative transforms as

$$\partial_x=\delta^{-1}\partial_y\,.\tag{4.56}$$

In the case of the BH-mode $\widetilde{\lambda}=1$, one obtains the equation

$$\begin{aligned}&\varepsilon^2\delta^{-2}\Psi''(y)+\varepsilon^2\delta^{-2}y^{-1}\Psi'(y)\\&+\varepsilon^2\delta^{-1}\left(\frac{1}{1-\frac{r_c}{r_+}+\delta y}+\frac{1}{1-\frac{r_-}{r_+}+\delta y}+\frac{1}{1-\frac{(-r_+-r_c-r_-)}{r_+}+\delta y}\right)\Psi'(y)\\&+\left(\frac{1}{g(\delta y)(1+\delta y)}+\varepsilon\delta^{-1}\frac{\widetilde{\rho}}{yg(\delta y)}\right)^2\Psi(y)=0\,.\end{aligned}\tag{4.57}$$

Now one can see that the ambiguity in taking the limit can be removed by choosing the scale $\delta(\varepsilon) = \varepsilon$, in which case (4.57) becomes

$$\Psi''(y) + y^{-1}\Psi'(y) + \varepsilon\left(\frac{1}{1-\frac{r_c}{r_+}+\varepsilon y} + \frac{1}{1-\frac{r_-}{r_+}+\varepsilon y} + \frac{1}{1-\frac{(-r_+-r_c-r_-)}{r_+}+\varepsilon y}\right)\Psi'(y) + \left(\frac{1}{g(\varepsilon y)(1+\varepsilon y)} + \frac{\widetilde{\rho}}{y g(\varepsilon y)}\right)^2 \Psi(y) = 0. \tag{4.58}$$

Note that it is important to choose the BH mode $\widetilde{\lambda} = 1$ to obtain an equation without the non-commuting limit problem (4.58). If any other value $\widetilde{\lambda}_0 \neq 1$ had been chosen the term proportional to $(\widetilde{\lambda} - 1)$ in (4.51) would have prevented the scaling $\delta(\varepsilon) = \varepsilon$ from being effective.

4.3.3.2 Leading-order equation

Since Eq. (4.58) still depends on the charge parameter ε, the function $\Psi(y)$ is expanded in ε:

$$\Psi(y) = \psi_0(y) + \varepsilon\psi_1(y) + \mathcal{O}\left(\varepsilon^2\right); \tag{4.59}$$

One obtains the following equation for ψ_0:

$$\psi_0''(y) + \frac{1}{y}\psi_0'(y) + \gamma^2\left(1+\rho_0 y^{-1}\right)^2\psi_0(y); \tag{4.60}$$

where the following constant has been introduced:

$$\gamma \equiv \frac{Q}{2r_+\kappa_+}. \tag{4.61}$$

In the asymptotic analysis carried out in 4.3.2 the coefficient ρ_0^{BH} in the asymptotic expansion of the QNM-frequency of the leading BH-mode was calculated. With the QNM-fequency re-scaling $\rho \to \widetilde{\rho}$ given in Eq. (4.49), the re-scaled coefficient $\widetilde{\rho}_0^{\mathrm{BH}}$ of is given by

$$\widetilde{\rho}_0^{\mathrm{BH}} \equiv \frac{-\mathrm{i}}{4\gamma}. \tag{4.62}$$

The equation (4.60) for the BH mode then becomes

$$\psi_0''(y) + \frac{1}{y}\psi_0'(y) + \gamma^2\left(1 - \frac{\mathrm{i}}{4\gamma}y^{-1}\right)^2\psi_0(y)\,; \tag{4.63}$$

The general solution to the BH mode equation (4.63) has the following form:

$$\begin{aligned}\psi_0(y) &= \mathrm{e}^{\mathrm{i}\gamma y}\left(C_1 y^{-\frac{1}{4}} + C_2 y^{-\frac{1}{4}}\mathrm{erf}\left((1+\mathrm{i})\sqrt{y\gamma}\right)\right)\\ &= \mathrm{e}^{\mathrm{i}\gamma y}\left(C_1 y^{-\frac{1}{4}}\left(1+\mathcal{O}\left(y^{-1}\right)\right) + C_2 y^{\frac{1}{4}}\left(1+\mathcal{O}\left(y^{-1}\right)\right)\right)\,.\end{aligned} \tag{4.64}$$

Eq. 4.64 is a linear combination of two independent solutions, one of which obeys the correct ingoing boundary condition at the BH horizon $y = 0$. By comparing Eq. (4.60) to our previous Frobenius analysis, in particular to Section 4.3.1.3, one finds that the solution multiplying C_1 in Eq. (4.64) has the same Frobenius factor $y^{-1/4}$ up to order $\mathcal{O}\left(\varepsilon^0\right)$ as the Frobenius expansion which satisfies the correct boundary condition, and so $C_2 = 0$ for the BH-mode. Moreover, the exponential factor $\mathrm{e}^{\mathrm{i}\gamma y}$ is also in agreement with the solution found in Section 4.3.2. Hence the multiple scale analysis is consistent with the asymptotic analysis in Sections 4.3.1 and 4.3.2 for the BH-mode solution. There is however, one subtlety which is interesting from a mathematical perspective. The Frobenius analysis in Section 4.3.1 leads to the two Frobenius exponents

$$\begin{aligned}p_1(\varepsilon) &= -\frac{1}{4} + \mathcal{O}(\varepsilon)\,;\\ p_2(\varepsilon) &= +\frac{1}{4} + \mathcal{O}(\varepsilon)\,,\end{aligned} \tag{4.65}$$

for the BH-mode frquency $\omega = \omega^{\mathrm{BH}}$. However, if one expands the field $\phi(r,\varepsilon)$ in ε first as done in Eq. (4.30), and then performs a Frobenius analysis, the Frobenius exponents degenerate by $-1/4$, that is, one obtains the two exponents

$$\begin{aligned}p_1(\varepsilon) &= -\frac{3}{4} + \mathcal{O}(\varepsilon)\,;\\ p_2(\varepsilon) &= -\frac{1}{4} + \mathcal{O}(\varepsilon)\,,\end{aligned} \tag{4.66}$$

Note that because p_1 in (4.65) is the same as p_2 in (4.66), in both cases it is possible to represent the solution satisfying the physical boundary conditions using one of the two Frobenius expansions. However, in the second case where the Frobenius exponents are degenerate as shown in (4.66), the unphysical solution no longer agrees with the unphysical solution from the original Frobenius expansion. It is not clear to the

author why this phenomenon happens and what the significance of it is, and further investigation into the matter is necessary. To conclude, the results from the multiple scales analysis have been found to be consistent with the results from the asymptotic analysis in Section 4.3.1 to leading order as long as one only considers the physical solution satisfying the correct boundary condition. Moreover, it is expected that going to higher orders in ε will confirm that the two methods, expanding out in ε-first on the one hand and introducing a boundary layer and performing a multiple scales analysis on the other, are consistent with each other.

4.4 Asymptotic analysis of the QNMs

In the previous section the QNM wave equation was solved to leading order for the BH-mode ω^{BH} with angular momentum number $\ell = 0$. It was found that there exist two linearly independent solutions with exponential weights $A_-(r)$ and $A_+(r)$. The boundary conditions define a constraint on the solution and fix the leading order coefficient in the perturbative expansion, $\omega^{\mathrm{BH}}_{-1} = Q/r_+$. Moreover, near the horizons r_+ and r_c, only the solution with $A_-(r)$ satisfies the boundary condition. Since the goal is to understand the full non-perturbative picture of the problem, an analysis of the singularities in the Borel plane of both $\omega(\varepsilon)$ and the field $\psi(r,\varepsilon)$ will be useful. To carry out such an anlysis it is necessary to obtain many coefficients of the perturbative expansions of both $\omega(\varepsilon)$ and $\psi(r,\varepsilon)$. In this section, an algorithm will be given which allows one to compete these coefficients via recursion relations. Further, the Borel plane of $\omega(\varepsilon)$ will be analysed, and the results of the computation will be discussed for two different sets of parameters, once away from extremality $Q = Q_{\mathrm{ext}}$, and once for near extremal parameters.

4.4.1 Perturbative computation of the leading QNM-frequency

In the following section only the leading BH-mode satisfying $\lambda_0 = \lambda_0^+ = Q/r_+$ will be considered, and the numerical computation of the perturbtive coefficients in [6] is reproduced.

By expanding the differential equation in powers of ε and matching the different orders, one obtains a sequence of ODEs which can be solved recursively. The ODE for $\phi_n(r)$

depends also on the functions $\phi_j(r)$ with $j < n$ as well as λ_k with $k \leq n+1$. The ε-rescaled QNM-frequency coefficients λ_k may be computed by expanding the ODE (4.34) around $r = r_+$ and requiring the $1/(r-r_+)$ term to vanish. The goal is to compute as many orders as possible in the ε-expansion of $\lambda(\varepsilon)$. For convenience one redefines $\lambda(\varepsilon)$ in terms of the new quantity $\rho(\varepsilon)$

$$\lambda(\varepsilon) = \varepsilon\,\omega(\varepsilon) = \frac{Q}{r_+} + \frac{\kappa_+}{2}\varepsilon\rho(\varepsilon), \tag{4.67}$$

such that the leading order behaviour is

$$\rho(\varepsilon) = -\mathrm{i} + \rho_1\varepsilon + \dots . \tag{4.68}$$

Moreover, one defines

$$x = r - r_+, \tag{4.69}$$

and $\phi_n(x)$ will be written to denote $\phi_n(r = r_+ + x)$. The ODEs one obtains are all of the form

$$L\phi_n(x) = G_n\big[\{\phi_j, j<n\}, \{\rho_k, k \leq n\}\big](x), \tag{4.70}$$

where L is a linear, first order derivative operator and the inhomogeneity G_n (also) includes derivatives of the ϕ_j. For the leading order, the inhomgeneity vanishes, i.e. $G_0(x) = 0$. Hence ϕ_0 satisfies the homogeneous equation $L\phi_0(x) = 0$. This allows to further simplify the equations by re-scaling our function ϕ:

$$\begin{aligned} \phi(x,\varepsilon) =& \phi_0(x)\psi(x,\varepsilon); \\ \psi(x,\varepsilon) =& 1 + \psi_1(x)\varepsilon + \psi_2(x)\varepsilon^2 + \dots; \end{aligned} \tag{4.71}$$

One is free to choose $\psi(x=0,\varepsilon) \equiv \mathrm{Init}(\varepsilon)$, i.e. $\mathrm{Init}(\varepsilon)$ may be any function of ε. To simplify the computation, $\psi(x=0,\varepsilon) = 1$ will be chosen for all ε, which means that $\psi_n(x=0) = 0$ for all $n \geq 1$. The LHS of (4.70) becomes (the exact expressions for $W(x)$ and $Z(x)$ are unimportant)

$$\begin{aligned} L\phi_n(x) \equiv& W(x)\phi_n'(x) + Z(x)\phi_n(x) \\ =& \psi_n(x)\left(\underbrace{W(x)\phi_0'(x) + Z(x)\phi_0(x)}_{=L\phi_0(x)=0}\right) + W(x)\phi_0(x)\psi_n'(x). \end{aligned} \tag{4.72}$$

This leads to the equation (for $n \geq 1$):

$$\psi_n'(x) = \frac{G_n(x)}{W(x)\phi_0(x)}. \tag{4.73}$$

Now one expands (remember that $\psi_n(0) = 0$ for $n \geq 1$)

$$\psi_n(x) = \sum_{j=1}^{+\infty} \psi_{n,j} x^j \,. \tag{4.74}$$

By substituting these expansions into (4.70) one obtains the following equations for the perturbative coefficients $\psi_{n,m}$:

$$\begin{aligned}
\psi_{n,m} =& \frac{1}{m}\Bigg\{ g_{1,m-1}\rho_{n-1} + g_{2,m-1}\left(\sum_{\ell=0}^{n-1}\rho_\ell\rho_{n-1-\ell}\right) + g_{3,m-1}\rho_n \\
&+ \sum_{j=-1}^{m-1}\Bigg[g_{1,j}\sum_{\ell=1}^{n-1}\rho_{n-1-\ell}\psi_{\ell,m-1-j} + g_{2,j}\sum_{\ell=1}^{n-1}\left(\sum_{k=0}^{n-1-\ell}\rho_k\rho_{n-1-\ell-k}\right)\psi_{\ell,m-1-j} \\
&+ g_{3,j}\sum_{\ell=1}^{n-1}\rho_{n-\ell}\psi_{\ell,m-1-j} + g_{4,j}\psi_{n-1,m-1-j} \\
&+ (m-j)\left(g_{5,j}\sum_{\ell=1}^{n-1}\rho_{n-1-\ell}\psi_{\ell,m-j} + g_{6,j}\psi_{n-1,m-j}\right)\Bigg] \\
&+ \sum_{j=0}^{m-1}(m-j)(m-j+1)g_{0,j}\psi_{n-1,m-j+1}\Bigg\}.
\end{aligned} \tag{4.75}$$

In this last expression, $g_0(x), g_1(x) \ldots g_6(x)$ are exactly known functions of order $\mathcal{O}(x^{-1})$ as $x \to 0$, except for $g_0(x)$, which is of order $\mathcal{O}(x^0)$ as $x \to 0$. The expressions $g_{j,k}$ denote the coefficients of the series expansions of those functions. Note that $G_n(x)$ is such that in order to compute $\psi_{n,j}$, we must know $\psi_{n-1,j+1}, \ldots \psi_{n-k,j+k}, \ldots \psi_{1,n+j-1}$. With our choice $\psi_n(0) = 0$ for $n \geq 1$ the equation for ρ_n is

$$\begin{aligned}
\rho_n =& \frac{-\mathrm{i}}{\alpha_0}\left(\alpha_0\delta_{n,0} + (\alpha_1\rho_{n-1} - 2\mathrm{i}\nu_{n-1})(1-\delta_{n,0}) + \mathrm{i}\alpha_2\sum_{j=0}^{n-1}\rho_j\rho_{n-1-j} - \sum_{j=0}^{n-1}\nu_j\rho_{n-1-j}\right); \\
\nu_j \equiv& \begin{cases} \phi_0'(0)/\phi_0(0) & \text{for } j = 0, \\ \psi_{j,1} & \text{for } j \geq 1. \end{cases}
\end{aligned} \tag{4.76}$$

Here α_0, α_1 and α_2 denote some constants which only depend on the parameters of our problem, i.e. r_+,r_c and Q. Remember that to compute $\psi_n(x)$, one needs to know $\rho_0, \ldots \rho_n$,

and to compute ρ_n, one needs to know $\psi_{j,1}$ for all $j < n$. Hence one can implement the algorithm for the computation of the ρ_n as follows:

i) The goal is to compute ρ_n for $n \leq N$. The algorithm starts with $n = 1$, since $\rho_0 = -\mathrm{i}$ and $\psi_0(x) = 1$ are already known.

ii) Compute ρ_n using (4.76).

iii) Compute $\psi_n(x)$ to order $N - n$ in x using (4.73). Set $n \to n + 1$.

iv) Repeat ii) and iii) until obtaining ρ_N.

The results of the above algorithm for ρ_n (and hence for the coefficients ω_n) have been cross-checked (visually) with the results given in [6] and have been found to be consistent. A plot of the asymptotic behaviour of the coefficients ω_n is given in Fig. 4.2. The above algorithm for calculating both the field $\phi(r, \varepsilon)$ and $\omega(\varepsilon)$ as perturbative expansions in both ε and r will be useful later in an analysis of the non-perturbative contributions. Remember that in this perturbative apprach the assumption was made that one can obtain correct results by first expanding in ε and then in $x = r - r_+$. In what follows a multiple scales analysis is presented and the validity of this assumption is examined.

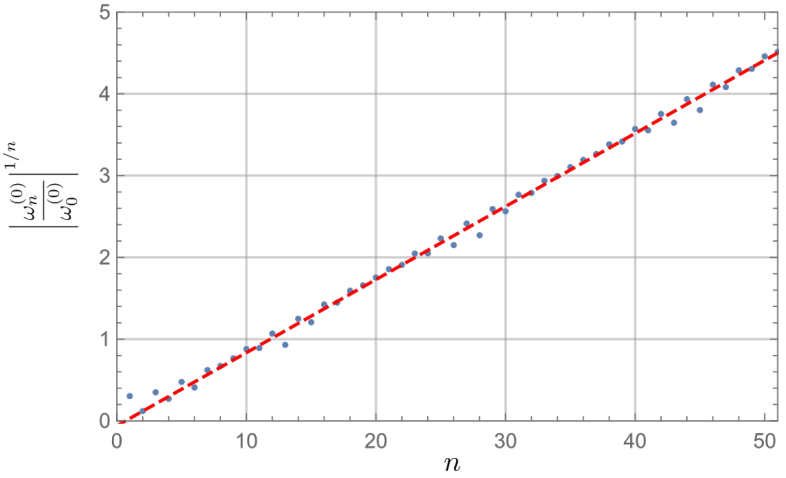

FIGURE 4.2: Visualisation of the coefficients of $\omega^{(0)}$ for $(r_c, r_+, Q) = (1, 1/2, 2/5)$ as a function of the expansion order n. The dotted red line is the same as the one in Fig. 2 from [6], $-0.059708(1) + 0.089413(2)\, n$. Our results seem to agree with those in [6]. NB: Our notation for the coefficients $\omega_n^{(0)} \leftrightarrow \omega_+^{(n)}$ differs from [6].

4.4.2 Borel-resummation of $\omega(\varepsilon)$

The Borel transform of the QNM-frequency ω for the black-hole family will be analysed (and the '+'label will be dropped). In the previous section an algorithm was given to calculate the first N terms of the perturbative expansion (the new index (0) is used to distinguish it from non-perturbative corrections $\omega^{(1)}(\varepsilon), \omega^{(2)}(\varepsilon)\dots$)

$$\omega^{(0)}(\varepsilon) = Q/r_+\varepsilon^{-1} + \sum_{n=0}^{+\infty} \omega_n^{(0)} \varepsilon^n \,. \tag{4.77}$$

This asymptotic series is divergent and hence we must rely on a resummation method to retrieve information from it. In what follows the analysis will be carried out via the method of Borel resummation. The minor of of $\omega^{(0)}$ is given by

$$\mathcal{B}[\breve{\omega}^{(0)}](\xi) = \sum_{n=0}^{+\infty} \frac{\omega_{n+1}^{(0)}}{n!} \xi^n, \qquad \text{as } \xi \to 0, \tag{4.78}$$

where the 'inverse hat' means that the terms of order $\mathcal{O}\left(\varepsilon^{-1}\right)$ and $\mathcal{O}\left(\varepsilon^{0}\right)$ have been subtracted. If the non-perturbative contributions are to be captured, it is useful to first analyse the singularity structure of the analytic continuation of (4.78). As only a finite number of terms are available, the symmetrical Padé-approximant of 4.78 is used for the approximation. This has already been introduced in previous chapters and is given here as a reminder:

$$\mathrm{BP}_N\left[\breve{\omega}^{(0)}\right](\xi) = \frac{\mathrm{Num}_{N/2}(\xi)}{\mathrm{Denom}_{N/2}(\xi)} \,, \tag{4.79}$$

where both numerator and denominator are polynomials of order $N/2$ (or the nearest integer below $N/2$ for odd N). The singularities in the Borel-plane show up as zeros in the denominator of the Borel-Padé approximant, and any logarithmic singularity will show up as a dense line (not in the technical sense) of poles of the Borel-Padé approximant.

Parameter values $r_c = 1$, $r_+ = 1/2$, $Q = 2/5$

The quasinormal mode frequency $\omega^{(0)}$ has been computed to order $N = 250$. The data agrees well with the results in [6], which can be seen by comparing our plot, Fig. 4.2, with Fig. 2 from [6]. One finds that the coefficients $\omega_k^{(0)}$ are real for even k and imaginary

for odd k, from which the following relation follows for the Borel transforms:

$$\left(\mathcal{B}\left[\breve{\omega}^{(0)}\right](-\xi^*)\right)^* = \mathcal{B}\left[\breve{\omega}^{(0)}\right](\xi)\,. \tag{4.80}$$

This implies that the set of singularities is symmetric with respect to reflections across the imaginary axis. On the positive real half-plane, one finds the singularity (see Fig. 4.3)

$$A_\omega \equiv 4.09881 - 0.342825\,\mathrm{i}\,. \tag{4.81}$$

This singularity is indicative of a Stokes phenomenon. If the perturbative series $\omega^{(0)}$ is resummed by calculating the Laplace integral of the minor $\mathcal{B}[\breve{\omega}^{(0)}](\xi)$, one expects non-perturbative contributions to be turned on when moving the angle of resummation over the singularity:

$$\begin{aligned}\mathrm{Disc}_{\arg(A_\omega)}\,\omega(\varepsilon) &\equiv \mathcal{S}_{\theta_2}\,\breve{\omega}^{(0)}(\varepsilon) - \mathcal{S}_{\theta_1}\,\breve{\omega}^{(0)}(\varepsilon)\\ &= \delta\sigma\,\mathrm{e}^{-A_\omega/\varepsilon}\,\mathcal{S}_{\theta_1}\,\breve{\omega}^{(1)}(\varepsilon) + \mathcal{O}\left(\left(\delta\sigma\mathrm{e}^{-A_\omega/\varepsilon}\right)^2\right),\end{aligned} \tag{4.82}$$

where $\omega^{(1)}(\varepsilon)$ is the asymptotic series of the first non-perturbative sector and $\delta\sigma$ is the change in the transseries parameter σ which is induced by the action of the Stokes automorphism at the Stokes line. Using numerical integration and choosing

$$\begin{aligned}\theta_1 &\equiv \arg(A_\omega) + \frac{\pi}{6};\\ \theta_2 &\equiv \arg(A_\omega) - \frac{\pi}{6},\end{aligned} \tag{4.83}$$

one finds that the discontinuity obeys the expected non-perturbative behaviour (4.82). Fig. 4.4 shows both resummations evaluated along the real positive q-line. Figs. 4.5 and 4.6 illustrate that behaviour of the discontinuity as a function of q is consistent with our expectation from Eq. (4.82).

Near extremal parameter values $r_c = 1$, $r_+ = 1/3$, $Q/Q_{\mathbf{ext}} = 1 - 10^{-4}$

Since the violation of SCC only happens at near-extremal parameters, it is instructive to consider the case of a near-extremal black-hole with

$$r_c = 1; \quad r_+ = 1/3; \quad Q/Q_{\mathrm{ext}} = 1 - 10^{-4}. \tag{4.84}$$

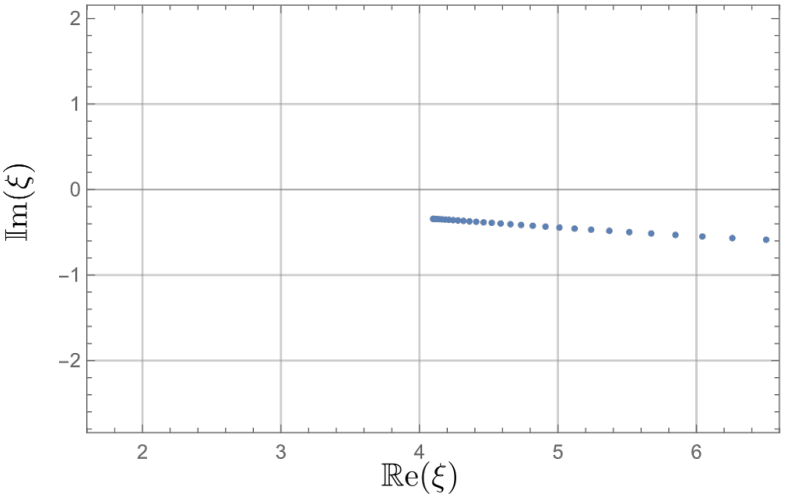

FIGURE 4.3: The poles of the Borel-Padé-approximant $\mathrm{BP}_N[\widehat{\omega^{(0)}}](\xi)$ for $(r_c,\, r_+,\, Q) = (1, 1/2, 2/5)$ and $N = 250$. One can interpret the condensation of poles onto a line for large N as an indication of a branch-cut singularity, possibly a logarithmic one. The position of the singularity is $A \equiv 4.09881 - 0.342825\mathrm{i}$.

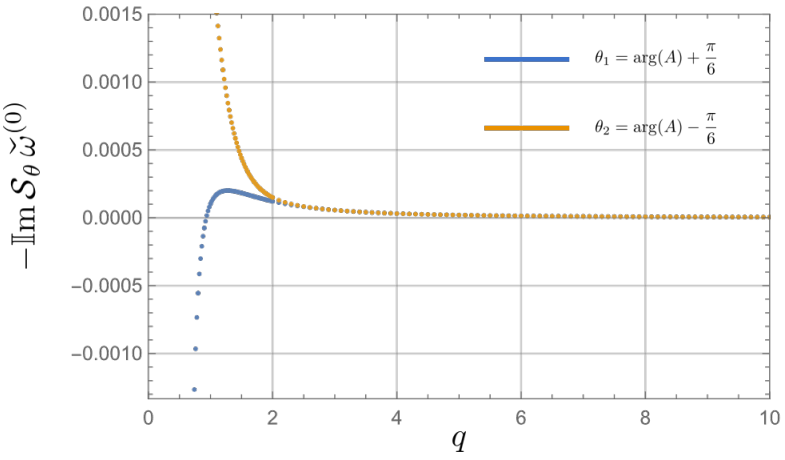

FIGURE 4.4: The negative imaginary part of the resummations $\mathcal{S}_\theta\,\breve{\omega}^{(0)}(q = \varepsilon^{-1})$ for $(r_c,\, r_+,\, Q) = (1, 1/2, 2/5)$ and two different values of $\theta_2 < \arg(A) < \theta_1$ above and below the Stokes line. The blue line is equivalent to a resummation of $\breve{\omega}^{(0)}$ along the real axis, whereas the orange line shows the resummation of $\breve{\omega}^{(0)}$ with the non-perturbative contributions turned-on.

A number of $N = 350$ coefficients have been computed in the expansion of $\omega^0(\varepsilon)$. Since the zeros and singularities of the Borel-Padé transform of $\omega^{(0)}(\varepsilon)$ are again symmetric w.r.t. reflections across the imaginary axis, only the singularities with positive real part need to be considered w.l.o.g. Repeating the previous analysis for the near extremal parameters, one now finds more than only one singularity in the Borel plane of $\omega^{(0)}$. Apart from the singularity closest to the origin,

$$A_{\omega,0} = 2.86651 - 6.59978\,\mathrm{i}\,, \tag{4.85}$$

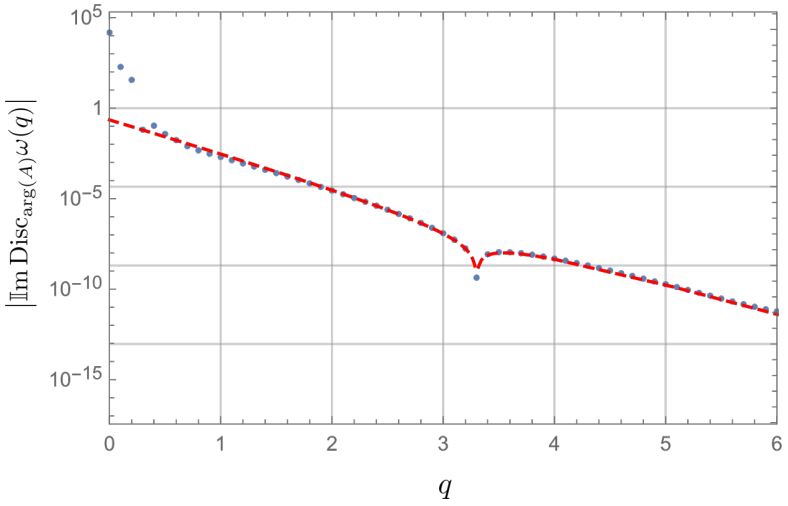

FIGURE 4.5: Blue: The absolute value of the imaginary part of the discontinuity $\mathrm{Disc}_{\arg(A)}\,\omega(q)$ as a function of charge q for $(r_c,\, r_+,\, Q) = (1, 1/2, 2/5)$, displayed logarithmically. The spike between $q = 3$ and $q = 4$ is due to a change of sign from the oscillatory behaviour (A has a non-vanishing imaginary part). Dotted red: The function $\left|\mathbb{I}\mathrm{m}\left(Ce^{-Aq}\right)\right|$, where $C \equiv -0.12 + 0.25\mathrm{i}$.

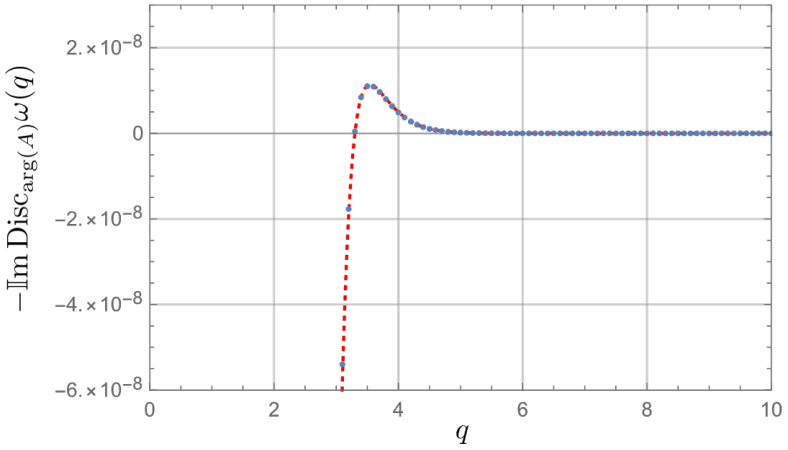

FIGURE 4.6: The negative imaginary part of the discontinuity $\mathrm{Disc}_{\arg(A)}\,\omega(q)$ for $(r_c,\, r_+,\, Q) = (1, 1/2, 2/5)$, plotted on a linear scale to illustrate the behaviour near the zero. Dotted red: The function $-\mathbb{I}\mathrm{m}\left(Ce^{-Aq}\right)$, where $C \equiv -0.12 + 0.25\mathrm{i}$.

one also finds singularities at the positions

$$A_{\omega,\ell} \equiv A_{\omega,0} + \ell\, C_-, \qquad \ell \in \{-2, -1, 0, 1, 2, 3\}; \tag{4.86}$$

$$C_- \equiv -5.73318. \tag{4.87}$$

The notation of the constant C_- was chosen in this way because it is related to the ambiguity of the action at r_- due to a logarithmic term.

4.5 Resummation of the scalar field $\psi(r, \varepsilon)$

In what follows the results of the BH-mode computation for the field $\psi(r, \varepsilon)$ will be discussed for two different sets of parameters, first for $r_c = 1$, $r_+ = 1/2$, $Q = 2/5$ far away from extremality, as well as for the near-extremal case where $r_c = 1$, $r_+ = 1/3$, $Q/Q_{\text{ext}} = 1 - 10^{-4}$. Analysing the Borel plane of the perturbative expansion of the field $\psi(r, \varepsilon)$ will turn out to be useful since it hints at a Stokes phenomenon and provides information on what the full non-perturbative picture of the problem may look like.

Parameter values $r_c = 1$, $r_+ = 1/2$, $Q = 2/5$

One may ask whether the non-perturbative corrections to the perturbative ε-expansion of ω are related to the non-perturbative corrections to the perturbative ε-expansion of the scalar field $\psi(x, \varepsilon)$ from Eq. (4.71). To investigate the non-perturbative behaviour and possible Stokes phenomena, one calculates the ε-expansion for different values of $x = r - r_+$ and performs a Borel transform in the ε-variable:

$$\mathcal{B}\left[\breve{\psi}\right](x, \xi) = \sum_{m=0}^{+\infty} \frac{\psi_{m+1}(x)}{m!} \xi^m, \tag{4.88}$$

where again the 'inverse hat' means that the $\mathcal{O}\left(\varepsilon^0\right)$-term is dropped. As before with the minor $\breve{\omega}^{(0)}$, one can now calculate the Padé transform of (4.88) for different values of x. Remember that originally two distinct exponential weights $A_{\text{sgn}}(r)$ were found (see Eq. (4.38)), each of which corresponds to one of two linearly independent solutions to the ODE (4.34), one for each choice sgn $\in \{+, -\}$. The weight $A_{\text{sgn}}(r)$ is regular at $r = r_c$ for sgn $= (-)$ and regular at $r = r_+$ for sgn $= (+)$, and the leading order coefficient of the QNM-frequency, $\omega_{-1}^{(0)} = \lambda_0$, is chosen in such a way as to make $A_-(r)$ regular at $r = r_+$ as well. However, if we consider the possibility of Stokes-phenomena, this is not the only possibility for all values of r. For the black hole mode and values of r close to r_c, only $A_-(r)$ is allowed under the regularity constraint, since $A_+(r)$ diverges at $r = r_c$ for the black hole mode. However, both weights, $A_-(r)$ and $A_+(r)$ are regular at $r = r_+$. If there is a Stokes line in between, then $A_+(r)$ could be turned on at the Stokes line. For a Stokes phenomena to occur, the solution with the exponential weight $A_-(r)$ must get mapped into a linear combination of the $A_-(r)$ and the $A_+(r)$-solution. Since the field

$\psi(r,\varepsilon)$ comes multiplied with a non-perturbative factor

$$\exp\left(\frac{-1}{\varepsilon}A_-(r)\right), \tag{4.89}$$

The exponential factor that must be turned on for the $\psi(r,\varepsilon)$ when crossing a Stokes line is

$$\exp\left(-\frac{1}{\varepsilon}\left(A_+(r)-A_-(r)\right)+\frac{K}{\varepsilon}\right), \tag{4.90}$$

where K is some constant. If one is resumming along the real line, a Stokes phenomenon at $r=r_*$ would correspond to the function

$$\mathrm{Sing}(r) = -\left(A_+(r)-A_-(r)\right)+K \tag{4.91}$$

crossing the real line at r_*, i.e.

$$\mathbb{I}\mathrm{m}\left(\mathrm{Sing}(r_*)\right)=0. \tag{4.92}$$

Since the ODE only uniquely determines the derivatives of $A_1(r)$ and $A_2(r)$, one can only know $\mathrm{Sing}(r)$ up to the constant K from the analysis carried out up so far. The behaviour of the singularities of the Borel-Padé transform

$$\mathrm{BP}_N\left[\breve{\psi}\right](x,\xi) \tag{4.93}$$

can be used to determine the constant K and serves as a consistency check for the hypothesis that the r-dependence of the singularities is given by (4.91). One finds that for $x=0$, there is one singularity with $\mathbb{R}\mathrm{e}\,(\xi)>0$, and that singularity corresponds exactly to the exponential weight which was found for the QNM-frequency $A_\omega \equiv 4.099-0.343\mathrm{i}$ (see Eq. (4.81)). For the constant K one finds

$$K = 0.482 - 10.010\,\mathrm{i}\,. \tag{4.94}$$

As x is increased, the singularity at $\xi=A_\omega$ splits up into two distinct singularities. One with the constant location at $\xi=A_\omega$, and another one emerging from it which follows the function $\mathrm{Sing}(r)$, just as expected (see Fig. 4.7). Because the derivative of $\mathrm{Sing}(r)$ is pure imaginary for real r, this second moving singularity crosses the real line, and this

happens at

$$\begin{aligned} x_\star &= 0.015795; \\ r_\star &= 0.515795. \end{aligned} \tag{4.95}$$

When the crossing happens a Stokes phenomenon is expected to take place since the singularity moves to the other side of the real integration path in the Borel resummation.

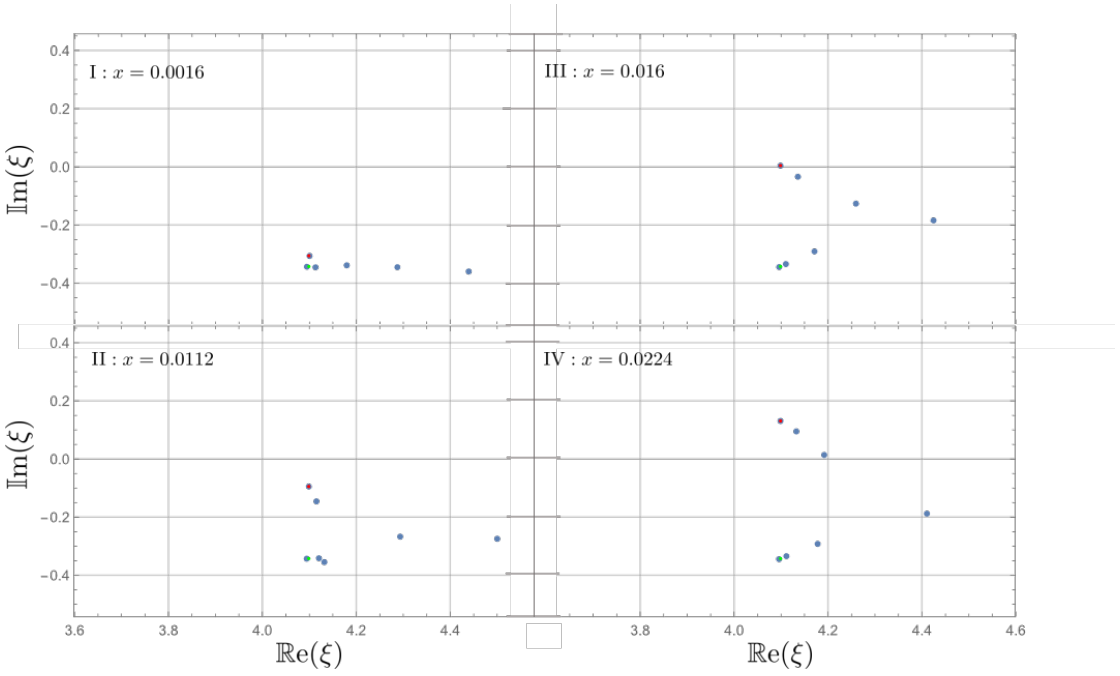

FIGURE 4.7: Singularities of the Borel-Padé transform $\mathrm{BP}_N\left[\breve{\psi}\right](x,\xi)$ for $N = 82$ for different values of x in increasing order from I-IV. The chosen parameters are $r_c = 1$, $r_+ = 1/2$, $Q = 2/5$. The green dot is located at $A_\omega = 4.099 - 0.343\mathrm{i}$, whereas the red dot represents the analytic prediction of the moving singularity at $\mathrm{Sing}(r = r_+ + x)$. The choice of smaller N than in the previous analysis of $\omega(\varepsilon)$ is necessary due to a trade-off between the orders in the x-expansion and the orders in the ε-expansion.

Near extremal parameter values $r_c = 1$, $r_+ = 1/3$, $Q/Q_{\mathbf{ext}} = 1 - 10^{-4}$

By considering the Borel-Padé transform of ψ one finds an emergence of moving singularities from those in Eq. (4.85), which can be expressed as

$$\begin{aligned} \mathrm{Sing}_\ell(r) &\equiv A_+(r) - A_-(r) + K + \ell\, C_- \,; \\ \ell &\in \{-4,-3,-2,-1,0,1,2,3\}. \end{aligned} \tag{4.96}$$

As before, the constant K is chosen such that $\mathrm{Sing}_\ell(r=r_+) = \mathrm{Sing}_{\omega,0}$. One obtains

$$K = -0.717905 - 70.134\,\mathrm{i}\,. \tag{4.97}$$

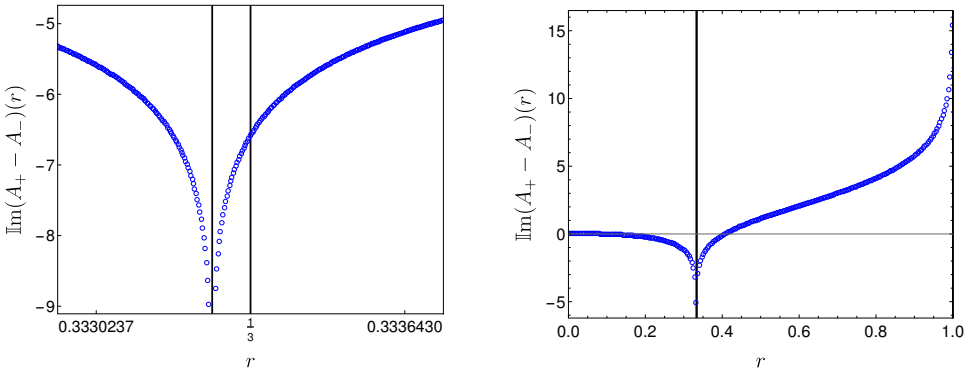

FIGURE 4.8: The difference of the two actions A_- (regular at r_+ and r_c) and A_+ (regular only at r_+) for the black hole family for near-extremal parameters $r_+ = 1/3$, $r_c = 1$, $Q/Q_{\mathrm{ext}} - 1 = 10^{-4}$ near the black hole horizon (left) and on a wider range from $r \in [0,1]$. The singularity in the first picture is located at $r = r_-$.

It is possible to understand the exact positions of the new actions by considering the properties of the functions $A_-(r)$ and $A_+(r)$. For the BH-mode one has $\lambda_0 = Q/r_+$ in Eq. (4.38), the 'singularity function' $\mathrm{Sing}_k(r)$ has three logarithmic singularities at the positions $r = r_-, r_+, r_{\mathrm{neg}}$, where

$$r_{\mathrm{neg}} = -\left(r_+ + r_c + r_-\right). \tag{4.98}$$

Hence the monodromy of $\mathrm{Sing}_k(r)$ is non-trivial. Each time one 'walks' in a circle around one of the singularities r_*, $* \in \{(-), (+), \mathrm{neg}\}$ (i.e. along a 2π-loop in the complex plane), the function $\mathrm{Sing}_k(r)$ changes by a constant,

$$\mathrm{Sing}_k(r_* + \delta) \mapsto \mathrm{Sing}_k(r_* + \delta\,\mathrm{e}^{2\pi\mathrm{i}}) = \mathrm{Sing}_k(r_* + \delta) + C_*. \tag{4.99}$$

The constants C_* are

$$\begin{aligned} C_{\mathrm{neg}} &= \frac{-2\pi Q(r_+ - r_{\mathrm{neg}})}{r_+ r_{\mathrm{neg}} \kappa_{\mathrm{neg}}}\,[= 7.16883]\,; \\ C_- &= \frac{2\pi Q(r_+ - r_-)}{r_+ r_- \kappa_-}\,[= 5.73318]\,; \\ C_c &= \frac{2\pi Q(r_c - r_+)}{r_+ r_c \kappa_c}\,[= 12.9020]\,, \end{aligned} \tag{4.100}$$

where the values in the values in the brackets are obtained by evaluating the above expressions at the chosen near-extremal parameters. In principle, it would be consistent with our analysis so far if all three translation constants from (4.100) would define a grid of singularities in the Borel-plane which could be parameterised by three integers. However, as it turns out one only finds the singularities defined by the C_--translations, namely (4.96). The singularities of the Borel-Padé transform of ψ are plotted in Fig. 4.9. One can see the Padé singularities accumulating around the positions of the Borel singularities of ω. The further away the singularity lies from the origin, the fewer Padé singularities are present around the Borel singularities. In Fig. 4.9 only four singularities are visible, but it is expected that more singularities would appear if one were to increase the order of the Padé approximation.

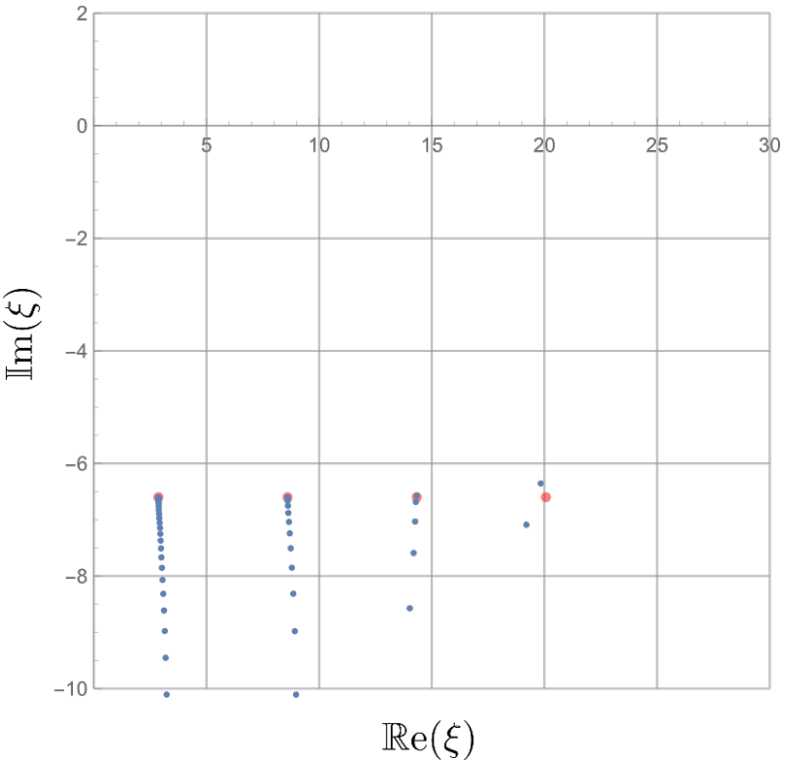

FIGURE 4.9: Singularities of Borel-Padé transform of $\omega^{(0)}(\varepsilon)$ for $N = 280$ and $r_+ = 1/3$, $r_c = 1$, $Q/Q_{\text{ext}} = 1 - 10^{-4}$. The red dots show the singularities which are expected from Eq. (4.86).

4.5.1 Stokes phenomenon

The implications of the previous analysis for the behaviour of the QNM wave function $\psi(r, \varepsilon)$ at the Stokes transition will now be discussed. The following observations and conclusions form part of ongoing research and may change as new findings emerge.

While the exact form of the non-perturbative contributions to the QNM wave function $\psi(r,\varepsilon)$ is still unknown, one can deduce which kinds of corrections are possible from the structure of the Borel singularities and the knowledge of the boundary conditions. It was found that without taking into account the boundary conditions, two r-dependent exponential weights $A_+(r)$ and $A_-(r)$ are allowed, each one corresponding to one of two linearly independent Frobenius expansions. At each of the two horizons only one of the two linearly independent is allowed under the constraint imposed by the boundary conditions. This leads to an interesting problem when considering Stokes transitions. One could expect that if at a certain position r near the Stokes line only one of the two solutions (corresponding to one the two exponential weights $A_+(r)$ or $A_-(r)$) is present, the other solution will be turned on upon crossing the Stokes line, as is often the case in problems involving WKB expansions. However, since at each of the two horizons r_+ and r_c only one of the solutions is allowed by the boundary conditions, two explanations are possible:

1. There are several Stokes lines present, and the solution which does not obey the correct boundary conditions is turned off again before reaching the next horizon.
2. The non-perturbative exponentials which are turned on at a Stokes transition are independent of r. Hence the asymptotic expansion is merely re-scaled by an r-independent factor.

The problem with option 1 is that the singularities $\mathrm{Sing}_\ell(r)$ in the Borel plane only cross the real line once, which seems to exclude the possibility of the existence of more than one Stokes transition between $r = r_+$ and $r = r_c$. This observation seems to takes us in the direction of option 2.

To understand this issue better, consider the following re-scaling of the scalar field $\widehat{\Phi}$ from (4.12):

$$\widehat{\Phi}(r) \equiv \left(\frac{r}{r_+} - 1\right)^{-\mathrm{i}\beta_+(\varepsilon)/\varepsilon} \left(1 - \frac{r}{r_c}\right)^{-\mathrm{i}\beta_c(\varepsilon)/\varepsilon} \Psi(r,\varepsilon) \tag{4.101}$$

Note that in the field redefinition (4.101), the leading order r-dependent exponential behaviour $\sim \mathrm{e}^{-A(r)/\varepsilon}$ is not part of the re-scaling and is therefore part of the field Ψ. With the re-scaling (4.101), the boundary conditions imply that $\Psi(r,\varepsilon)$ be regular at both horizons r_+ and r_c.

The two linearly independent solutions for Ψ (disregarding the boundary conditions) behave asymptotically in ε as

$$\Psi^{(\pm)}(r,\varepsilon) \simeq \mathrm{e}^{-A_\pm(r)/\varepsilon} \times \underset{\text{perturbative in } \varepsilon}{\psi^{(\pm)}(r,\varepsilon)}\ , \tag{4.102}$$

where $A_\pm$ are given in (4.38) by choosing sgn $= \pm$. The functions $\psi^{(\pm)}$ are perturbative divergent WKB expansions in ε, but both linearly independent solutions do not need to be regular in r at the horizons. In fact, one and only one of the $\psi^{\pm}(r,\varepsilon)$ is a regular function of r at both horizons, as can be seen from the Frobenius analysis, as we shall see next. In Section 4.3.1 it was found that the leading-order exponents in the Frobenius expansion around any of the two horizons r_j, where $j \in \{+,c\}$, are of the form

$$\pm \mathrm{i}\,\alpha_j(\varepsilon) = \pm \mathrm{i}\,\beta_j(\varepsilon)/\varepsilon. \tag{4.103}$$

The function $\beta_j(\varepsilon)$ admits a perturbative expansion (starting at order ε^0 or higher) around $\varepsilon = 0$. If one considers as a variable the distance from an horizon r_j, $x = r - r_j$, then the solution $\widehat{\Phi}(r)$ can be expanded in the following way around $x = 0$ ($r = r_j$):

$$\widehat{\Phi}(r_j + x) = x^{-\mathrm{i}\alpha_j} f_-(x) + x^{+\mathrm{i}\alpha_j} f_+(x); \tag{4.104}$$

where $f_-(x)$ and $f_+(x)$ are regular expansions in x and hence the two terms in (4.104) are linearly independent. The re-scaling in (4.102) corresponds to factoring out $x^{-\mathrm{i}\alpha}$ in (4.104):

$$\widehat{\Phi}(r_j + x) = x^{-\mathrm{i}\alpha_j} \underbrace{\left(\underset{\text{regular}}{f_-(x)} + \underset{\text{not regular}}{x^{+2\mathrm{i}\alpha_j} f_+(x)} \right)}_{\propto \Psi(r_j+x)}; \tag{4.105}$$

Since α does not vanish generically, $x^{-2\mathrm{i}\alpha}$ is generally not regular at $x = 0$. The linearly independent solutions $\Psi^{(\pm)}(r,\varepsilon)$ in (4.102) thus correspond to the terms inside the bracket (4.105). Since factoring out the non-perturbative exponential as done in (4.102) can at most cancel the leading order ε^{-1}-term in the exponent $\alpha(\varepsilon)$, at least one of the two functions $\psi^{(\pm)}$ in (4.102) is not regular in the variable r at the horizon r_j. Therefore one and only one of the two functions $\psi^{(\pm)}(r,\varepsilon)$ is regular in r at any horizon.

The equation of motion (4.12) is linear and homogeneous and does not involve any derivatives in ε. Hence one can re-scale any solution $\Psi(r,\varepsilon)$ with an arbitrary function

of ε and the resulting function will also be a solution. As a consequence the weight functions $A_\pm(r)$ are a priori only defined up to an additive constant. However, function re-scalings affect both linearly independent solutions in the same way, and so the *difference of the weight functions*

$$A_+(r) - A_-(r) \tag{4.106}$$

should have no ambiguity. Consequently, after factoring out $A_-(r)$, the remaining non-perturbative weight is given by the difference (4.106) and is unambiguous. Due to the boundary conditions one requires the field $\Psi(r,\varepsilon)$ to be regular at r_+ and r_c. For each of the four horizons r_j (also including the negative horizon $r = r_{\text{neg}} = -(r_+ + r_- + r_c)$) there is a logarithmic term $\sim \log(r - r_j)$ in $A_{\text{sgn}}(r)$ (see (4.38)), and there are two ways of cancelling each of the singularities at r_+ and r_c: either by choice of λ_0 (defining the mode family), or by choice of the sign sgn $\in \{+,-\}$, that is choosing one of the linearly independent solutions.

Now consider the black hole family, which means choosing

$$\lambda_0 = \lambda_0^{(+)} = \frac{Q}{r_+}. \tag{4.107}$$

In Section 4.3 as well as in [6] it was assumed that the only allowed weight function $A_{\text{sgn}} \in \{A_-, A_+\}$ must be regular at both horizons r_+ and r_c. For the black hole family this is the case with $A_-(r)$. If all that mattered in the analysis was the regularity of the exponential prefactor

$$\mathrm{e}^{-A_{\text{sgn}}(r)/\varepsilon}, \tag{4.108}$$

then it would be possible that for the BH-mode, both actions $A_-(r)$ and $A_+(r)$ would be turned on near the BH horizon $r = r_+$, since both are regular at that point. Moreover, after crossing the Stokes line the solution with $A_+(r)$ could be turned off (or, equivalently, one would start only with the $A_-(r)$ solution near the cosmological horizon $r = r_c$ coming from the right and the $A_+(r)$ could be turned on by a Stokes crossing from right to left). However, each of the two solutions defined by a prefactor (4.108) corresponds to exactly one Frobenius expansion. Moreover, only one of the Frobenius expansions can be regular after having factored out the leading order term in the Frobenius expansion which satisfies the boundary conditions. It follows that if the other solution is turned on by the Stokes line, it must be turned off again before reaching the next horizon. But since $A_-(r) - A_+(r)$ only crosses the real line once with increasing r, there cannot be

more Stokes transitions where this turning-off could take place. This seems to indicate that we need to consider option 2 above, and that the Stokes automorphism leads to a re-scaling of $\psi(r,\varepsilon)$ by a factor which includes non-perturbative exponentials in ε, but is constant in r.

4.6 Discussion

In the previous chapters, it was found that both the QNM wave function $\psi(r,\varepsilon)$ and the QNM-frequency $\omega(\varepsilon)$ have singularities in the Borel plane. It was also found that the positions of these singularities are closely related to each other. In particular, the Borel singularities of the QNM-frequency ω, denoted by $A_{\omega,\ell}$, are also present in the Borel plane of the QNM wave function $\psi(r,\varepsilon)$, together with another set of r-dependent singularities $\mathrm{Sing}_\ell(r)$ emerging from the singularities $A_{\omega,\ell}$. The singularities $\mathrm{Sing}_\ell(r)$ move upward as the radial variable r is increased and cross the real axis at a certain point. This behaviour hints at the existence of a Stokes phenomenon and the turning-on of non-perturbative exponentials. The objective of this project is to understand the full non-perturbative picture of the problem. The following three research questions lie at the main focus of the ongoing work on this project.

1. The Borel singularities $A_{\omega,\ell}$ have been calculated numerically by computing the positions of the Padé singularities in the Borel plane. While the real part $\mathbb{R}\mathrm{e}\,(A_{\omega,\ell})$ has also been determined in closed form, it is still unclear how to obtain exact expressions for the imaginary part $\mathbb{I}\mathrm{m}\,(A_{\omega,\ell})$.

2. For the BH-mode which determines the validity of the SCC conjecture, a multiple-scale analysis has been carried out by introducing a boundary layer around the black hole horizon $r = r_+$. It is possible that a similar multiple scales analysis around the cosmological horizon $r = r_c$ may yield new insights about analytical properties of the problem such as the exact positions of the Borel singularities $A_{\omega,\ell}$, or about the full non-perturbative picture of the problem.

3. The structure of the moving Borel singularities $\mathrm{Sing}_\ell(r)$ in the Borel plane of the QNM wave function $\psi(r,\varepsilon)$ provides evidence for the existence of a Stokes phenomenon. Further analysis of the ODE is necessary to gain a better understanding

of the non-perturbative contributions which are turned on at the Stokes line. In particular, it is unclear whether the Stokes phenomenon involves a turning on of a linearly independent solution, or whether the non-perturbative exponentials which arise at the Stokes transition are constants in the radial variable r.

Answering the above research questions will allow one to use the asymptotic techniques of Borel resummation and Hyperasymptotics to calculate the QNM frequency of the leading BH-mode $\omega^{\text{BH}}(\varepsilon)$ as a function of the charge parameter $\varepsilon = 1/q$ with exponential accuracy. In particular, if one manages to calculate the first non-perturbative correction in $\omega^{\text{BH}}(\varepsilon)$, it would be possible to obtain the non-perturbative 'wiggles' around the critical regularity value $\beta = 1/2$ to high accuracy with very little computational power, and thus extend the results in [6, 122]. Furthermore, the approach which was developed in this work can also be applied to similar problems in which QNMs are calculated using WKB expansions.

Outlook

In each of the three projects presented in this thesis, the asymptotic techniques described in Chapter 1 have been essential to unravel the global analytic behaviour of observables from the original local asymptotic analysis. In Chapters 2 and 4 Borel techniques have been used to thoroughly analyse the asymptotic properties of the respective perturbative observables, and to find a complete non-perturbative solution in the form of a formal transseries. This is a crucial step in the general goal of understanding some global analytic properties of these observables, which can then be obtained by extremely accurate summation methods.

The non-perturbative structure of the observable studied in Chapter 3 was previously known [123], but an analysis of its analytic properties, based on exponentially accurate summations was non-existent. These novel results were presented in Chapter 3 , where a thorough comparison of different asymptotic methods of summation, and their respective strengths and weaknesses can also be found. In Chapters 2 and 3 it was shown explicitly that the transasymptotic summation is a very powerful method to analytically access the non-perturbative domain and to deduce global properties of the solution. In particular, the transasymptotic summation can be used to connect different asymptotic regimes by analytically continuing a function of interest from a region where the non-perturbative exponentials are small to regions in which they are very large. The method also enables one to determine poles, zeros or branch points on the complex plane. This approach is generic and has recently been successfully applied to locate the complex singularities of Burger's equation [124]. For the ongoing project discussed in Chapter 4, one of the next steps is to apply the transasymptotics approach to find the critical values of the scalar field charge. To do this a general understanding of the the non-perturbative corrections is needed and is currently underway.

The work in this thesis showed that the non-perturbative methods built on resurgence are highly effective in describing intricate mathematical phenomena in a variety of mathematical problems. The most important results which have been developed in this thesis can be summarised as follows. Chapter 2 provides a completely novel understanding of the bifurcations arising in discrete non-linear systems in terms of the behaviour of non-perturbative exponentials in a transseries expansion. In addition to providing quantitative approximations to the solutions using transasymptotic summation, analytic expressions allow for a qualitative understanding of the 'canard' bifurcations in terms of the change in dominance of different exponential scales. A similar analysis can be performed to analyse changes in period dominance for other discrete/finite difference equations such as string equations coming matrix models *e.g.* [125, 126].

In Chapter 3, a systematic way of linking the known transseries expansion at late times to the early time behaviour is developed in the context of relativistic hydrodynamics. The method relies on known Borel techniques and will likely be of great use in many hydrodynamics problems where a late-time attractor is present *e.g.* [127, 128]. Furthermore, the method is generic and not tied to how the transseries expansion of an observable is obtained, which makes the findings in Chapter 3 highly applicable to a wide range of problems in physics, see *e.g.* [95]. In fact, in this Chapter the transasymptotic summation has been used to deduce analytic global properties of the observable such as the location of square-root branch point singularities, and a thorough understanding of the relationship between the asymptotic expansions in different regions of the complex plane has been obtained.

As previously mentioned, summation techniques such as transasymptotic summation will be crucial to the analytic understanding of the critical points of quasi-normal modes in the context of strong cosmic censorship. This work is on-going and is presented in Chapter 4. Here an extensive analysis of the expected non-perturbative corrections to the least suppressed quasi-normal mode was carried out, and preliminary summations have been analysed.

To summarise, the great potential which lies in the asymptotic summation techniques described made it possible to gain a fundamental understanding of the mathematical mechanism behind the bifurcations leading to deterministic chaos in non-linear systems, link the early-time behaviour to the late-time behaviour in an expanding relativistic

strongly-coupled fluid, as well as understand non-perturbative effects arising in the calculation of quasinormal modes in the context of the Strong Cosmic Censorship conjecture. The results obtained in each of the three projects are also highly applicable to problems in different physical contexts. Non-perturbative effects in quasinormal modes arise in many spacetime and matter models. Thus the methodology developed in Chapter 4 may also be used to compute quasinormal mode frequencies in cases where the expansion parameter is different from the scalar field charge, *e.g* like in the WKB analysis of [129]. The matching method which was developed in Chapter 3 can be applied to much more general fluid models. In principle it can be applied in many situations in which a hydrodynamics model is used to model the macroscopic evolution of a system which is microscopically described by some quantum field theory. This is the case with $\mathcal{N} = 4$ SYM strongly coupled fluids [127, 128], whose macroscopic evolution is very difficult to obtain without using the AdS/CFT correspondence to calculate phenomenological parameters such as the shear viscosity, and then solving the phenomenological evolution equation. Another example of physical observables in which the methods used in this thesis can be extremely useful are in integrable field theories [130, 131]. In some of these problems, partial transseries results already exist, and applying summation techniques could lead to promising new insights.

Based on a three-month internship on the topic of quantum machine learning several techniques have been studied in the context of image processing and classification, and another future direction of work is to understand how take advantage of the asymptotic toolbox in the study of certain non-linear properties of machine learning models based on neural networks.

Appendix A

Logistic equation

A.1 Explicit transseries terms

In (2.31), the transseries for $R(\tau_0, \varepsilon)$ is written in terms of a base approximation $R_0(\varepsilon)$, a sum of odd terms in τ_0, denoted $\Omega_{o,k}$, and a sum of even terms in τ_0, denoted $\Omega_{e,k}$. One may further simplify this by writing $R(\tau_0, \varepsilon; \sigma_0) = R(\varepsilon) + S(\tau_0, \varepsilon)$, where

$$S(\tau_0, \varepsilon) = \sqrt{\varepsilon} \sum_{k=0}^{\infty} \varepsilon^k \Omega_{o,k}(\tau_0) + \varepsilon \sum_{k=0}^{\infty} \varepsilon^k \Omega_{e,k}(\tau_0). \tag{A.1}$$

Note that $\tau_0(x + \varepsilon) = -(1 + \varepsilon)\tau_0(x)$. Consequently,

$$S(\tau_0(x + \varepsilon), \varepsilon) = S(-(1 + \varepsilon)\tau_0(x), \varepsilon). \tag{A.2}$$

Applying (A.1) and (A.2) to the logistic equation (2.16) gives

$$S(-(1 + \varepsilon)\tau_0, \varepsilon) = -(1 + \varepsilon)S(\tau_0, \varepsilon) - (3 + \varepsilon)S(\tau_0, \varepsilon)^2. \tag{A.3}$$

Expanding the left-hand side of this expression as a Taylor series in ε gives

$$\begin{aligned} S(-(1 + \varepsilon)\tau_0, \varepsilon) &= \sum_{j=0}^{\infty} \frac{(-\tau_0 \varepsilon)^j}{j!} R^{(j)}(-\tau_0) \\ &= -\sqrt{\varepsilon} \sum_{m=0}^{\infty} \varepsilon^m \sum_{k=0}^{m} \frac{\tau_0^k}{k!} \Omega_{o,m-k}^{(k)}(\tau_0) + \varepsilon \sum_{m=1}^{\infty} \varepsilon^n \sum_{k=0}^{m-1} \frac{\tau_0^k}{k!} \Omega_{e,n-1-k}^{(k)}(\tau_0), \end{aligned} \tag{A.4}$$

where the fact that $\Omega_{o,k}$ and $\Omega_{e,k}$ are odd and even in τ_0 respectively was used. The remaining expansions in (A.3) may be obtained by substitution of (A.1) into (A.3). It is straightforward to show that

$$R(\tau_0,\varepsilon)^2 = 3\sum_{m=1}^{\infty}\varepsilon^m\sum_{k=0}^{m-1}\Omega_{o,k}(\tau_0)\Omega_{o,m-1-k}(\tau_0) \tag{A.5}$$

$$+\sqrt{\varepsilon}\sum_{m=1}^{\infty}\varepsilon^m\sum_{k=0}^{m-1}\Omega_{o,k}(\tau_0)\Omega_{e,m-1-k}(\tau_0)+\sum_{m=2}^{\infty}\varepsilon^m\sum_{k=0}^{m-2}\Omega_{e,k}(\tau_0)\Omega_{e,m-2-k}(\tau_0). \tag{A.6}$$

These expansions may now be used to equate powers of ε and obtain the expressions given in (2.42).

A.2 Initial Condition for 4-Periodic Equation

In order to calculate the initial condition for the 4-periodic problem, first recall that $\hat{R}(x,\varepsilon)$ was derived in order to satisfy the initial condition for small ϵ. The 4-periodic solution arises for $\varepsilon > -2+\sqrt{6}$, or $\eta > 0$. Hence, one determines the initial condition by perturbing around the leading-order behaviour of $\hat{R}(x,\varepsilon)$, which is initially 2-periodic for the parameter regime under consideration. One then determines σ_1 by matching with the initial condition in the limit that $\eta \to 0$.

One first obtains the stable 2-periodic behaviour of $R(x,\varepsilon)$ from (2.12), letting $x = 0$ in order to describe the initial state. This expression may be written in terms of η, to allow a small η expansion in this limit. This gives

$$\begin{aligned}\hat{R}(0,\varepsilon) =& \frac{4+\varepsilon+\sqrt{\varepsilon(4+\varepsilon)}}{2(3+\varepsilon)}\\ \sim& \frac{1}{5}\left(2-\sqrt{3}+\sqrt{2+\sqrt{3}}\right)+\frac{\eta}{50}\left(3\sqrt{2}-16\sqrt{3}-7\sqrt{6}+12\right)\\ &+\frac{3\eta^2}{250}\left(-47\sqrt{2}+84\sqrt{3}+18\sqrt{6}-38\right)+\mathcal{O}(\eta^3).\end{aligned} \tag{A.7}$$

Setting $x = 0$, letting $\sigma_1 = \sigma_{1,0} + \eta\sigma_{1,1} + \ldots$, and expanding S in powers of η gives

$$\begin{aligned} S(0,\varepsilon) \sim & \eta\sigma_{1,0} \\ & + \eta^2 \left(-\tfrac{5}{12}(14 - 7\sqrt{2} - 4\sqrt{3} + 4\sqrt{6})\sigma_{1,0}^3 + (3\sqrt{3} - \sqrt{6} + \tfrac{3}{2}\sqrt{2} - 1)\sigma_{1,1}^2 + \sigma_{1,1} \right) \\ & + \mathcal{O}(\eta^3) \end{aligned} \tag{A.8}$$

To determine the appropriate initial condition, $\eta = 0$ is set, which gives

$$R(0,\varepsilon) = \frac{1}{5}\left(2 - \sqrt{3} + \sqrt{2 + \sqrt{3}}\right). \tag{A.9}$$

By setting $R(0,\varepsilon) = \hat{R}(0,\varepsilon) + S(0,\varepsilon)$, and matching powers of η, one obtains

$$\begin{aligned} \sigma_1 = & -\frac{1}{50}\left(3\sqrt{2} - 16\sqrt{3} - 7\sqrt{6} + 12\right) + \frac{\eta}{500}\left(297\sqrt{2} - 709\sqrt{3} - 189\sqrt{6} + 399\right) \\ & + \mathcal{O}(\eta^2), \end{aligned} \tag{A.10}$$

This is sufficient information to approximate the solution using the transseries behaviour, although it is straightforward to continue this process to obtain higher corrections for σ_1.

A.3 Proof that a multi-parameter transseries is not required

Here it will be explained why a single parameter transseries is sufficient even though the dynamical logistic equation admits several different exponential weights parametrised by a constant γ and and integer p:

$$A_\gamma(x) \equiv \gamma - 1 - (1 + x)\left(\log(1 + x) - 1\right) - \mathrm{i}\pi(2p + 1)x\,. \tag{A.11}$$

They all satisfy

$$\begin{aligned} \frac{\tau(x+\varepsilon)}{\tau(x)} &= \exp\left[-\left(\frac{A_\gamma(x+\varepsilon) - A_\gamma(x)}{\varepsilon}\right)\right] \\ &= \exp\left[-\left(\frac{A_0(x+\varepsilon) - A_0(x)}{\varepsilon}\right)\right]. \end{aligned} \tag{A.12}$$

This implies that the ratio $\tau(x+\varepsilon)/\tau(x)$ is the same for all possible weights. Now consider the following transasymptotic summation of a two-parameter transseries in

the variables τ_1 and τ_2 corresponding to the parameters σ_1 and σ_2.

$$R(\tau_1, \tau_2, x, \varepsilon) \;=\; \sum_{n,m\geq 0} \tau_1^m \tau_2^n \, \Phi_{n,m}(x, \varepsilon)\,. \tag{A.13}$$

One can substitute this ansatz (A.13) into the dynamical logistic equation (2.90), and obtain equations for the $\Phi_{m,n}$ by matching all the terms with given powers of σ_1 and σ_2. As a consequence of (A.12), the functions $\Phi_{m,n}(x, \varepsilon)$ satisfy the resulting difference equations if one sets

$$\Phi_{m,n}(x, \varepsilon) \;\equiv\; \binom{m+n}{m} R_{m+n}(x, \varepsilon)\,, \tag{A.14}$$

where the functions R_k are the transseries-sectors of the one-parameter transseries (2.92) satisfying Eq. (A.44). One may now write

$$\begin{aligned} R(\tau_1, \tau_2, x, \varepsilon) \;&=\; \sum_{n,m\geq 0} \tau_1^m \tau_2^n \binom{m+n}{m} R_{n+m}(x, \varepsilon) \;=\; \sum_{n=0}^{+\infty} (\tau_1 + \tau_2)^n R_n(x, \varepsilon) \\ &= \sum_{k=0}^{+\infty} \varepsilon^k \, \Omega_k(\tau_1 + \tau_2, x), \end{aligned} \tag{A.15}$$

where the functions Ω_k are the same as in (A.18). In fact this argument can be generalised to any number of transseries parameters $\{\tau_m\}$ as long as the ratio $\tau_m(x+\varepsilon)/\tau_m(x)$ does not depend on m. Eq. (A.15). This implies that if for n distinct transasymptotic variables τ_m one may always define a new variable

$$\tau \;\equiv\; \tau_1 \,+\, \tau_2 \,\ldots\, +\, \tau_n\,, \tag{A.16}$$

such that the transasymptotic summation effectively only depends on a single variable τ. As a consequence, the treatment of the dynamical logistic equation using a one-parameter transseries is justified.

A.3.1 Derivation of equations for $\Omega_0(y)$ and $\Omega_1(y)$

In this section the transasymptotic approach to solving the DLE (2.90) is taken. Instead of expanding in powers of the parameter σ, that is, in non-perturbative sectors, one instead changes the order of summation by grouping together all the exponentials multiplying the same power of ϵ. Note that the whole expansion is performed over two indices (m, n) corresponding to $\sigma^m \epsilon^n$. The whole summation can be thought of as a summation

over all the points in the grid $\mathbb{N}_0 \times \mathbb{N}_0$. The approach that was taken before corresponds to summing over all the points along the direction $(0,1)$, whereas now one will first sum over all the points along the direction $(1,0)$. It is useful to perform a change of variables:

$$\begin{aligned} \sigma \mapsto \tau \equiv \sigma\, \mathrm{e}^{-A(x)/\epsilon}\, \epsilon\,; \\ x \mapsto x\,; \\ \epsilon \mapsto \epsilon\,. \end{aligned} \tag{A.17}$$

The transseries then takes the form

$$R(\tau,\, x, \epsilon) \;=\; \sum_{k=0}^{+\infty} \epsilon^k \sum_{j=0}^{+\infty} \tau^j\, R_{j,k}(x) \;\equiv\; \sum_{k=0}^{+\infty} \epsilon^k\, \Omega_k(\tau,\, x)\,. \tag{A.18}$$

The variable τ behaves in the following way under translations $x \mapsto x+\epsilon$ while keeping σ constant:

$$\tau(x+\epsilon) \;=\; \mathrm{e}^{-(A(x+\epsilon)-A(x))/\epsilon}\, \tau(x)\,. \tag{A.19}$$

One also has

$$\tau'(x) \;=\; -\frac{A'(x)}{\epsilon}\, \tau(x)\,. \tag{A.20}$$

This is a very useful property. It implies that the translation operator $x \mapsto x+\epsilon$ can be rewritten as

$$[x \mapsto x+\epsilon] \;=\; \exp\left(\epsilon \frac{\mathrm{d}}{\mathrm{d}x}\right) \;=\; \exp\left(-A'(x)\tau(x)\partial_\tau\big|_x \;+\; \epsilon\, \partial_x\big|_\tau\right)\,. \tag{A.21}$$

The ansatz Eq. (A.18) will be used to solve the difference equation

$$R(x+\epsilon,\epsilon) \;=\; (3+x)\, R(x,\epsilon)\; (1-R(x,\epsilon)) \tag{A.22}$$

First, the left hand side needs to be computed:

$$R(\tau(x+\epsilon), x+\epsilon, \epsilon) \;=\; \sum_{n=0}^{+\infty} \epsilon^n\, \Omega_n(\tau(x+\epsilon), x+\epsilon)\,. \tag{A.23}$$

$\Omega_n(\tau(x+\epsilon), x+\epsilon)$ must be expanded in ϵ. To simplify notation, whenever the arguments are not written explicitly, this will mean 'evaluation without shift in the argument',

so τ will stand for $\tau(x)$.

$$\Omega_n(\tau(x+\epsilon), x+\epsilon) \;= \exp\left(\epsilon \frac{\mathrm{d}}{\mathrm{d}x}\right) \Omega_n(\tau(x), x)\,, \tag{A.24}$$

where (see Eq. (A.21))

$$\epsilon \,\frac{\mathrm{d}}{\mathrm{d}x} \;=\; -A'(x)\tau\, \partial_\tau\big|_x + \epsilon\, \partial_x\big|_\tau\,. \tag{A.25}$$

Now a change of coordinates from (x, τ) to (y, x) will be performed, given by

$$\begin{pmatrix} x \\ \tau \end{pmatrix} \mapsto \begin{pmatrix} x \\ y \end{pmatrix} \;=\; \begin{pmatrix} x \\ -\frac{x}{A'(x)} \log\, \tau \end{pmatrix}\,. \tag{A.26}$$

In these coordinates, one can write (from now on, ∂_x means $\partial_x\big|_y$ and $\partial_y \equiv \partial_y\big|_x$)

$$\begin{aligned} \epsilon \,\frac{\mathrm{d}}{\mathrm{d}x} \;&=\; A \,+\epsilon B\,; \qquad A \;\equiv\; x\,\partial_y; \qquad B \;\equiv\; x\, g(x,y)\,\partial_y \,+\, \partial_x\,; \\ g(x,y) \;&\equiv\; \frac{y}{x}\,\left(1 - x\,\frac{A''(x)}{A'(x)}\right)\,. \end{aligned} \tag{A.27}$$

Now $\exp\,(A \,+\, \epsilon B)$ has to be expanded in powers of ϵ in order solve the problem perturbatively. In a first step, all the terms up to linear order in ϵ are considered. The following lemma will be needed:

Lemma A.1 (Binomial expansion)**.** *Let A and B be linear operators on a vector space V, i.e. $A,\, B \in L(V, V)$. If the commutator of A and B is of the form*

$$[A,\, B] \;=\; \alpha\, A\,,$$

where $\alpha \in L(V, V)$ with $[\alpha, A] \;=\; 0$. Then

$$(A \,+\, \epsilon\, B)^n \;=\; A^n + \epsilon\, A^{n-1}\left(n\, B \,-\, \frac{n(n-1)}{2}\,\alpha\right) \,+ \mathcal{O}(\epsilon^2)\,.$$

Proof:

The binomial expansion $(A + \epsilon B)^n$ is computed to order ε under the assumptions

$[A, B] = \alpha A$ and $[\alpha, A] = 0$:

$$\begin{aligned}(A + \epsilon B)^n &= A^n + \epsilon \left(BA^{n-1} + ABA^{n-2} + \ldots + A^{n-1}B \right) \\ &= A^n + \epsilon \sum_{k=1}^{n} A^{k-1} B A^{n-k} .\end{aligned} \tag{A.28}$$

In order to further simplify this, consider (for some positive integers k and ℓ)

$$\begin{aligned}A^k B A^\ell &= A^k [B,\, A] A^{\ell-1} + A^{k+1} B A^{\ell-1} \\ &= A^{k+\ell}(-\alpha) + A^{k+1} B A^{\ell-1} \\ &= A^{k+\ell}(-\alpha) + A^{k+\ell}(-\alpha) + A^{k+2} B A^{\ell-2} \\ &= \ldots = -\ell\, \alpha\, A^{k+\ell} + A^{k+\ell} B \\ &= A^{k+\ell}\, (B - \ell\, \alpha) \,,\end{aligned} \tag{A.29}$$

where the condition $[\alpha,\, A] = 0$ has been used by commuting the operator α through the A. If this is applied to Eq. (A.28), one can simplify the expression further:

$$\begin{aligned}(A + \epsilon B)^n &= A^n + \epsilon \sum_{k=1}^{n} A^{n-1} \big(B - (n-k)\, \alpha \big) + \mathcal{O}(\epsilon^2) \\ &= A^n + \epsilon \left[A^{n-1} B\, n - \left(\sum_{k-0}^{n-1} k \right) \alpha\, A \right] + \mathcal{O}(\epsilon^2) \\ &= A^n + \epsilon \left[n\, B - \frac{n(n-1)}{2}\, \alpha \right] A^{n-1} + \mathcal{O}(\epsilon^2) \,,\end{aligned} \tag{A.30}$$

which completes the proof.

Now one can compute the exponential

$$\begin{aligned}\exp\left(A + \epsilon\, B\right) &= \sum_{n=0}^{+\infty} \frac{1}{n!} \left(A + \epsilon\, B\right)^n \\ &= \sum_{n=0}^{+\infty} \left(A^n + \epsilon\, n A^{n-1} B - \frac{\epsilon}{2} \alpha\, n(n-1) A^{n-1} \right) + \mathcal{O}(\epsilon^2) \\ &= \exp(A) + \epsilon \left(\sum_{n=1}^{+\infty} \frac{A^{n-1}}{(n-1)!} \right) B - \frac{\epsilon}{2} \alpha \left(\sum_{n=2}^{+\infty} \frac{1}{(n-2)!} A^{n-2} \right) A \\ &\quad + \mathcal{O}(\epsilon^2) \\ &= \exp(A) \left(1 + \epsilon \left[B - \frac{\alpha}{2} A \right] \right) + \mathcal{O}(\epsilon^2) \,.\end{aligned} \tag{A.31}$$

So far, this result holds for all A and B which satisfy the requirements of Lemma A.1. Now it will be shown that the A and B which was defined in Eq. (A.27) satisfy those requirements. One has

$$\begin{aligned}[A,\, B] \;&=\; [x\,\partial_y,\, g\,\partial_y + \partial_x] \;=\; [x\,\partial_y, g\,\partial_y] + [x\,\partial_y,\, \partial_x] \;=\; (\partial_y g)\,x\,\partial_y \;-\; \partial_y \\ &=\; \left((\partial_y g)x - 1\right)\,\partial_y = \left(\frac{g}{y} - \frac{1}{x}\right)\,x\,\partial_y \equiv \alpha\,A\,.\end{aligned} \tag{A.32}$$

where α is given by

$$\alpha(x) \;=\; \left(\frac{g}{y} - \frac{1}{x}\right) \;=\; -\frac{A''(x)}{A'(x)}\,. \tag{A.33}$$

Note that $\alpha(x)$ only depends on x and not on y, hence it commutes with $x\,\partial_y$ and so $[\alpha,\, A] = 0$ is satisfied. In the following the notation $\tilde{f}$ will be used to denote the representation of some function f in the (x, y)-coordinate system:

$$f(\tau(x,y), x) \;=\; \tilde{f}(y, x)\,. \tag{A.34}$$

When one uses (x, y)-coordinates, the operator $\exp(A) = \exp\left(x\,\partial_y\right)$ just shifts the y-coordinate of whatever expression it acts upon by x, so $y \mapsto y + x$. One finds

$$\begin{aligned}\left(1 + \epsilon\,\left[B - \frac{\alpha}{2}A\right]\right)\,\tilde{f} \;&=\tilde{f} + \left(g\,\partial_y\tilde{f} \;+\; \partial_x\tilde{f}\right) \;-\; \frac{1}{2}\left(\frac{x}{y}g - 1\right)\partial_y\tilde{f} \\ &=\tilde{f} + \left(g \;+\; \frac{1}{2} \;-\; \frac{x}{2y}g\right)\tilde{f}^{(1,0)} \;+\; \tilde{f}^{(0,1)}\,.\end{aligned} \tag{A.35}$$

And so for the whole expansion one obtain

$$\begin{aligned}\exp\left(A + \epsilon\,B\right)\tilde{f}(y,x) \;=\; \tilde{f}(y+x,x) \;&+\epsilon\left[\tilde{f}^{(0,1)}(y+x,x) + \right. \\ &+\left.\left(g(x,y+x)\left(1 - \frac{x}{2(y+x)}\right) + \frac{1}{2}\right)\,\tilde{f}^{(1,0)}(y+x,x)\right] \;+\; \mathcal{O}(\epsilon^2)\,.\end{aligned} \tag{A.36}$$

Define the coefficients $O_{n,j}$ as

$$\Omega_n(\tau(x+\epsilon), x) \;\equiv\; O_{n,0} \;+\; \epsilon\,O_{n,1} \;+\; \epsilon^2\,O_{n,2} \;+\; \ldots\,. \tag{A.37}$$

It follows from the above calculation that the first two are given by

$$\begin{aligned} O_{n,0} &= \tilde{\Omega}_n(y+x,x)\,; \\ O_{n,1} &= \left(g(x,y+x)\left(1-\frac{x}{2(y+x)}\right)+\frac{1}{2}\right)\tilde{\Omega}_n^{(1,0)}(y+x,x) \;+\; \tilde{\Omega}_n^{(0,1)}(y+x,x)\,. \end{aligned} \tag{A.38}$$

Now expand the original series

$$\begin{aligned} \sum_{n=0}^{+\infty}\epsilon^n\,\Omega_n(\tau(x+\epsilon),x+\epsilon) &= \Omega_0(\tau(x+\epsilon),x+\epsilon) \\ &\quad +\;\Omega_1(\tau(x+\epsilon),x+\epsilon)\;+\mathcal{O}(\epsilon^2) \\ &= O_{0,0}+\epsilon\;(O_{0,1}\;+\;O_{1,0})\;+\;\mathcal{O}(\epsilon^2)\,. \end{aligned} \tag{A.39}$$

Dropping the tilde in the notation, the zeroth-order equation is

$$\Omega_0(y+x,x) \;=\; (3+x)\,\Omega_0(y,x)\;(1-\Omega_0(y,x))\;. \tag{A.40}$$

Notice that the equation for f_0 is just the static logistic equation. Hence the results for f_0 can be used. The equation for f_1 is

$$\Omega_1(y+x) \;=\; C(y,x)\,\Omega_1(y,x)\;+\;D(y+x,x)\,; \tag{A.41}$$

$$\begin{aligned} C(y,x) &= (3+x)\big(1-2\Omega_0(y,x)\big)\,; \\ D(y+x,x) &= -\left[g(x,y+x)\left(1-\frac{x}{2(y+x)}\right)+\frac{1}{2}\right]\Omega_0^{(1,0)}(y+x,x) \\ &\quad -\;\Omega_0^{(0,1)}(y+x,x)\,. \end{aligned} \tag{A.42}$$

A.3.2 Equations for $R_{n,0}$, $R_{n,1}$, $R_{n,2}$

One first calculates

$$\begin{aligned} &\exp\left[-\left(\frac{A(x+\varepsilon)-A(x)}{\varepsilon}\right)\right] = \\ &= \exp\left\{\frac{+1}{\varepsilon}\left[\mathrm{i}\pi\varepsilon+(1+x)\log\left(1+\frac{\varepsilon}{1+x}\right)+\varepsilon\log(1+x+\varepsilon)-\varepsilon\right]\right\} \\ &= (-1)(1+x+\varepsilon)\exp\left[\frac{1+x}{\varepsilon}\log\left(1+\frac{\varepsilon}{1+x}\right)-1\right] \\ &= (-1)(1+x)\underbrace{\mathrm{e}^{-1}\Big(1+\delta(x,\varepsilon)\Big)^{1+1/\delta(x,\varepsilon)}}_{\equiv\,\eta(x,\varepsilon)}\,; \quad \delta(x,\varepsilon)\;\equiv\;\frac{\varepsilon}{1+x}\,. \end{aligned} \tag{A.43}$$

Note that for fixed x and $\varepsilon \to 0$, one has $\delta \to 0$ and $\eta \to 1$. Also note that $\eta(x,\varepsilon)$ is analytic for $x, \varepsilon \geq 0$. Then one obtains

$$\begin{aligned}&(-1)^n(1+x)^n\eta(x,\varepsilon)^n\Phi_n(x+\varepsilon,\varepsilon)\\ &= (3+x)\left[\Phi_n(x,\varepsilon)\,(1-2\Phi_0(x,\varepsilon)) - \sum_{\ell=1}^{n-1}\Phi_\ell(x,\varepsilon)\Phi_{n-\ell}(x,\varepsilon)\right]; \quad n \geq 1;\end{aligned} \tag{A.44}$$

$$\begin{aligned}\eta(x,\varepsilon) &= \mathrm{e}^{-1}\left(1+\frac{\varepsilon}{1+x}\right)^{1+\frac{1+x}{\varepsilon}}\\ &= \exp\left[\left(1+\frac{1+x}{\varepsilon}\right)\log\left(1+\frac{\varepsilon}{1+x}\right)-1\right]\\ &= \exp\left[\left(1+\frac{1}{\delta(x,\varepsilon)}\right)\log\left(1+\delta(x,\varepsilon)\right)-1\right].\end{aligned} \tag{A.45}$$

Now the coefficients $R_{n,k}$ in the expansions of the Φ_n will be calculated. To do this, all the terms of the same order in ε are matched after expanding all the terms Eq. (A.44) in ε. Doing this order by order leads to a (countably infinite) family of differential equations $\mathrm{EQ}(n,k)$ for the coefficients $R_{n,k}$, where n stands for the sector Φ_n and k for the order of ε^k which is being matched. To derive the equations up to order ε^2 the following expansion is needed:

$$\eta(x,\varepsilon)^n = 1 + \frac{n}{2(1+x)}\varepsilon - \frac{n(3n-4)}{24(1+x)^2}\varepsilon^2 + \mathcal{O}(\varepsilon^3). \tag{A.46}$$

For $n \geq 2$ and order ε^0 one has

$$\left[(-1)^n(1+x)^n + (1+x)\right]R_{n,0}(x) = -(3+x)\sum_{k=1}^{n-1}R_{k,0}(x)R_{n-k,0}(x); \quad n \geq 0. \tag{A.47}$$

For $n \geq 2$ and order ε^1 one obtains

$$\begin{aligned}&\left[(-1)^n(1+x)^n + (1+x)\right]R_{n,1} =\\ &(-1)^{n+1}(1+x)^n\partial_x R_{n,0} + \left[\frac{2}{(2+x)(3+x)} + \frac{n}{2}(-1)^{n+1}(1+x)^{n-1}\right]R_{n,0}\\ &- 2(3+x)\sum_{k=1}^{n-1}R_{k,0}R_{n-k,0}.\end{aligned} \tag{A.48}$$

And at order ε^2 the equation is

$$\begin{aligned}(-1)(1+x)^n\Bigg[&\frac{n(3n-4)}{24(1+x)^2}R_{n,0} + \frac{n}{2(1+x)}\left(R_{n,1} + \partial_x R_{n,0}\right)\\ &+\left(R_{n,2} + \partial_x R_{n,1} + \frac{1}{2}\partial_x^2 R_{n,0}\right)\Bigg]\\ = (3+x)\Bigg[&-2R_{n,0}R_{0,2} - 2R_{n,1}R_{0,1} + R_{n,2}\left(1-2R_{0,0}\right)\\ &-\sum_{k=1}^{n-1}\left(2R_{k,0}R_{n-k,2} + R_{k,1}R_{n-k,1}\right)\Bigg].\end{aligned} \tag{A.49}$$

Note that for $n = 1$ the leading order equation corresponding to ε^0 is trivially satisfied, which means that $R_{1,0}(x)$ is unconstrained by Eq. (A.47). The equation $\mathrm{EQ}(1,1)$ is

$$\begin{aligned}(1+x)\partial_x R_{1,0} &= \frac{1}{2}\left(-1+4(3+x)R_{0,1}\right)R_{1,0}\\ &= -\left(\frac{1}{2}+\frac{2}{x+2}+\frac{2}{x+3}\right)R_{1,0}\,;\end{aligned} \tag{A.50}$$

$$\mathrm{d}\log R_{1,0} = \left[-\frac{3}{2}\frac{1}{1+x} + \frac{2}{2+x} - \frac{1}{3+x}\right]\mathrm{d}x\,, \tag{A.51}$$

where Eq. (2.115) was used to find

$$R_{0,1} = -\frac{1}{(x+2)(x+3)^2}\,. \tag{A.52}$$

If the integration constant is fixed by requiring $R_{1,0}(x=0) = 1$, one arrives at the expression

$$R_{1,0} = \frac{3}{4}\frac{(2+x)^2}{(3+x)(1+x)^{3/2}}\,. \tag{A.53}$$

A.4 Algorithm for the approximate computation of the $Y_k = R_{1,k}$ using Taylor expansions

One could in principle determine all the $Y_k(x)$ exactly. However, this is computationally expensive and hence a different method is needed. Instead of trying to obtain an exact solution, an approximation scheme is used in which all the expressions in Eq. (2.139) are Taylor-expanded

$$F(x) = \sum_{s=0}^{+\infty} F_s x^s\,;\quad G_k(x) = \sum_{s=0}^{+\infty} G_{k,s}x^s\,;\quad Y_k(x) = \sum_{s=0}^{+\infty} Y_{k,s}x^s\,. \tag{A.54}$$

By substituting these expressions into Eq. (2.139) one obtains

$$\sum_{s=0}^{+\infty} \left[(s+1) Y_{k,s+1} + \sum_{\ell=0}^{s} \left(Y_{k,\ell} F_{s-\ell} \right) - G_{k,s} \right] x^s = 0 . \tag{A.55}$$

W.l.o.g. one can set $Y_{k,0} = 0$. Since the x^s are linearly independent, this results in

$$(s+1) Y_{k,s+1} + \sum_{l=1}^{s} \left(Y_{k,l} F_{s-l} \right) - G_{k,s} = 0 , \quad s \geq 0 . \tag{A.56}$$

Now an algorithm can be specified to calculate the $Y_k(x)$ for $k \leq \bar{k}$ to order n in x. Define $n + \bar{k} = \tilde{n}$.

(i) Compute the functions $R_{0,j}(x)$ to order $\tilde{n} + 2 - j$ in x for $j \leq \bar{k} + 1$.

(ii) Compute the functions $F(x)$ and $\left\{ \eta_k(x) \,|\, k \leq \bar{k} + 1 \right\}$ as well as $Y_0(x)$ (initial step) to order $\tilde{n}$ in x.d

(iii) Given $Y_j(x)$ to order $\tilde{n} - j$ in x for all $j \leq k - 1$, compute $G_k(x)$ to order $\tilde{n} - (k+1)$ in x using Eq. (2.137).

(iv) Compute Taylor coefficients $Y_{k,s}$ for $s \leq \tilde{n} - k$ using the recursion equation Eq. (A.56).

(v) Repeat the last two steps until reaching $Y_{\bar{k}}$, which will be given at order $n = \tilde{n} - \bar{k}$ in x

The choice of $\tilde{n}$ in the algorithm must yet be justified. The difficulty is to calculate the right number of Taylor coefficients in each step. Note that each derivative 'kills off' one order of precision. That is, if $f(x)$ is given as a Taylor expansion to order n, then f'(x) is an expansion to order $n - 1$ and so on. To see what this means for the calculation, the functions $R_{0,j}(x)$ need to be computed, since they appear in the formula for $G_k(x)$. Assume $R_{0,0}$ is computed to order n_0, then it follows from the recursion relation Eq. (2.93) that $R_{0,j}$ can be computed to order $n_0 - j$. For general k, the following expressions are

part of the formula for $G_k(x)$:

$$\begin{aligned}
&\partial_x^k Y_0,\ \partial_x^{k-1} Y_1,\ \dots\ \partial_x Y_{k-1}\\
&Y_0,\ \partial_x Y_0,\ \dots\ \partial_x^{k-1} Y_0\\
&Y_1,\ \partial_x Y_1\ \dots\ \partial_x^{k-2} Y_1\\
&\dots\\
&Y_{k-2},\ \partial_x Y_{k-2}\\
&Y_{k-1}\\
&Y_{k-1} R_{0,2},\ Y_{k-2} R_{0,3},\ \dots\ Y_0 R_{0,k+1}\,.
\end{aligned} \tag{A.57}$$

The notation $F \to \mathrm{ord}(m)$ is introduced to denote that the expansion of F is precise up to order n in x. In the case of $G_1(x)$, the orders to which these expressions are precise are (remember that $\tilde{n}$ is the order to which Y_0 is given as a Taylor series):

$$\begin{aligned}
\partial_x^2 Y_0 &\to \mathrm{ord}(\tilde{n}-2)\,;\\
\partial_x Y_0 &\to \mathrm{ord}(\tilde{n}-1)\,;\\
Y_0 R_{0,2} &\to \mathrm{ord}\left(\min\left\{\tilde{n}, n_0-2\right\}\right)\,.
\end{aligned} \tag{A.58}$$

The coefficient $R_{0,2}$ is given to $\mathrm{ord}(n_0-2)$ and will limit the precision of the result. W.l.o.g. it can therefore be assumed that $\tilde{n} \leq n_0 - 2$. On the other hand, if $\tilde{n} < n_0 - 2$, the $R_{0,j}$ would have been calculate to a higher precision than is useful. Therefore $\tilde{n} = n_0 - 2$ is chosen. So then one has $\min\{\tilde{n}, n_0-2\} = \tilde{n}$ and $G_1 \to \mathrm{ord}(\tilde{n}-2)$. In Eq. (A.56) s varies between 0 and $\tilde{n}-2$ and one finds $Y_1 \to \mathrm{ord}(\tilde{n}-1)$ (note that the

coeffcient $Y_{k,0} = 0$). For $G_2(x)$ the following contributions are present:

$$\begin{aligned}
\partial_x^2 Y_0 &\to \mathrm{ord}(\tilde{n}-2)\,;\\
\partial_x Y_1 &\to \mathrm{ord}(\tilde{n}-2)\,;\\
\partial_x^3 Y_0 &\to \mathrm{ord}(\tilde{n}-3)\,;\\
\partial_x^2 Y_1 &\to \mathrm{ord}(\tilde{n}-3)\,;\\
Y_0 &\to \mathrm{ord}(\tilde{n})\,;\\
Y_1 &\to \mathrm{ord}(\tilde{n}-1)\,;\\
\partial_x Y_0 &\to \mathrm{ord}(\tilde{n}-1)\,;\\
Y_1 R_{0,2} &\to \mathrm{ord}(\min\{\tilde{n}-1, n_0-2\})\\
&\quad = \mathrm{ord}(\tilde{n}-1)\,;\\
Y_0 R_{0,3} &\to \mathrm{ord}(\min\{\tilde{n}, n_0-3\})\\
&\quad = \mathrm{ord}(\tilde{n}-1) \text{ or } \mathrm{ord}(\tilde{n})\,.
\end{aligned} \tag{A.59}$$

As a result $G_2(x) \to \mathrm{ord}(\tilde{n}-3)$ and $Y_2 \to \mathrm{ord}(\tilde{n}-2)$. For G_3, the precision-limiting contribution comes from the terms

$$\partial_x^4 Y_0,\, \partial_x^3 Y_1,\, \partial_x^2 Y_2 \quad \to \quad \mathrm{ord}(\tilde{n}-4)\,. \tag{A.60}$$

Hence $G_3 \to \mathrm{ord}(\tilde{n}-4)$ and $Y_3 \to \mathrm{ord}(\tilde{n}-3)$. The general pattern is:

$$\begin{aligned}
G_k &\to \mathrm{ord}(\tilde{n}-k-1)\,;\\
Y_k &\to \mathrm{ord}(\tilde{n}-k)\,.
\end{aligned} \tag{A.61}$$

To calculate all the Y_k for $k \le \bar{k}$ to order n, one must choose

$$\tilde{n} \;=\; n + \bar{k}\,. \tag{A.62}$$

This explains the choice of expansion orders in this algorithm.

Appendix B

Late to early time behaviour of an expanding plasma in MIS theory

B.1 The Stokes constant S_1 and median summation

An approximation for S_1 relying on hyperasymptotics is given by [132]:

$$\begin{aligned} S_1 \approx & 2\pi \mathrm{i}\, \Phi_{N_0}^{(0)} \left(\sum_{m=0}^{\lfloor N_0/2 \rfloor - 1} \frac{\Phi_m^{(1)} \Gamma(N_0 + \beta - m)}{A^{N_0+\beta-m}} \right)^{-1} \\ \approx & 0.00547029852521058876501313500533268164639903851030642446773261 62\mathrm{i}. \end{aligned} \tag{B.1}$$

S_1 was computed with (B.1) with an accuracy of $\mathcal{O}\left(10^{-65}\right)$ using $N_0 = 200$. Eq. (B.1) requires knowledge of the coefficients of both the perturbative and the first non-perturbative sector. Note that it is possible to compute S_1 without knowing the coefficients of the first non-perturbative sector using the so-called large-order relations

$$\Phi_n^{(0)} \sim \frac{\Gamma(n+\beta)}{A^{n+\beta}} S_1 \left(\Phi_0^{(1)} + \mathcal{O}\left(n^{-1}\right) \right), \text{as} \quad n \to \infty \tag{B.2}$$

The leading order behaviour in (B.2) provides a sequence which converges to S_1 as $\mathcal{O}\left(n^{-1}\right)$ and involves only the free coefficient $\Phi_0^{(1)}$ from the first non-perturbative sector, which *defines* the Stokes constant. The value in Eq. (B.1) corresponds to the choice

$\Phi_0^{(1)} = 3/2$, which was chosen in such a way that the value of the Stokes constant is the same as in [30, 31, 69].

There is a connection between the value of the Stokes constant and the value of the parameter σ across the real axis. The positive real axis is a Stokes line, meaning that the Borel transform $\mathcal{B}[\Phi](\xi)$ has branch-cut singularities at the locations $\xi = A, 2A, 3A, \ldots$. Therefore the definition (3.37) is ambiguous in the choice of angle θ.

When the integration path is moved across the Stokes line from below and thus the angle θ in (3.37) is increased from $\theta_- = -\varepsilon$ to $\theta_+ = +\varepsilon$, this results in a discontinuity in the value of the Borel resummation (3.37). Crossing the Stokes line in (3.37) while keeping the value of the transseries parameter σ from (3.25) constant corresponds to moving from one Riemann sheet to the other. Alternatively, the value of the transseries parameter can be changed according to $\sigma \to \sigma - S_1$ to avoid a discontinuity. The result of the resummation for the whole transseries (3.25) has to be real-valued on the positive real axis, which is known as Median-resummation. The reality constraint fixes the imaginary part of the transseries parameter σ. Median resummation requires[18]

$$\mathrm{i}\,\mathbb{I}\mathrm{m}(\sigma) = \pm\frac{S_1}{2}, \quad \text{for} \mp\theta > 0. \tag{B.3}$$

If a convention is chosen on the path along the integration in (3.37) is carried out (below/above the real axis in the Borel plane), the only degree of freedom that is left is the real part of the parameter σ, which is expected given that there is a one-parameter family of real solutions.

B.2 Recurrence relations for $\Phi^{(1)}$ and $\Phi^{(2)}$

The recurrence relations for the coefficients of the perturbative and first non-perturbative sectors can be derived by substituting the expression

$$f(w) = \Phi^{(0)}(w) + \sigma w^{\beta} \mathrm{e}^{-Aw} \Phi^{(1)}(w) \tag{B.4}$$

[18] For more details see *e.g.* the review [7]

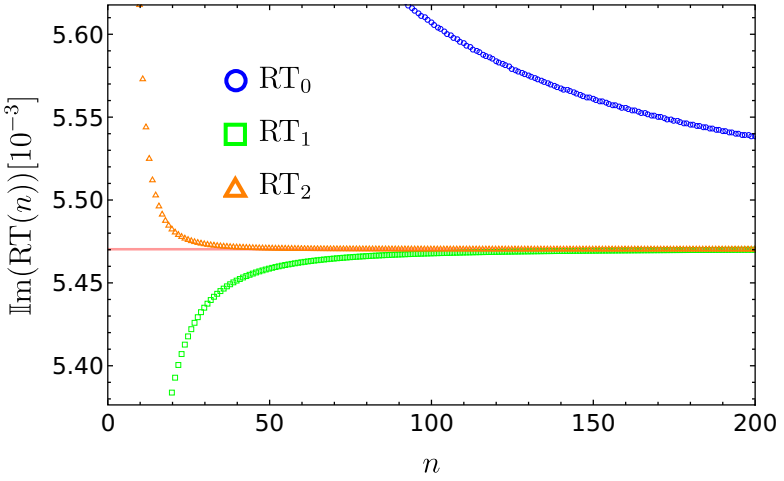

FIGURE B.1: The Richardson transforms RT_0, RT_1 and RT_2 of the imaginary part of the leading order sequence in the large order relations (B.2) (only the first term without the $\mathcal{O}\left(n^{-1}\right)$ corrections). The Richardson transforms are a method of speeding up the convergence of a series (see e.g. [7]), and the zeroth Richardson transform RT_0 is just the original sequence. One can see the convergence to the imaginary part of the Stokes constant S_1 from (B.1).

into the MIS ODE (3.19). At order $\mathcal{O}\left(\sigma^0\right)$ the same ODE is obtained, but for $\Phi^{(0)}$ instead of f. At order $\mathcal{O}\left(\sigma^1\right)$ one obtains the equation

$$\begin{aligned}\Phi^{(1)}(w)\left(-8+Aw+(8-Aw+\beta)\,\Phi^{(0)}(w)+w\partial_w\Phi^{(0)}(w)\right)+\\ +w\Phi^{(0)}(w)\partial_w\Phi^{(1)}(w)=0.\end{aligned} \tag{B.5}$$

With the series ansatz

$$\Phi^{(n)}(w)=\sum_{j=0}^{\infty}a_j^{(n)}w^{-j}, \tag{B.6}$$

the following recurrence relations for $\Phi^{(0)}$ and $\Phi^{(1)}$ are obtained:

$$\begin{aligned}a_0^{(0)}&=1;\quad a_1^{(0)}=\frac{\beta}{A};\\ a_j^{(0)}&=\frac{1}{A}\left[8a_{j-1}^{(0)}+\frac{j-9}{2}\sum_{\ell=0}^{j-1}a_\ell^{(0)}a_{j-1-\ell}^{(0)}\right],\quad \text{for } j\geq 2;\\ a_0^{(1)}&\equiv\frac{3}{2};\\ a_j^{(1)}&=\frac{1}{j}\left[(8+\beta-j)\sum_{\ell=0}^{j-1}a_\ell^{(1)}a_{j-\ell}^{(0)}-A\sum_{\ell=0}^{j-1}a_\ell^{(1)}a_{j+1-\ell}^{(0)}\right],\quad \text{for } j\geq 1.\end{aligned} \tag{B.7}$$

The coefficient $a_0^{(1)}$ is undetermined by (B.5), and any redefinition of $a_0^{(1)}$ can be absorbed into the transseries parameter σ.

B.3 Coefficient functions $F_r(W)$

The ODEs (3.45) can be rewritten as

$$\mathcal{L}F_r(W) = g_r(W); \qquad \mathcal{L} \equiv (1+W)W\frac{\mathrm{d}}{\mathrm{d}W} - 1, \tag{B.8}$$

where the homogeneous equation $\mathcal{L}F_r(W) = 0$ is the same for all F_r, and $g_r(W)$ is the inhomogeneity which does depend on the functions $\{F_s \,|\, s \leq r-1\}$ and their derivatives. It is easy to check that the function $\Theta(W) = W/(1+W)$ solves the homogeneous equation $\mathcal{L}\Theta = 0$. This motivates re-scaling the F_r to simplify the left-hand-side of (B.8):

$$F_r(W) = \frac{W}{1+W}Y_r(W); \qquad \mathcal{L}F_r(W) = W^2 Y_r'(W). \tag{B.9}$$

The advantage of working with $Y_r(W)$ is that an explicit formula can be given for the solutions

$$Y_r(W) = \int \mathrm{d}W\, W^{-2} g_r(W) + c_r. \tag{B.10}$$

The integrand of (B.10) is given by the recurrence relation

$$\begin{aligned} Y_r'(W) = W^{-2}g_r(W) =& \frac{(4-\beta)(1+W)}{AW^2}\delta_{1,r} - \frac{8}{AW}Y_{r-1}(W) \\ &+ \sum_{k=0}^{r-1}\Bigg[\frac{9-r}{2A(1+W)}Y_k(W)Y_{r-k-1}(W) \\ &+ \frac{1}{(1+W)^3}\,Y_k(W)\left(\frac{\beta}{A}Y_{r-k-1}(W) - (1-\delta_{k,0})Y_{r-k}(W)\right) \\ &+ \frac{W}{(1+W)^2}\,Y_k(W)\left(\frac{\beta}{A}Y_{r-k-1}'(W) - (1-\delta_{k,0})Y_{r-k}'(W)\right)\Bigg]. \end{aligned} \tag{B.11}$$

Adding an integration constant c_r in (B.10) corresponds to adding a multiple of the function $\Theta(W)$, $F_r(W) \to F_r(W) + c_r\Theta(W)$. In general, the rational decomposition of the integrand in (B.10) includes a term of order W^{-1}, which leads to logarithms in the $Y_r(W)$. There is a unique choice of the set $\{c_r \,|\, r \geq 0\}$ for which the $Y_r(W)$ are rational functions in W without any logarithmic terms. Once the Y_r have been computed, the functions F_r are easily obtained by multiplying the Y_r with the factor $W(1+W)^{-1}$. With this method one can compute as many of the functions F_r as desired. The first few

functions are given by:

$$
\begin{aligned}
F_0(W) &= 1+W;\\
F_1(W) &= \frac{2W^3+(\beta+4)W^2+\beta(\beta+7)W+\beta}{A(1+W)};\\
F_2(W) &= \frac{1}{2A^2\left(1+W\right)^3}\Big(4W^6+(7\beta+22)\,W^5+\left(8\beta^2+70\beta+32\right)W^4\\
&\qquad +\left(\beta^3+29\beta^2+145\beta+10\right)W^3+\left(2\beta^3+34\beta^2+110\beta-8\right)W^2\\
&\qquad +\Big(\beta^4+11\beta^3+34\beta^2+10\beta\Big)\,W+2\Big);\\
F_3(W) &= \frac{1}{6A^3\left(1+W\right)^5}\Big(6W^9+(26\beta+60)\,W^8+\left(45\beta^2+317\beta+210\right)W^7\\
&\qquad +\left(30\beta^3+438\beta^2+1212\beta+336\right)W^6\\
&\qquad +\Big(11\beta^4+252\beta^3+1677\beta^2+2050\beta+254\Big)\,W^5\\
&\qquad +\Big(44\beta^4+708\beta^3+3210\beta^2+1522\beta+92\Big)\,W^4\\
&\qquad +\Big(72\beta^4+903\beta^3+3054\beta^2+297\beta+42\Big)\,W^3\\
&\qquad +\Big(-2\beta^6-30\beta^5-82\beta^4+410\beta^3+1524\beta^2-220\beta+48\Big)\,W^2\\
&\qquad +\beta\Big(\beta^5+15\beta^4+86\beta^3+188\beta^2-36\beta+68\Big)\,W-18\beta^2+12\beta\Big).
\end{aligned}
\tag{B.12}
$$

Note that to keep the notation simple no distinction between $F_r(\tau)$ and $F_r(W(\frac{3}{2}\tau))$ is made. To obtain the original transasymptotic coefficient functions $F_r(\tau)$ from (3.42), the variable W in (B.12) must be replaced by $W(\frac{3}{2}\tau)$.

B.4 Coefficients of $\gamma(w)$

The the perturbative expansion of $\gamma(w)$ (see (3.48)) is given by

$$\gamma(w) = \sum_{n=0}^{\infty} \gamma_n w^{-n}. \tag{B.13}$$

This expansion solves (3.47). To simplify the notation, one defines

$$c \equiv f_{\rm ac}(w_0) - 1, \tag{B.14}$$

where $f_{\mathrm{ac}}(w_0)$ is the (numerical) analytical continuation of $f(w)$ from $w = 0$ to $w = w_0$, as explained in Section 3.4. The first four coefficients γ_n are then given by:

$$\begin{aligned}
\gamma_0 =& \frac{2}{3} c\, e^c; \\
\gamma_1 =& -\frac{2e^c}{3A}\left(\beta + 2c^3 + (\beta+4)c^2 + \beta(\beta+7)c\right); \\
\gamma_2 =& \frac{e^c}{3A^2}\Big(2\beta\left(\beta^2+7\beta-1\right) + 4c^5 + 4(\beta+7)c^4 + \left(5\beta^2+41\beta+38\right)c^3 \\
&+ 2\left(\beta^3+12\beta^2+34\beta+4\right)c^2 + \beta\left(\beta^3+15\beta^2+55\beta+10\right)c\Big); \\
\gamma_3 =& -\frac{e^c}{9A^3}\Big(3\beta\left(\beta^4+15\beta^3+51\beta^2-18\beta+4\right) + 8c^7 + 12(\beta+10)c^6 \\
&+ 6\left(3\beta^2+33\beta+83\right)c^5 + \left(13\beta^3+207\beta^2+872\beta+620\right)c^4 \\
&+ 3\left(3\beta^4+52\beta^3+261\beta^2+349\beta+78\right)c^3 \\
&+ 3\left(\beta^5+21\beta^4+142\beta^3+321\beta^2+74\beta+16\right)c^2 \\
&+ \beta\left(\beta^5+24\beta^4+188\beta^3+507\beta^2+198\beta+20\right)c\Big).
\end{aligned} \tag{B.15}$$

B.5 Lambert-W function

The Lambert-W function (see [133, §4.13]) is defined as the solution to the equation

$$W(z)\mathrm{e}^{W(z)} = z. \tag{B.16}$$

The function $W(z)$ has infinitely many branches, which are known as $W_k(z)$, where k is an integer. Only two of those branches, $W_{-1}(z)$ and $W_0(z)$, return real values on subsets of the real line. In the case of the MIS equation (3.19), the Lambert-W function appears in the context of the transasymptotic summation (3.42), where the leading-order contribution in w^{-1} is given by

$$F_0(\tau(w)) = 1 + W\left(\frac{3}{2}\sigma w^{\beta}\mathrm{e}^{-Aw}\right). \tag{B.17}$$

As $w \to +\infty$, one requires $f(w) \to 1$. This means that $W(\dots) \to 0$ in (B.17). For $k \neq 0$ the branches $W_k(z)$ diverge as $z \to 0$. Therefore, the branch W_0 has to be chosen at $w = +\infty$, which admits the Taylor expansion $W_0(z) = z + \dots$ around $z = 0$. This is consistent with the behaviour of $f(w)$ near $w = +\infty$. For large arguments, the branch

W_0 admits the following expansion [97]:

$$W_0(z) = L_1 - L_2 + \sum_{k=0}^{\infty}\sum_{m=1}^{\infty} C_{km} L_1^{-(k+m)} L_2^m, \tag{B.18}$$

where

$$\begin{aligned} L_1 &= \log w\,; \\ L_2 &= \log(\log w)\,; \\ C_{km} &= \frac{(-1)^{k+m+1}}{m!}\mathrm{Stir}(k+m, k+1)\,. \end{aligned} \tag{B.19}$$

The expression $\mathrm{Stir}(n, m)$ denotes Stirling circle numbers of the first kind. The presence of logarithmic terms in the expansion (B.18) explain how logarithmic terms arise in the transseries Ψ in (3.27) from the transseries $\mathcal{F}$ in (3.25) when going from $w = +\infty$ to $w = -\infty$. Note that the magnitude of the exponential scale $\tau \sim \mathrm{e}^{-Aw}$ changes from small to large when the sign of w is flipped from $(+)$ to $(-)$, which makes it necessary to use the expansion (B.18). Note that the Lambert-W function has a square root branch point at $z = -\mathrm{e}^{-1}$.

B.6 Taylor-series method

In the Taylor-series method (see [133, §3.7(ii)]), at a regular point $w = w_0$, the Taylor series $f(w) = \sum_{n=0}^{\infty} b_n (w - w_0)^n$ is combined with the differential equation (3.19) and one obtains the recurrence relation

$$\begin{aligned} w_0(n+1)b_0 b_{n+1} =& A\delta_{n,1} + (Aw_0 + \beta - 4)\delta_{n,0} - \tfrac{1}{2}w_0(n+1)\sum_{m=1}^{n} b_m b_{n+1-m} \\ & - \tfrac{1}{2}(n+8)\sum_{m=0}^{n} b_m b_{n-m} - Ab_{n-1} - (Aw_0 - 8)b_n, \qquad n \geq 0. \end{aligned} \tag{B.20}$$

With this method it is very easy to "walk" in the complex w-plane. Once $b_0 = f(w_0)$ is known (either from a local expansion at the origin, or a branch-point, or from the asymptotic expansion) one can compute many coefficients in the Taylor-series expansion, and use this Taylor series to make a small step in the complex w-plane, that is, compute $f(w_0 + h)$ and use this as the new b_0.

B.7 Recursion relation for the coefficients $Z_{r,m}$

The coefficients $Z_{r,m}$ are the coefficients of the Taylor expansion of the functions $Z_r(E)$ (see Eq. (3.78)). They can be calculated through the following recursion relation:

$$
\begin{aligned}
Z_{r,m} = \frac{1}{m - N(r)} \Bigg\{ & - \delta_{r,1}\, \phi_{1,m} \quad - g_{c(r),m} \sum_{p=0}^{m-c(r)} Z_{r-1,p}\, \phi_{2,m-c(r)-p} \\
& + \sum_{k=0}^{r-1} \Bigg[g_{\mu(r,k),m}\, \psi_{k,0} \sum_{\ell=0}^{m-\mu(r,k)} Z_{k,\ell}\, Z_{r-k-1,m-\mu(r,k)-\ell} \\
& + g_{\mu(r,k)+2,m} \psi_{k,2} \sum_{\ell=0}^{m-\mu(r,k)-2} Z_{k,\ell}\, Z_{r-k-1,m-\mu(r,k)-2-\ell} \\
& + g_{1+\nu(r,k),m} g_{1,k} \sum_{\ell=0}^{m-\nu(r,k)-1} Z_{k,\ell}\, Z_{r-k,m-\nu(r,k)-1-\ell} \\
& + g_{1+\mu(r,k),m} \frac{\beta}{A}\, \widetilde{\psi}_0 \\
& \times \left(\sum_{\ell=0}^{m-1-\mu(r,k)} Z_{k,\ell}\, Z_{r-k-1,m-1-\mu(r,k)-\ell} \Big(- N(r-k-1) + m - 1 - \mu(r,k) - \ell \Big) \right) \\
& + g_{2+\mu(r,k),m} \frac{\beta}{A}\, \widetilde{\psi}_1 \\
& \times \left(\sum_{\ell=0}^{m-2-\mu(r,k)} Z_{k,\ell}\, Z_{r-k-1,m-2-\mu(r,k)-\ell} \Big(- N(r-k-1) + m - 2 - \mu(r,k) - \ell \Big) \right) \\
& - g_{\nu(r,k),m} g_{1,k} \widetilde{\psi}_0 \sum_{\ell=0}^{m-\nu(r,k)} Z_{k,\ell}\, Z_{r-k,m-\nu(r,k)-\ell} \Big(- N(r-k) + m - \nu(r,k) - \ell \Big) \\
& - g_{\nu(r,k)+1,m} g_{1,k} \widetilde{\psi}_1 \\
& \times \left(\sum_{\ell=0}^{m-\nu(r,k)-1} Z_{k,\ell}\, Z_{r-k,m-\nu(r,k)-1-\ell} \Big(- N(r-k) + m - \nu(r,k) - 1 - \ell \Big) \right) \\
& \Bigg] \Bigg\}.
\end{aligned}
\tag{B.21}
$$

In the above expression the following notations have been used (any additional indices on the symbols denote the coefficients in the E-expansion):

$$
\begin{aligned}
N(k) &\equiv \begin{cases} (k+1) & \text{for } k \leq 4 \\ k & \text{for } k \geq 5 \end{cases} ; \\
\phi_1(E) &\equiv \frac{E^2(4-\beta)}{A(1-E)^2} ; \\
\phi_2(E) &\equiv \frac{-8E}{A(1-E)} ; \\
\psi_k(E) &\equiv A^{-1}\left((k-4) - \beta E^2\right) ; \\
\widetilde{\psi}(E) &\equiv (1-E) ; \\
\Theta(n) &\equiv \begin{cases} 0 & \text{for } n \leq 0 ; \\ 1 & \text{for } n > 0 ; \end{cases} \\
c(r) &\equiv -\Theta(r-4) + \Theta(r-5) + 1 ; \\
\mu(r,k) &\equiv -\Theta(r-4) + \Theta(k-4) + \Theta(r-k-5) ; \\
\nu(r,k) &\equiv -\Theta(r-4) + \Theta(k-4) + \Theta(r-k-4) .
\end{aligned}
\tag{B.22}
$$

References

[1] D. Manchon, S. Marmi, D. Sauzin and I. Aniceto, *Resurgence, Physics and Numbers*. Edizioni della Normale Pisa, 2017, 10.1007/978-88-7642-613-1.

[2] I. Aniceto, D. Hasenbichler, C. J. Howls and C. J. Lustri, *Capturing the cascade: a transseries approach to delayed bifurcations*, *Nonlinearity* **34** (2021) 8248 [2012.09779].

[3] C. L. Hall and C. J. Lustri, *Multiple scales and matched asymptotic expansions for the discrete logistic equation*, *Nonlinear Dynamics* **85** (2016) 1345 [1601.03137].

[4] I. Aniceto, D. Hasenbichler and A. O. Daalhuis, *The late to early time behaviour of an expanding plasma: hydrodynamisation from exponential asymptotics*, *J. Phys. A* **56** (2023) 195201 [2207.02868].

[5] O. J. C. Dias, H. S. Reall and J. E. Santos, *Strong cosmic censorship: taking the rough with the smooth*, *JHEP* **10** (2018) 001 [1808.02895].

[6] O. J. Dias, H. S. Reall and J. E. Santos, *Strong cosmic censorship for charged de Sitter black holes with a charged scalar field*, *Classical and Quantum Gravity* **36** (2019) 045005 [1808.04832].

[7] I. Aniceto, G. Başar and R. Schiappa, *A primer on resurgent transseries and their asymptotics*, *Physics Reports* **809** (2019) 1 [1802.10441].

[8] M. V. Berry and C. J. Howls, *Hyperasymptotics*, *Proceedings: Mathematical and Physical Sciences* **430** (1990) 653.

[9] O. Costin, *Correlation between pole location and asymptotic behavior for Painlevé I solutions*, *Communications on Pure and Applied Mathematics: A Journal Issued by the Courant Institute of Mathematical Sciences* **52** (1999) 461 [math/9709223].

[10] A. B. Olde Daalhuis, *Hyperasymptotic solutions of higher order linear differential equations with a singularity of rank one*, *R. Soc. Lond. Proc. Ser. A Math. Phys. Eng. Sci.* **454** (1998) 1.

[11] E. Delabaere, *Introduction to the Ecalle theory*. Cambridge University Press, 2011, 10.1017/cbo9780511565816.004.

[12] J. Écalle, *Les fonctions résurgentes:(en trois parties)*, vol. 1-3. Université de Paris-Sud, Département de Mathématique, Bât. 425, 1981.

[13] D. Tong, *TASI lectures on solitons*, *arXiv* (2005) 1 [hep-th/0509216].

[14] M. Marino, *Instantons and large N: an introduction to non-perturbative methods in quantum field theory*. Cambridge University Press, 2015, 10.1017/CBO9781107705968.

[15] B. R. Holstein, *Understanding alpha decay*, *American Journal of Physics* **64** (1996) 1061.

[16] G. H. Winslow, *Alpha-Decay Theory and a Surface Well Potential*, *Physical Review* **96** (1954) 1032.

[17] R. J. McMahon, *Chemical Reactions Involving Quantum Tunneling*, *Science* **299** (2003) 833.

[18] G. Edgar, *Transseries for beginners*, *Real Analysis Exchange* **35** (2010) 253 [0801.4877].

[19] S. Coleman, *Aspects of symmetry: selected Erice lectures*. Cambridge University Press, 1988.

[20] M. D. Schwartz, *Quantum Field Theory and Standard Model*. Cambridge University Press, 2013, 10.1017/9781139540940.

[21] C. M. Bender and S. A. Orszag, *Advanced Mathematical Methods for Scientists and Engineers I*. Springer Science & Business Media, 1999, 10.1007/978-1-4757-3069-2.

[22] D. Sauzin, *Introduction to 1-summability and resurgence*, *arXiv* (2014) [1405.0356].

[23] D. Dorigoni, *An introduction to resurgence, trans-series and alien calculus*, *Annals of Physics* **409** (2019) [1411.3585].

[24] E. Delabaere, H. Dillinger and F. Pham, *Exact semiclassical expansions for one-dimensional quantum oscillators*, *Journal of Mathematical Physics* **38** (1997) 6126.

[25] J. M. Lee and J. M. Lee, *Introduction to Smooth manifolds*. Springer, 2012, 10.1007/978-1-4419-9982-5.

[26] A. A. Agrachev and R. V. Gamkrelidze, *The exponential representation of flows and the chronological calculus*, *Matematicheskii Sbornik* **149** (1978) 467.

[27] M. Nakahara, *Geometry, topology and physics*. CRC press, 2003.

[28] C. Howls and S. Trasler, *Weyl's wedges*, *Journal of Physics A: Mathematical and General* **31** (1998) 1911.

[29] I. Aniceto, J. Jankowski, B. Meiring and M. Spaliński, *The large proper-time expansion of Yang-Mills plasma as a resurgent transseries*, *JHEP* **02** (2019) 073 [1810.07130].

[30] I. Aniceto and M. Spaliński, *Resurgence in extended hydrodynamics*, *Physical Review D* **93** (2016) 085008 [1511.06358].

[31] G. Başar and G. V. Dunne, *Hydrodynamics, resurgence, and transasymptotics*, *Physical Review D* **92** (2015) 125011 [1509.05046].

[32] M. Marziani, *Convergence of a class of borel-padé-type approximants*, *Nuovo Cim., B* **99** (1987) 145.

[33] M. V. Berry and C. J. Howls, *Hyperasymptotics for integrals with saddles*, *Proceedings of the Royal Society of London. Series A: Mathematical and Physical Sciences* **434** (1991) 657.

[34] Dingle, Robert B., *Asymptotic Expansions: Their Derivation and Interpretation*. Academinc Press, 1973.

[35] A. B. Olde Daalhuis, *Hyperasymptotics for nonlinear ODEs II. The first Painlevé equation and a second-order Riccati equation*, *Proc. Roy. Soc. Lond.* A **461** (2005) 3005.

[36] A. B. Olde Daalhuis and F. W. J. Olver, *On the asymptotic and numerical solution of linear ordinary differential equations*, *SIAM Rev.* **40** (1998) 463.

[37] M. Wechselberger, *À propos de canards (Apropos canards)*, *Trans. Amer. Math. Soc.* **364** (2012) 3289.

[38] É. Benoit, A. Fruchard, R. Schäfke and G. Wallet, *Solutions surstables des équations différentielles complexes lentes-rapides à point tournant*, in *Annales de la Faculté des sciences de Toulouse: Mathématiques*, vol. 7, pp. 627–658, 1998.

[39] A. Fruchard and R. Schäfke, *Bifurcation delay and difference equations*, *Nonlinearity* **16** (2003) 2199.

[40] W. Eckhaus, *Relaxation oscillations including a standard chase on french ducks*, in *Asymptotic Analysis II, Springer Lecture Notes Math. 985*, pp. 449–497, Springer, (1983).

[41] R. Goh, T. J. Kaper and T. Vo, *Delayed Hopf Bifurcation and Space–Time Buffer Curves in the Complex Ginzburg–Landau Equation*, *IMA Journal of Applied Mathematics* **87** (2022) 131 [2012.10048].

[42] P. P. d'Escurac, *The Borel transform of canard values and its singularities*, in *Formal and Analytic Solutions of Diff.(differential, partial differential, difference, q-difference, q-difference-differential,...) Equations*, pp. 149–175, Springer, 2017.

[43] A. B. Olde Daalhuis, *Inverse factorial-series solutions of difference equations*, *Proceedings of the Edinburgh Mathematical Society* **47** (2004) 421.

[44] C. Baesens, *Slow sweep through a period-doubling cascade: Delayed bifurcations and renormalisation*, *Physica D: Nonlinear Phenomena* **53** (1991) 319.

[45] H. G. Davies and K. Rangavajhula, *Dynamic period–doubling bifurcations of a unimodal map*, *Proc. Roy. Soc. Lond.* A **453** (1997) 2043.

[46] C. Baesens, *Noise effect on dynamic bifurcations: The case of a period-doubling cascade*, in *Dynamic Bifurcations*, pp. 107–130, Springer, (1991), DOI.

[47] H. G. Davies and K. Rangavajhula, *A period–doubling bifurcation with slow parametric variation and additive noise*, *Proc. Roy. Soc. Lond.* A **457** (2001) 2965.

[48] H. G. Davies and K. Rangavajhula, *Noisy parametric sweep through a period-doubling bifurcation of the Hénon map*, *Chaos, Solitons & Fractals* **14** (2002) 293.

[49] A. El-rabih, *Canards solutions of difference equations with small step size*, *Journal of Difference Equations and Applications* **9** (2003) 911.

[50] A. Fruchard, *Existence of bifurcation delay: the discrete case*, in *Dynamic Bifurcations*, pp. 87–106, Springer, (1991), DOI.

[51] A. Fruchard, *Sur l'équation aux différences affine du premier ordre unidimensionnelle*, in *Annales de l'institut Fourier*, vol. 46, pp. 139–181, 1996, DOI.

[52] A. Fruchard and R. Schäfke, *A survey of some results on overstability and bifurcation delay*, *Discrete & Continuous Dynamical Systems-S* **2** (2009) 931.

[53] N. Joshi and C. J. Lustri, *Stokes phenomena in discrete Painlevé I*, *Proc. Roy. Soc. Lond. A* **471** (2015) 20140874 [1503.01302].

[54] N. Joshi, C. J. Lustri and S. Luu, *Stokes phenomena in discrete Painlevé II*, *Proc. Roy. Soc. Lond. A* **473** (2017) 20160539 [1607.04494].

[55] N. Joshi, C. J. Lustri and S. Luu, *Nonlinear q-Stokes phenomena for q-Painlevé I*, *J. Phys. A* **52** (2019) 065204 [1807.00450].

[56] J. R. King and S. J. Chapman, *Asymptotics beyond all orders and Stokes lines in nonlinear differential-difference equations*, *Eur. J. Appl. Math.* **12** (2001) 433.

[57] N. Joshi and C. J. Lustri, *Generalized solitary waves in a finite-difference Korteweg-de Vries equation*, *Stud. Appl. Math.* **142** (2019) 359 [1808.09654].

[58] G. L. Alfimov, A. S. Korobeinikov, C. J. Lustri and D. E. Pelinovsky, *Standing lattice solitons in the discrete NLS equation with saturation*, *Nonlinearity* **32** (2019) 3445 [1809.10828].

[59] C. J. Howls, *Exponential asymptotics and boundary-value problems: keeping both sides happy at all orders*, *Proc. Roy. Soc. Lond. A* **466** (2010) 2771 [1005.4421].

[60] H. Pastijin, *Chaotic Growth with the Logistic Model of P.-F.Verhulst*, in *The Logistic Map and the route to chaos*, M. Ausloos and M. Dirickx, eds., (2006), DOI.

[61] M. V. Berry, *Uniform asymptotic smoothing of stokes's discontinuities*, *Proc. Roy. Soc. Lond. A* **422** (1986) 7–21.

[62] J. T. Stone, R. H. Self and C. J. Howls, *Aeroacoustic catastrophes: upstream cusp beaming in lilley's equation*, *Proc. Roy. Soc. Lond. A* **473** (2017) 0880.

[63] J. T. Stone, R. H. Self and C. J. Howls, *Cones of silence, complex rays and catastrophes: high-frequency flow–acoustic interaction effects*, *Journal of Fluid Mechanics* **853** (2018) 37–71.

[64] C. Shen and L. Yan, *Recent development of hydrodynamic modeling in heavy-ion collisions*, *Nucl. Sci. Tech.* **31** (2020) 122 [2010.12377].

[65] C. Gale, S. Jeon and B. Schenke, *Hydrodynamic modeling of heavy-ion collisions*, *International Journal of Modern Physics A* **28** (2013) 1340011 [1301.5893].

[66] P. Romatschke, *New developments in relativistic viscous hydrodynamics*, *Int. J. Mod. Phys. E* **19** (2010) 1 [0902.3663].

[67] U. Heinz and R. Snellings, *Collective flow and viscosity in relativistic heavy-ion collisions*, *Ann. Rev. Nucl. Part. Sci.* **63** (2013) 123 [1301.2826].

[68] J. D. Bjorken, *Highly relativistic nucleus-nucleus collisions: The central rapidity region*, *Physical review D* **27** (1983) 140.

[69] M. P. Heller and M. Spaliński, *Hydrodynamics beyond the gradient expansion: resurgence and resummation*, *Physical review letters* **115** (2015) 072501 [1503.07514].

[70] W. Florkowski, M. P. Heller and M. Spalinski, *New theories of relativistic hydrodynamics in the LHC era*, *Rept. Prog. Phys.* **81** (2018) 046001 [1707.02282].

[71] C. M. Bender and S. A. Orszag, *Advanced mathematical methods for scientists and engineers I: Asymptotic methods and perturbation theory*, vol. 1. New York: Springer Science & Business Media, 1999.

[72] O. Costin, *On the formation of singularities of solutions of nonlinear differential systems in antistokes directions*, *Inventiones mathematicae* **145** (2001) 425 [math/0202234].

[73] E. Caliceti, M. Meyer-Hermann, P. Ribeca, A. Surzhykov and U. D. Jentschura, *From useful algorithms for slowly convergent series to physical predictions based on divergent perturbative expansions*, *Physics reports* **446** (2007) 1 [0707.1596].

[74] M. Berry and C. Howls, *Hyperasymptotics*, *Proceedings of the Royal Society of London. Series A: Mathematical and Physical Sciences* **430** (1990) 653.

[75] A. B. Olde Daalhuis and F. W. J. Olver, *Hyperasymptotic solutions of second-order linear differential equations. I*, *Methods Appl. Anal.* **2** (1995) 173.

[76] O. Costin, R. Costin and M. Huang, *Tronquée solutions of the Painlevé equation PI*, *Constructive Approximation* **41** (2015) 467 [1310.5330].

[77] I. Aniceto, R. Schiappa and M. Vonk, *In preparation*, .

[78] J. Bhattacharya, S. Bhattacharyya, S. Minwalla and A. Yarom, *A theory of first order dissipative superfluid dynamics*, *Journal of High Energy Physics* **2014** (2014) 1 [1105.3733].

[79] I. Müller, *Zum Paradoxon der Wärmeleitungstheorie*, *Zeitschrift für Physik* **198** (1967) 329.

[80] W. Israel and J. M. Stewart, *Transient relativistic thermodynamics and kinetic theory*, *Annals of Physics* **118** (1979) 341.

[81] T. Ruggeri, I. S. Liu and T. Müller, *Relativistic thermodynamics of gases*, *Ann. of Phys* **169** (1986) 191.

[82] R. Geroch and L. Lindblom, *Causal theories of dissipative relativistic fluids*, *Annals of Physics* **207** (1991) 394.

[83] M. P. Heller, R. A. Janik and P. Witaszczyk, *The characteristics of thermalization of boost-invariant plasma from holography*, *Phys. Rev. Lett.* **108** (2012) 201602 [1103.3452].

[84] S. Bhattacharyya, S. Minwalla, V. E. Hubeny and M. Rangamani, *Nonlinear fluid dynamics from gravity*, *Journal of High Energy Physics* **2008** (2008) 045 [0712.2456].

[85] R. Baier, P. Romatschke, D. T. Son, A. O. Starinets and M. A. Stephanov, *Relativistic viscous hydrodynamics, conformal invariance, and holography*, *Journal of High Energy Physics* **2008** (2008) 100 [0712.2451].

[86] A. Behtash, S. Kamata, M. Martinez, T. Schäfer and V. Skokov, *Transasymptotics and hydrodynamization of the Fokker-Planck equation for gluons*, *Physical Review D* **103** (2021) 056010 [2011.08235].

[87] A. Behtash, S. Kamata, M. Martinez and H. Shi, *Dynamical systems and nonlinear transient rheology of the far-from-equilibrium Bjorken flow*, *Phys. Rev. D* **99** (2019) 116012 [1901.08632].

[88] M. V. Berry and C. J. Howls, *Hyperasymptotics for integrals with saddles*, *Proceedings of the Royal Society of London. Series A: Mathematical and Physical Sciences* **434** (1991) 657.

[89] A. B. Olde Daalhuis, *Hyperasymptotic solutions of second-order linear differential equations. II*, *Methods Appl. Anal.* **2** (1995) 198.

[90] A. B. Olde Daalhuis, *Hyperasymptotics for nonlinear ODEs I. A Riccati equation*, *Proc. Roy. Soc. Lond.* A **461** (2005) 2503.

[91] A. B. Olde Daalhuis, *Hyperterminants. II*, *J. Comput. Appl. Math.* **89** (1998) 87.

[92] E. Delabaere and F. Pham, *Resurgent methods in semi-classical asymptotics*, *AIHP* **A71** (1999) 1.

[93] I. Aniceto and R. Schiappa, *Nonperturbative ambiguities and the reality of resurgent transseries*, *Commun. Math. Phys.* **335** (2015) 183 [1308.1115].

[94] I. Aniceto, *Talk at StringMath 2019, "From asymptotics to exact results in string and gauge theories", in Uppsala, Sweden*, .

[95] M. Borinsky and G. V. Dunne, *Non-perturbative completion of Hopf-algebraic Dyson-Schwinger equations*, *Nucl. Phys. B* **957** (2020) 115096 [2005.04265].

[96] L. N. Trefethen and J. A. C. Weideman, *The exponentially convergent trapezoidal rule*, *SIAM Rev.* **56** (2014) 385.

[97] R. M. Corless, G. H. Gonnet, D. E. G. Hare, D. J. Jeffrey and D. E. Knuth, *On the LambertW function*, *Advances in Computational Mathematics* **5** (1996) 329.

[98] I. Aniceto, D. Hasenbichler and A. B. Olde Daalhuis, *In preparation*, .

[99] M. P. Heller, A. Serantes, M. Spaliński, V. Svensson and B. Withers, *Relativistic hydrodynamics: A singulant perspective*, *Phys. Rev. X* **12** (2022) 041010 [2112.12794].

[100] M. P. Heller and V. Svensson, *How does relativistic kinetic theory remember about initial conditions?*, *Physical Review D* **98** (2018) 054016 [1802.08225].

[101] A. Behtash, S. Kamata, M. Martinez and H. Shi, *Global flow structure and exact formal transseries of the Gubser flow in kinetic theory*, *Journal of High Energy Physics* **2020** (2020) 1 [1911.06406].

[102] I. Aniceto, *The resurgence of the cusp anomalous dimension*, *Journal of Physics A: Mathematical and Theoretical* **49** (2016) 065403 [1506.03388].

[103] D. Dorigoni and Y. Hatsuda, *Resurgence of the Cusp Anomalous Dimension*, *JHEP* **09** (2015) 138 [1506.03763].

[104] P. Romatschke, *Relativistic hydrodynamic attractors with broken symmetries: Non-conformal and non-homogeneous*, *JHEP* **12** (2017) 079 [1710.03234].

[105] X. Du, M. P. Heller, S. Schlichting and V. Svensson, *Exponential approach to the hydrodynamic attractor in yang-mills kinetic theory*, *Phys. Rev. D* **106** (2022) 014016 [2203.16549].

[106] M. Mokdad, *Reissner–Nordstrøm–de Sitter manifold: photon sphere and maximal analytic extension*, *Class. Quant. Grav.* **34** (2017) 175014 [1701.06982].

[107] S. W. Hawking and G. F. R. Ellis, *The Large Scale Structure of Space-Time*, Cambridge Monographs on Mathematical Physics. Cambridge University Press, 2, 2023, 10.1017/9781009253161.

[108] R. Penrose, *The question of cosmic censorship*, *Journal of Astrophysics and Astronomy* **20** (1999) 233.

[109] M. Dafermos, *Black holes without spacelike singularities*, *Commun. Math. Phys.* **332** (2014) 729 [1201.1797].

[110] J. Sbierski, *The C_0-inextendibility of the Schwarzschild spacetime and the spacelike diameter in Lorentzian geometry*, *J. Diff. Geom.* **108** (2018) 319 [1507.00601].

[111] J. Luk and S.-J. Oh, *Strong cosmic censorship in spherical symmetry for two-ended asymptotically flat initial data ii: the exterior of the black hole region*, *Annals of PDE* **5** (2019) 6 [1702.05716].

[112] D. Christodoulou, *The Formation of Black Holes in General Relativity*, in *12th Marcel Grossmann Meeting on General Relativity*, pp. 24–34, 5, 2008, 0805.3880, DOI.

[113] M. Dafermos and Y. Shlapentokh-Rothman, *Rough initial data and the strength of the blue-shift instability on cosmological black holes with $\Lambda > 0$*, *Class. Quant. Grav.* **35** (2018) 195010 [1805.08764].

[114] P. Hintz and A. Vasy, *Analysis of linear waves near the Cauchy horizon of cosmological black holes*, *J. Math. Phys.* **58** (2017) 081509 [1512.08004].

[115] F. Mellor and I. Moss, *Stability of Black Holes in De Sitter Space*, *Phys. Rev. D* **41** (1990) 403.

[116] K. D. Kokkotas and B. G. Schmidt, *Quasinormal modes of stars and black holes*, *Living Rev. Rel.* **2** (1999) 2 [gr-qc/9909058].

[117] V. Cardoso, J. a. L. Costa, K. Destounis, P. Hintz and A. Jansen, *Quasinormal modes and Strong Cosmic Censorship*, *Phys. Rev. Lett.* **120** (2018) 031103 [1711.10502].

[118] R. Luna, M. Zilhão, V. Cardoso, J. a. L. Costa and J. Natário, *Strong cosmic censorship: The nonlinear story*, *Phys. Rev. D* **99** (2019) 064014 [1810.00886].

[119] O. J. C. Dias, F. C. Eperon, H. S. Reall and J. E. Santos, *Strong cosmic censorship in de Sitter space*, *Phys. Rev. D* **97** (2018) 104060 [1801.09694].

[120] L. C. Evans, *Partial differential equations*, Graduate studies in mathematics. American Mathematical Society, 2 ed., 1998.

[121] D. Hasenbichler, *Cosmic censorship in de Sitter and quasinormal modes*, Master's thesis, Imperial College London, 2019.

[122] C. J. Howls, P. J. Langman and A. B. Olde Daalhuis, *On the higher–order Stokes phenomenon*, *Proc. Roy. Soc. Lond. A* **460** (2004) 2285.

[123] M. P. Heller and M. Spaliński, *Hydrodynamics Beyond the Gradient Expansion: Resurgence and Resummation*, *Phys. Rev. Lett.* **115** (2015) 072501 [1503.07514].

[124] C. J. Lustri, I. Aniceto, D. J. VandenHeuvel and S. W. McCue, *Locating complex singularities of burgers' equation using exponential asymptotics and transseries*, *Proceedings of the Royal Society A* **479** (2023) 20230516 [2307.10508].

[125] I. Aniceto, R. Schiappa and M. Vonk, *The resurgence of instantons in string theory*, *Communications in Number Theory and Physics* **6** (2012) 339 [1106.5922].

[126] P. A. Clarkson, K. Jordaan and A. Loureiro, *Generalized higher-order freud weights*, *Proceedings of the Royal Society A* **479** (2023) 20220788 [2211.13645].

[127] M. Spaliński, *On the hydrodynamic attractor of Yang–Mills plasma*, *Phys. Lett. B* **776** (2018) 468 [1708.01921].

[128] M. P. Heller, R. A. Janik and P. Witaszczyk, *Hydrodynamic gradient expansion in gauge theory plasmas*, *Phys. Rev. Lett.* **110** (2013) 211602 [1302.0697].

[129] A. Davey, O. J. C. Dias and J. E. Santos, *Scalar QNM spectra of Kerr and Reissner-Nordström revealed by eigenvalue repulsions in Kerr-Newman*, *arXiv* (2023) [2305.11216].

[130] M. Marino, R. Miravitllas and T. Reis, *On the structure of trans-series in quantum field theory*, *arXiv* (2023) [2302.08363].

[131] Z. Bajnok, J. Balog and I. Vona, *The full analytic trans-series in integrable field theories*, *Physics Letters B* **844** (2023) 138075 [2212.09416].

[132] A. B. Olde Daalhuis and F. W. J. Olver, *On the calculation of Stokes multipliers for linear differential equations of the second order*, *Methods Appl. Anal.* **2** (1995) 348.

[133] "*NIST Digital Library of Mathematical Functions*." http://dlmf.nist.gov/, Release 1.1.5 of 2022-03-15.